

Neuronal circuits and behavior of *Hydra* in the context of the metaorganism

Dissertation

in fulfilment of the requirements for the degree
Doctor rerum naturalium
of the Faculty of Mathematics and Natural Sciences at the
University of Kiel

Submitted by Christoph Giez
Department of Cell- and Developmental Biology
Zoological Institute, Kiel University
Kiel, 2023

First referee: Prof. Dr. Thomas Bosch

Second referee: Prof. Dr. Hinrich Schulenburg

Date of oral examination: December 15th, 2023

Signature:

Declaration

I, Christoph Giez, declare that:

Apart from my supervisor's guidance the content and design of the thesis is all
my own work.

Specific aspects of my thesis were supported by colleagues; their contribution is
specified in detail in the following section "Contribution of authors".

The thesis has not already been submitted neither partially nor wholly as part of
a doctoral degree to another examining body. Apart from the included published
papers no other part of the thesis has been published nor submitted for
publishing; Furthermore, I declare that I have not yet attempted a doctoral
degree.

The thesis has been prepared subject to the Rules of Good Scientific Practice of
the German Research Foundation (DFG).

Signature: _____

Acknowledgements

Over the last four years, my work on the interaction of the nervous system of *Hydra* and the associated microbes have been a time I am very grateful for and very much enjoyed. However, it would have been not nearly as much fun without a large group of people supporting me along the way.

Firstly, and most importantly, I want to express my gratitude to you, Thomas Bosch, for the guidance, support, trust, and freedom you provided as a supervisor. You always inspired me to go further and to stay curious. I also cannot thank you enough for the many opportunities you made possible during my development.

I would like to express my gratitude to Karen Guillemin and Hinrich Schulenburg for the time they devoted to overseeing my progress and providing invaluable suggestions that significantly enhanced my work.

Thank you to Tim Lachnit and Alexander Klimovich, for smoothing the way for me by providing the needed expertise and fruitful discussions. Alexander Klimovich for the help to develop the required tools, Tim Lachnit for the dedication to identify the microbial molecule.

I also want to thank Andreas Tholey, Jan Leipert, Christian Treitz, Christoph Kaleta, Georgios Marinos, Karlis Moors, Jan Taubenheim, Jenny Uhl, Urska Repnik, and Marc Bramkamp for their help, expertise, and the different points of view on my project, leading to stimulating discussions.

I would also like to thank all former and current members of the Bosch lab: Jay Bathia, Johana Fajardo Castro, Hanna Domin, Maria Franck, Yan Giencke, Jinru He, Mirjam Hecht, Eva-Maria Herbst, Anika Hintz, Alexander Klimovich, Tim Lachnit, Janina Lange, Benedikt Mortzfeld, Ornina Merza, Christopher Noack, Dijana Pavleska, Denis Pinkle, Kai Rathje, Ehsan Sakib, Benedict Staack, Jan Taubenheim, Laura Ulrich, Doris Willoweit-Ohl and Jörg Wittlieb for helping me along the way and making my journey more joyful.

Jörg Wittlieb without whom the project would have not been possible; Eva-Maria Herbst for helping and supporting me since my start in the lab and always spreading joy.

I also want to thank my bachelor and master students Denis Pinkle, Yan Giencke and Ehsan Sakib who I was lucky to supervise and support. Thank you for your trust in me and for helping me to decipher the interaction between neuronal populations and microbes.

Thank you to Ute Jülly for helping me during challenging times, helping me to reflect and giving me support.

Without the unwavering support and encouragement of my family, my parents, and my friends I would not have been able to accomplish this chapter of my life. Special thanks to you, Lena Peters, for taking the same journey, being an inspiration, and support. Thank you also to Janna Wülbern for taking your time and improving my thesis at the end.

Finally, I would like to thank my wife Tabea for her emotional support, motivation, being immensely patient, making challenges appear simple and always believing in me. Without you I would have lost myself, you keep me grounded.

Content

Acknowledgements	5
Content	9
Contribution of authors	11
Summary	15
Zusammenfassung	17
Introduction	21
Animals evolved in a microbial world: The concept of a metaorganism	21
Neuro-Microbe interaction	26
Evolution of the nervous system	33
Hydra – a model system for neurobiology	35
Hydra – a simple metaorganism	47
Hydra as a chance for a mechanistic understanding	50
Objectives and overview of this thesis.	52
Chapter I:	53
Neurons interact with the microbiome: an evolutionary-informed perspective.....	53
Chapter II:	73
Spontaneous body wall contractions stabilize the fluid microenvironment that shapes host-microbe associations.	73
Chapter III:	103
Multiple neuronal populations control the eating behavior in Hydra and are responsive to microbial signals	103
Chapter IV:	155
The internal metabolic state controls behavior in Hydra through an interplay of enteric and central nervous system-like neuron populations.....	155
Epilogue.....	179
Connection between behavior, nervous system, and microbiota – can we understand the “why”?.....	181
Does Hydra have a brain?	191
References (Introduction and Epilogue).....	201

Contribution of authors

Chapter I:

Neurons interact with the microbiome: an evolutionary-informed perspective.

Neuroforum, Review article, 2021

Christoph Giez, Alexander Klimovich and Thomas C. G. Bosch

CG, AK and TCGB reviewed the relevant literature and contributed to the main text.

Chapter II:

Spontaneous body wall contractions stabilize the fluid microenvironment that shapes host-microbe associations.

eLife, 2023

Janna C Nawroth^a, **Christoph Giez**^a, Alexander Klimovich, Eva Kanso, Thomas CG Bosch

^a contributed equally

C. G., Data curation, Data analysis, Investigation, Visualization, Methodology, Writing – original draft, Writing – review and editing. All behavioral experiments, data analysis and visualization. All 16S RNA Seq sampling, analysis, and visualization. Labelling of *Curvibacter* to visualize fluid boundary layer-bacteria interaction.

Chapter III:

Microbes as part of ancestral neuronal circuits: Bacterial produced signals affect neurons controlling eating behavior in *Hydra*.

Accepted by Current Biology, BioRxiv, 2023

Christoph Giez, Denis Pinkle, Yan Giencke, Jörg Wittlieb, Eva Herbst, Tobias Spratte, Tim Lachnit, Alexander Klimovich, Christine Selhuber-Unkel, Thomas Bosch

C.G. and T.C.G.B. conceptualized the project and wrote the manuscript. C.G. designed, established new constructs, and performed experiments on transgenesis. C.G. designed and performed histological, behavioral experiments. C.G. designed and performed neuronal activity and microbiota experiments. C.G. designed and analyzed the RNA Seq experiments and data. C.G. wrote first version of the manuscript.

Chapter IV:

The internal metabolic state controls behavior in *Hydra* through an interplay of enteric and central nervous system-like neuron populations.

Manuscript submitted, 2023

Christoph Giez, Christopher Noack, Ehsan Sakib, Thomas Bosch

C.G. conceptualized the project and conducted the experiments. C.G. generated the transgenic constructs and designed experiments for behavioral analysis. C.G. and performed cell ablation experiments. C.G. performed calcium imaging experiments. C.G. did data analysis. C.G. wrote first version of manuscript.

As supervisor I confirm the above stated contributions

Signature, Doctorand:

Signature, Supervisor:

Summary

How do spontaneous body wall contractions, eating behavior, the evolution of the nervous system and the microbiota fit together? In my thesis I show that all four are connected and form a feedback loop that is omnipresent in the animal kingdom and might shed new light on the evolution of the metaorganism. My major findings were:

1. A puzzling behavior within *Hydras*' repertoire is the spontaneous contractions of its body walls. We combined experimental fluid dynamics analysis and mathematical modeling to shed light on this phenomenon. It turns out that these spontaneous body wall contractions play a functional role by enhancing the transport of chemical compounds to and from the tissue surfaces where symbiotic bacteria reside. Interestingly, reducing the frequency of these contractions is associated with alterations in the composition of the colonizing microbiota.
2. Further, we delved into the eating behavior of Hydra, investigating the interplay between neuronal circuits and the symbiotic microbiota. Multiple neuronal subpopulations work together to control eating behavior and integrate a microbial metabolite. This observation underscores how microbes can affect neuronal circuits and eating behavior in a community-dependent manner.
3. Additionally, hunger and satiety have been found to influence behavior. Our work revealed that two distinct neuronal populations, N3 and N4, are responsible for feeding-dependent behavioral changes in *Hydra*. The endodermal N4 population is essential for food intake and digestion, like the enteric nervous system, while the ectodermal N3 population influences and inhibits other motor-related behaviors, similar to the central nervous system. These intriguing findings highlight the evolution and complexity of even the simplest nervous systems.

In summary, research on *Hydra* illuminates the importance of spontaneous body wall contractions, eating behavior and microbes, and neuronal activity in response to feeding. Our data highlight that one major function of the nervous system is to control eating behavior and maintain a stable and beneficial microbiota which are in the end linked to each other via feedback loops. These discoveries provide valuable insights into the dynamics of host-microbe interactions and the functionality of rudimentary nervous systems.

Zusammenfassung

Wie passen spontane Kontraktionen, Essverhalten, die Evolution des Nervensystems und Mikroben zusammen? In meiner Arbeit zeige ich, dass alle diese Elemente miteinander verbunden sind und diese Verbindung in allen Tieren zu finden ist und womit diese Erkenntnis möglicherweise ein neues Licht auf die Evolution des Metaorganismus und des Nervensystems wirft. Hier eine kurze Zusammenfassung der wichtigsten Erkenntnisse aus meiner Arbeit:

1. Um das Phänomen der Kontraktionen in *Hydra* zu verstehen, kombinierten wir experimentelle Fluidodynamikanalysen und mathematische Modellierungen. Dadurch konnten wir feststellen, dass diese spontanen Kontraktionen eine wichtige Rolle spielen im Transport von Stoffen zu und von der Körperoberfläche von *Hydra*. Interessanterweise sind Veränderungen in der Häufigkeit dieser Kontraktionen mit einer Veränderung in der Zusammensetzung der assoziierten Mikrobiota verbunden.
2. Des Weiteren haben wir das Essverhalten der *Hydra* untersucht und das Zusammenspiel zwischen neuronalen Schaltkreisen und der Mikrobiota erforscht. Wir stellten fest, dass mehrere neuronale Zellpopulationen zusammenarbeiten, um das Essverhalten zu steuern. Gleichzeitig wird in diesen Schaltkreis ein mikrobielles Molekül integriert. Die Integration ist abhängig von der Zusammensetzung der mikrobiellen Gemeinschaft, was zu Veränderungen im Verhalten führen kann. Diese Beobachtung unterstreicht, wie Mikroben neuronale Schaltkreise und Essverhalten in einer gemeinschaftsabhängigen Weise beeinflussen können.
3. Darüber hinaus haben wir festgestellt, dass zwei unterschiedliche neuronale Populationen, N3 und N4, für sättigungsabhängige Verhaltensänderungen in der *Hydra* verantwortlich sind. Die endodermale N4-Population ist entscheidend für die Nahrungsaufnahme und endodermalen Kontraktionen während der Verdauung, ähnlich dem enterischen Nervensystem, während die ektodermale N3-Population andere motorische Verhaltensweisen in einer sättigungsabhängigen

Weise moduliert, ähnlich dem zentralen Nervensystem. Diese faszinierende Entdeckung verdeutlicht die Evolution und Komplexität selbst einfacher Nervensysteme.

Meine Arbeit zeigt, dass eine Hauptfunktion des Nervensystems darin besteht, das Essverhalten zu kontrollieren und eine stabile und nützliche Mikrobiota aufrechtzuerhalten, wobei beides über Rückkopplungsschleifen miteinander verbunden ist. Diese Erkenntnisse bieten wertvolle Einblicke in die Dynamik von Wechselwirkungen zwischen Wirt und Mikrobe sowie die Funktionalität und Evolution von Nervensystemen.

Introduction

Animals evolved in a microbial world: The concept of a metaorganism

Let me take you on a trip back to the origin of life on our planet earth. Picture a time when everything was just about chemical reactions. In this soup, suddenly, the basis of all life emerged in a beautiful spontaneous reaction (Harold Urey, 1952). One intriguing theory speculates that this pivotal moment was driven by the miraculous birth of self-replicating macromolecules. These humble beginnings set the stage for the rise of RNA in the so-called "RNA world" and eventually paving the way for the DNA, the genetic code as we know it (Cooper, 2000; Robertson and Joyce, 2012). Now let's fast forward to about 3.8 billion years ago, when the young planet earth was on the brink of turning mere billion years old. During this epoch, prokaryotes evolved as the first life form on earth (Cooper, 2000). From now on, these prokaryotes shaped the earth, thriving in the harshest of environments. Yet, it was not until another 1.8 billion years had passed that the first eukaryotic cell evolved in this prokaryotic world. In a mesmerizing twist, it has been proposed that the eukaryotic cell is an outcome of a bacterium living in an archaeon (Sagan, 1967). Another 1.2 billion years come and go, ushering in an era around 600 million years ago, when the first multicellular organism is belived to have emerged (Erwin et al., 2011; Grosberg and Strathmann, 2007; Zhu et al., 2016). Let us now reflect upon this magnificent story of life, where the first multicellular organisms evolved in a world solely shaped by microbial organisms and their molecules. It is a remarkable testament to the unbreakable connection that exists among every living being and the everlasting heritage of our earliest days.

The whole trajectory of the metazoan evolution happened in the context of a microbial world (McFall-Ngai et al., 2013). There was never a time and environment without microbes or microbial products which caused microbes to have a crucial impact on the evolution of eukaryotes. It is highly probable that the organelles mitochondria and chloroplasts evolved as a result of an uptake of a microbial cell (Dyall et al., 2004; McFadden and Van Dooren, 2004). Further, in the emergence of the first form of multicellularity, bacterial metabolites are thought

to be the inducers of the transition from a unicellular to a multicellular lifestyle (Woznica et al., 2016). Continuing along the trajectory of the evolution of complex lifeforms, one can find a multitude of different degrees of symbiotic interactions (McFall-Ngai et al., 2013). This highlights that there is no organism without an associated microbial community and every organism can be seen as a metaorganism (Fig. 1) (Bosch and McFall-Ngai, 2011).

Over the last two decades, the interactions within the metaorganism were investigated on a wide variety of model systems ranging from unicellular organisms, (such as choanoflagellates), over early branching metazoan (sponges and cnidarian) and invertebrates (*Caenorhabditis elegans*, *Drosophila melanogaster*) to vertebrates (zebrafish, mice, humans) highlighting the manifold impact of microbes on animals' development, physiology and behavior (Bosch and McFall-Ngai, 2021; Carrier and Bosch, 2022; Fraune and Bosch, 2010).

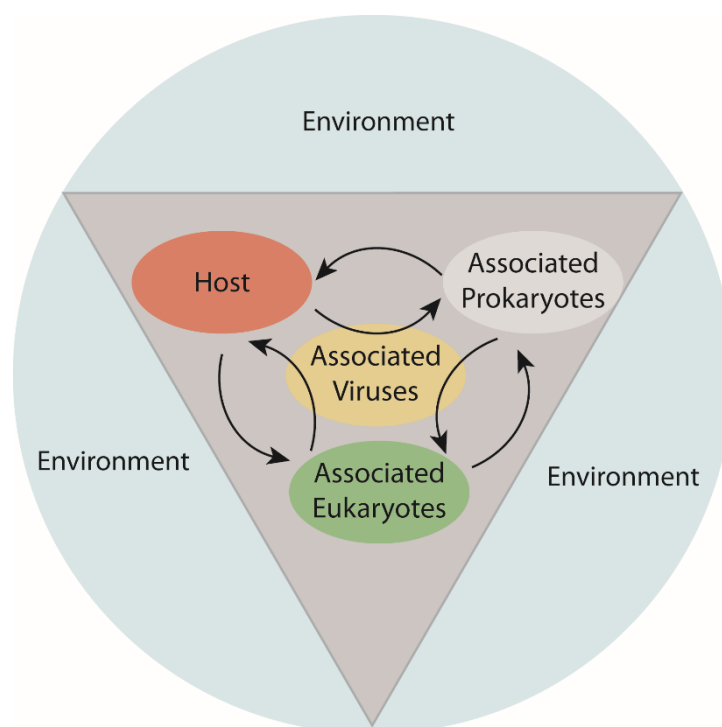


Figure 1. The metaorganism concept. Multicellular organisms are hosts to prokaryotes, eukaryotes, and viruses thereby forming a metaorganism which is embedded in a certain environment. (Modified from (Bosch and McFall-Ngai, 2011))

Microbes and host development

In invertebrates, microbial symbionts can have a major impact on developmental transitions, development *per se*, life history, and fitness. Many marine invertebrates use bacterial cues to decide where to settle and undergo metamorphosis such as the tubeworm *Hydroides elegans* (Hadfield, 2010; Shikuma et al., 2016). In a different instance, in the bobtail squid *Euprymna scolopes*, the colonization of the crypts by *Vibrio fischeri* leads to light-organ morphogenesis (Nyholm and McFall-Ngai, 2021). This includes cellular changes, epithelial swelling, and an increase in microvillar density. In *Drosophila melanogaster* the microbiota influences stem cell proliferation, tissue homeostasis, mating preferences and life span (Erkosar et al., 2013). Interestingly, in invertebrates, one can see the most intimate interactions and co-dependency between microbes and hosts. One such exceptional case can be observed in the aphid *Acyrtosiphon pisum* where a specialized cell, the bacteriocytes, houses the obligative endosymbiont *Buchnera*. *Buchnera* provides essential amino acids that compensate for the essential amino acid deficient diet enabling the host to grow and reproduce (Akman Gündüz and Douglas, 2008; Shigenobu et al., 2000). Such intimate and essential symbiosis occurs frequently in insects and can get as fascinating as the fungus-growing ants (Currie, 2003). All those examples highlight the importance of microbes and their manifold impact on invertebrate development and physiology.

In vertebrates, microbial symbionts are required for the development and maturation of the intestinal epithelium, as well as for the immune and nervous system (John F Cryan et al., 2019; Sommer and Bäckhed, 2013). In zebrafish the gut microbiota promotes intestinal epithelia proliferation (Cheesman et al., 2011), maturation and enteroendocrine and goblet cell differentiation (Bates et al., 2006). Here, bacteria seem to interfere with the developmental pathway Notch thereby changing cell fates. The phenotypes and transcriptional response to the microbiota were found to be similar between germ-free (GF) zebrafish and mice which suggests a conserved response to the microbiota in vertebrates (Hooper et al., 2001; Rawls et al., 2004; Sharma and Schumacher, 1995; Uribe et al., 2009). Looking into immune system maturation in mammals, the impact of the microbiota has been shown in multiple studies and it already starts during early life (Gensollen et al., 2016; Hooper et al., 2012; Lee and Mazmanian, 2010). Another aspect of vertebrate physiology where microbes can play a crucial role

includes the phenomenon of aging. In the killifish *Nothobranchius furzeri*, the microbiota has a major impact on the aging process. This is evident through transplantation experiments where the transfer of the microbiota from a young donor to an old individual extended their life span and delayed the behavioral decline (Smith et al., 2017). A similar phenotype was also observed in mice when the microbiota from either old or young mice is transplanted (Boehme et al., 2021; Parker et al., 2022). However, the underlying mechanism is still unclear. Nevertheless, those mechanisms might be solved in the future with the establishment of new technologies such as single cell sequencing, spatial transcriptomics, and metabolomics (Michellod et al., 2023; Williams et al., 2022). The elucidation of the global impact of the microbiota on the host has already been emphasized by studying the hosts with a single cell resolution. In zebrafish, this approach revealed a global effect across all tissues by microbes (Massaquoi et al., 2023). While highlighting all the importance of microbes on the host, most studies remain correlative and lack to elucidate the mechanism of interaction. Also, the extent to which these interactions affect animal fitness, life history, and evolution in their natural environment remains unclear since germ-free animals can still survive and reproduce under laboratory conditions.

Host-microbe interaction – a micro-scaled ecosystem

Based on what has been described so far in invertebrates and vertebrates, we can conclude that there are different levels of interactions between metazoan hosts: from endosymbionts to hosts forming specialized organs to an associated microbial community (Alberdi et al., 2021). In the following, the focus will be on associated microbial communities. These associated communities can be found in most animals and are often described as microbiota. Characterizing the dynamic interactions among the host and the members of the microbial community one can describe and think about them as an “ecosystem on a leash” (Foster et al., 2017). Since all surfaces are colonized by a myriad of microbes, each species down to strain level has the potential to interact with each other. Some can kill (Kommineni et al., 2015) or cross-feed conspecifics (Rakoff-Nahoum et al., 2016) leading to a complex and dynamic ecosystem. Interestingly, to understand such a complex micro-scaled-environment, theories developed in ecology find their way into microbiome research (Costello et al., 2012). In addition, the concept of host-microbe interactions and their origin has been enriched by the integration of evolutionary thinking. This integration has contributed to a more

comprehensive understanding of these interactions (Obeng et al., 2021; Sieber et al., 2021, 2019). However, most studies focused on the mammalian-microbe interaction, but this is just one of a myriad of symbioses that evolved over time. Comparing different organisms, one can find striking similarities which suggest common underlying principles (Foster et al., 2017). In summary one can find three main characteristics: microbe-host, host-microbe, and microbe-microbe interactions (Foster et al., 2017). As suggested, most functions of the microbiota can be explained by the latter two and in the next paragraph the point of host-microbe interaction will be explored further (Foster et al., 2017). In summary, the metaorganism is a complex nested ecosystem with a multitude of potential interactions, and a substantial part is still ignored since unicellular eukaryotes, *archaea*, and fungi are underrepresented in most studies.

The host to microbe interaction is one of the factors that have been proposed to explain most function of the microbiota (Foster et al., 2017). While the host can affect and influence the whole microbiota, an individual microbe is unlikely to have the same degree of impact on the myriad of other microbes. Following this way of thinking, the host is supposed to have a strong natural selection on the control of the microbiota (Schluter and Foster, 2012). To effectively regulate one's microbiota, it is necessary to possess the capacity to perceive and comprehend it, thereby facilitating the ability to react to any potentially harmful changes. How exactly the host senses the microbial colonizers, and their different states is an exciting question. A classical and conserved way of sensing characteristic molecules of bacteria is over pattern recognition receptors (PRR) which can sense for example cell wall components such as lipopolysaccharides. These PRR can be found in plants as well as in basal metazoans and even in mammals (Li and Wu, 2021). Those receptors play a key role in the innate immune system. To mention one example, one of the conserved signaling pathways is the Toll-Like receptor with MyD88 which can be found in *Cnidarian* to mammals (Akira and Takeda, 2004; Cheesman et al., 2011; Franzenburg et al., 2012; van der Vaart et al., 2013). It can recognize different surfaces and intracellular components of microbes and trigger inflammatory cytokine production via MyD88 (Franzenburg et al., 2012). However, there are a multitude of different signaling pathways to sense and respond to the microbiota, and the manifold of channels to sense and regulate microbes has not been revealed yet.

In the next chapter, neurons are proposed to work as immunocompetent cells which have been able to sense and regulate microbial symbionts since the evolution of the nervous system. Since nearly all hosts exhibit a neuronal response to the lack or existence of specific microbial species, implying a shared motif across all animal species. The common underlying mechanism of the interaction between neurons and microbes still lacks causal data.

Neuro-Microbe interaction

In the last two decades, a paradigm shift happened in neuroscience since it has been shown that distant gut bacteria can influence neuronal physiology in the brain (Mayer et al., 2014). From that point on, a large body of work has demonstrated the multifaceted effects that the microbiota can have on the host nervous system in a variety of model organisms (Nagpal and Cryan, 2021). However, most work focuses on rodents and remains at a correlative level, linking the gut metabolome to neurological phenotypes. To reach a causal level, the search for synergies between different model systems along the tree of life will be the next step.

Behavioral changes due to bacteria

Strikingly, there are multiple behaviors affected similarly by bacteria across multiple model systems such as *C. elegans*, *Drosophila*, zebrafish, and mice. In the absence of microbes, axenic, *Drosophila*, zebrafish, and mice show hyperactivity (Heijtz et al., 2011; Phelps et al., 2017; Schretter et al., 2018). *Drosophila melanogaster* exhibit an increase in walking speed and daily activity in the absence of microbes. *Lactobacillus brevis* mono-colonization rescues the effect via octopaminergic neurons and sugar metabolism (Schretter et al., 2018). In zebrafish larvae, the absence of microbes results also in hyperactivity but via a neuronal developmental impairment. Interestingly, heat-killed bacteria cannot abrogate the effect (Phelps et al., 2017). Mice show hyperactivity under germ-free conditions compared to specific pathogen free mice. Here, the behavioral changes were associated with gene expression changes in the brain. The effect was reversible when colonizing germ-free mice during early life (Heijtz et al., 2011). Another interesting behavioral phenotype that is changing due to the manipulation of the microbiota is social behavior. Male *Drosophila melanogaster* flies exhibit aggressive behavior against other males (Zhou et al., 2008; Zwarts et al., 2012). In germ-free flies, inter-male aggression is reduced, and the germ-

free males are not as competitive for female flies as colonized flies (Jia et al., 2021). The deficit can be restored by recolonization and mono-association with *Lactobacillus plantarum* which acts via octopaminergic neurons. The recolonization must happen within a specific developmental window to fully rescue the aggression behavior (Jia et al., 2021). Zebrafish larvae develop their first social behaviors such as aggression, shoaling, and kin recognition after 12 to 16 days post fertilization (dpf) (Dreosti et al., 2015; Hinz and De Polavieja, 2017; Madeira and Oliveira, 2017; Stednitz et al., 2018; Stednitz and Washbourne, 2020). When they develop in the absence of microbes, zebrafish show abnormal social behavior (Bruckner et al., 2022). Associated with the behavioral change, neurite complexity is decreased of forebrain neurons, and microglia localization altered. Interestingly, multiple bacteria taxa are able to rescue the phenotype (Bruckner et al., 2022). In mice, social behavior is impaired in a reversible way within a developmental window of time (Desbonnet et al., 2013). Germ-free mice show an impairment in social preferences and social cognition. Colonization postweaning only reversed the impairment of social preference but not social cognition, which suggests a critical developmental phase during weaning (Desbonnet et al., 2013; Luczynski et al., 2016). In summary, the microbiota influences similar behaviors in different animals, whether through an influence in a specific developmental window or through a direct and general influence.

Eating behavior and bacteria

One behavior that is modulated by microbes and has a direct influence on the gut environment, is the regulation of appetite, feeding and food choice. *C. elegans* can sense food ingestion via a conserved acid sensing ion channel, DEL-3 and DEL-7, which is expressed in serotonergic sensory neurons (NSM neuron) and has a global effect on behavior such as locomotion (Rhoades et al., 2019). The molecule, which is triggering the NSM neuron response, is heat stable and most likely a membrane component. This work shows a new way of how the enteric nervous system can influence behavior in general (Rhoades et al., 2019). The protein appetite of *Drosophila melanogaster* is influenced by the *Acetobacter pomorum* which cross-feeds on the lactate of *Lactobacillus plantarum* and provides the fly with essential amino acids and thereby allows the fly to grow on an imbalanced diet (Henriques et al., 2020). Further, the fly can sense the amount of essential amino acids in the gut and change its food choice appropriately via

the neuropeptide CNMamide produced by enterocytes of the anterior midgut (Kim et al., 2021). Thereby the production of essential amino acids by the microbiota is sufficient to alter the food choice (Kim et al., 2021). In mammals and mice, gut microbial metabolites can affect appetite via multiple routes for example by acting directly as appetite-related signaling molecules to regulate hormone secretion or by directly acting on hypothalamic neurons (Han et al., 2021). In a recent publication, the pattern recognition receptor NOD2 which is expressed throughout the brain and can sense muropeptides, components of bacterial cell wall, affects among others the eating behavior of mice (Gabanyi et al., 2022). Thereby, the brain may sense changes in gut bacteria as a measure of food intake. As a final focus of this section, one change in behavior on a much smaller scale is the contraction pattern of the gut (peristalsis), which is the habitat of the microbes. In *Drosophila melanogaster* the sensing of potential pathogens has been proposed to induce a change in gut peristalsis to expel or transfer pathogens to more hostile environments (ROS, AMPs) (Buchon et al., 2013; Vallet-Gely et al., 2008). Since the gut peristalsis is supposed to be under the control of the nervous system, there has to be a circuit that integrates the information of the colonizing microbial community. In zebrafish, gut peristalsis has a key effect on the persistence and stability of the microbial members (Logan et al., 2018; Wiles et al., 2020, 2016). Similar to mice, the gut motility changes as a reaction to different conditions such as dysbiosis or diet (Obata and Pachnis, 2016). More recently, the aryl hydrocarbon receptor (AHR) has been shown to be a biosensor for the microbial environment and integrator of this information into the neuronal circuit which regulates gut motility (Obata et al., 2020). Overall, all these examples highlight that the effect of microbes on different hosts can have striking similarities which suggests conserved ways of interaction. However, the causal underlying mechanisms of the conserved routes are still not yet fully revealed, and the next part will highlight the different ways of communication and impacts on the host.

Microbial-produced neuroactive molecules

Seeing similar behavioral modulations due to changes in the microbiota across different model organisms suggests common themes of interactions. Here, the focus will be on the synthesis of neuroactive metabolites by bacteria and since there is a multitude of findings the focus will be on molecules that have a behavioral effect and mechanistic validation. A way in which bacteria can influence the nervous system is by producing precursors of neurotransmitters or

neurotransmitters and thereby modulating behavioral pattern. Although in mammals some members of the microbiota have the potential to produce precursors and neurotransmitters, most studies remain on a correlative level showing an increase of neurotransmitter in proximity and distant tissue (Miri et al., 2023; Nagpal and Cryan, 2021). So far, the direct link between bacterial produced neurotransmitter, uptake, and integration by the host into neuronal circuits lacks a mechanistic understanding and evidence. Most work shows that bacterial metabolites lead to the production of neurotransmitter by the host due to binding to a receptor in a certain tissue (Cussotto et al., 2018; Dohnalová et al., 2022; Jia et al., 2021; Masuzzo et al., 2020; Nagpal and Cryan, 2021). A causal insight into the communication via precursor of a neurotransmitter is currently gained by the model organisms *C. elegans* and zebrafish (Nagpal and Cryan, 2021). In *C. elegans*, the gut colonizing *Providencia* influences host sensory decision making by producing tyramine – a precursor of the neurotransmitter octopamine (O'Donnell et al., 2020). Octopamine itself targets the ASH nociceptive neuron, which affects an aversive olfactory behavior. In zebrafish, enteroendocrine cells can get directly stimulated by a bacterial subset of indole derivatives of tryptophan catabolism via an ion channel that leads to the secretion of serotonin (Ye et al., 2021). In mice, the examples discussed so far show an influence of the nervous system via a pattern recognition receptor, Nod2, for bacterial cell wall components (Gabanyi et al., 2022) and a receptor that functions as a transcription factor in the enteric nervous system (Obata et al., 2020). However, there are also examples in which bacteria produce metabolites which affect sensory neurons (Dohnalová et al., 2022). Here, bacteria produce endocannabinoid metabolites which affect sensory neurons via the ion channel TRPV1 and increase motivation to exercise. This increases dopamine levels in the brain during exercise (Dohnalová et al., 2022). Nevertheless, the mechanism of how and if the molecules reach the sensory neurons is still not solved. Following this, even though a myriad of bacteria from mammal guts has the potential to produce neurotransmitters such as glutamate, GABA, and serotonin (Strandwitz, 2018), the translation from *in vitro* to *in vivo* is not yet fully made and future work has to reveal the whole picture. One way to reach a mechanistic understanding might be provided by including simpler model organisms and searching for overlaps.

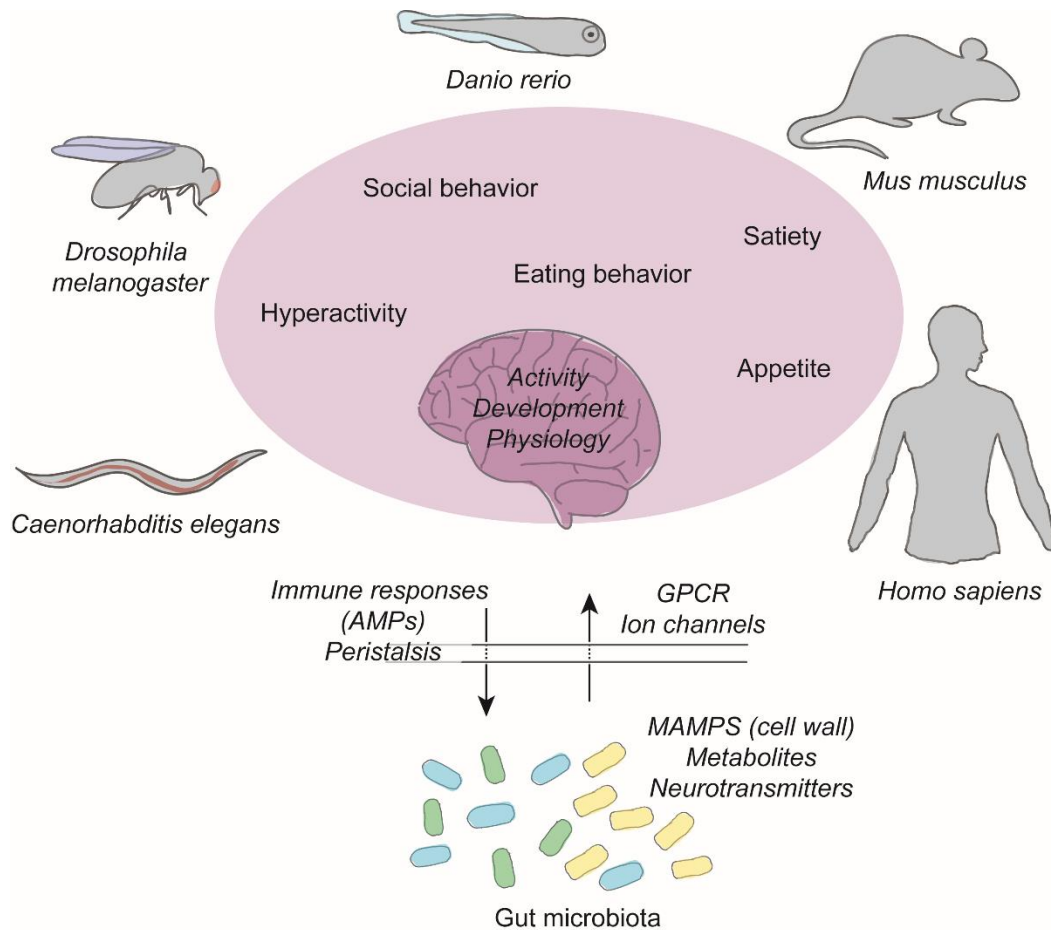


Figure 2. The gut microbiota influences similar behaviors across multiple model organisms. The gut microbiota produces metabolites which are detected over multiple signaling pathways. In the end they all reach the brain and affect the behavior of the host. Hyperactivity, social behavior, and eating behavior are modulated by microbes across multiple model systems.

Host repertoire of receptors

Discussing the ways of behavioral changes and the production of neuroactive molecules, leaves the question open of how the host is detecting the microbial signals. Interestingly, most hosts have developed a manifold of receptors that can sense and get activated by microbial metabolites. Those channels can be divided into ion channels, such as TRPVA1 (Dohnalová et al., 2022), and G-protein coupled receptors (GPCR) (Cohen et al., 2017; Colosimo et al., 2019). Within the GPCRs, many have not been annotated and are taxonomically restricted (Chen et al., 2019). In mammals there have been multiple *in vitro* screenings of GPCRs highlighting the ability to sense microbial metabolites in a host specific manner (Chen et al., 2019; Cohen et al., 2017; Colosimo et al., 2019). In *Drosophila*, a GPCR is proposed to sense the uracil of opportunistic pathobionts and provoke

chronic inflammation (Ha et al., 2009; Lee et al., 2013) and in addition different ion channel receptors can detect microbial metabolites (Depetris-Chauvin et al., 2017). In *C. elegans*, an ion channel from the family of acid sensing ion channels detects microbes in the gut (Rhoades et al., 2019). However, a systematic approach to identify GPCR and ion channels that can respond to microbial products is missing for most hosts. The identification and analysis of the potential to sense microbial products and their location might help to close the gap in knowledge about the communication between gut and brain.

Bacterial effects on the nervous system

The impact of microbes on the central nervous system seems to be manifold besides the impact on behavior: it can affect neuronal activity and neurogenesis across multiple hosts. In mice and zebrafish, the absence of microbes leads to changes in the anatomy of the nervous system. Such as a decrease in axon growth and a decrease in arborization of neurons (Bruckner et al., 2022; Vuong et al., 2020). These effects abrogated due to an early-life recolonization or exposure to microbial products. Bacterial metabolites can change the neuronal activity of the enteric nervous system as well as the central nervous system. In mice, the gut microbiota is necessary for the normal excitability of the gut sensory neurons (Mcvey Neufeld et al., 2013). Similarly, the presence of distinct bacteria and metabolites can activate the enteric nervous system in zebrafish (Ye et al., 2021). Bacterial cell membrane components, muropeptides, can reach the brain and reduce neuronal activity in mice (Gabanyi et al., 2022). The presence of bacterial metabolites is also able to activate the dorsal root ganglion and thereby induces neurochemical changes in the brain (Dohnalová et al., 2022). Interestingly, not much is known about the influence of bacteria on neuronal activity and anatomy in invertebrates although there are behavioral changes (Nagpal and Cryan, 2021). In *Drosophila* peptidoglycan is inhibiting the activity of a subset of octopaminergic neurons in the brain which control egg laying (Masuzzo et al., 2019). Nevertheless, given the different and prominent effects on behavior in invertebrates, changes in neuronal activity and neurogenesis are to be expected and worth pursuing further. This can give a better understanding of conserved principles across systems and elucidating new mechanisms.

Going through the exciting findings about the importance of microbes on animal behavior, only in a few cases a deep mechanistic understanding has been

reached as highlighted above. Challenging enough, results tackling the impact of microbes on animal behavior and even work solely focusing on behavior showed a variety of inconsistencies between different working groups and over different model systems (Nagpal and Cryan, 2021; Richter et al., 2009). This shows that so far not all relevant factors are known or discovered. To increase complexity, the question that often remains unanswered is: why do microbes have an impact on behavior or why has the host adapted to bacterial signals in a certain way? Since the decoding of the nervous system is a tremendous challenge in itself, the inclusion of the effect of an associated microbial community seems unsolvable. The proposal outlined at the start suggests that finding synergies across the phylogenetic tree and new model organisms, involving simpler organisms with genetic accessibility, can clarify the complex interplay.

Open questions:

- How do animals integrate bacterial/microbial signals in neuronal circuits and respond almost immediately? (**Chapter III**)
- How are microbial metabolites sensed and in which way is the information translated and integrated in distal tissues such as the brain? (**Chapter III**)
- Are there universal mechanisms for how hosts detect and integrate bacterial metabolites? (**Chapter III**)
- Why do microbial metabolites influence host behavior? (**Chapter II**)

Evolution of the nervous system

The nervous system is one of the most diverse structures in the animal kingdom, both in its anatomy and in cell type diversity (Arendt, 2018; Bucher and Anderson, 2015; Martín-Durán and Hejnal, 2021; Squire et al., 2012). It comprises diffuse nerve nets (Cnidarian) to complex brains (Vertebrates) as well as nervous systems with just 302 neurons (*C. elegans*) and ones with billions of neuronal cells (Squire et al., 2012). The evolution of such diverse and complex structures is still an enigma and multiple works draw different scenarios of how neurons and complex structures emerged (Arendt, 2020, 2018; Bucher and Anderson, 2015; Martín-Durán and Hejnal, 2021). Before starting this chapter, we need to ask: what defines a neuron as a neuron? The features which one would assign first are that (1) a neuron possesses long processes (axons, dendrites, neurites), (2) it can generate and/or transmit action potentials, (3) it has an input (from sensory neuron or other stimuli), and (4) an output via synaptic structures to another cell (neuron, muscle etc.) (Kristan, 2016). However, not every neuron has all those features. There are neurons which have no processes or do not use action potentials (Kristan, 2016). Thus, the key characteristics all neurons have in common are that they can communicate via specialized synaptic connections (Bucher and Anderson, 2015; Hobert et al., 2010). The evolution of the cell type neuron is still discussed, and it is not clear if neurons evolved only once or multiple times independently (Moroz et al., 2014; Moroz and Kohn, 2016; Ryan et al., 2013). However, since the phylogeny of the cell type neuron is not clear, here, the focus will be on the origin of some of the molecular neuronal features instead of elucidating the phylogenetic reconstruction.

If we take the three common associated characteristics with neurons – action potential, neurotransmitter, and synaptic molecules, – and elaborate on their origin, one finds that those characteristics are not exclusively neuron and metazoan-specific but can be already found in unicellular organisms and prokaryotes. Action potentials are one of the key features of a neuron, but it is not restricted to neurons even in metazoans. In *Cnidarian*, epithelia cells can transmit and generate action potentials which allows for example nerve-free *Hydra* to still contract due to mechanical stimuli (Bosch et al., 2017; Tran et al., 2017). In sponges, certain species can use electrical signaling without the presence of a neuron (Leys and Anderson, 2015; Leys and Mackie, 1997). However, the first organisms to use electrical signaling to communicate are prokaryotes (Bavaharan and Skilbeck, 2022; Benarroch and Asally, 2020; Leys and Anderson, 2015;

Shimomura et al., 2020; Vien and DeCaen, 2016). They already possessed voltage-gated ion channels and use electrical signaling at a single cell and biofilm level (Leys and Anderson, 2015; Leys and Mackie, 1997). Classical neurotransmitters such as glutamate and GABA can be found in microbial communities as well as their receptors to detect those molecules (Dagorn et al., 2013; Kuner et al., 2003; Roshchina, 2016). For example, in *Agrobacterium tumefaciens* GABA may modulate the level of quorum sensing signal (Chevrot et al., 2006). Last, classical synaptic molecules such as Homer and SNAREs can be already found forming fine cytoplasmatic bridges in their colonial life stages in choanoflagellates (Burkhardt and Sprecher, 2017; Fairclough et al., 2013). In conclusion, many components of the neuronal molecular characteristics were invented by microbes to communicate between conspecifics. Reassembly and cell type specialization may have led to the evolution of the cell type neuron, suggesting that fundamental structures are still working in a similar way as in prokaryotes. This might have implications for understanding the prominent crosstalk between the nervous system and the microbiota.

From diffuse nerve net to complex brain

Since there are multiple theories on how the nervous system evolved, we will focus here on one which also translates to our findings in **Chapter IV**. The evolution of complex structures as the brain is still an unresolved question. The answer to this question would greatly improve our understanding of how the brain works, which would have far-reaching implications. One potential scenario is proposed by Arendt *et al.* 2015 who propose that the evolution of complex nervous systems started with the integration of distinct integration centers which are already found in the Cnidarian phylum (Arendt et al., 2015). The predictions are mainly drawn from a comparative developmental biological point of view but are also partially supported by functional data. The authors indicated that the apical nervous system (ANS) and blastoporal nervous system (BNS) underwent evolutionary changes to emerge as centers of integration situated on opposite sides of the body. The ANS is responsible for controlling the overall physiology of the organism, settlement, and locomotion, while the BNS coordinates feeding movements. The integration centers are defined by their location in the gastrula-shaped ancestor (Arendt et al., 2015). In Bilaterian, the two centers merged and then formed the complex structures of the brain and the nerve chords (Fig. 3A). However, how exactly the transition from a rather diffuse structure in Cnidarian to

the Bilaterian brain happened is still highly speculative. To resolve this enigma, one needs to get a better understanding of the nervous systems prior to cephalization as they already can perform similar functions as the complex central nervous system in Bilaterian (Bosch et al., 2017). In **Chapter IV**, we approach this by deciphering the sub-functionalization of a simple nervous system.

***Hydra* – a model system for neurobiology**

The freshwater Cnidarian *Hydra vulgaris* is a unique model system that provides the prospect to address all the questions raised in the previous sections and gain a mechanistic understanding. First, because of its phylogenetic position, the common ancestor of Cnidarian and Bilaterian is supposed to have evolved one of the first nervous systems by using the same building blocks which makes it suitable for investigating evolutionarily conserved traits (Fig. 3A) (Jékely et al., 2015; Pisani et al., 2015). Second, it has a simple body plan consisting of two epithelia layers – the ecto- and the endoderm – which are separated by a matrix called mesoglea (Fig. 3B-C). Together they form the body column with a head and a basal foot (Fig. 3B). The lumen of the body column where the food is digested is also known as the gastric cavity. Third, it is colonized with a simple microbiota that sits on the outside in a mucus layer similar to the mucus structures in the gut of vertebrates (Fig. 3C) (Fraune and Bosch, 2007; Schröder and Bosch, 2016a). Fourth and last, the nervous system is rather simple compared to other model systems but still able to control complex behaviors (Fig. 3D-J) (Han et al., 2018; Siebert et al., 2019). In this chapter, the model system *Hydra vulgaris* will be reviewed and the open question highlighted.

Neuronal cell types

The first accepted confirmation of neurons in *Hydra* was made in 1964 which led to several investigations on the structure of the nervous system in *Hydra* (Fig. 3D) (Burnett and Diehl, 1964). The nervous system of *Hydra* was commonly assumed to be a diffuse and primitive nervous system but already in 1978 eleven different morphological neurons were described (Epp and Tardent, 1978; Tardent and Weber, 1976). Forty-two years later, this cell-type diversity could be confirmed based on molecular signatures (Siebert et al., 2019). The first attempt to describe the diversity of neurons was solely based on the morphology of dissociated cells using maceration (David, 1973; Epp and Tardent, 1978; Tardent

and Weber, 1976). Based on the observations, two different multipolar cells (M_1 , M_2), two symmetrical bipolars (B_1 , B_2) and two unipolar cells (U_1 , U_2) were found in the ecto- and endoderm. Asymmetrical bipolars (B_3 - B_7) were only found in the endoderm. The distribution of the neurons follows a U-shape where the highest densities were found in the head (including tentacles) and the foot (Bode et al., 1973). Overall, two main neuronal cell types were described: sensory neurons (bipolar and unipolar, Fig. 3D) and ganglion neurons (multipolar, Fig. 3D) (Tardent and Weber, 1976). Recently the diversity of neuronal cell types was revisited by investigating the molecular signatures of the different cell types in *Hydra* (Klimovich et al., 2020; Siebert et al., 2019). Based on this approach, nine distinct main neuronal populations were identified, while some could be divided further, which leads to twelve neuronal populations (Fig. 3E). From those populations, three were identified to be in the endoderm and the other nine populations were in the ectoderm. The distribution of neuronal cell types between ecto- and endoderm is not in consistency with the work from 1978. However, both works highlight that on the morphological and molecular level the nervous system seems to be more complex than just a diffuse nerve net.

Chemical and electrical synaptic structures

The identification of different neuronal populations (either based on morphology or molecular data) raised the question of how they are connected or to epitheliomuscular cells. With the first ultrastructural evidence of neurons, multiple other studies followed investigating the synaptic structures (Lentz and Barnett, 1965) as well as conducting molecular and genomic analysis (Chapman et al., 2010). On the molecular level, multiple gap junctions, innexins, were identified allowing electrical coupling between neurons and epithelia cells (Chapman et al., 2010). With the single cell data sets, neuronal populations were identified which can or are electrically coupled and which are not. All populations express innexins except for population N6 (Ec4A/B) and N7 (Ec2) while there is no such clear distinction seen with genes associated with chemical synapsis (Klimovich et al., 2020). However, electron microscopy revealed both chemical and electrical synapsis decades earlier, but here assigning a neuron to one of the different neuronal populations is highly speculative. Therefore, the body of work on the ultrastructure of *Hydras* nervous system is a highlight of all potential structures that can be found in neurons of *Hydra* but not a systematic approach to link molecular and structural data.

Investigation of the nervous system of *Hydra* on an ultrastructural level defined various modes of synaptic connections. One of the first studies identified polarized chemical synaptic structures in neurons that contain dense core vesicles filled with neuropeptides (Koizumi et al., 1989; Westfall et al., 1971). Those chemical connections can be found between neurons (sensory-sensory, sensory-ganglion, ganglion-ganglion), neuro-epitheliomuscular cells and neuro-nematocytes (Westfall and Kinnamon, 1984). The synaptic structures can be reciprocal synapsis (between sensory cells, sensory-ganglion and ganglion-ganglion) or two-way chemical synapsis (only between ganglion-ganglion cells and ganglion-sensory cells). Based on serial sectioning and tracing there were also either two-cell pathways, which are formed by direct sensory-nematocyte/-epitheliomuscular cells, and three-cell pathways where a ganglion cell is interposed between sensory and epitheliomuscular cells (Westfall and Kinnamon, 1984). In addition, ganglion cells can form axo-axo-epitheliomuscular synapsis. Interestingly, a high percentage of neurons (ganglion cells in particular) in the head and foot have stereo ciliary complexes (between 84% and 96%)(Kinnamon and Westfall, 1981; Westfall and Epp, 1985). Further, in the head ganglion cells are often found in groups since 64 neuronal clusters with more than three neurons were identified (5 neurons on average per cluster, maximum of eleven)(Kinnamon and Westfall, 1981). In summary synaptic connections in *Hydra* are characterized by dense core vesicles which often form reciprocal structures.

Interestingly, while investigating the ultrastructural anatomy of *Hydras* neurons, multifunctional properties were identified based on cell structures (Westfall, 1973; Westfall and Kinnamon, 1978a). Sensory and ganglion cells seem to be multifunctional and were described as sensory-motor-interneuron. The ganglion neurons have a cilium, as a characteristic of a sensory cell, they both have contact with epitheliomuscular cells, a characteristic of a motor neuron, and they both have synaptic connections to other neurons, a characteristic of an interneuron (Kinnamon and Westfall, 1981; Westfall et al., 1991; Westfall and Kinnamon, 1978b). The sensory cells can have complicated synaptic connections with each other and the surrounding epitheliomuscular cells as they can reach a ratio of one epithelia cell to up to four sensory cells in the apical region of the head/hypostome (Westfall and Kinnamon, 1984). Most of the work mentioned focused on chemical synapsis, but adjacent electrical and chemical synapses were observed as well by the same neuron to an epitheliomuscular cells, multiple gap-junctions between neurons, and even neurons which have both chemical and

electrical synapsis (Westfall et al., 1980). All those features make the nervous system of *Hydra* an interesting neurobiology model system. To summarize, *Hydra's* neurons seem to be multifunctional since they have characteristics of sensory, inter-, and motor neurons in one neuronal cell and can have both electrical and chemical synapses in the same neuron, suggesting a highly flexible nervous system where a neuron can overtake multiple roles at once. However, the functional significance of the observed structures and arrangements is still not clear.

The behavioral pattern in *Hydra*

Even though *Hydra* has a rather simple body plan and no central nervous system structure, it can already perform complex behavioral patterns (Fig. 3J). The behavior of *Hydra* can be divided into spontaneous and stimulus-triggered movements which were initially documented by Trembley (1744) (Trembley, 1744). Spontaneous actions encompass contraction (Passano and McCullough, 1964) as well as locomotion including somersaulting and inchworming (Mackie, 2013). However, both behaviors can be triggered by light and mechanical stimuli such as pinching (L. M. Passano and McCullough, 1964; L M Passano and McCullough, 1964; Passano and McCullough, 1965, 1963, 1962). Contraction behavior can be triggered by light such as that in the dark/night the contraction frequency decreases and increases during light/day (Kanaya et al., 2019; Passano and McCullough, 1964). The starvation state as well as other behaviors (feeding behavior) can affect or inhibit contractions (Rushforth, 1965). In a state dependent manner, *Hydra* is moving via locomotion towards a light-source which contains the blue spectrum (400-450nm)(Kim and Robinson, 2023; Tardent et al., 1976). On the other hand, the classical stimulus evoked behavior is the feeding behavior in *Hydra* (Lenhoff, 1961; Loomis, 1955). Food-related stimuli elicit a stereotypical feeding behavior that consists of three distinctive stages: tentacle writhing, tentacle ball formation and mouth opening (Koizumi et al., 1983; Lenhoff, 1961; Loomis, 1955). This behavior is crucial to the survival of *Hydra*. Furthermore, feeding behavior can be robustly induced by small molecules such as glutathione and S-methyl-glutathione (GSH, more later) (Loomis, 1955). Apart from the relatively complex actions, *Hydra* also exhibits fewer complex movements in various body parts and magnitudes, such as flexion, autonomous tentacle motion, as well as radial and longitudinal contractions (Han et al., 2018). To show that a neuronal control underlies all those behaviors, nerve free *Hydra*

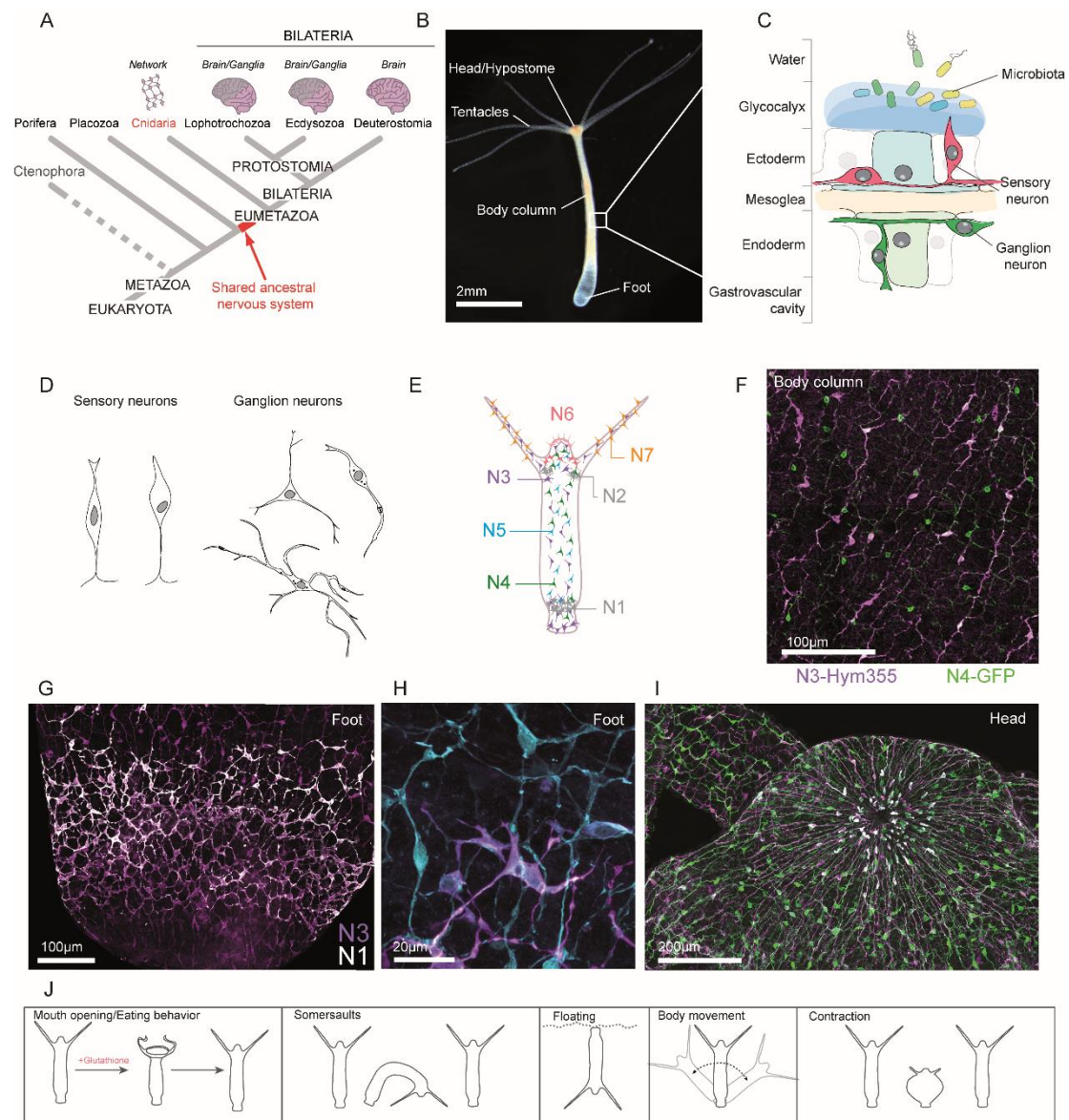


Figure 3. *Hydra* as a model system for neuroscience. **A.** Phylogenetic tree which highlights the evolution of the nervous system and transition from a nerve net to a centralized nervous system (modified from (Bosch et al. 2017)). **B.** *Hydra*'s body plan consisting of a head with tentacles, body column, and a foot. **C.** Schematic of the tissue organization and localization of the microbiota. **D.** Drawings of neurons isolated from *Hydra* by A. Burnett 1964, separating into sensory and ganglion morphotypes (Burnett and Diehl, 1964). **E.** Schematic drawing of all major neuronal cell populations identified by single-cell analysis (modified from (Klimovich et al., 2020)). **F-I.** Immunohistochemistry of *Hydra* visualizing different neuronal population at different body locations. **J.** The major behavioral pattern of *Hydra*.

were used (i-cell lineage free). Work on nerve free *Hydra* revealed that all complex behaviors (contractions, locomotion, feeding) are controlled by the interstitial cell lineage and most likely by neurons (Campbell et al., 1976; Tran et al., 2017). In summary, *Hydra* exhibits an already complex repertoire of movements with different degrees of complexity despite the simple nervous system.

Neuronal circuits: electrophysiology and calcium imaging

The major current focus was and still is on the contraction behavior of *Hydra*, which led to studies investigating its underlying neuronal circuit and activity. Even though there was pioneer work analyzing the activity of the whole animal little is known about other neuronal circuits underlying behaviors besides contractions. Electrophysiological analysis 40 years ago identified different electrical activity patterns associated with different behaviors in *Hydra* without determining neurons as their source (Passano and McCullough, 1965, 1964, 1964, 1962; Rushforth, 1971, 1965; Norman B Rushforth and Hofman, 1972). More recently, the nervous system of *Hydra* was characterized in its activity pattern using calcium imaging tools which identified a non-overlapping activity pattern aligning with the electrophysiological data from 40 years ago (Dupre and Yuste, 2017).

In both approaches - the electrophysiological and calcium imaging approaches - intrinsic activated spiking activity was detected. In the electrophysiological studies, two main pacemaker systems were identified: the contraction burst (CB, ~6-10 spikes, speed 15cm/sec, originates from sub-hypostome) and rhythmic potentials (RP, every ~13±0.1sec, 4cm/sec, <0.4mV, originates from bottom)(Passano and McCullough, 1964, 1963, 1962). Additionally, tentacle pulses, which happened occasionally, and locomotor contraction bursts (faster and more spikes than CBs), which happened before retraction of the foot (Kass-Simon et al., 2003; L. M. Passano and McCullough, 1964). However, the origin of the signal could not be determined, and the question remained whether neurons are the source of it. In the calcium imaging analysis, the source was pinned down to neurons while the main pacemaker systems were identified as well (CB and RP) but the RPs were divided into a network in the ectodermal RP1 and endodermal RP2 (Dupre and Yuste, 2017). Further, they identified a sub-tentacle network which was located underneath the base of the tentacles. This nicely shows how the two independent approaches identified similar activity patterns of *Hydra's* nervous system even though using different methods.

In addition, both approaches started to align their identified activity patterns with behaviors which was a first attempt to identify neuronal circuits in *Hydra*. While identifying the two different neuronal networks, it has been observed that CBs are associated with contractions while RP (RP1) has been associated with the elongation of the body column(Passano and McCullough, 1963). This

suggests an antagonistic activity. Based on electrophysiological measurements, RPs increase after a CB and decrease before a CB in their spiking activity (Passano and McCullough, 1963). Further, when analyzing the spiking frequency for over an hour, a high frequency of RPs was associated with a reduced CBs occurrence (McCullough, 1965). A negative relationship was also observed while using calcium imaging. Both systems are also sensible to light and mechanical stimuli as well as nutritional state. In the case of CBs, they are inhibited during eating behavior whereas RPs show no drastic change (Passano and McCullough, 1964, 1962). The previously mentioned discoveries concerning the understanding of the evolutionary conserved properties of a nervous system effectively highlight the fact that diffuse pacemaker activity is a fundamental and necessary characteristic of the nervous system.

The accessibility of calcium imaging and the ability to record the whole animal together with the development of analytical tools (Han et al., 2018; Lagache et al., 2021) led to a series of studies that focused on the integration of environmental information into the contraction burst and rhythmic potential 1 circuit. The contraction burst circuits have been associated with osmoregulation of the animals since its activity decreases in hyper-osmolar media and increases in hypo-osmolar media. The neuronal activity reflected the increase in contraction frequencies (Yamamoto and Yuste, 2020a). The rhythmic potential 1 network seems to be unresponsive to changed osmolarity. Another work provides evidence that the integration of mechanical stimuli depends on two different networks, one in the oral and one in the aboral region (Badhiwala et al., 2021). Within the same line, it has also been shown that contraction burst neurons change their spiking frequency depending on the temperature (Tzouanas et al., 2021). However, none of these studies provide a mechanistic understanding of how the neurons sense environmental changes. Further, the question remains if neurons are the first responding cell type or rather the epithelia cells which then affect the neuronal circuits downstream.

Now, with the activity and single cell molecular information, the link between both data sets must be made to deepen the mechanistic understanding of the different circuits and neuronal populations. However, a systematic approach to connect those data is still missing. In a recent study, that focusses on the somersaulting behavior of *Hydra*, the molecular information was used to identify and understand the rhythmic potential 1 network with the N3/Ec3 population

(Yamamoto and Yuste, 2023). A burst of spikes was known to be associated with the detachment of the foot since the electrophysiological studies, but it was thought to be a separate network from the rhythmic potential (Passano and McCullough, 1964). Here, they showed that N3 is associated with somersaulting by increasing in spiking frequency prior to the detachment of the foot, while also playing a role in the elongation behavior. In addition, they could provide further proof by ablation and activation experiments (intrinsic property to respond to blue light of N3) for the involvement in the somersaulting behavior. This behavior is under the control of a neuropeptide expressed in N3 neurons, Hym-248, which can induce somersaulting behavior (Yamamoto and Yuste, 2023). An interesting observation is also that one neuronal population, N3/RP1 is responsible for two different behaviors, elongation and somersaulting, and exhibits different spiking patterns while doing so. In summary, this study emphasizes the power of linking molecular information with activity data to decipher a neuronal circuit underlying behavior in *Hydra*. Additionally, it highlights the necessity of connecting neuronal activity with molecular information to resolve the mechanisms that underlie a circuit.

The effect of neurotransmitters

Hydra uses classical neurotransmitters to modulate various aspects of its behavioral repertoire. Recent single-cell analysis of *Hydras* nervous system has shown that neurons express receptors for GABA, glutamate, glycine, dopamine, and acetylcholine (Klimovich et al., 2020). Pharmacological interference experiments from more than 20 years ago support these findings with functional data (Bosch et al., 2017; Kass-Simon and Pierobon, 2007). Historically caused, the main read outs to investigate the role of neurotransmitters in *Hydra* were contraction bursts, rhythmic potential and feeding behavior. Further investigations will be needed to fully explore the effect of neurotransmitters on other behavioral patterns.

Contraction bursts are modulated by the inhibitory neurotransmitter GABA and the excitatory neurotransmitter acetylcholine and glutamate. GABA decreased the occurrence of contraction bursts most likely via the (ionotropic) GABA_a receptor (Kass-Simon et al., 2003). Glutamate on the other hand increases contraction bursts by low concentration probably via an AMPA receptor. Blocking acetylcholine receptors with nicotinic antagonists and serotonergic inhibitors

(methysergide) decreased the contraction burst pattern by reducing the number of pulses per burst and the number of bursts per hour (G. Kass-Simon and Passano, 1978). Follow up studies showed that the effect on the contraction burst system most likely happens over a nicotinic receptor (nAChR) since the antagonist of nAChR tubocurarine (DTC) drastically reduced spontaneous body contractions (Klimovich et al., 2020). In summary, the contraction burst pacemaker system is controlled by classical excitatory and inhibitory neurotransmitters.

Rhythmic potentials are modulated in a similar way as the contraction bursts by glutamate and GABA but inhibited by acetylcholine and glycine. The same modulatory effects with glutamate and GABA were also observed for the rhythmic potentials (Kass-Simon et al., 2003). GABA reduces the frequency and glutamate increases the frequency of rhythmic potentials. Activation of the glycine receptor GlyR via glycine and taurine decreased the frequency of rhythmic potential (Ruggieri et al., 2004). Disabling the receptor via strychnine did not affect rhythmic potentials but decreased contraction bursts. Nicotinic antagonists and serotonergic inhibitors (methysergide) increased the frequency of rhythmic potentials (G Kass-Simon and Passano, 1978). In contrast, atropine (anticholinergic agent) decreased rhythmic potentials while increasing contraction bursts (G Kass-Simon and Passano, 1978; Ruggieri et al., 2004). To summarize, rhythmic potentials and contraction bursts are modulated by similar neurotransmitters. However, there are also clearly opposing modulating systems.

Besides the contractile behavior and the modulation of rhythmic potentials and contraction bursts, neurotransmitter seem to also play a role in the modulation of nematocyte discharge (Kass-Simon and Scappaticci, 2004; Scappaticci and Kass-Simon, 2008). GABA and glutamate increase the sensitivity of two different nematocyte cell populations. On one hand, GABA seems to modulate (increases) the discharge of the desmonemes nematocytes most likely via metabotropic GABA receptors. This was shown by the metabotropic antagonists phaclofen that inhibits their discharge (Kass-Simon and Scappaticci, 2004). On the other hand, glutamate modulates the sensitivity (increases) of the stenoteles nematocytes to mechanical stimuli probably via the NMDA receptor given that NMDA has a similar effect (Scappaticci and Kass-Simon, 2008).

To conclude this chapter, a more recent study also showed that *Hydra* has a sleep-like behavior (reduced activity) which can be induced by GABA as well as by dopamine (Kanaya et al., 2020). What highlights the interesting role of neurotransmitters in Cnidarian, but more work is needed to understand how the mechanisms underlying those behaviors work and where the neurotransmitters are synthesized. Overall, all the mentioned studies work with pharmacological interference approaches, and a clear localization, or a genetic manipulation of the respective receptor or transporter is still missing. Furthermore, the enzymes producing the different neurotransmitters are also unexplored and a colocalization with neuronal populations is missing.

The feeding response

One of the most complex behavioral patterns in *Hydra* is the feeding response which requires a sequence of coordinated movements and so far, the underlying neuronal circuit has not been revealed (Fig. 3J). The feeding response consists of a complex series of consecutive movements (Koizumi et al., 1983; Norman B. Rushforth and Hofman, 1972; Trembley, 1744). First, the prey (small Crustaceans) is captured by the tentacles and immobilized by the nematocytes which penetrate the cuticula. Upon prey capture, the tentacles start to move towards the head/hypothome and push it against the hypostome which leads to the mouth opening. The mouth ingests the prey with the help of the tentacles which push it inside. As soon as the prey is inside, the mouth closes again and the tentacles relax (Norman B. Rushforth and Hofman, 1972). The first description of this behavior was given by Trembley in 1744 (Trembley, 1744). Since then, the search for the molecule which can induce this fascinating behavior has been started.

Reduced glutathione can induce the feeding response via an unknown receptor which is located in the tentacles and head of *Hydra*. For the first time, Loomis showed in 1955 that shrimp-extract and in particular reduced glutathione (not oxidized) can elicit the feeding behavior (Loomis, 1955). Shrimp-extract and later nematocytes were identified as the source of glutathione (Burnett et al., 1963; Loomis, 1955). Further, the work showed that the effect of glutathione depends on the concentration and on the feeding state (Loomis, 1955). For the feeding response, glutathione needs to be continuously around, and the response stops by itself after 36 ± 2.95 min (Lenhoff, 1961). The time an animal needs to

respond to the presence of GSH is around 0.43-0.6 min. Interestingly, the feeding response is not an all-or-none response since the duration of the response is concentration dependent (Lenhoff, 1961). After an induced feeding response an animal needs a recovery period before responding again which can take up to 48h. Based on multiple observations, there was a prediction of a receptor sensing glutathione which is most likely localized around the mouth and tentacles (Lenhoff, 1961). In addition, a mechanism was proposed that prevents another response immediately after a finished sequence of the feeding behavior. However, exposure to live shrimp still induces a feeding response even if the excessive glutathione is still around (Burnett et al., 1963). In contrast, well-fed animals did not respond anymore in a feeding state-dependent manner which led to the suggestion that an internal state controls the eating behavior (Koizumi and Maeda, 1981). In summary, reduced glutathione is capable of provoking the feeding response through an unidentified receptor that is situated in the tentacles and head region of *Hydra*.

The feeding behavior-inducing effect is specific to glutathione, but glutathione is not solely present in the prey. Trypsin, hyaluronidase, and lactic acid can also induce the feeding response and induce nematocyte discharge (Burnett et al., 1963). Interestingly, the ability to induce the feeding behavior by those molecules was abolished by removal of tentacles while reduced glutathione still induces the behavior. Inducing nematocyte discharge in truncated tentacles and transferring the medium to normal polyps also induced the eating behavior (Burnett et al., 1963). The proposed mechanism is that nematocytes by themselves contain glutathione which they release during discharge and together with the prey induce the feeding response. Therefore, the feeding response can be elicited by reduced glutathione from either the prey or the nematocytes as well as by other chemicals in a tentacle dependent way.

Hydra possess a receptor for glutathione which is expressed by cells of the interstitial lineage. An initial observation and personal communication suggested that nerve-free animals did not show any feeding behavior (Marcum and Campbell, 1978). Therefore, nerve free animals need to be force-fed to maintain them over longer periods of time (Tran et al., 2017). More evidence was given by doing glutathione binding assays with *Hydra* tissue. Removing nematocytes by propargylglycine led to a reduced binding of glutathione. Further, this reduced binding was dramatically amplified when all interstitial cells were removed

(Hufnagel et al., 1985; Venturini, 1987). In addition, glutathione was binding to membrane fractions in a specific and non-replaceable manner (Grosvenor et al., 1992). However, even though there is accumulating evidence of a specific receptor, the location and molecular identity have not yet been identified.

The main neurotransmitters involved in the feeding response are GABA and glutamate which have opposite effects. GABA prolongs the feeding behavior, in particular the mouth opening duration, by 25% via ionotropic GABA_A receptors (Concas et al., 1998; Pierobon et al., 2004b, 1995). The response time to glutathione was not affected and animals responded as fast as the control. In addition, glycine, taurine, and β -alanine had a similar effect, but glycine rather works via glycine (GlyR) and NMDA receptors (Pierobon et al., 2001). In contrast, glutamate inhibits the mouth opening in a glutathione-to-glutamate ratio dependent way (Lenhoff, 1961). The same effect was also seen with AMPA and kainate whereas NMDA, a glutamate receptor agonist, only reduced the response duration and did not inhibit the behavior (Pierobon et al., 2004b, 2004a). Further examination was conducted to investigate classical neurotransmitters and their involvement in the regulation of feeding behavior. Based on their observation, dopamine increases the duration of the mouth opening whereas endocannabinoid, anandamide, accelerates the mouth closing (De Petrocellis et al., 1999; Venturini and Carolei, 1992). Nevertheless, the identification of the specific cellular subtype that detects and reacts to the neurotransmitter remains elusive in all of the aforementioned investigations.

In summary, the feeding response is an essential behavior for the survival of organisms involving intricate movements instigated by both prey and glutathione, originating from endogenous or exogenous sources. The feeding response depends on the interstitial cell line, namely neurons, however, the underlying neural circuitry responsible for this phenomenon remains elusive, as does the receptor that recognizes glutathione. The modulation and inhibition of the feeding response can be attributed to classical neurotransmitters such as GABA and glutamate.

***Hydra* – a simple metaorganism**

The microbiota of *Hydra* consists of a rather simple community with a few dominant bacterial species which sits on the outside in a mucus-like structure, glycocalyx (Bosch, 2014, 2013; Fraune and Bosch, 2007). Those features make it a great system for investigating host-microbe interactions. On one side because of the simplicity of the bacterial community. On the other side because of the easy accessibility and possibility to manipulate.

The microbiota of *Hydra* is shaped predominantly by environmental factors and to a lesser extent by host factors. Nevertheless, there are still similarities between laboratory animals and wild-caught animals as well as differences between different *Hydra* species. Therefore, *Hydra vulgaris* and *Hydra oligactis* have a distinct microbial composition which is mainly based on the different abundance of β -proteobacteria and α -proteobacteria (Fraune and Bosch, 2007). *Hydra vulgaris*' main class of bacteria are β -proteobacteria (dominant family: *Burkholderiaceae*) whereas *Hydra oligactis*' main class of bacteria are α -proteobacteria (dominant order: *Rickettsiales*). Expanding the number of *Hydra* species highlighted that the differences still hold partially true (Franzenburg et al., 2013b). Interestingly, *Hydra vulgaris* AEP rather clusters together with *H. carnea* and *H. magnipapillata* instead of *Hydra vulgaris*. However, during the analysis of the bacterial communities, reads of a *Spirochaetia* (*Turneriella parva*) were removed from *Hydra vulgaris* AEP which potentially introduced a bias in the analysis and interpretation (Franzenburg et al., 2013b). Further, in later studies the dominant order *Rickettsiales* of *H. oligactis* was lost, suggesting a more flexible community composition than initially suggested (Mortzfeld et al., 2018). In a more recent study, environmental factors were shown to drive the diversity of the host associated communities more strongly than host factors (Taubenheim et al., 2022). Here, different *Hydra* populations in the wild were investigated under different environmental conditions (Taubenheim et al., 2022). In conclusion, similar bacteria can be detected in association with *Hydra vulgaris* such as *Curvibacter* but the abundance and the diversity of the community can vary depending on the environmental situation.

Hydra controls the associated microbial community via neurons and by using the conserved Toll-like receptor and MyD88 signaling pathway as well as antimicrobial peptides and potentially other innate immune pathways (Bosch, 2014; Klimovich and Bosch, 2018). Single-cell analysis revealed that neurons of

Hydra express many genes associated with the innate immune system which suggests a role in detection and interaction with the microbiota (Klimovich et al., 2020). Among the many genes were TLR/MyD88 associated genes as well different antimicrobial peptides expressed in neurons. Interestingly, many of those observations have already been experimentally proven before the availability of the single cell atlas. For MyD88, it has been shown that Toll-like receptors (TLR) and MyD88 play a mild role in regulating a species-specific recolonization (Franzenburg et al., 2012). In MyD88 knock-down animals many taxonomic restricted genes are (*Hydra* specific without annotation) differentially expressed and the recolonization by bacteria is delayed (Franzenburg et al., 2012). Furthermore, the role of neurons was elegantly shown by following interstitial stem cell lineage free (nerve free) animals over time and analyzing the microbial community (Fraune et al., 2009). The interstitial stem cell lineage was removed by a heat shock which allows the ablation of the interstitial stem cell in the naturally occurring mutant *H. magnipapillata* sf1. In the absence of neurons and gland cells, the microbial community changed significantly by a reduced abundance of β -Proteobacteria (Rhodoferax) and an increased abundance of Bacteroidetes (Fraune et al., 2009). Further evidence for the role of neurons has been given by showing that a neuropeptide had antimicrobial properties against the main colonizer *Curvibacter* (Augustin et al., 2017). The antimicrobial peptide, NDA-1, was expressed specifically in neurons in the head, body, and foot while missing in the tentacles. Interestingly, the abundance of *Curvibacter* in the tentacles is found to be 10-fold higher in comparison to the other regions of the body, thereby raising a question as to whether neurons are accountable for the spatial distribution of bacteria (Augustin et al., 2017). In NDA-1 knock-down animals the abundance of *Curvibacter* increased 2-fold in the body and foot region. To summarize, the neural regulation and utilization of Toll-like receptor and MyD88 signaling pathway, along with antimicrobial peptides and other innate immune pathways, play a crucial role in governing the microbial community associated with *Hydra*.

Community assembly in *Hydra* is based on host factors, such as quorum quenching and antimicrobial peptides which lead to frequency-dependent interactions. Starting from the embryogenesis over to hatchling till the adulthood of *Hydra* the colonization pattern highlighted an interplay between host-derived factors, the environment, and frequency dependent interactions (Franzenburg et al., 2013a). Among the host factors, it has been shown that *Hydra* can modulate

the behavior of its bacterial symbionts by modifying quorum sensing molecules using an oxidoreductase leading to increased colonization (Pietschke et al., 2017). Furthermore, antimicrobial peptides such as arminins or other antimicrobial peptides controlled by the transcription factor Foxo, affect the reassembly of the species-specific microbiota (Franzenburg et al., 2013b; Mortzfeld et al., 2018). In addition, the community stability in *Hydra* depends on bacteria-bacteria interactions and host factors. *Curvibacter* domination of the community and its coexistence with *Duganella* is only possible because of the host (Deines et al., 2020). *Duganella* is outcompeting *Curvibacter* when the factor host is removed from the equation. In conclusion, the model system *Hydra* provides a unique playground to study community dynamics while considering host, environment, and bacteria-bacteria interactions.

The fact that *Hydra* has an associated microbial community which is rather simple is well established but what are the benefits of having the symbionts and why does *Hydra* invest in regulating the community. On one hand, one of the most important traits is the protection against other pathogenic microbes such as the fungi *Fusarium sp.* The bacterial community protects against the fungal infection in a community dependent manner and not based on the trait of a single bacterium (Fraune et al., 2015). Another example is the tissue disturbance by the interaction of two bacteria, a *Spirochaetia* and a *Pseudomonas*, which only occurs when both are present (Rathje et al., 2020). On the other hand, bacteria can have modulatory effects on the behavior and development of the host. The frequency of the spontaneous body contraction behavior of *Hydra* is reduced to 60% compared to the control when there are no bacteria (Murillo-Rincon et al., 2017). The effect can be partially reversed by recolonization with the bacterial community, indicating either that part of the effect is due to a failed community assembly or another unknown factor. Another work shows that bacteria can influence taxonomically restricted genes which further affect Wnt-signaling and lead to a softening of the head regulation (Taubenheim et al., 2020). Overall, the mentioned examples highlight the modulatory effects and importance of the associated microbial community on the well-being of *Hydra*.

Hydra with its long history of behavioral and neurobiological work as well as its associated natural microbiota offer a unique opportunity to address questions about the conserved ways of interaction between neurons and microbes. The well described behavioral pattern such as the feeding response, the insights in

neurotransmitter modulation paired with the new molecular data sets and the development of new methods on host side as well as on symbiont side make the time perfect to dive into mechanisms underlying the nervous system and the interplay with the environment.

***Hydra* as a chance for a mechanistic understanding**

Metazoan evolution unfolded amidst a microbial world, profoundly shaping eukaryotic development. Symbiotic interactions extended across organisms, modulating developmental trajectories, enhancing fitness, and influencing behavior. Metazoan evolution and microbial dynamics are interwoven, yielding intricate symbiotic connections that continue to captivate both evolutionary and microbiological exploration. Nevertheless, while the field is nearly exploding in publications, many papers overinterpret their results while failing to resolve the underlying mechanism of the interaction. One such field is the study of the interaction between the nervous system and microbes and the impact of the microbial molecules on behavior and the central nervous system. Even though the field has made major advancements in the last decade, many fundamental questions have not been solved yet. Among those questions are: how do animals integrate microbial signals into neuronal circuits and respond almost immediately? How are microbial signals sensed and translated or transported to distal tissues such as the brain? Are there universal principles of mechanisms of how hosts detect and integrate microbial molecules?

To explore such fundamental questions, history has shown that doing comparative studies among a high variety of model organisms yield an understanding of groundbreaking mechanisms (Bosch et al., 2017). Especially in neuroscience, the exploration of organisms with simpler nervous systems enabled insights into the workings of a brain and opened an emerging field looking into the evolution of the nervous system (Arendt, 2018; Arendt et al., 2015; Bosch et al., 2017; Dupre and Yuste, 2017; Weissbourd et al., 2021). Taking the simplicity of a nervous system of an early branching metazoan and also including the environment – such as the microbial world – might be a powerful approach to understand the fundamental functions of a nervous system and neuro-microbe interaction. Such an exemplary system is *Hydra*, which falls under the phylum of *Cnidarian*. It is proposed that this organism shares a common ancestor with *Bilaterian*, one of the earliest ones, which already possessed a neural network. *Hydra* already has a long history of work focusing on neurobiology and symbiotic

bacteria. However, in recent years, many new tools have been developed for exploring *Hydras* behavior and underlying neuronal circuits which currently makes it a promising field of research.

However, despite all the work on the nervous system and the interaction of *Hydra* and the associated microbes, many questions remain unanswered. On one hand, the neuronal circuits of complex behaviors such as feeding behavior are unknown even though many predictions have been made (Pierobon, 2015, 2012). This is particularly interesting because here a coordination of movements has to be done without a central nervous system, which can give new insights into nervous system functions. On the other hand, neurons produce neuropeptides and are responsible for shaping the microbial community (Augustin et al., 2017; Franzenburg et al., 2013b; Fraune et al., 2009). However, there is no evidence that microbes influence neuronal activity directly and thereby behavior so far. In the work on spontaneous contractions, an effect of microbes on the behavior has been shown but the link to neuronal activity or neurons *per se* is missing (Murillo-Rincon et al., 2017). Furthermore, why bacteria stimulate spontaneous body contractions and create a dynamic environment has not been explained and is mind boggling. In addition, there is no knowledge if neurons do respond also on a transcriptional level to the presence of bacteria. All those questions raised, can be answered and further explored with the development of new methods for *Hydra* such as calcium imaging (Dupre and Yuste, 2017).

Objectives and overview of this thesis.

In this thesis, I aim to explore the effect of symbiotic bacteria on the behavior of *Hydra* and the coordination of complex behaviors with a simple nervous system. I think this work will advance the understanding of conserved functions of the nervous system and bacteria-neuron interactions. The acquired insights will hopefully inspire to explore unsolved questions in more complex systems with a new perspective gained by this work.

Chapter II aims to investigate which effect spontaneous body contractions have on the microbial community and if we can understand the “why” of this phenomenon.

Chapter III will focus in a first step on the underlying neuronal circuitry of the eating/feeding behavior of *Hydra*. In the second step it will explore the impact of symbiotic bacteria on the identified circuit and decipher the underlying mechanism.

Chapter IV will focus on the evolution of the enteric nervous and central nervous system and how they can be found in an organism without a brain.

Chapter I:

Neurons interact with the microbiome: an evolutionary-informed perspective.

Neuroforum

Review article

Christoph Giez, Alexander Klimovich and Thomas C. G. Bosch*

*Corresponding author: Thomas C. G. Bosch, Christian-Albrechts-Universität zu Kiel, Kiel, Germany, E-mail: tbosch@zoologie.uni-kiel.de. Christoph Giez and Alexander Klimovich, Christian-Albrechts-Universität zu Kiel, Kiel, Germany, E-mail: cgiez@zoologie.uni-kiel.de

Apr 01, 2021 - DOI: <https://doi.org/10.1515/nf-2021-0003>

Abstract:

Animals have evolved within the framework of microbes and are constantly exposed to diverse microbiota. Microbes colonize most, if not all, animal epithelia and influence the activity of many organs, including the nervous system. Therefore, any consideration on nervous system development and function in the absence of the recognition of microbes will be incomplete. Here, we review the current knowledge on the nervous systems of *Hydra* and its role in the host–microbiome communication. We show that recent advances in molecular and imaging methods are allowing a comprehensive understanding of the capacity of such a seemingly simple nervous system in the context of the metaorganism. We propose that the development, function and evolution of neural circuits must be considered in the context of host–microbe interactions and present *Hydra* as a strategic model system with great basic and translational relevance for neuroscience.

Keywords: antimicrobial peptides; evolution; *Hydra*; metaorganism; nerve nets.

Introduction: neurons interact with the microbiome

Nervous systems allow animals to perceive signals from the environment and to respond to them. Novel technologies including sequencing and imaging has unveiled that an important component of the immediate environment of many if not all organisms is a coevolved and resident microbiota (Baquero and Nombela, 2012; Blaser et al., 2016). Microbes shaped the Earth since billions of years before the “invention” of any nervous system, and they continue to shape the Earth. In animals, including humans, microbes are colonizing all epithelia. Animal evolution therefore appears intimately linked to the presence of microbes. Considering organisms as “metaorganisms” or “holobionts” (Bosch and Mcfall-Ngai, 2011, 2021) incorporates this impact of the microbial world and attempts to drive the neurosciences to the next level of enquiry.

Previous studies on germ-free (GF) animals, i.e., organisms treated with broad-spectrum antibiotics to completely eliminate their microbes or animals born and raised in absolutely axenic conditions, show that specific microbiota can impact central nervous system (CNS) physiology and neurochemistry (Sharon et al., 2016). GF mice that are devoid of associated microflora exhibit neurological deficiencies in learning, memory, recognition, and emotional behaviours (Foster et al., 2017; Gareau, 2014). In developing mice embryos, proliferation of neurons in the dorsal hippocampus is greater in GF mice than in conventionalized mice. However, post-weaning exposure of GF mice to microbial clones did not influence neurogenesis, suggesting that neuronal growth is stimulated by microbiota at an early stage (Ogbonnaya et al., 2015).

It is now well established that microbiota not only affect the CNS but also influence the enteric nervous system (Cryan et al., 2019). For example, mice kept under sterile conditions show reduced excitability of enteric neurons, resulting in slower gut peristalsis and protracted intestinal transit time. Interestingly, colonization of adult GF mice with microbes taken from the intestine of animals kept under standard laboratory conditions restores the peristaltic activity to normal levels (De Vadder et al., 2018; Obata et al., 2020), indicating that the gut monitors continuously the contents of the lumen and responds to potential changes. It also has been shown that intestinal microbiota directly affects transcriptional programs



Figure 1: The nervous system of Hydra is a diffuse nerve net. Here, a population of neurons expressing a Hydra-specific Hym355 neuropeptide (green) and muscular fibers of epithelial cells (magenta) are visualized in a juvenile polyp.

in enteric neurons (Obata et al., 2020). These observations are medically relevant because changes in the composition of microbiota (known as dysbiosis) are also observed in common gastrointestinal disorders, including those characterized by changes in intestinal motility, such as irritable bowel syndrome (De Palma et al., 2017).

Most if not all of these studies were done in laboratory mice. How relevant are they for our understanding of neurobiology in general? From our evolutionary point of view, the discovery of an interaction of microbes with the mouse nervous system(s) comes as no surprise. Below we show that similar interactions between the microbiota and the neurons are in place already at the beginning of animal evolution, suggesting that animal–bacteria interactions are likely as ancient as animals themselves.

***Hydra*, a model to study neuron– microbiome interactions**

Hydra, a member of the animal phylum Cnidaria, is close to the earliest animals in evolution that had nervous systems (Figures 1, 2A and B). Cnidaria occupy a

sister phylogenetic position to bilaterians. The fact that they encode most of the gene families found in bilaterians makes them a suitable model to study the “genetic tool kit” present in the cnidarian–bilaterian ancestor. This includes their repertoire of ion channels, synaptic proteins, small neurotransmitters, receptors and the corresponding processing machinery. In *Hydra*’s simple tube-like body structure, the single layer of ectodermal epithelial cells covered by a multilayered glycocalyx represents a physical barrier toward the environment, whereas a single layer of endodermal epithelial cells separates the body from the content of the gastric cavity. Very much to our surprise, and made possible by novel sequencing technologies, we discovered very early that *Hydra*’s ectodermal epithelial surface is densely colonized by a stable multispecies bacterial community (Fraune and Bosch, 2007) (Figure 2C). Since that discovery, *Hydra* has proven itself as an excellent model for studying host–microbe interactions and how metaorganisms function in vivo (Bosch, 2013, 2014; Klimovich and Bosch, 2018; Schröder and Bosch, 2016). The presence and composition of *Hydra*’s microbiota is critical for the tissue homeostasis and health of the polyps (Rathje et al., 2020). Remarkably, each *Hydra* species supports long-term associations with a different set of bacteria, suggesting that the host imposes specific selection pressure onto its microbiome (Franzenburg et al., 2013; Fraune and Bosch, 2007). Both, ecto- and endodermal epithelial cells produce a rich repertoire of antimicrobial peptides that regulate the microbiome (Franzenburg et al., 2013).

In addition to ectodermal and endodermal epithelial cells, *Hydra* has an anatomically simple nervous system (Figures 1, 2D–G) which consists of approximately 3000 neurons in an adult and 70 neurons in a newly hatched polyp (Klimovich and Bosch, 2018; Martin et al., 1997). Although in the early studies, we had considered the epithelial cells as prime regulators of the microbiome (Bosch, 2013, 2014), we recognized over time that neurons per se are involved and that they somehow interact with microbes. When assessing antibacterial activity in *Hydra*, we observed a strong correlation between the number of neurons present and the antibacterial activity (Kasahara and Bosch, 2003). Moreover, when we removed all neurones from the epithelium, we observed significant changes in *Hydra*’s microbial community (Fraune et al., 2009). Based on these observations, meanwhile, we have established an experimental platform to investigate the neuron–microbe interactions in *Hydra* not only at a descriptive level, but also to uncover the underlying molecular mechanisms (causalities).

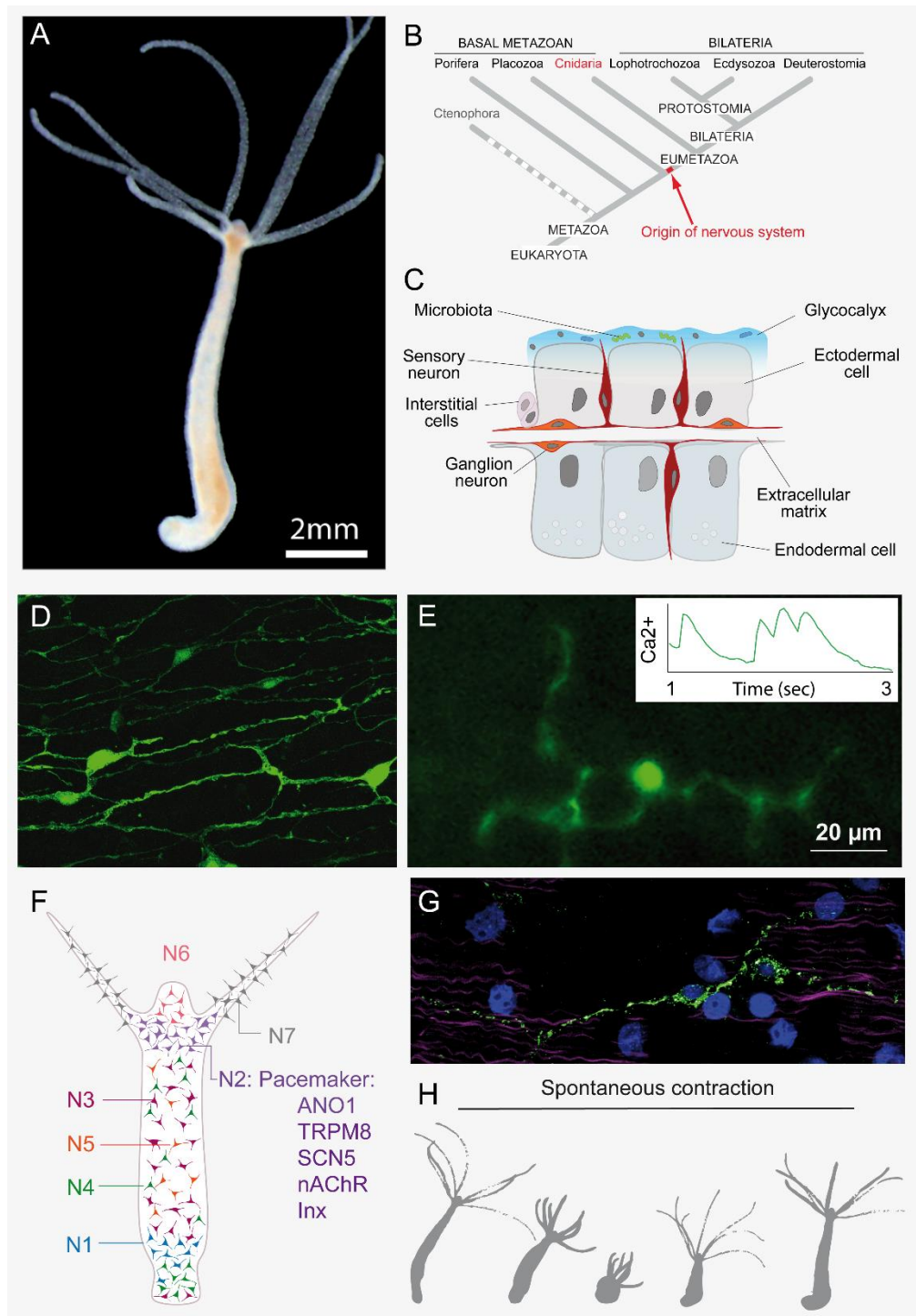


Figure 2: Hydra as a model to study neuron-microbe interactions.

A. An adult polyp contains a nervous system comprising approximately 3000 neurons. **B.** Hydra belongs to the phylum Cnidaria, the sister group to the Bilateria. Their common ancestor developed the first nervous system. **C.** The tissue structure of Hydra with the microbiota in the glycocalyx. **D.** The nerve net of Hydra. **E.** In vivo recording and quantification (inset) of neuronal activity using a genetically encoded Ca^{2+} -sensor GCaMP expressed specifically in neurons in transgenic Hydra. **F.** The spatial distribution of the seven distinct neuronal populations in Hydra. N2 as the pacemaker population with the conserved signature of ion channels. **G.** A pacemaker neuron of Hydra visualized using an antibody against SCN5-like channel (green). Nuclei are stained with TO-PRO (blue) and actin filaments of epitheliomuscular cells are stained with Phalloidin (magenta). **H.** Schematic illustration of the spontaneous contraction behavior.

What neuronal circuits do in *Hydra*

Nervous systems are commonly interpreted as information processing input–output devices. They receive environmental information from their sensors as input, subsequently process or integrate this information, and use the result to control effectors, providing some kind of output. Although this interpretation seems beyond dispute, from an evolutionary perspective, it requires some clarification and reflection. First, neuronal circuits evolve by the Darwinian processes of variation and selection. Given the extremely high costs of building and maintaining nervous systems, selective optimization seems to shape neuroanatomy rather than neutral evolutionary processes (Jekely, 2011). Second, in evolutionary ancient neuronal circuits, input is provided by sensory cells having receptors for neurotransmitters, neuropeptides and other signaling molecules in the neural membrane which may still have been incompletely genetically individualized compared to more complex animals (Schlosser, 2018). In animals such as *Hydra*, the few neuronal cell types are multifunctional, and later during a long evolutionary history may have diversified and specialized for different sensory modalities and larger and more complex sense organs. Third, as emphasized by Jekely (2011), behaviour evolved before nervous systems. Various single-celled eukaryotes (protists) and the ciliated larvae of sponges devoid of neurons can display sophisticated behaviours, including phototaxis, gravitaxis or chemotaxis. Fourth, animal behaviour allows individuals to adapt to the environment at a time scale that is much faster than natural selection, and therefore drives the rapid evolution of the nervous system (Anderson and Perona, 2014). Last, there is increasing evidence that human and animal's social behaviour, hyperactivity and maybe even anxiety are influenced by microbes (Bruckner et al., 2020; Vuong et al., 2017).

Hydra behaviour has been studied for centuries. It was first described by Trembley (1744) and consists of both spontaneous and stimulus-evoked, reactive behaviours (Trembley, 1744). Spontaneous behaviours include the rhythmic spontaneous body contractions that are correlated with a specific electrophysiological activity termed contraction bursts and are modulated by light, among other stimuli (Passano and McCullough, 1964). The stereotypical feeding response, a typical reactive behaviour induced by food-associated stimuli consists of three distinct stages: tentacle writhing, tentacle ball formation and mouth opening (Koizumi et al., 1983; Lenhoff, 1968). This reactive and elaborate

reflex-like behaviour is fundamental to the survival of *Hydra* and sensitive to its needs: well-fed animals do not appear to show feeding behaviour when exposed to a food stimulus (Grosvenor et al., 1996; Koizumi and Maeda, 1981; Loomis, 1955). In addition, feeding behaviour can be robustly induced by small molecules, such as glutathione (Lehoff, 1961). Mounting evidence suggests that all these behaviours represent a motor output of neuronal circuits that may comprise sensory and ganglion neurons which are controlling the effectors, i.e. the multifunctional epitheliomuscular cells. However, the architecture of these circuits, the principles of neuronal connectivity and signal transduction within the *Hydra* nerve net and the neural mechanisms underlying the behaviour changes under environmental, physiological, nutritional or pharmacological manipulations are still largely in the dark.

Ontogeny, architecture and activity of *Hydra*'s nervous system

In a *Hydra* embryo, the first neurons appear to develop relatively late and just before hatching (Martin et al., 1997). A juvenile polyp (hatchling) emerges with a few dozens of neurons. After hatching, the growth of a polyp is accompanied by a gradual increase in the number of neurons, which reaches approximately 3000 two weeks after hatching. Since *Hydra* proliferates asexually continuously by budding, in an adult *Hydra*, neurogenesis also takes place continuously to maintain tissue homeostasis. The simplicity and difference in neural architecture between an embryo and an adult polyp offer great potential for understanding the basic design principles and minimal size of a nervous system to still perform basic sensory information processing tasks.

Currently, it is unknown which level of neuronal organization is required for *Hydra*'s spontaneous and stimulus-evoked, reactive behaviour. Moreover, we do not know the essential components of the nerve net that enable spontaneous and reactive behaviour as an indication of functional neuronal circuit growth. A rich repertoire of methods including in vivo labelling and tracking of trans-genic neurons, cell cycle analysis and expression analysis at the protein and transcriptome level is available to explore how neuronal circuits are established and maintained by continuously integrating stem-cell-derived migratory neuronal precursor cells into the nervous system. In addition, improved imaging techniques enable neuroscientists to observe the entire activity of certain nervous systems at a glance, providing completely new insights in neural circuit architecture and

functioning (Figure 2E). This becomes obvious in the recent work by Dupre and Yuste (Dupre and Yuste, 2017) who demonstrated by calcium imaging technology in *Hydra* the existence of multiple circuits within these nerve nets. They proposed that three major functional networks extend through the entire animal and are activated selectively during longitudinal contractions, elongations in response to light, and radial contractions. From these and other studies, it is obvious that the advent of novel imaging technologies leverages the great potential of *Hydra* as a model system to get in-depth insight into the functional sophistication of apparently simple nerve nets.

Rhythmic spontaneous body contractions require both pacemaker cells and the presence of microbes

Spontaneous contractions of the digestive tract play an important role in almost all animals. From simple invertebrates to humans, there are consistently similar patterns of movement, through which rhythmic contractions of the muscles facilitate the transport and mixing of the bowel contents. The triggers for the spontaneous contractions of the muscle tissue are so-called pacemaker cells of the nervous system. In a specific rhythm and without any external stimulation, they emit electrical impulses, that ultimately reach the smooth muscles of the intestinal wall and cause them to contract. Although the impulses as such occur autonomously, their frequency, regularity and intensity are subject to external influences. The factors underlying the control of these impulses are not known yet.

Hydra turned out to be a very suitable system for understanding the control of this simple spontaneous behaviour and the underlying neuronal circuits. An undisturbed adult *Hydra* polyp will contract spontaneously with a frequency in the order of 5–10 contractions per hour (Figure 2H). The regularity and frequency of these contractions are highly sensitive to environmental conditions—such as light intensity and spectrum, presence of food, and osmolarity (Benos and Prusch, 1973; Kanaya et al., 2019, 2020; Passano, 1963; Rushforth et al., 1963; Yamamoto and Yuste, 2020). The contractions are electrically induced by central pattern generator neurons or pacemaker cells (Figure 2F and G). Previous extracellular electrophysiological recordings (Passano and McCullough, 1964) suggest that the pacemaker cells operate at a higher intrinsic frequency than the contraction burst frequency, and thus imply existence of an additional mechanism

or cell type that relays their motor output. To identify additional components of the control machinery, we remembered that the *Hydra* epithelium is colonized by a specific microbiota, and compared normal *Hydra* which had typical bacterial colonisation with those that had their microbiome completely removed (Murillo-Rincon et al., 2017). In comparison, organisms without bacterial colonisation exhibited a reduction in contractions by about half. At the same time, the rhythm of the movements became disrupted, and some of the breaks between the contractions were much longer. Thus, the absence of the specific microbiome in *Hydra* compromised the peristaltic movements in the body cavity. In a further step, we restored the specific bacterial colonisation in the germ-free organisms. Initially, we introduced each of the five most common bacterial species found in the *Hydra* microbiome individually back into the sterile polyps. It turned out that this individual bacterial colonisation has no appreciable effect on the frequency and timing of contractions. Only the joint reintroduction of the five main representatives of the microbiome led to a marked improvement in peristalsis, although even then, the pattern of contractions was not fully normalised. The point was made even stronger by the fact that an extract produced from the colonising bacteria had a similarly positive influence (Murillo-Rincon et al., 2017). Taken together, these observations indicate that only the natural and complete *Hydra* microbiome is indispensable for regular spontaneous contractility. Not yet identified molecules secreted by the bacteria can intervene in the control mechanism of the pacemaker cells. As such, bacterial metabolites or signals can have a decisive effect on the pattern of spontaneous peristaltic contractions. In sum, the microbiome appears to have an indispensable function in the frequency and timing of tissue contractions.

The molecular signature of pacemaker cells

Based on the differential expression of transcripts encoding neurotransmitter receptors, ion channels, neuropeptides, and transcription factors, the neuronal population of *Hydra* can be subdivided into distinct clusters that are likely to include neurons with unique functions (Klimovich et al., 2020; Siebert et al., 2019). By using cluster-specific transcripts as molecular markers, certain neuronal classes were found to be restricted to specific domains in the *Hydra* body column. One such neuronal subpopulation is located at the base of the tentacles and expresses nicotinic acetylcholine receptors as well as genes encoding SCN-like sodium channels, ANO1-like chloride channels and TRPM-like cation channels

(Figure 2F and G). When we blocked the activity of these genes in *Hydra*, this immediately led to a drastic reduction in rhythmic body contractions. Modulation of the activity of these “pacemaker” channels disturbed both the rhythm and the frequency of the spontaneous contractions of the *Hydra* body, indicating that they depend on the unique combination of ion channels. For this reason, we are convinced that these neurons are indeed the pacemaker cells that control the peristalsis; and that they are able to perceive signals from microorganisms and react to them. Interestingly, the human orthologs of these channels are expressed by the intestinal pacemaker cells in mammals (first identified by Ramón y Cajal and called interstitial cells of Cajal) and linked to the pathogenesis of irritable bowel syndrome (Beyder et al., 2014; Mazzone et al., 2019; Strege et al., 2018). This evolutionary connection can be stretched even further since the unique molecular architecture of pacemakers appears to be conserved between *Hydra* neurons, the pharyngeal pacemaker complex of *Caenorhabditis elegans* and the above mentioned enteric nervous system of the mouse. The peristaltic activity of the gut turns out as an evolutionarily ancient neurogenic behaviour dependent on microbial signals and essential for life.

Bidirectional communication between pacemaker neurons and the symbiotic bacteria

Our studies uncovered that *Hydra* neurons not only receive signals from the microbiome, but also actively affect the composition of the associated microbiota. A detailed molecular genetic analysis of *Hydra*'s individual nerve cells using single cell RNA sequencing technology showed (Klimovich et al., 2020) that distinct subpopulations of neurons exert a direct influence on the density and composition of the symbiotic bacteria using the tools of the innate immune system. Distinct neuronal types, including the pacemakers, produce neuropeptides that display highly selective antimicrobial activity and alter the composition and spatial distribution of the microbial communities on *Hydra* body (Augustin et al., 2017; Klimovich et al., 2020). In addition, neurons in *Hydra* produce many components of microbe associated molecular pattern (MAMP) receptors, such as Toll-like receptors, NOD-like receptors, C-type lectin, etc., indicating that neurons in *Hydra* are immunocompetent cells with critical roles in immune signaling function (Klimovich et al., 2020). Emphasizing further the role of *Hydra* neurons in immunity, bioinformatics and machine learning algorithms revealed that a large fraction of neuronal genes unique to this genus (so called taxonomically restricted

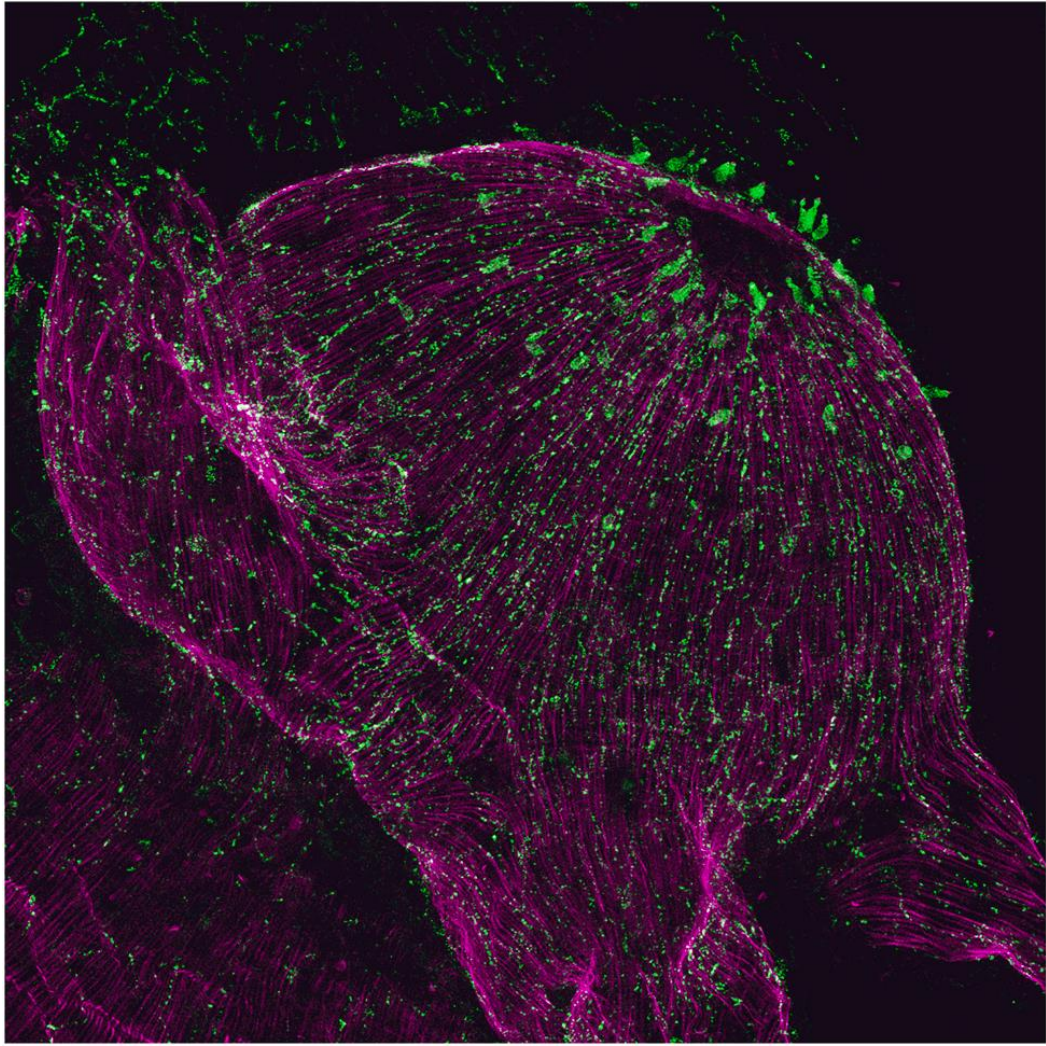


Figure 3: The nerve net of Hydra is composed of at least seven distinct spatially restricted neuronal populations. Here, one of them – a population of neurons expressing the RF-amide neuropeptide (green) in the hypostome of a polyp are visualized using specific antibodies. Muscular fibers of epithelial cells (magenta) are counterstained with Phalloidin.

genes), are capable of encoding antimicrobial peptides (Klimovich et al., 2020). To our surprise, we uncovered that a number of *Hydra*-specific neuropeptides known to mediate neurotransmission and motor control have a second function; they act as antimicrobial peptides and shape the microbiome (Augustin et al., 2017). Intriguingly, a bidirectional interaction between neurons and microbes can also be observed in vertebrates. While defensin family AMPs are expressed in the murine enteric neurons (Klimovich et al., 2020), a plethora of other peptides, produced in the mammalian brain, may also play a role in controlling resident beneficial microbes (Holzer and Farzi, 2014). Moreover, similar to dual-function neuropeptides of *Hydra*, a neuropeptide PACAP known to regulate neurodevelopment, emotion and stress responses in the mammalian brain has been recently identified as an antimicrobial peptide (Lee et al., 2021). Strikingly,

antimicrobial peptides have structural features that make them prone to aggregation into plaques similar to those characteristics for the amyloids in the brain (Lee et al., 2020). Even more intriguingly, the β -amyloid protein also has antimicrobial potential and may normally function in the innate immune system (Soscia et al., 2010). These observations provide an exciting perspective that the accumulation of amyloid, considered a toxic waste product, may in fact be an immune reaction of the brain to the presence of microbes or their products (Abbott, 2020). Taken together, these observations uncover the existence of a common evolutionary conserved principle and support an emerging paradigm that the communication between the nervous system(s) and the microbiota are indeed bidirectional. The nervous system receives signals from the gut (gut–brain axis) affecting host behaviour and development; and on the other hand, is producing neuropeptides with antimicrobial activity and a possible role in controlling the microbiota.

Conclusions: Open questions, and future perspectives: a new way of exploring neuronal circuits.

Here we have reviewed that nerve cells are involved in controlling resident beneficial microbes in the early emerging metazoan *Hydra*, and that microbes affect the animal's behaviour by directly interfering with neuronal receptors. Recent progress in molecular and imaging analysis allows us to present *Hydra* as a powerful system for studying neural interactions and neural circuit formation which allows easy access to combined genetic, cell biological, molecular, and biocomputational tools. It is increasingly evident that bidirectional interactions exist in many vertebrates among the gastrointestinal tract, the intestinal microbiota and the enteric and central nervous systems.

The path taken so far enables us to address specific and evolutionary informative questions with regard to the evolutionary origin of host neuron–microbe interactions. Open questions include:

- How do microbes affect innate behaviour such as *Hydra*'s feeding reflex?
- What are the microbial taxa involved and the responsive neuron populations?
- How different are these signals and factors closely related but different *Hydra* species? Preliminary observations point to a surprising difference in

neuroanatomy in closely related and apparently similar *Hydra* species; yet functional consequences of these differences remain unclear.

- Does the resident microbiota influence neurogenesis in embryos and/or in adults?
- Is the resident microbiota involved in educating neuronal precursor cells/stem cells which, in turn, influence the composition of the microbiota?
- How do the commensal microbiota support the development of the complex nerve net made of distinct spatially restricted neuronal populations (Figures 3 and 4)?
- Ample histochemical, biochemical and functional data has been accumulated, indicating the presence of different small molecule neurotransmitters such as catecholamines, serotonin, acetylcholine, glutamate and GABA in *Hydra*. Do the resident microbes contribute to the repertoire of neurotransmitters?
- Last: what are the fundamental principles of the nerve net topology, dynamics and function that allow the simple nervous system of *Hydra* to be highly effective, multifunctional and energy-efficient? Understanding these basic rules of network design, implemented in the simple nervous systems of *Hydra* and other models, will be instrumental for development of highly efficient yet less energy-demanding microprocessors and computers (Bosch et al., 2017; Dupre and Yuste, 2017; Martinez and Sprecher, 2020).

Some of these questions are already under study in laboratories around the globe, but a more focused effort is required. The fascinating perspective is that these efforts will assist our understanding of how all of the parts of a living organism operate together within the metaorganismic framework. The comprehensive elucidation of the neural code for behavior in an experimental system where one can have in principle access to either connectivity or functional data from every single neuron also enables the rigorous modeling of neural circuits, with simulations that are constrained completely in terms of the number of neurons, connections between the neurons and activity patterns. Model systems such as *Hydra* therefore may open new pathways to mimic basal neuronal mechanisms by electronic systems. Such studies will have relevance for understanding neural circuits in all animal species. In conclusion, the evidence is now irrefutable that “from so simple a beginning” (Charles Darwin) the neurobiology of animals has been, and is being, shaped by interactions with the microbial world.

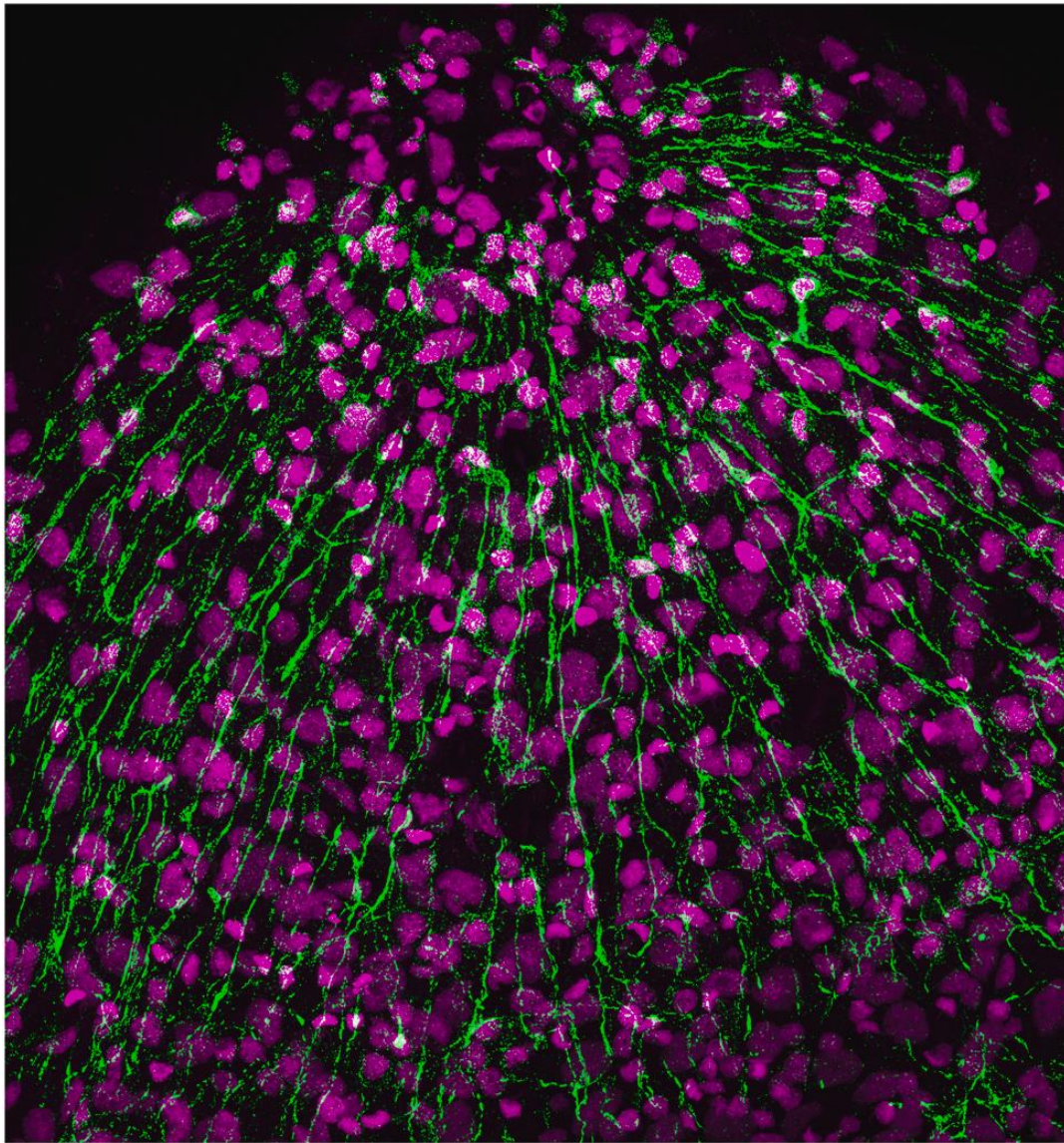


Figure 4: Modern microscopy technologies allow analysing the complex anatomy of the Hydra nerve net with unprecedented resolution. Here, the cell bodies and neurites of RF-amide-positive neurons in the hypostome (green) are visualized using a specific antibody. Cell nuclei are counterstained with TO-PRO (magenta).

Glossary

Antimicrobial peptides (AMPs): Small molecular mass proteins with broad spectrum antimicrobial activity against bacteria, viruses and fungi. These peptides are usually positively charged and have both a hydrophobic and hydrophilic side that enable the molecule to be soluble in aqueous environments yet also enter lipid-rich membranes.

Axenic condition: Condition of animal culture, in which only a single species of organism is present and entirely free of all other contaminating organisms. This state is achieved by sterilizing the housing equipment, supplied food and air. Axenic culture is an essential tool for studies on symbiotic interactions in a controlled environment.

Commensal microbe: A bacterial, viral, fungal or archaeal organism that under normal circumstances resides in or on host tissue, does not cause disease, and forms a symbiotic relationship with the host in which one derives some benefit, while the other is unaffected.

Conventionalized host organisms: Carrying the full (undefined) load of organisms usually associated with this species.

Dysbiosis: An altered state (or disbalance) of microbiota associated with a change in species composition, abundance and/or spatial distribution and typically associated with a disease.

Germfree: Host organisms that are devoid of any other living germs or microorganisms.

Holobiont: The cnidarian host organism and all of its symbiotic algae and stably associated microbiota. While the term “meta-organism” defines a superordinate entity that is applicable to all kinds of interdependent associations, the term “holobiont” is constrained to specific taxonomic groups.

Metaorganism: An association composed of a uni-or multicellular macroscopic host and diverse microorganisms, including bacteria, Archaea, fungi, viruses, and various other microbial eukaryotic species including algal symbionts.

Microbes: Microbial life forms including bacteria, archaea, fungi and viruses.

Microbiota: Microbial life forms within a given habitat or host. **Microbiome:** The totality of microorganisms and their collective genetic material present in or on the body of a macroscopic host organism or in another environment.

Symbiotic interactions: A close and usually obligatory association between two or more different organisms of different species that live together, often but not necessarily to their mutual benefit.

Author contributions:

All the authors have accepted responsibility for the entire content of this submitted manuscript and approved submission. Research funding: This work was supported in part by grants from the Deutsche Forschungsgemeinschaft, the CRC 1182 “Origin and Function of Metaorganisms”(to TCGB.) and funded by the Deutsche Forschungsgemeinschaft (DFG, German Research Foundation) – Project-ID 434434223 –SFB 1461 “Neurotronics: Bio-Inspired Information Pathways” (to TCGB and AK). T.C.G.B. appreciates support from the Canadian Institute for Advanced Research. Conflict of interest statement: The authors declare no conflicts of interest regarding this article.

References

- Abbott, A. (2020). Are infections seeding some cases of Alzheimer’s disease? *Nature* 587,22–25.
- Anderson, D.J. and Perona, P. (2014). Toward a science of computational ethology. *Neuron* 84,18–31.
- Augustin, R., Schröder, K., Rincón, A.P.M., Fraune, S., Anton-Erxleben, F., Herbst, E.M., Wittlieb, J., Schwentner, M., Grötzinger, J., Wassenaar, T.M., et al. (2017). A secreted antibacterial neuropeptide shapes the microbiome of Hydra. *Nat. Commun.* 8,1–8.
- Baquero, F. and Nombela, C. (2012). The microbiome as a human organ. *Clin. Microbiol. Infect.* 18,2–4.
- Benos, D.J. and Prusch, R.D. (1973). Osmoregulation in Hydra: Column contraction as a function of external osmolality. *Comp. Biochem. Physiol. Part A Physiol.* 44, 1397–1400.
- Beyder, A., Mazzone, A., Strega, P.R., Tester, D.J., Saito, Y.A., Bernard, C.E., Enders, F.T., Ek, W.E., Schmidt, P.T., Dlugosz, A., et al. (2014). Loss-of-function of the voltage-gated sodium channel NaV1.5 (Channelopathies) in patients with irritable bowel syndrome. *Gastroenterology* 146, 1659–1668.
- Blaser, M.J., Cardon, Z.G., Cho, M.K., Dangl, J.L., Donohue, T.J., Green, J.L., Knight, R., Maxon, M.E., Northen, T.R., and Pollard, K.S. (2016). Toward a predictive understanding of Earth’s microbiomes to address 21st century challenges. *mBio* 7, e00714–16.
- Bosch, T.C.G. (2013). Cnidarian-microbe interactions and the origin of innate immunity in metazoans. *Annu. Rev. Microbiol.* 67, 499–518.
- Bosch, T.C.G. (2014). Rethinking the role of immunity: Lessons from Hydra. *Trends Immunol.* 35, 495–502.
- Bosch, T.C.G. and McFall-Ngai, M. (2021). Animal development in the microbial world: Re-thinking the conceptual framework. *Curr. Top. Dev. Biol.* 141, 399–427.
- Bosch, T.C.G. and Mcfall-Ngai, M.J. (2011). Metaorganisms as the new Frontier. *Zoology* 114, 185–190.
- Bosch, T.C.G., Klimovich, A., Domazet-Lošo, T., Gründer, S., Holstein, T.W., J’

- ékely, G., Miller, D.J., Murillo-Rincon, A.P., Rentzsch, F., Richards, G.S., et al. (2017). Back to the basics: Cnidarians start to fire. *Trends Neurosci.* 40,92–105.
- Bruckner, J.J., Stednitz, S.J., Grice, M.Z., Larsch, J.J., Tallafuss, A., Washbourne, P., and Eisen, J. (2020). The microbiota promotes social behavior by neuro-immune modulation of neurite complexity. *BioRxiv* 2020.05.01.071373.
- Cryan, J.F., O’Riordan, K.J., Cowan, C.S.M., Sandhu, K.V., Bastiaanssen, T.F.S., Boehme, M., Codagnone, M.G., Cusotto, S., Fulling, C., and Golubeva, A.V. (2019). The microbiota-gut-brain axis. *Physiol. Rev.* 99, 1877–2013.
- Dupre, C. and Yuste, R. (2017). Non-overlapping neural networks in *Hydra vulgaris*. *Curr. Biol.* 27, 1085–1097.
- Foster, J.A., Rinaman, L., and Cryan, J.F. (2017). Stress & the gut-brain axis: Regulation by the microbiome. *Neurobiol. Stress* 7, 124–136.
- Franzenburg, S., Walter, J., Künzel, S., Wang, J., Baines, J.F., Bosch, T.C.G., and Fraune, S. (2013). Distinct antimicrobial peptide expression determines host species-specific bacterial associations. *Proc. Natl. Acad. Sci. Unit. States Am.* 110, E3730–E3738.
- Fraune, S. and Bosch, T.C.G. (2007). Long-term maintenance of species-specific bacterial microbiota in the basal metazoan *Hydra*. *Proc. Natl. Acad. Sci. Unit. States Am.* 104, 13146–13151.
- Fraune, S., Abe, Y., and Bosch, T.C.G. (2009). Disturbing epithelial homeostasis in the metazoan *Hydra* leads to drastic changes in associated microbiota. *Environ. Microbiol.* 11, 2361–2369.
- Gareau, M.G. (2014). Microbiota-gut-brain axis and cognitive function. *Adv. Exp. Med. Biol.* 817, 357–371.
- Grosvenor, W., Rhoads, D.E., and Kass-Simon, G. (1996). Chemoreceptive control of feeding processes in *Hydra*. *Chem. Senses* 21, 313–321.
- Holzer, P. and Farzi, A. (2014). Neuropeptides and the microbiota-gut-brain axis. *Adv. Exp. Med. Biol.* 817, 195–219.
- Jékely, G. (2011). Origin and early evolution of neural circuits for the control of ciliary locomotion. *Proc. R. Soc. B Biol. Sci.* 278, 914–922.
- Kanaya, H.J., Kobayakawa, Y., and Itoh, T.Q. (2019). *Hydra vulgaris* exhibits day-night variation in behavior and gene expression levels. *Zool. Lett.* 5,1–12.
- Kanaya, H.J., Park, S., Kim, J., Kusumi, J., Krenenou, S., Sawatari, E., Sato, A., Lee, J., Bang, H., and Kobayakawa, Y. (2020). A sleep-like state in *Hydra* unravels conserved sleep mechanisms during the evolutionary development of the central nervous system. *Sci. Adv.* 6, eabb9415.
- Kasahara, S. and Bosch, T.C.G. (2003). Enhanced antibacterial activity in *Hydra* polyps lacking nerve cells. *Dev. Comp. Immunol.* 27, 79–85.
- Klimovich, A.V. and Bosch, T.C.G. (2018). Rethinking the role of the nervous system: Lessons from the *Hydra* holobiont. *Bioessays* 40, 1800060.
- Klimovich, A., Giacomello, S., Björklund, Å., Faure, L., Kaucka, M., Giez, C., Murillo-Rincon, A.P., Matt, A.-S., Willoweit-Ohl, D., Crupi, G., et al. (2020). Prototypical pacemaker neurons interact with the resident microbiota. *Proc. Natl. Acad. Sci. U. S. A.* 117, 17854–17863.
- Koizumi, O. and Maeda, N. (1981). Rise of feeding threshold in satiated *Hydra*. *J. Comp. Physiol.* 142,75–80.
- Koizumi, O., Haraguchi, Y., and Ohuchida, A. (1983). Reaction chain in feeding behavior of *Hydra*: Different specificities of three feeding responses. *J. Comp. Physiol.* 150,99–105.
- Lee, E.Y., Srinivasan, Y., de Anda, J., Nicastro, L.K., Tükel, Ç., and Wong, G.C.L. (2020). Functional reciprocity of amyloids and antimicrobial peptides: Rethinking the role of supramolecular assembly in host defense, immune activation, and inflammation. *Front. Immunol.* 11, 1629.
- Lee, E.Y., Chan, L.C., Wang, H., Lieng, J., Hung, M., Srinivasan, Y., Wang, J., Waschek, J.A., Ferguson, A.L., Lee, K.F., et al. (2021). PACAP is a pathogen-inducible resident antimicrobial neuropeptide affording rapid and contextual molecular host defense of the brain. *Proc. Natl. Acad. Sci. U. S. A.* 118, e1917623117.

- Lenhoff, H.M. (1968). Behavior, hormones, and Hydra. Research on behavior of lower invertebrates may help elucidate some cellular actions of hormones. *Science* 161, 434–442.
- Lenhoff, H.M. (1961). Activation of the feeding reflex in *Hydra littoralis*.
- I. Role played by reduced glutathione and quantitative assay of the feeding reflex. *J. Gen. Physiol.* 45, 331–344. Loomis, W.F. (1955). Glutathione control of the specific feeding reactions of *Hydra*. *Ann. N. Y. Acad. Sci.* 62, 211–227. Martin, V.J., Littlefield, C.L., Archer, W.E., and Bode, H.R. (1997). Embryogenesis in *Hydra*. *Biol. Bull.* 192, 345–363.
- Martinez, P. and Sprecher, S.G. (2020). Of circuits and brains: The origin and diversification of neural architectures. *Front. Ecol. Evol.* 8, 82.
- Mazzone, A., Gibbons, S.J., Eisenman, S.T., Strege, P.R., Zheng, T., D'Amato, M., Ordog, T., Fernandez-Zapico, M.E., and Farrugia, G. (2019). Direct repression of anoctamin 1 (ANO1) gene transcription by Gli proteins. *Faseb. J.* 33, 6632–6642.
- Murillo-Rincon, A.P., Klimovich, A., Pemöller, E., Taubenheim, J., Mortzfeld, B., Augustin, R., and Bosch, T.C.G. (2017). Spontaneous body contractions are modulated by the microbiome of *Hydra*. *Sci. Rep.* 7, 15937.
- Obata, Y., Castaño, Á., Boeing, S., Bon-Frauches, A.C., Fung, C., Fallesen, T., de Agüero, M.G., Yilmaz, B., Lopes, R., and Huseynova, A. (2020). Neuronal programming by microbiota regulates intestinal physiology. *Nature* 578, 284–289.
- Ogbonnaya, E.S., Clarke, G., Shanahan, F., Dinan, T.G., Cryan, J.F., and O'Leary, O.F. (2015). Adult hippocampal neurogenesis is regulated by the microbiome. *Biol. Psychiatr.* 78,e7–9.
- De Palma, G., Lynch, M.D.J., Lu, J., Dang, V.T., Deng, Y., Jury, J., Umeh, G., Miranda, P.M., Pastor, M.P., and Sidani, S. (2017). Transplantation of fecal microbiota from patients with irritable bowel syndrome alters gut function and behavior in recipient mice. *Sci. Transl. Med.* 9, eaaf6397.
- Passano, L.M. (1963). Primitive nervous systems. *Proc. Natl. Acad. Sci. Unit. States Am.* 50, 306–313.
- Passano, L.M. and McCullough, C.B. (1964). Co-ordinating systems and behaviour in *Hydra*: I. Pacemaker system of the periodic contractions. *J. Exp. Biol.* 41, 643–664.
- Rathje, K., Mortzfeld, B., Hoeppner, M., Bosch, T.C.G., and Klimovich, A. (2020). Dynamic interactions within the host-associated microbiota cause tumor formation in the basal metazoan *Hydra*. *PLoS Pathog* 16, e1008375.
- Rushforth, N.B., Burnett, A.L., and Maynard, R. (1963). Behavior in *Hydra*: Contraction responses of *Hydra pirardi* to mechanical and light stimuli. *Science* 139, 760–761.
- Schlosser, G. (2018). A short history of nearly every sense—the evolutionary history of vertebrate sensory cell types. *Integr. Comp. Biol.* 58, 301–316.
- Schröder, K. and Bosch, T.C.G. (2016). The origin of mucosal immunity: Lessons from the holobiont *Hydra*. *mBio* 7,e01184–16.
- Sharon, G., Sampson, T.R., Geschwind, D.H., and Mazmanian, S.K. (2016). The central nervous system and the gut microbiome. *Cell* 167, 915–932.
- Siebert, S., Farrell, J.A., Cazet, J.F., Abeykoon, Y., Primack, A.S., Schnitzler, C.E., and Juliano, C.E. (2019). Stem cell differentiation trajectories in *Hydra* resolved at single-cell resolution. *Science* 365, eaav9314.
- Soscia, S.J., Kirby, J.E., Washicosky, K.J., Tucker, S.M., Ingelsson, M., Hyman, B., Burton, M.A., Goldstein, L.E., Duong, S., Tanzi, R.E., et al. (2010). The Alzheimer's disease-associated amyloid β -protein is an antimicrobial peptide. *PloS One* 5, e9505.
- Strege, P.R., Mazzone, A., Bernard, C.E., Neshatian, L., Gibbons, S.J., Saito, Y.A., Tester, D.J., Calvert, M.L., Mayer, E.A., and Chang, L. (2018). Irritable bowel syndrome patients have SCN5A channelopathies that lead to decreased Nav1.5 current and mechanosensitivity. *Am. J. Physiol. Liver Physiol.* 314, G494–G503.
- Trembley, A. (1744). *Mémoires pour servir à l'histoire d'un genre de polypes d'eau douce, à bras en forme de cornes* (Leiden: Jean and Herman Verbeek).

- De Vadder, F., Grasset, E., Holm, L.M., Karsenty, G., Macpherson, A.J., Olofsson, L.E., and Bäckhed, F. (2018). Gut microbiota regulates maturation of the adult enteric nervous system via enteric serotonin networks. *Proc. Natl. Acad. Sci. Unit. States Am.* 115, 6458–6463.
- Vuong, H.E., Yano, J.M., Fung, T.C., and Hsiao, E.Y. (2017). The microbiome and host behavior. *Annu. Rev. Neurosci.* 40, 21–49.
- Yamamoto, W. and Yuste, R. (2020). Whole-body imaging of neural and muscle activity during behavior in *Hydra vulgaris*: Effect of osmolarity on contraction bursts. *enNeuro* 7, ENEURO.0539-19.2020, <https://doi.org/10.1523/eneuro.0539-19.2020>.

Spontaneous body wall contractions stabilize the fluid microenvironment that shapes host-microbe associations.

Research Article

Physics of Living Systems

Spontaneous body wall contractions stabilize the fluid microenvironment that shapes host–microbe associations.

Janna C Nawroth^{1, 3, a}, **Christoph Giez**^{2, a}, Alexander Klimovich², Eva Kanso³, Thomas CG Bosch²

^a contributed equally

¹ Helmholtz Pioneer Campus and Institute of Biological and Medical Imaging (IBMI), Helmholtz Munich (GmbH), Germany; Chair of Biological Imaging at the Central Institute for Translational Cancer Research (TranslaTUM), School of Medicine, Technical University of Munich, Germany;

² Zoological Institute, Kiel University, Germany

³ Aerospace and Mechanical Engineering, University of Southern California, United States;

Jul 3, 2023 - DOI: doi.org/10.7554/eLife.83637

Abstract

The freshwater polyp *Hydra* is a popular biological model system; however, we still do not understand one of its most salient behaviors, the generation of spontaneous body wall contractions. Here, by applying experimental fluid dynamics analysis and mathematical modeling, we provide functional evidence that spontaneous contractions of body walls enhance the transport of chemical compounds from and to the tissue surface where symbiotic bacteria reside. Experimentally, a reduction in the frequency of spontaneous body wall contractions is associated with a changed composition of the colonizing microbiota. Together, our findings suggest that spontaneous body wall contractions create an important fluid transport mechanism that (1) may shape and stabilize specific host–microbe associations and (2) create fluid microhabitats that may modulate the spatial distribution of the colonizing microbes. This mechanism may be more broadly applicable to animal–microbe interactions since research has shown that rhythmic spontaneous contractions in the gastrointestinal tracts are essential for maintaining normal microbiota.

Introduction

The millimeter-scale freshwater polyp *Hydra* with its simple tube-like body structure (Figure 1A) and stereotypic movement patterns is a popular biological model organism for immunology (Bosch and McFall-Ngai, 2021; Bosch, 2014; Bosch, 2013; Klimovich and Bosch, 2018a; Schröder and Bosch, 2016), developmental and evolutionary biology, and neurobiology (Klimovich and Bosch, 2018a; Bosch et al., 2017). Despite *Hydra*'s relevance for fundamental research, one of the animal's most salient behaviors remains a mystery since its first description in 1744 (Bayer et al., 1744): it is unclear why *Hydra* undergoes recurrent full-body contraction-relaxation cycles, approximately one every 10–30 min (Figure 1B), while attached to the substratum. Most, if not all, animals exhibit such spontaneous contractions of muscular organs and body walls to pump internal fluids, create mixing flows, feed, locomote, or clean surfaces (Schierwater et al., 1991; Kremien et al., 2013; Trojanowski et al., 2016; Rich, 2018; Kornder et al., 2022). Other animals perform rhythmic pulsations, which differ from spontaneous contractions by occurring in predictable intervals and usually serve similar functions. For example, rhythmic pulsation of tentacles in corals, first noted

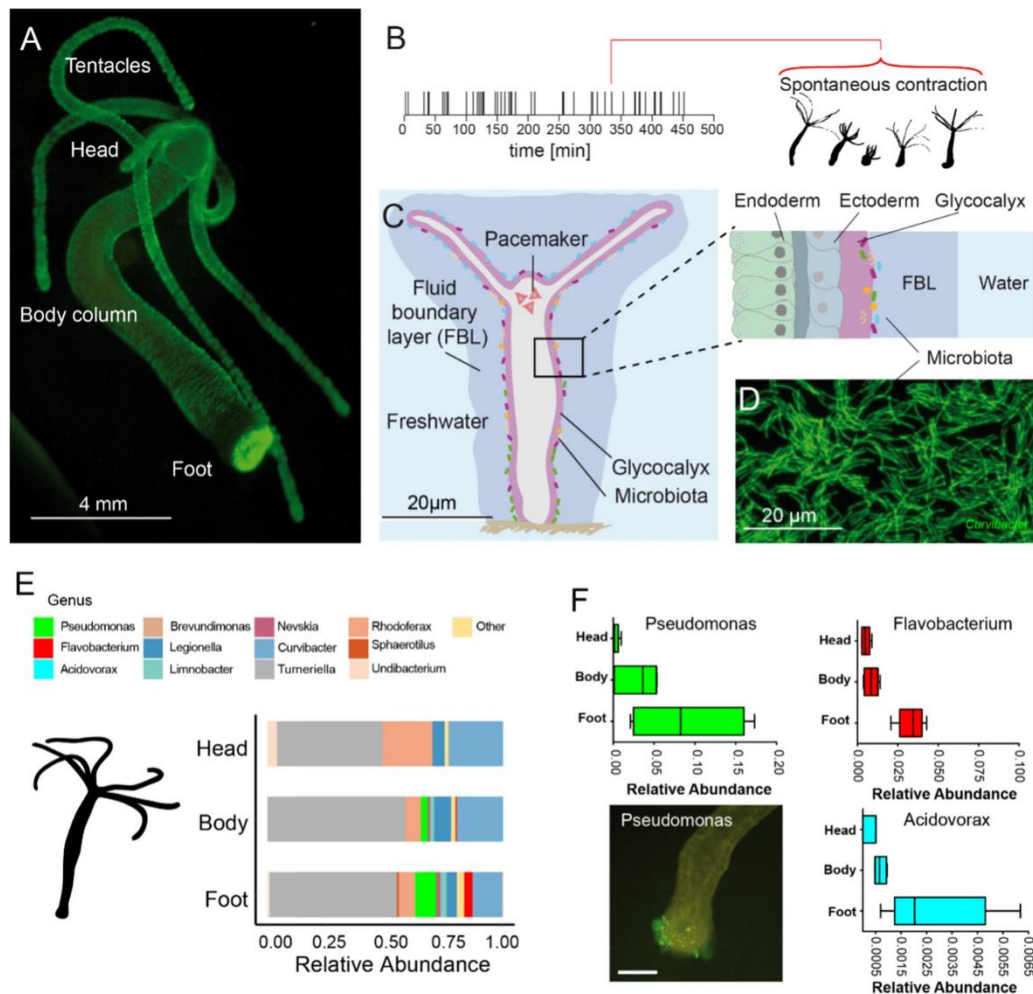


Figure 1. The freshwater polyp *Hydra*, a model system for the role of spontaneous body wall contractions in shaping microbe biogeography. (A) Polyp colonized with fluorescently labeled betaproteobacteria. (B) A representative contractile activity pattern of an individual polyp recorded over 8 hr (left). Each dash on the timeline represents an individual spontaneous contraction-relaxation cycle (right). (C) Schematic representation of a *Hydra* with a fluid boundary layer surrounding the polyp with the glycocalyx layer adjacent to the polyp's tissue. Inset: tissue architecture covered outside by the mucus-like glycocalyx that provides the habitat for a specific bacterial community on the interface with the fluid boundary layer. (D) Dense community of fluorescently labeled bacteria (main colonizer *Curvibacter* sp.) colonizing the polyp's head. (E) The biogeography of *Hydra*'s symbionts under undisturbed/control conditions follows a distinct spatial colonization pattern along the body column ($n = 4$). (F) Bacteria mostly colonizing the foot region include *Pseudomonas*, *Flavobacterium*, and *Acidovorax* ($n = 4$). Scale bar: 500 µm.

by Lamarck nearly 200 years ago, lead to increased turbulent mixing, which enhances photosynthesis via fast removal of excess oxygen and prevents refiltration of surrounding water by neighboring polyps (Kremien et al., 2013). However, *Hydra*'s size, morphology, and spontaneous contraction characteristics do not fit any of the known functions of rhythmic or spontaneous contractions. In particular, *Hydra*'s small dimensions likely prevent it from the generation of turbulent mixing (Purcell, 1977). Here, we sought to investigate the functional underpinnings of *Hydra*'s spontaneous contractions from a fluid mechanics perspective. We hypothesized that the spontaneous contractions might generate

fluid transport patterns of relevance to *Hydra*'s microbial partners that colonize the so-called glycocalyx on the outer body wall (Schröder and Bosch, 2016; Fraune et al., 2015; Figure 1C). Typically, the composition and distribution of symbiotic microbial communities residing at solid–liquid interfaces, such as in the gut and lung, are regulated both by interaction with host cells and by the properties of the fluid medium (Fang et al., 2021; Franzenburg et al., 2013). Therefore, we asked whether *Hydra*'s microbiome might be influenced by fluid flow associated with spontaneous contractions.

Results

First, we mapped the abundance and distribution of microbiota that reside on the glycocalyx (Figure 1C and D). The glycocalyx is a multilayered extracellular cuticle covering *Hydra*'s ectodermal epithelial cells, has mucus-like properties, and shapes the microbiome by providing food and antimicrobial peptides (Franzenburg et al., 2013). Regional differences in the glycocalyx have not been reported; however, using 16S rRNA profiling on different sections of *Hydra*, we found that different microbial species favor different regions along the body column, including foot- and head-dominating microbiota (Figure 1E and F). Based on these intriguing data and recent insights into how fluid flow shapes spatial distributions of bacteria (Wheeler et al., 2019), we hypothesized that the spontaneous contractions might generate fluidic microhabitats that facilitate the microbial biogeography along the body column.

Kinematics and flow physics of individual spontaneous contractions

To explore this hypothesis, we used video microscopy and analyzed the animal's body kinematics to assess the differential impact of spontaneous contractions on the fluid microenvironment. We examined the contraction activity (Figure 2A) of multiple animals over 8 hr and recorded an average contraction frequency of 2.5 spontaneous contractions per hour (Figure 2—figure supplements 1 and 2, Figure 2—figure supplement 3 control conditions), corresponding to an average duration (T_{IC}) of the inter-contraction intervals of 24 min. To arrive at estimates rooted in probability theory that take into consideration the distribution of T_{IC} , we collected the measured T_{IC} from all animals in the form of a histogram (Figure 2—figure supplement 3B, control condition). The resulting distribution of T_{IC} is best fit by an exponential distribution, implying that contraction events of individual polyps

follow a stochastic Poisson process. We computed the average frequency based on the exponential fit to these biological data. We found that the so-computed contraction frequency is equal to 2.9 contractions per hour, which is slightly larger than the 2.5 contractions per hour obtained by taking a direct average of the data.

Each stage of the inter-contraction intervals and spontaneous contraction cycle is characterized by stereotypic kinematic patterns of *Hydra*'s motion trajectories and velocities (Figure 2A, bottom). During inter-contraction intervals, which on

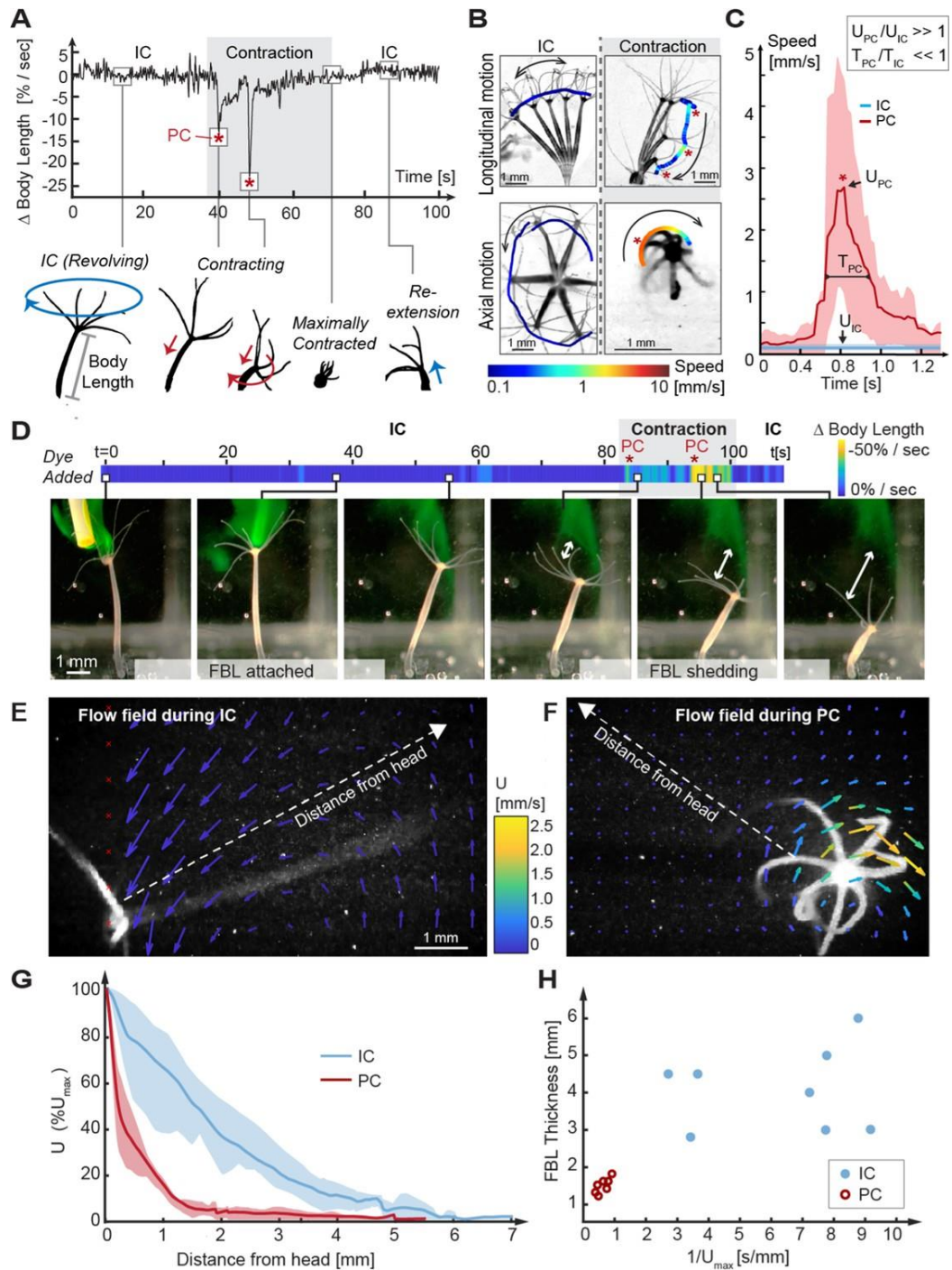


Figure 2. Kinematic and fluid dynamics analysis of individual contraction events reveal the shedding of the fluid boundary layer (FBL) during each spontaneous contraction event. (A) Top: representative plot of the change in relative body length in *Hydra* as a function of time shows transition from an inter-contraction interval (IC) to a spontaneous contraction with two peak contraction events (PC, asterisks), and the return to an IC interval. Bottom: typical kinematic pattern associated with IC intervals and contractions. Arrows indicate distinct body trajectories during IC intervals (blue) compared to contractions (red). (B) Typical body trajectories in longitudinal and axial plane during IC intervals and spontaneous contractions visualized by time-lapse microscopy. Maximal speeds (log10 scale) are indicated by color-coded trajectories of the head (oral end or tentacles). Trajectories are slightly offset to avoid obscuring the animal. Asterisks denote PC events. (C) Comparison of maximal velocities near head reached during IC intervals ($n = 3$ animals) and PC ($n = 5$ animals). Lines: average curves. Shaded areas: interquartile range. Inset: relative scaling of PC duration (TPC), IC interval duration (TIC), PC velocity magnitudes (UPC), and IC interval velocity magnitudes (UIC). (D) Application of a fluorescent dye reveals existence of a FBL during the IC interval and its shedding upon a contraction event. A representative time-lapse series. White arrows indicate FBL shedding after PCs, that is, the growing separation between the original, stained FBL and *Hydra*'s head. (E) Quantification of *Hydra*'s flow velocity field during IC intervals and (F) during a typical PC with axial rotation (top view). Flow vectors and velocities are indicated by color-coded arrows. (G) Relative change of fluid flow speed as a function of distance from *Hydra*'s surface measured along dotted lines in (E, F) during IC intervals (blue) and during PCs with rotation (red). Lines: average curves. Shaded areas: interquartile range. (H) FBL thickness, defined as distance from *Hydra* at which 90% freestream speed is reached, is inversely correlated to maximal flow speed (U_{max}).

The online version of this article includes the following figure supplement(s) for figure 2: Figure supplement 1. The experimental setup for measuring and manipulating the contraction rates in *Hydra*. Figure supplement 2. Behavioral analysis of *Hydra* over 8 hr. Figure supplement 3. Spontaneous contractions are modeled mathematically as a Poisson process. Figure supplement 4. The 2D space covered by *Hydra*'s resting motion and re-extensions in the period of nine contractions is revealed by this overlay of detected motion. Figure supplement 5. Typical flow speed profiles derived from the particle imaging velocimetry (PIV) data. Figure supplement 6. Spontaneous contraction frequencies of *Hydra* when placed in small liquid volumes can reach up to 12 contractions per hour (CPH).

average last tens of minutes (Figure 2—figure supplement 3B), *Hydra*'s body column remains nearly fully extended and slowly revolves at full length around its foothold, tracing a cone-shaped volume over time (Figure 2B, Video 1). By contrast, spontaneous contraction events typically last a few seconds and are characterized by a stepwise shortening of the body column with one or more peak contraction events until the body column has shortened to 20% or less of its original length (Figure 2A–C). A peak contraction is defined as any part of the spontaneous contraction during which *Hydra* contracts at a rate of 25% change in body length per second or more. spontaneous

contractions are frequently accompanied by axial rotation in a spiraling downward motion (Figure 2A and B, Video 1) and are typically followed by slow re-extension to inter-contraction interval length (Figure 2A) in a random direction (Figure 2—figure supplement 4). We quantified the speeds and timescales that different regions of *Hydra*'s body column experience during inter-contraction intervals and spontaneous contractions. During spontaneous contractions, specifically during

peak contractions characterized by simultaneous linear shortening and axial rotation, the oral region accelerates to peak velocities UPC of 10 mm/s. This is almost two orders of magnitude faster than maximal head speeds UIC during inter-contraction intervals, which are on the order of 0.1 mm/s in both longitudinal and axial directions (Figure 2B and C). Further, peak contraction rarely last longer than $T_{PC} = 1$ s and hence operate at 1000-fold smaller timescales than inter-contraction intervals (with mean duration of ca. 24 min, i.e., 1440 s).

To assess the effects of *Hydra*'s body kinematics on its fluid environment, we computed the Reynolds number $Re = \ell U / \mu$ at the tentacles near *Hydra*'s mouth, where the tentacle diameter is $\ell = 0.1$ mm, the kinematic viscosity of water at 20°C is $\mu = 1.0034$ mm²/s, and the tentacle speed U is in mm/s. The Re number compares the effects of fluid inertia to viscous drag forces. During inter-contraction intervals, $U = UIC$ is on the order of 0.1 mm/s, and Re is on the order of 0.01. At such low Re number, fluid flow is dominated by viscous effects and distinguished by the presence of a laminar and expansive fluid boundary layer. The fluid boundary layer can be envisioned as an envelope of fluid enclosing *Hydra* and moving at the same velocity as *Hydra*'s surface. The thickness of the fluid boundary layer is defined as the distance from the surface at which the fluid speed decreases by 90% compared to *Hydra*'s speed, that is, the distance at which the fluid is no longer following *Hydra*'s surface (Vogel, 2020). During peak contraction, *Hydra*'s speed $U = UPC$ is on the order of 10 mm/s, Re increases to the order of 1, which indicates greater inertial effects that result in thinning of the fluid boundary layer (Schlichting and Gersten, 2000).

To label the fluid boundary layer and assess the animal–fluid interactions experimentally (Nawroth and Dabiri, 2014), we added fluorescent dye adjacent to *Hydra*'s oral region while in the intercontraction interval state. In one representative recording (Figure 2D, left, Video 2), the dye faithfully followed the fully extended animal's slow revolutions during the inter-contraction interval for more than 1 min, qualitatively confirming the presence of a stably attached fluid boundary layer. Intriguingly, as the animal underwent a spontaneous contraction (with two peak contraction events), the dye separated from the animal's surface and stayed behind as *Hydra* retracted, indicating shedding of the original fluid boundary layer (Figure 2D, right, Video 2). Since the animals tend to slowly re-extend into a random direction (Figure 2—figure supplement 4), their chances of re-encountering the shed fluid are small. To confirm these observations

quantitatively and to measure the dynamically changing fluid boundary layer thickness, we recorded the microscale fluid motion using particle imaging velocimetry (PIV) as described previously (Nawroth et al., 2017). During inter-contraction intervals, fluid parcels at distances far from the body column followed the animal's trajectory, reflecting an expansive fluid boundary layer of almost one full-body length in thickness (fluid boundary layer thickness = 5 mm) (Figure 2E and G, Figure 2—figure supplement 5A, Video 3). In contrast, during peak contractions, only the fluid close to *Hydra*'s surface accelerated with the body, whereas fluid at further distances remained unaffected (fluid boundary layer thickness = 1.5 mm) (Figure 2F and G, Figure 2—figure supplement 5B, Video 3). The thickness of the fluid boundary layer correlated inversely with body speed (Figure 2H). These measurements demonstrate shedding of the fluid boundary layer during contractions and significant reduction in the thickness of the fluid boundary layer that had developed during the inter-contraction interval. Thus, recurrent spontaneous contractions result in regular shedding of the fluid boundary layer (as illustrated by the streak of dye left behind in Figure 2D), enabling *Hydra* to partially escape from its previous fluid environment and thereby transiently reshape the chemical microenvironment at the epithelial surface where the microbial symbionts are localized. Importantly, the contraction events form a brief perturbation of the inter-contraction interval flow regime at the oral region, while the foot region remains motionless even during peak contractions (Figure 2B) and experiences slow flow speeds of maximal values on the order of 0.1 mm/s (Figure 2—figure supplement 5B). These flow speeds are comparable to flow speeds experienced at the head between contractions (Figure 2—figure supplement 5A). Taken together, these results suggest that *Hydra*'s spontaneous contractions lead to a maximal shedding of viscous boundary layers near the head's surface, and minimal shedding near the foot's surface. This differentiation in the fluid environment could be relevant because of our finding that *Hydra*'s surface is colonized by foot- and head-dominating microbiota (Figure 1D and E). Contraction-induced fluid boundary layer shedding may enhance the transport of bacteria-relevant compounds, such as metabolites, antimicrobials, and extracellular vesicles (Fischbach and Segre, 2016; Ñahui Palomino et al., 2021), between *Hydra*'s head and the fluid environment, compared to lower transport near the foot, hence generating biochemical microhabitats that could promote the observed microbial biogeography. This hypothesis is not readily amenable to experimental interrogation. To date, there are no universal tools for experimentally identifying individual and combinations of the many chemical compounds

released or absorbed by microbes (Thorn and Greenman, 2012). We therefore probed this hypothesis indirectly. We developed a simple mathematical model of chemical transport in a fluid environment that gets regularly reset by shedding events, as discussed next.

Physics-based model predicts that contractions increase the exchange rate of chemical compounds to and from the surface

We formulated a simple physics-based mathematical model of the transport of chemical compounds to and from *Hydra*'s surface where the microbes reside. We exploited two key findings from our experimental data. First, between contractions, transport of chemical compounds to and from *Hydra*'s surface is best described by molecular diffusion rather than fluid advection. Second, peak contractions are much shorter and faster than movement during inter-contraction intervals ($T_{PC} \ll T_{IC}$ and $U_{PC} \gg U_{IC}$, see Figure 2C), and each peak contraction causes intermittent shedding of the fluid boundary layer and re-extension of *Hydra*'s head in a random direction. Thus, each contraction resets the fluid microenvironment and replenishes the chemical concentration around *Hydra*'s head, while the fluid environment at *Hydra*'s foot remains always at rest, akin to a permanent inter-contraction interval state.

Our dye visualization and flow quantification showed no noticeable background flows between contraction events (Figure 2D). The fact that diffusion is dominant between contractions can be formally shown by computing the Péclet number $Pe = LU/D$, which compares the relative importance of advection versus diffusion for the transport of a given compound, such as oxygen. Using the length L of *Hydra*'s body column, the mean flow speed U over 1 hr (averaging over both inter-contraction intervals and contracting periods), and the constant oxygen diffusion D at 15°C, we find that Pe is $0.005 \ll 1$, implying that diffusion is dominant between contraction events, even when the flow speed U is overestimated by averaging over both inter-contraction intervals and spontaneous contraction periods.

To reflect the different fluid microenvironments in the highly motile head and static foot, we approximated the respective head and foot surfaces by two non-interacting spheres of radii a and b separated by a distance L (Figure 3A, box). When even a few percent of *Hydra*'s head or foot surface are covered by living

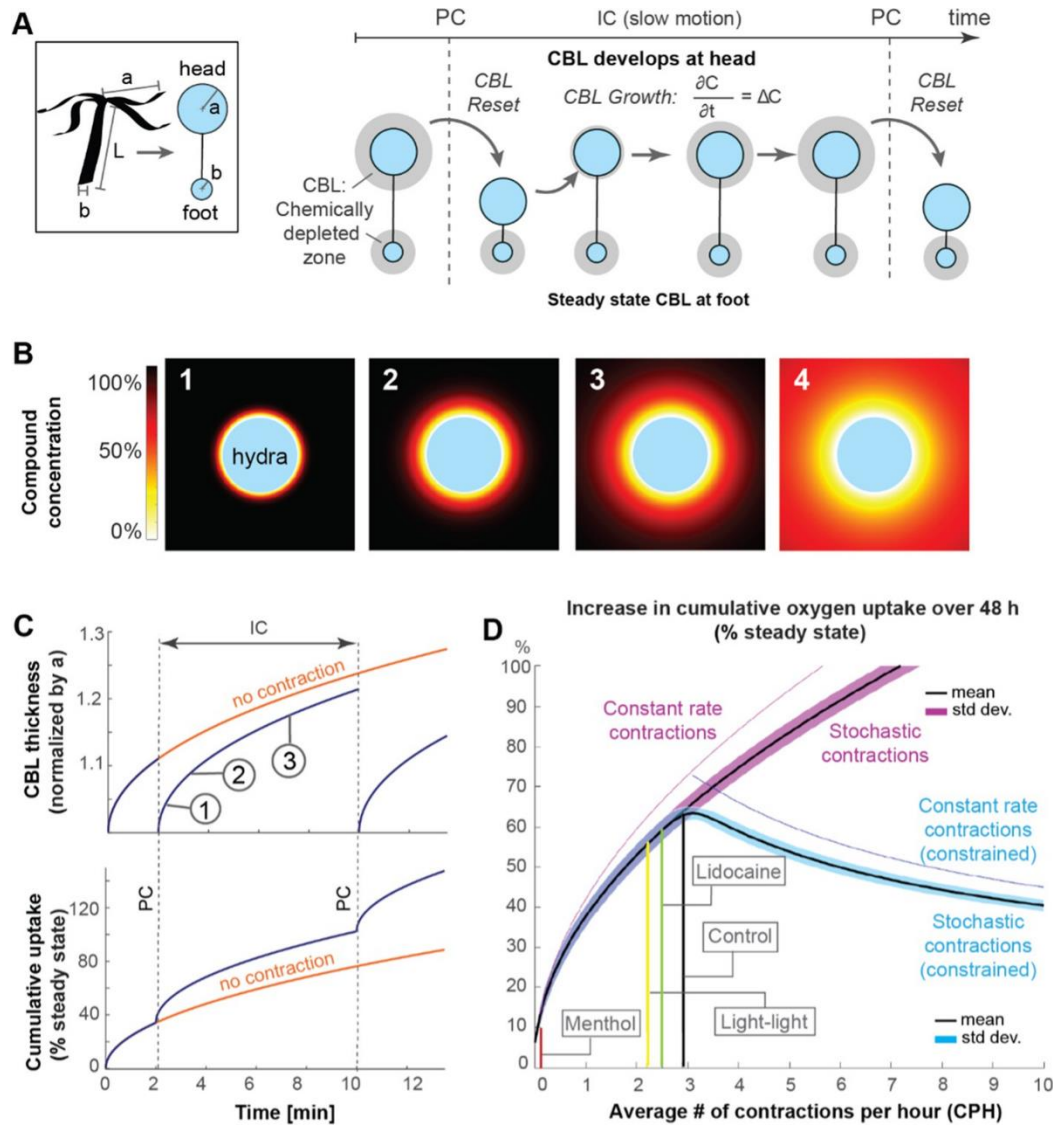


Figure 3. Mathematical model suggests that spontaneous contractions enhance mass transport to and from the surface. (A) Left, box: simplified animal geometry assumed in model consists of a sphere representing the head and a smaller sphere representing the basal foot. Right: by Fick's law, a chemically depleted concentration boundary layer (CBL) forms around Hydra's head and foot region through continuous uptake of chemical compounds at the surface during the inter-contraction interval (IC). The CBL is shed from the head region, but not the foot region, through spontaneous contractions (PC). (B) Computationally modeled growth of chemically depleted CBL around Hydra's head over time until steady state is reached (panel 4), assuming continuous uptake at surface and unlimited supply at far distance. (C) Top: growth of chemically depleted CBL as a function of time with and without contractions. Bottom: instantaneous and cumulative uptake rate, respectively, of a given chemical compound (here: oxygen) during the CBL dynamics above; (D) Predicted increase in cumulative uptake rate (as percentage of steady state) of a given chemical compound over 48 hr as a function of spontaneous contraction frequencies within the observed range (purple), and of increasing frequencies with unconstrained number of spontaneous contractions (magenta) compared to a constrained number of spontaneous contractions (blue graph).

microbes or host cells, the diffusion-limited rate of absorption or emission of a chemical compound by these cells is well approximated by a uniformly covered surface (Berg and Purcell, 1977). Assuming equivalence of the transport of

emitted and absorbed chemical substances (see ‘Materials and methods’), we focus here on absorption only. This implies zero concentration of the chemical compound of interest, say oxygen, at *Hydra*’s surface. Starting in a compound-rich environment, a concentration boundary layer (CBL) depleted of that chemical compound forms and grows near the surface. In the absence of contractions, the concentration field reaches a steady state with zero rate of change of the compound concentration. Each spontaneous contraction event sheds the chemically depleted fluid boundary layer near the head and effectively resets the depletion zone growth process (Figure 3A). Accounting for unsteady diffusion following each spontaneous contraction, we computed the growth of the depletion boundary layer over time (stages 1–3 in Figure 3B), using as an example the diffusion coefficient D of oxygen to derive a dimensional timescale $\tau = a^2/D$ (see ‘Materials and methods’). In the absence of fluid boundary layer shedding, such as near *Hydra*’s static foot, steady state is approached as time increases (stage 4 in Figure 3B). Near *Hydra*’s head, however, each spontaneous contraction resets the CBL thickness to zero (Figure 3C, top), resulting in an instantaneous and increased uptake of molecules, such as oxygen, in the head region (blue) compared to the foot (orange). Consecutive contractions increase the maximal cumulative uptake of compounds near *Hydra*’s head (blue) compared to the foot (orange) (Figure 3C, bottom).

To investigate the functional implications of experimentally observed temporal distribution of spontaneous contractions over many hours, we combined our physics-based model of chemical transport (Figure 3A) with a stochastic model of contraction events. Specifically, the temporal sequence of *Hydra*’s spontaneous contractions can be estimated mathematically by a Poisson distribution of mean λ , given that the distribution of inter-contraction intervals are best fitted by an exponential distribution of mean $1/\lambda$ (Figure 2—figure supplement 3B). We calculated analytically the expected mean and standard deviation of the cumulative uptake J_{IC} over a single inter-contraction period T_{IC} and of the cumulative uptake J over an extended period T (containing multiple T_{IC}) (see ‘Materials and methods’). We found that the expected mean value of J_{IC} , given by $\langle J_{IC} \rangle = \sqrt{(a^2\lambda/D)}$, decreases with increasing contraction frequency λ , while the expected mean value of J , given by $\langle J \rangle = \sqrt{(a^2\lambda/D)}$, increases with increasing λ . This is intuitive: as the contraction frequency increases, the inter-contraction time T_{IC} decreases, so does the expected uptake J_{IC} over a single inter-contraction period T_{IC} . However, the fluid environment gets reset more often, with each

resetting event replenishing the chemical concentration, leading to an increase in the expected cumulative uptake J over an extended period T containing multiple contraction events.

Next, we numerically simulated data sets of inter-contraction intervals T_{IC} (Figure 2—figure supplement 3C) drawn from exponential distributions of mean $1/\lambda$, where we let λ range from 0 to 10 at 0.05 intervals. For each λ , we conducted 10,000 numerical experiments, each lasting for a fixed total time period $T = 48$ hr. The obtained number of contraction events in each numerical experiment consisted of one realization taken from a Poisson distribution of mean λ . The total number of contraction events over all experiments was normally distributed, as expected from the law of large numbers (see ‘Materials and methods’). We computed numerically the cumulative oxygen uptake J over $T = 48$ hr for each realization (normalized by the cumulative uptake at steady state), and for each λ , we calculated the mean and standard deviation of the computed J . Plotting the mean and standard deviation of J as a function of λ (Figure 3D), we found that increasing λ increases the cumulative uptake J and that the mean (solid black line) and standard deviation (thick purple segment) are in excellent agreement with analytical predictions (see ‘Materials and methods’).

Spontaneous contraction frequencies on the order of 10 contractions per hour and more have been reported in the *Hydra* (Murillo-Rincon et al., 2017, Yamamoto and Yuste, 2020), indicating that, in theory, increases in uptake rates are possible. In our experience, however, such high frequencies occur only transiently when *Hydra* has been stressed, for example, by transferring the animals into very small containers such as concave glass for imaging purposes. At later time points, the contraction frequency of animals in these conditions converge towards an spontaneous contraction rate around three contractions per hour (Figure 2—figure supplement 6), similar to what we observed in our regular setup condition using a large beaker setup (Figure 2—figure supplement 2A, control condition). This suggests that under unconstrained conditions, *Hydra*’s baseline contraction rate per hour is near 3, rather than 10.

We used the model to test the effect of limiting the maximal number of contractions over 48 hr to 144 contractions, which is the total number of contractions at an average spontaneous contraction frequency $\lambda = 3$ contractions per hour. Effectively, this constraint means that once the maximum number of

contractions is reached, no additional contractions are permitted during the remainder of the 48 hr, mimicking, for example, a finite energy budget for spontaneous contractions. Interestingly, imposing this constraint showed that maximal uptake gains are achieved at contractions frequencies consistent with the imposed constraint (Figure 3D, thick blue graph), and that increasing λ beyond three contractions per hour decreases the cumulative uptake.

When testing the effect of a constant-rate contraction activity, that is, with a constant TIC approximately equal to $48/\lambda$ hours, the model predicts a slightly increased uptake compared to stochastic activity, indicating that a precise rhythm would only confer a small benefit over the stochastic mechanism (Figure 3D, thin purple and blue graphs). Analogous results hold for the removal of accumulated chemicals produced by microbes at *Hydra*'s surface (see 'Materials and methods').

Our model indicates that *Hydra*'s spontaneous contractions facilitate a greater exchange rate – including both uptake and release – of chemical compounds in the oral region as compared to the static foot region. When spontaneous contraction frequency is reduced, the maximal exchange rate near the head is reduced as well and, in the extreme case of zero contractions, becomes almost identical to the steady state in the foot region.

The simplicity of the model should not distract from the universality of the mechanism it probes: the effect of stochastic contractions on the transport of chemicals to and from a surface exhibiting spontaneous wall contractions. To make analytical progress, we assumed the surface is spherical, but, by continuity arguments, the conclusions we arrived at are qualitatively valid even for non-spherical surfaces. These conclusions can be restated concisely as follows: fast spontaneous contractions of an otherwise slowly moving surface in a stagnant fluid medium cause impromptu shedding of the fluid boundary layer and lead to improved transport of chemicals to and from the surface between contraction events. Higher contraction frequencies are beneficial, but require additional, may be prohibitive, metabolic cost. A stochastic distribution of contraction events over time, following a Poisson process, produces benefits that are nearly as good as those produced by regular contractions, but without the need for a biological machinery to maintain a precise rhythm. Limiting the total number of contractions

leads to decreased performance at contraction frequencies beyond what would allow the contraction events to be Poisson distributed.

Taken together, our model suggests that changing the spontaneous contraction frequency will alter the fluid microenvironment and biochemical concentrations experienced by *Hydra*'s microbial community; in particular, reducing the spontaneous contraction frequency would make the microenvironment near *Hydra*'s head, where the greatest fluid boundary layer shedding occurs during spontaneous contractions, more similar to the foot, where minimal fluid boundary layer shedding occurs.

Reducing the spontaneous contraction frequency changes the colonizing microbiota

To directly probe the impact of spontaneous contractions on the associated microbial community, we decreased *Hydra*'s spontaneous contraction frequency by two established methods: (1) continuous exposure to either light or darkness (Kanaya et al., 2019, Rushforth et al., 1963) and (2) chemical interference with the ion channel inhibitors menthol and lidocaine (Klimovich et al., 2020; Figure 2—figure supplement 1). Continuous exposure to light and treatment with ion channel inhibitor lidocaine reduced the spontaneous contraction frequency slightly from an average value of 2.5 contractions per hour in control conditions to 2.3 contractions per hour in continuous light and to 2.0 contractions per hour in lidocaine treatment (Figure 2—figure supplement 2A) (note that we were unable to make the measurements in the continuous dark condition). Treatment with ion channel inhibitor menthol almost completely abolished the occurrence of contractions. The treatments reduced spontaneous contraction frequency without significantly changing the frequency of other common fast contractile behaviors, such as somersaulting (Figure 2—figure supplement 2B and C; Han et al., 2018). Consistent with earlier studies (Kanaya et al., 2019, Klimovich et al., 2020), lidocaine and constant light treatment increased the likelihood of longer T_{IC} ; the contraction events remained, however, Poisson distributed, and T_{IC} remained exponentially distributed (Figure 2—figure supplement 3B), as assumed in our mathematical model. Computing the average contraction frequency based on the best exponential fit to biological data, we found that it to be equal to 2.5, and 2.2 contractions per hour for the lidocaine, and continuous light treatments,

respectively, as opposed to 2.9 contractions per hour for the control, again confirming the reduced contraction rate in the treatment groups.

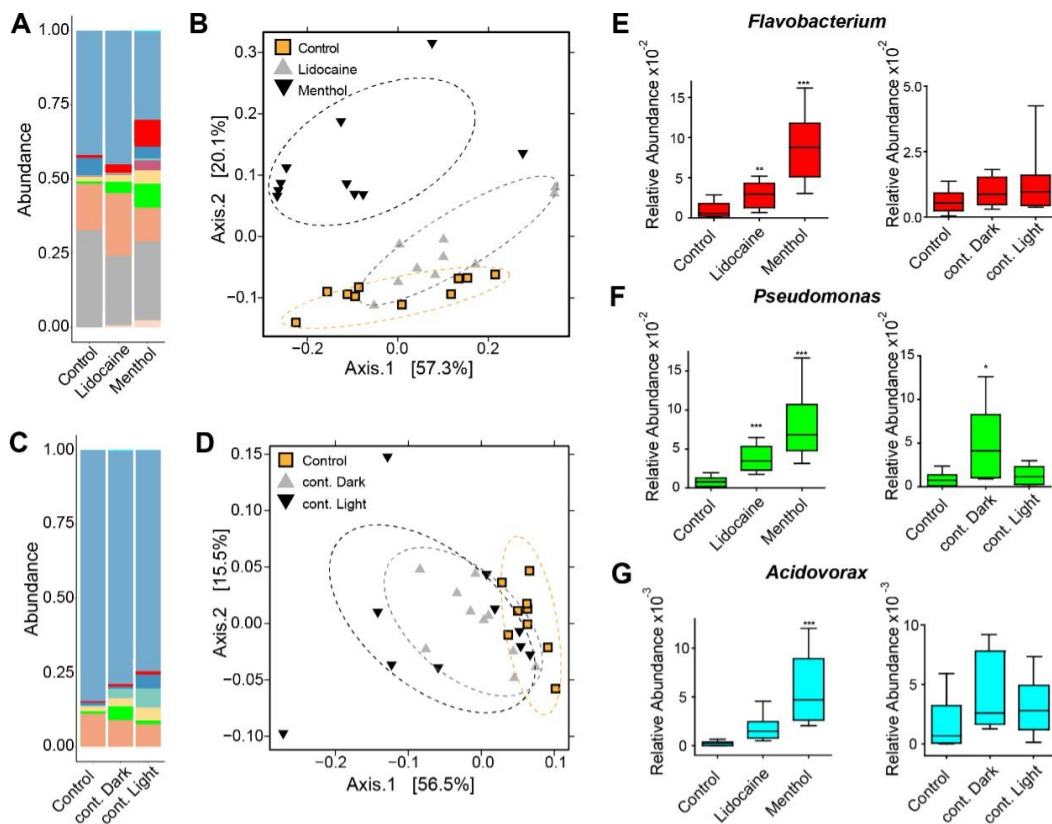


Figure 4. Perturbing the frequency of spontaneous contractions over extended time periods shifts the microbial composition in *Hydra*. Reducing the spontaneous contraction frequency with 48 hr treatment of ion channel inhibitors (menthol and lidocaine), continuous light exposure (cont. light), or continuous dark (cont. dark) exposure significantly affects the bacterial community. Control is incubation in freshwater (*Hydra* medium) and 12 hr of light alternating with 12 hr of dark conditions. (A) Bar plot of the relative abundance on the genus level showing the effect of the ion channel inhibitors. (B) Bar plot of the relative abundance on the genus level showing the effect of the light treatments. (C, D) Analysis of the bacterial communities associated with the control and disturbed conditions using principal coordinate analysis of the Bray–Curtis distance matrix. The polyps with disturbed contraction frequency show distinct clustering (ellipses added manually). (E–G) Box plots displaying the fold change of the relative abundance compared to the control of *Flavobacterium*, *Pseudomonas*, and *Acidovorax* in response to the different treatments. (For all plots: $n = 8-10$) * $p \leq 0.05$; ** $p \leq 0.01$; *** $p \leq 0.001$ (ANOVA and Kruskal–Wallis).

The online version of this article includes the following source data and figure supplement(s) for figure 4: Figure supplement 1. The microbiota changes due to reduced contraction frequency. Figure supplement 2. Analysis of the bacterial communities using different distance matrixes. Figure supplement 2—source data 1. Statistical analysis of the PCoAs using Anosim and Adonis. Figure supplement 3. The bacterial load is not affected by ion channel inhibitors or light treatments. Figure supplement 4. Video recording of fluorescently labeled *Curvibacter* reveals a very stable colonization pattern during a full contraction cycle. Figure supplement 5. Reduction in contraction frequency does not alter the glycocalyx of *Hydra*.

We next investigated the effects of the altered spontaneous contraction frequency on *Hydra's* microbiota. A 48 hr exposure to either pharmacological agents (menthol and lidocaine) or exposure to different light regimes led to a similar and significant shift in the microbial community (Figure 4, Figure 4—figure supplement 1). The relative abundance bar plot and principal coordinate analysis (PCoA) of the microbial composition showed a clustering of the different treatments in response to a disturbed contraction frequency. The extent of the shift was positively correlated with the magnitude of the decrease in contraction frequency and, consequently, was the greatest in menthol-treated animals. This shift consisted of a change in the relative abundance rather than a disappearance of bacterial taxa or bacterial load (Figure 4—figure supplement 2). The fact that both light and pharmacological manipulations resulted in similar effects provides strong evidence that the change in relative bacterial abundance is related to the altered spontaneous contraction frequencies. We further verified by using a minimal inhibitory concentration (MIC) assay that there were no inhibitory effects of the pharmacological substances on the bacteria (Figure 4—figure supplement 3). We evaluated the differences between control and treatment groups for up- or downregulated bacteria using linear discriminant analysis effect size (LEfSe) (Segata et al., 2011). When spontaneous contractions were reduced, the foot-specific microbial colonizers *Flavobacterium*, *Pseudomonas*, and *Acidovorax* (Figure 1E and F) became more abundant (Figure 4E–G). Taken together, these data suggest that a reduced spontaneous contraction frequency alters the microbial composition and potentially expands the biogeography of foot-associated bacteria. Our fluid and transport analysis suggests that these changes in the microbiota result from an altered biochemical microenvironment near *Hydra's* head, which is shaped by the spontaneous contraction frequency. In particular, our mathematical model, which faithfully mimics the distribution of inter-contraction intervals under control and disturbed conditions (Figure 2—figure supplement 3B and C), predicts that the reduction in spontaneous contraction frequency seen in the experimental treatments (lidocaine, methanol, continuous light) decreases the cumulative uptake or release of any bacteria-relevant chemical compound near *Hydra's* head (Figure 3C), such that the head's biochemical microenvironment becomes more similar to the static foot region (Figure 3C). However, another explanation of the observed changes in the microbiota could be that the contractions are important for the direct displacement of the microbes to other parts of the body. To investigate whether spontaneous contraction have a direct physical impact on the microbiome, we first took video

recordings of a normal *Hydra* polyp colonized with fluorescently labeled bacteria during a full contraction cycle. We could neither observe an overall change in the colonization pattern nor the physical detachment of labeled bacteria (Figure 4—figure supplement 4, Videos 4 and 5). Thus, at short time scale (few seconds), an individual contraction cycle does not affect the biogeography of the microbiome. We also probed whether a lack of recurrent spontaneous contractions may lead to a remodeled glycocalyx, for example, by hindering its redistribution during spontaneous contractions, and thereby alter the growth conditions of bacteria. Here, we used an antibody specific for a component of *Hydra*'s glycocalyx (Böttger et al., 2012) and visualizing the glycocalyx in animals immobilized for a prolonged (48 hr) time period (Figure 4—figure supplement 5). Since we could not detect major changes in the glycocalyx layer, we concluded that the observed changes in the microbiota are unlikely the cause of glycocalyx remodeling. These results strongly suggest that the fluid boundary layer shedding and resultant chemical exchange by *Hydra*'s spontaneous contractions stabilize microbial colonization and contribute to shaping the microbial biogeography along the body column (Figure 1D and E).

Discussion

The epithelia and microbial symbionts of *Hydra*'s body walls interface with slow-moving or highly viscous fluids. They rely on diffusion for the transport of chemical compounds to and from the surface. *Hydra* cannot engage in more efficient transport mechanisms via fluid advection (Nawroth et al., 2017, Gilpin et al., 2017, Pepper et al., 2010) because it lacks the ciliary or muscular appendages used by other organisms in the low and intermediate Reynolds number regimes to generate unsteady flows and vortices. Soft corals, for example, operate at intermediate Reynolds numbers and use rhythmic pulsations of their tentacles to generate bulk flow that removes oxygen waste (Samson et al., 2019). Although individual corals reach diameters similar to that of fully extended *Hydra* (ca. 1 cm), they usually occur in dense clusters and contract rhythmically at 0.5 Hz, leading to collective fluid advection with Péclet numbers on the order of 10–1000, compared to $Pe = 0.005$ computed for a single *Hydra* with only a handful of contractions per hour, indicating that the two organisms represent different scenarios. Our study suggests that *Hydra* does not leverage fluid advection but instead facilitates the diffusion process through its spontaneous contractions, which cause transiently and locally higher flow rates and greatly improve the

exchange of fluid near the epithelial surface by shedding the so-called fluid boundary layer. This is analogous to a recently discovered ‘sneezing’ mechanism by which marine sponges remove mucus from their surface by recurrent spontaneous contractions (Kornder et al., 2022). Combining high-throughput microbiota profiling, in vivo flow analysis, and mathematical modeling, we found that such exchange facilitates the transport of compounds, including nutrients, waste, antimicrobials, and gases, to and from surface-residing symbiotic microbiota and may take part in maintaining a specific microbiota biogeography along the *Hydra*’s body column (Augustin et al., 2017). Interestingly, this distinct spatial colonization pattern along the body column could not only be essential for pathogen defense (Bosch, 2013, Fraune et al., 2015) but could also be important for modulating the frequency of *Hydra*’s spontaneous contractions (Murillo-Rincon et al., 2017), suggesting a feedback loop that could be the focus of future studies.

Our results may also have broader applicability. *Hydra*’s mucous layer covering the epithelium – an inner layer with stratified organization devoid of bacteria, beneath an outer loose layer colonized by symbionts – is similar to the mammalian colon. Like *Hydra*, the peristaltic gut displays recurrent spontaneous contractions (Gill et al., 1986, Koch et al., 1988, Swaminathan et al., 2016) and a viscosity dominated, low Reynolds number flow regime (Janssen et al., 2007). Disturbance of this contractile activity (e.g., intestinal dysmotility) is correlated with dysbiosis (Hadizadeh et al., 2017, Scott and Cahall, 1982, Vandeputte et al., 2016), which can lead to bacterial overgrowth in the small intestine and irritable bowel syndrome (Kostic et al., 2014, Toskes, 1993). Microfluidic models mimicking the viscous environment and laminar flow of the gut suggest that intestinal contractions mix the luminal content, which appears to modulate microbial density and composition (Cremer et al., 2016). These observations are consistent with our findings in *Hydra* and suggest that spontaneous contractions might both depend on microbial colonizers and also regulate host–bacteria associations.

Finally, our non-dimensional model enables the generalized prediction that body wall contractions, whether in *Hydra*, the gut, or other systems, cause relative improvement of transport for any compound that is produced or consumed near an epithelial surface in low Reynolds number conditions, thereby simultaneously preventing the build-up of metabolic waste and restoring depleted nutrients. Lowering the frequency of spontaneous contractions by 10–15%, as seen in our

experiments, is predicted to reduce the uptake (or removal) rates of individual compounds by a similar order of magnitude. It is intriguing that such a relatively small change in spontaneous contraction rate altered the microbiome significantly and consistently across treatments. One explanation is that since fluid boundary layer shedding by contractions affects the transport of any chemical compound near the surface, decreasing the contraction rate might alter the uptake or removal of many compounds at once. As shown in a recent study on the response of microbial populations to altered soil properties, such combinatorial effects can greatly exceed, and complicate, the impact of any single factor (Rillig et al., 2019). Intuitively, and confirmed by our model, increasing the frequency of contractions results in greater transport to and from the surface. Since spontaneous contractions are energetically expensive processes, *Hydra* under normal conditions may get along well with a moderate rate of about three contractions per hour. Our computational model indicates that this rate still provides significant enhancement over purely diffusive transport, and our experimental data show that lower rates tend to destabilize the microbiome. Taken together, this suggests that *Hydra*'s rhythm of spontaneous contractions might be operating at a sweet spot of efficiency. Furthermore, we demonstrate that a stochastic distribution of a limited number of contractions over time results in a more effective transport than other strategies, such as alternating periods with a higher frequency of contractions with periods that are static. While contractions at regular time intervals would be slightly more effective still, this would require the presence and maintenance of pacemaker circuits with precisely controlled firing frequency. Though future work is needed, our results suggest that *Hydra* – and possibly other contractile epithelial systems – achieve near optimal efficiency without the need for a costly high precision pacemaker system.

Inspired by Dobzhansky's dictum that "nothing in biology makes sense but in the light of evolution" (Dobzhansky, 1964), we speculate that spontaneous contractions were critical early in the evolution of a gut system to maintain a stable microbiota. In this context, an observation in a new species of hydrothermal vent Yeti crabs, *Kiwa puravida* n.sp. is of interest (Thurber et al., 2011). The crabs farm symbiotic bacteria on the surface of their chelipeds (claws) and wave these chelipeds continuously in a constant rhythm. In search of an explanation, the authors stated: "We hypothesize that *K. puravida* n. sp. waves its chelipeds to shear off boundary layers formed by their epibionts productivity, increasing both the epibionts and, in turn, their own access to food" (Thurber et al., 2011). Pointing

in the same direction, a study on multiciliated surface cells in amphibian and some fish embryos ends with the hypothesis that the fluid flow generated by these cells may contribute to managing embryo-associated microbial consortia (Kerney, 2021). In light of these interesting hypotheses, well-controlled perturbation experiments in *Hydra* may offer a unique model to study both the mechanisms and the in vivo role of host generated water flow in maintaining a stable microbiome.

Materials and methods

Animal manipulation and data analysis

Animal culture

Experiments were carried out using *Hydra vulgaris* strain AEP. Animals were maintained under constant environmental conditions, including culture medium (*Hydra* medium; 0.28 mM CaCl₂, 0.33 mM MgSO₄, 0.5 mM NaHCO₃, and 0.08 mM KCO₃), temperature (18°C), and food according to standard procedures (Klimovich et al., 2019). Experimental animals were chosen randomly from clonally growing asexual *Hydra* cultures. The animals were typically fed three times a week with first-instar larvae of *Artemia salina*; however, they were not fed for 24 hr prior to pharmacological interference or light assays, or for 48 hr prior to RNA isolation.

Pharmacological interference and light assays

To alter the contraction frequency of *H. vulgaris* AEP polyps, the animals were treated for 48 hr with either 200 µM menthol (Sigma, Cat# 15785) or 100 µM lidocaine (Sigma, Cat# L5647), or exposed to 48 hr of continuous light or darkness. Control polyps were incubated in *Hydra* medium and were exposed to a 12 hr light/12 hr dark cycle over the same time period. Water temperature remained stable at 18°C for all conditions. From hour 24 to hour 32 of the 48 hr experiment, that is, for 8 hr total, 10 polyps each were simultaneously video recorded in a 50 mL glass beaker, using a frame rate of 20 frames per minute. For comparison with prior studies, single polyps were recorded for 8 hr in a concave slide with a medium volume of 200–500 µL as previously described (Murillo-Rincon et al., 2017). Using the video recordings, we quantified the

number of full-body contractions and somersaulting events in ImageJ/Fiji (Schindelin et al., 2012) and computed the average contraction frequency per hour.

DNA extraction and 16S rRNA profiling

To investigate the effects of a reduced contraction frequency on the microbiota, we exposed normal *H. vulgaris* AEP polyps to different pharmacological agents and light conditions over a 48 hr time period. Polyps were treated with 200 μ M menthol (Sigma, Cat# 15785), 100 μ M lidocaine (Sigma, Cat# L5647), continuous light or continuous darkness for 48 hr at 18°C. Control polyps were incubated in *Hydra* medium and were exposed to a 12 hr light/12 hr dark cycle. Afterward the genomic DNA was extracted from individual polyps with the DNeasy Blood and Tissue Kit (QIAGEN) as described in the manufacturer's protocol. Elution was performed in 50 μ L. Extracted DNA was stored at –20°C until sequencing. Prior to sequencing, the variable regions 1 and 2 (V1V2) of the bacterial 16S rRNA genes were amplified according to the previously established protocol using the primers 27F and 338R (Rausch et al., 2016). For bacterial 16S rRNA profiling, paired-end sequencing of 2 × 300 bp was performed on the Illumina MiSeq platform. The 16S rRNA sequencing raw data are deposited at the SRA and are available under the project ID PRJNA842888. The sequence analysis was conducted using the DADA2 pipeline in R 3.6.0 (Callahan et al., 2016). The downstream analysis of the 16S rRNA data (alpha diversity, relative abundance, and beta-diversity) was done in R including the packages phyloseq, vegan, DESeq2, and ggplot2 (McMurdie and Holmes, 2013; Oksanen et al., 2013; Love et al., 2014; Ginestet, 2011). ASVs with <10 reads were removed from the data set. The tables of bacterial abundance were further processed using LEfSe analysis to identify bacterial taxa that account for major differences between microbial communities (Segata et al., 2011). An effect size threshold of 3.0 (on a log₁₀ scale) was used for all comparisons discussed in this study. The results of LEfSe analysis were visualized by plotting the phylogenetic distribution of the differentially abundant bacterial taxa on the Ribosomal Database Project (RDP) bacterial taxonomy.

Statistics

Statistical analyses were performed using two-tailed Student's t-test or Mann–Whitney U-test where applicable. If multiple testing was performed, p-values were adjusted using Bonferroni correction.

Quantitative real-time PCR analysis (qRT-PCR)

In order to investigate the bacterial community change and validate if there is an increase in the bacterial load, we performed quantitative real-time PCR analysis. The samples from the 16S rRNA profiling experiment were used. Amplification was performed as previously described (Klimovich et al., 2018b) using GoTaq qPCR Master Mix (Promega, Madison, USA) and specific oligonucleotide primers (EUB 27F, EUB 338R). Also, 4–5 biological replicates of each treatment (light, darkness, menthol, and lidocaine) and control with two technical replications were analyzed. The data were collected using ABI 7300 Real-Time PCR System (Applied Biosystems, Foster City, USA) and analyzed by the conventional $\Delta\Delta C_t$ method.

Minimal inhibitory concentration assay (MIC)

To test whether the ion channel inhibitors (menthol and lidocaine) have an antimicrobial activity, their effect was tested in the MIC assays as previously described (Augustin et al., 2017). The following bacterial strain isolates from the natural *H. vulgaris* strain AEP microbiota were used: *Curvibacter* sp., *Acidovorax* sp., *Pelomonas* sp., *Undibacterium* sp., and *Duganella* sp. (Franzenburg et al., 2013; Klimovich et al., 2020). Microdilution susceptibility assays were performed in 96-microtiter-well plates. We tested a range of concentrations of the ion channel inhibitors in *Hydra* medium (with an additional 10% concentration of R2A agar) to match the nutrient-poor conditions of the behavioral assay. The concentration range was chosen such that the dose used in the behavioral assay was the middle of the dilution series. The following concentration were tested (in μM): menthol: 400, 300, 200, 100, and 10; and lidocaine: 10,000, 5000, 2500, 1000, and 100. The inoculum of approximately 100 CFU per well was used. The plates were incubated with the inhibitors for 5–7 d at 18°C. The MIC was determined as the lowest concentration showing the absence of a bacterial cell pellet. The run was designed in a way that every concentration had four replicates.

Immunochemical staining of the glycocalyx

To test whether alterations in the contraction frequency has any effect on the glycocalyx of *Hydra*, we incubated polyps for 48 hr in menthol solution or S-medium (control) and visualized the glycocalyx by immunochemical staining and confocal microscopy of whole-mount polyps. To facilitate the detection of the *Hydra*'s epithelial surface, we used transgenic polyps expressing eGFP in the ectoderm (ecto-GFP line A8; Wittlieb et al., 2006). The glycocalyx was stained using a polyclonal antibody raised in chicken against the PPOD4 protein, generously provided by Prof. Angelika Böttger. The PPOD4 protein has been previously shown to specifically localize to the glycocalyx layer adjacent to the membrane of ectodermal epithelial cells in *Hydra* (Böttger et al., 2012). Polyclonal rabbit-anti-GFP antibody (AB3080, Merck) was used to amplify the GFP signal. Immunohistochemical detection was carried out as described previously (Klimovich et al., 2018b). Briefly, polyps were relaxed in ice-cold urethane, fixed in 4% paraformaldehyde, incubated in blocking solution for 1 hr, and incubated further with the primary antibodies diluted to 1.0 µg/mL in blocking solution at 4°C. Following the protocol of Böttger and co-authors, tissue permeabilization steps were omitted to avoid detection of immature glycocalyx components within epithelial cells. Alexa Fluor 488-conjugated goat anti-rabbit antibodies (A11034, Thermo Fisher) and Alexa Fluor 546-conjugated goat anti-chicken anti-bodies (A11040, Thermo Fisher) were diluted to 2.0 µg/mL and incubations were carried out for 2 hr at room temperature. The samples were mounted into Mowiol supplemented with 1.0% DABCO antifade (D27802, Sigma). Confocal mid-body optical sections were captured using a Zeiss LSM900 laser scanning confocal microscope. To measure the glycocalyx thickness, the fluorescence profile across the ectoderm has been recorded and quantified for 10 transects, each 10 µm long, using Zen Blue v. 3.4.91 software (Zeiss).

GFP labeling of *Curvibacter* sp. AEP1.3

To visualize the colonization and dynamics during contraction events of *Curvibacter* sp. AEP1.3, we chromosomally integrated sfGFP behind the glmS-operon via the miniTn7-system as previously established by Wiles et al., 2018. The protocol was modified in order to manipulate the freshwater bacterium *Curvibacter* sp. AEP1.3 as follows: instead of the *Escherichia coli* SM10, we used the strain *E. coli* MFDpir as delivery system because bi- and triparental mating

was already observed (Wein et al., 2018; Ferrières et al., 2010). In addition, the growth medium was changed to the routinely used medium of *Curvibacter* sp. R2A and antibiotic concentration of the selection media was adjusted to 2 µg/mL.

Kinematics and fluid flow analysis

Fluid boundary layer visualization

The fluid boundary layer around *Hydra* was visualized as described previously (Nawroth et al., 2010; Nawroth and Dabiri, 2014). Briefly, animals were placed into custom-made cube-shaped acrylic containers filled with *Hydra* medium and allowed to acclimatize for 30 min. The fluid boundary layer was visualized using fluorescein dye (Sigma-Aldrich) added near *Hydra*'s head during inter-contraction periods using a transfer pipette. An LED light source was used to illuminate the dye from the side. Videos were recorded using a Sony HDR-SR12 camcorder (1440 × 1080 pixels, 30 frames per second; Sony Electronics, San Diego, CA) mounted to a tripod in front of the custom container. Videos were processed to enhance the contrast of the dye with respect to the background using Adobe Premiere Pro (San Jose, CA).

Fluid flow analysis

Fluid flow around *H. vulgaris* AEP polyps was quantified using particle image velocimetry under a stereo microscope as described previously (Nawroth et al., 2012). Briefly, *H. vulgaris* AEP polyps were placed in a custom-made acrylic container with glass walls filled with *Hydra*-medium that contained 1 µm green-fluorescent microspheres (Invitrogen). A violet laser pointer mounted on a custom micromanipulator stage was aligned with a plano-concave cylindrical lens with a focal length of -4 mm (Thorlabs, Newton, MA) to create an excitation light sheet that captured the particles in ca. 1 mm thick plane across or along the animal's body column. The green-emitting particles were recorded from top or side using a stereo microscope equipped with a long pass filter (to remove the violet excitation wavelength) and a camera (same as above) mounted to the eyepiece. Videos were recorded at 60 frames per second. We used MATLAB (MathWorks, Natick, MA) with an open-source code package (PIVlab Thielicke and Stamhuis, 2014) to measure the particle displacement field across the illuminated plane at each time point and derive the instantaneous planar flow velocity field. From this

vector field, the flow velocity magnitude (speed) profiles along lines extending perpendicular from *Hydra*'s surface (Figure 2E and F) were extracted to determine the fluid boundary layer thickness (Figure 2—figure supplement 5), defined here as the distance normal from the surface to the point in the fluid where flow velocity has reached 90% of free stream velocity (here assumed zero), as commonly done in biological systems (Vogel, 2020).

Acknowledgements

Research in the laboratory of TCGB was supported in part by grants from the Deutsche Forschungsgemeinschaft (DFG), the CRC 1182 'Origin and Function of Metaorganisms' (to TCGB) and the CRC 1461 'Neurotronics: Bio-Inspired Information Pathways' (Project-ID 434434223 – SFB 1461) (to TCGB and AK). AK is supported by a DFG grant KL3475/2-1. We thank the Central Microscopy Facility at the Biology Department of the University of Kiel for excellent technical support. TCGB appreciates support from the Canadian Institute for Advanced Research. JN and EK acknowledge support from the National Institute of Health grant 1R01 HL 15362201-A1 and the National Science Foundation INSPIRE grant 1608744.

Author contributions

Janna C Nawroth, Conceptualization, Data curation, Formal analysis, Validation, Investigation, Visualization, Methodology, Writing – original draft, Writing – review and editing; Christoph Giez, Data curation, Investigation, Visualization, Methodology, Writing – original draft, Writing – review and editing; Alexander Klimovich, Data curation, Formal analysis, Validation, Investigation, Visualization, Methodology, Writing – original draft, Writing – review and editing; Eva Kanso, Conceptualization, Formal analysis, Supervision, Funding acquisition, Validation, Investigation, Visualization, Methodology, Writing – original draft, Writing – review and editing; Thomas CG Bosch, Conceptualization, Formal analysis, Supervision, Funding acquisition, Investigation, Writing – original draft, Project administration, Writing – review and editing

References

- Augustin R, Schröder K, Murillo Rincón AP, Fraune S, Anton-Erxleben F, Herbst EM, Wittlieb J, Schwentner M, Grötzinger J, Wassenaar TM, Bosch TCG. 2017. A secreted antibacterial neuropeptide shapes the microbiome of hydra. *Nature Communications* 8:698. DOI: <https://doi.org/10.1038/s41467-017-00625-1>, PMID: 28951596
- Bayer FM, Lyonet P, Pronk C, van der Schley J, Trembley A. 1744. Mémoires pour Servir À L'Histoire d'un genre de Polypes D'Eau Douce, À Bras en forme de Cornes. *Memoire Sur Le Polypes* 1:1–404. DOI: <https://doi.org/10.5962/bhl.title.64073>
- Berg HC, Purcell EM. 1977. Physics of Chemoreception. *Biophysical Journal* 20:193–219. DOI: [https://doi.org/10.1016/S0006-3495\(77\)85544-6](https://doi.org/10.1016/S0006-3495(77)85544-6), PMID: 911982
- Bosch TCG. 2013. Cnidarian-microbe interactions and the origin of innate immunity in Metazoans. *Annual Review of Microbiology* 67:499–518. DOI: <https://doi.org/10.1146/annurev-micro-092412-155626>, PMID: 23808329
- Bosch TCG. 2014. Rethinking the role of immunity: lessons from Hydra. *Trends in Immunology* 35:495–502. DOI: <https://doi.org/10.1016/j.it.2014.07.008>, PMID: 25174994
- Bosch TCG, Klimovich A, Domazet-Lošo T, Gründer S, Holstein TW, Jékely G, Miller DJ, Murillo-Rincon AP, Rentzsch F, Richards GS, Schröder K, Technau U, Yuste R. 2017. Back to the basics: Cnidarians start to fire. *Trends in Neurosciences* 40:92–105. DOI: <https://doi.org/10.1016/j.tins.2016.11.005>, PMID: 28041633
- Bosch TCG, McFall-Ngai M. 2021. Animal development in the microbial world: re-thinking the conceptual framework. *Current Topics in Developmental Biology* 141:399–427. DOI: <https://doi.org/10.1016/bs.ctdb.2020.11.007>, PMID: 33602495
- Böttger A, Doxey AC, Hess MW, Pfaller K, Salvenmoser W, Deutzmann R, Geissner A, Pauly B, Altstätter J, Münder S, Heim A, Gabius H-J, McConkey BJ, David CN. 2012. Horizontal gene transfer contributed to the evolution of extracellular surface structures: the freshwater Polyp Hydra is covered by a complex fibrous Cuticle containing Glycosaminoglycans and proteins of the Ppod and Swt (sweet tooth) families. *PLOS ONE* 7:e52278. DOI: <https://doi.org/10.1371/journal.pone.0052278>, PMID: 23300632
- Callahan BJ, McMurdie PJ, Rosen MJ, Han AW, Johnson AJA, Holmes SP. 2016. Dada2: high-resolution sample inference from Illumina Amplicon data. *Nature Methods* 13:581–583. DOI: <https://doi.org/10.1038/nmeth.3869>, PMID: 27214047
- Carslaw HS, Jaeger JC. 1959. *Conduction of Heat in Solids* Clarendon Press.
- Cremer J, Segota I, Yang CY, Arnoldini M, Sauls JT, Zhang Z, Gutierrez E, Groisman A, Hwa T. 2016. Effect of flow and Peristaltic mixing on bacterial growth in a gut-like channel. *PNAS* 113:11414–11419. DOI: <https://doi.org/10.1073/pnas.1601306113>, PMID: 27681630
- Dobzhansky T. 1964. Biology, molecular and organismic. *American Zoologist* 4:443–452. DOI: <https://doi.org/10.1093/icb/4.4.443>, PMID: 14223586
- Fang J, Wang H, Zhou Y, Zhang H, Zhou H, Zhang X. 2021. Slimy partners: the mucus barrier and gut Microbiome in ulcerative colitis. *Experimental & Molecular Medicine* 53:772–787. DOI: <https://doi.org/10.1038/s12276-021-00617-8>, PMID: 34002011
- Ferrières L, Hémerly G, Nham T, Guérout AM, Mazel D, Beloin C, Ghigo JM. 2010. Silent mischief: Bacteriophage mu insertions contaminate products of Escherichia coli random Mutagenesis performed using suicidal Transposon delivery Plasmids mobilized by broad-host-range Rp4 Conjugative machinery. *Journal of Bacteriology* 192:6418–6427. DOI: <https://doi.org/10.1128/JB.00621-10>, PMID: 20935093
- Fischbach MA, Segre JA. 2016. Signaling in host-associated microbial communities. *Cell* 164:1288–1300. DOI: <https://doi.org/10.1016/j.cell.2016.02.037>, PMID: 26967294
- Franzenburg S, Walter J, Künzel S, Wang J, Baines JF, Bosch TC, Fraune S. 2013. Distinct antimicrobial peptide expression determines host species-specific bacterial associations. *PNAS* 110:E3730–E3738. DOI: <https://doi.org/10.1073/pnas.1304960110>, PMID: 24003149
- Fraune S, Anton-Erxleben F, Augustin R, Franzenburg S, Knop M, Schröder K, Willoweit-Ohl D, Bosch TCG. 2015. Bacteria-bacteria interactions within the Microbiota of the ancestral Metazoan Hydra contribute to fungal resistance. *The ISME Journal* 9:1543–1556. DOI: <https://doi.org/10.1038/ismej.2014.239>, PMID: 25514534

- Gill RC, Cote KR, Bowes KL, Kingma YJ. 1986. Human Colonic smooth muscle: spontaneous contractile activity and response to stretch. *Gut* 27:1006–1013. DOI: <https://doi.org/10.1136/gut.27.9.1006>, PMID: 3758812
- Gilpin W, Prakash VN, Prakash M. 2017. Vortex arrays and Ciliary tangles underlie the feeding–swimming trade-off in Starfish larvae. *Nature Physics* 13:380–386. DOI: <https://doi.org/10.1038/nphys3981>
- Ginestet C. 2011. Ggplot2: elegant Graphics for data analysis. *Journal of the Royal Statistical Society Series A* 174:245–246. DOI: https://doi.org/10.1111/j.1467-985X.2010.00676_9.x
- Hadizadeh F, Walter S, Belheouane M, Bonfiglio F, Heinsen FA, Andreasson A, Agreus L, Engstrand L, Baines JF, Rafter J, Franke A, D'Amato M. 2017. Stool frequency is associated with gut Microbiota composition. *Gut* 66:559–560. DOI: <https://doi.org/10.1136/gutjnl-2016-311935>, PMID: 27196592
- Han S, Taralova E, Dupre C, Yuste R. 2018. Comprehensive machine learning analysis of Hydra behavior reveals a stable basal behavioral repertoire. *eLife* 7:e32605. DOI: <https://doi.org/10.7554/eLife.32605>, PMID: 29589829
- Janssen PWM, Lentle RG, Asvarujanon P, Chambers P, Stafford KJ, Hemar Y. 2007. Characterization of flow and mixing regimes within the ileum of the Brushtail possum using residence time distribution analysis with simultaneous Spatio-temporal mapping. *The Journal of Physiology* 582:1239–1248. DOI: <https://doi.org/10.1113/jphysiol.2007.134403>, PMID: 17495038
- Kanaya HJ, Kobayakawa Y, Itoh TQ. 2019. Hydra Vulgaris exhibits day-night variation in behavior and gene expression levels. *Zoological Letters* 5:10. DOI: <https://doi.org/10.1186/s40851-019-0127-1>, PMID: 30891311
- Kerney R. 2021. Developing inside a layer of germs—a potential role for Multiciliated surface cells in vertebrate embryos. *Diversity* 13:527. DOI: <https://doi.org/10.3390/d13110527>
- Klimovich AV, Bosch TCG. 2018a. Rethinking the role of the nervous system: lessons from the Hydra Holobiont. *BioEssays* 40:e1800060. DOI: <https://doi.org/10.1002/bies.201800060>, PMID: 29989180
- Klimovich A, Rehm A, Wittlieb J, Herbst EM, Benavente R, Bosch TCG. 2018b. Non-Senescent Hydra Tolerates severe disturbances in the nuclear Lamina. *Aging* 10:951–972. DOI: <https://doi.org/10.18632/aging.101440>, PMID: 29754147
- Klimovich A, Wittlieb J, Bosch TC. 2019. Transgenesis in Hydra to characterize gene function and visualize cell behavior. *Nature Protocols* 14:2069–2090. DOI: <https://doi.org/10.1038/s41596-019-0173-3>, PMID: 31160787
- Klimovich A, Giacomello S, Björklund Å, Faure L, Kaucka M, Giez C, Murillo-Rincon AP, Matt A-S, Willoweit-Ohl D, Crupi G, de Anda J, Wong GCL, D'Amato M, Adameyko I, Bosch TCG. 2020. Prototypical pacemaker neurons interact with the resident Microbiota. *PNAS* 117:17854–17863. DOI: <https://doi.org/10.1073/pnas.1920469117>, PMID: 32647059
- Koch TR, Carney JA, Go VL, Szurszewski JH. 1988. Spontaneous contractions and some electrophysiologic properties of circular muscle from normal sigmoid colon and ulcerative colitis. *Gastroenterology* 95:77–84. DOI: [https://doi.org/10.1016/0016-5085\(88\)90293-4](https://doi.org/10.1016/0016-5085(88)90293-4), PMID: 3371626
- Kornder NA, Esser Y, Stoupin D, Leys SP, Mueller B, Vermeij MJA, Huisman J, de Goeij JM. 2022. Sponges sneeze mucus to shed particulate waste from their seawater inlet pores. *Current Biology* 32:3855–3861. DOI: <https://doi.org/10.1016/j.cub.2022.07.017>, PMID: 35952668
- Kostic AD, Xavier RJ, Gevers D. 2014. The Microbiome in inflammatory bowel disease: Current status and the future ahead. *Gastroenterology* 146:1489–1499. DOI: <https://doi.org/10.1053/j.gastro.2014.02.009>, PMID: 24560869
- Kremien M, Shavit U, Mass T, Genin A. 2013. Benefit of pulsation in soft corals. *PNAS* 110:8978–8983. DOI: <https://doi.org/10.1073/pnas.1301826110>, PMID: 23610420
- Love MI, Huber W, Anders S. 2014. Moderated estimation of fold change and dispersion for RNA-Seq data with Deseq2. *Genome Biology* 15:550. DOI: <https://doi.org/10.1186/s13059-014-0550-8>, PMID: 25516281

- McMurdie PJ, Holmes S. 2013. Phyloseq: an R package for reproducible interactive analysis and graphics of Microbiome census data. *PLOS ONE* 8:e61217. DOI: <https://doi.org/10.1371/journal.pone.0061217>, PMID: 23630581
- Murillo-Rincon AP, Klimovich A, Pemöller E, Taubenheim J, Mortzfeld B, Augustin R, Bosch TCG. 2017. Spontaneous body contractions are modulated by the Microbiome of Hydra. *Scientific Reports* 7:15937. DOI: <https://doi.org/10.1038/s41598-017-16191-x>, PMID: 29162937
- Ñahui Palomino RA, Vanpouille C, Costantini PE, Margolis L. 2021. Microbiota–host communications: bacterial extracellular Vesicles as a common language. *PLOS Pathogens* 17:e1009508. DOI: <https://doi.org/10.1371/journal.ppat.1009508>, PMID: 33984071
- Nawroth JC, Feitl KE, Colin SP, Costello JH, Dabiri JO. 2010. Phenotypic plasticity in juvenile Jellyfish Medusae facilitates effective animal–fluid interaction. *Biology Letters* 6:389–393. DOI: <https://doi.org/10.1098/rsbl.2010.0068>
- Nawroth JC, Lee H, Feinberg AW, Ripplinger CM, McCain ML, Grosberg A, Dabiri JO, Parker KK. 2012. A tissue-engineered Jellyfish with Biomimetic propulsion. *Nature Biotechnology* 30:792–797. DOI: <https://doi.org/10.1038/nbt.2269>, PMID: 22820316
- Nawroth JC, Dabiri JO. 2014. Induced drift by a self-propelled swimmer at intermediate Reynolds numbers. *Physics of Fluids* 26:091108. DOI: <https://doi.org/10.1063/1.4893537>
- Nawroth JC, Guo H, Koch E, Heath-Heckman EAC, Hermanson JC, Ruby EG, Dabiri JO, Kanso E, McFall-Ngai M. 2017. Motile cilia create fluid-mechanical Microhabitats for the active recruitment of the host Microbiome. *PNAS* 114:9510–9516. DOI: <https://doi.org/10.1073/pnas.1706926114>, PMID: 28835539
- Oksanen J, Blanchet FG, Kindt R, Legendre P, McGlinn D, Minchin PR, O'Hara RB, Simpson GL, Solymos P, Stevens MHH, Szöcs E, Wagner H. 2013. *Vegan*. 0ddfa4e. Github. <https://github.com/vegandevs/vegan>
- Pepper RE, Roper M, Ryu S, Matsudaira P, Stone HA. 2010. Nearby boundaries create eddies near microscopic filter feeders. *Journal of the Royal Society, Interface* 7:851–862. DOI: <https://doi.org/10.1098/rsif.2009.0419>, PMID: 19942677
- Purcell EM. 1977. Life at low Reynolds number. *American Journal of Physics* 45:3–11. DOI: <https://doi.org/10.1119/1.10903>
- Rausch P, Basic M, Batra A, Bischoff SC, Blaut M, Clavel T, Gläsner J, Gopalakrishnan S, Grassl GA, Günther C, Haller D, Hirose M, Ibrahim S, Loh G, Mattner J, Nagel S, Pabst O, Schmidt F, Siegmund B, Strowig T, et al. 2016. Analysis of factors contributing to variation in the C57Bl/6J fecal Microbiota across German animal facilities. *International Journal of Medical Microbiology* 306:343–355. DOI: <https://doi.org/10.1016/j.ijmm.2016.03.004>, PMID: 27053239
- Rich A. 2018. Improved imaging of Zebrafish motility. *Neurogastroenterology and Motility* 30:e13435. DOI: <https://doi.org/10.1111/nmo.13435>, PMID: 30240125
- Rillig MC, Ryo M, Lehmann A, Aguilar-Trigueros CA, Buchert S, Wulf A, Iwasaki A, Roy J, Yang G. 2019. The role of multiple global change factors in driving soil functions and microbial Biodiversity. *Science* 366:886–890. DOI: <https://doi.org/10.1126/science.aay2832>, PMID: 31727838
- Ross SM. 2014. *Introduction to Probability Models* Academic press.
- Rushforth NB, Burnett AL, Maynard R. 1963. Behavior in Hydra: contraction responses of Hydra Pirardi to mechanical and light stimuli. *Science* 139:760–761. DOI: <https://doi.org/10.1126/science.139.3556.760>
- Samson JE, Miller LA, Ray D, Holzman R, Shavit U, Khatri S. 2019. A novel mechanism of mixing by pulsing corals. *The Journal of Experimental Biology* 222:jeb192518. DOI: <https://doi.org/10.1242/jeb.192518>, PMID: 31315935
- Schierwater B, Murtha M, Dick M, Ruddle FH, Buss LW. 1991. Homeoboxes in Cnidarians. *The Journal of Experimental Zoology* 260:413–416. DOI: <https://doi.org/10.1002/jez.1402600316>, PMID: 1683896
- Schindelin J, Arganda-Carreras I, Frise E, Kaynig V, Longair M, Pietzsch T, Preibisch S, Rueden C, Saalfeld S, Schmid B, Tinevez J-Y, White DJ, Hartenstein V, Eliceiri K, Tomancak P, Cardona

- A. 2012. Fiji: an open-source platform for biological-image analysis. *Nature Methods* 9:676–682. DOI: <https://doi.org/10.1038/nmeth.2019>, PMID: 22743772
- Nawroth, Giez et al. *eLife* 2023;12:e83637. DOI: <https://doi.org/10.7554/eLife.83637> 22 of 23
- Schlichting H, Gersten K. 2000. *Boundary-Layer Theory* Berlin, Heidelberg: Springer. DOI: <https://doi.org/10.1007/978-3-642-85829-1>
- Schröder K, Bosch TCG. 2016. The origin of Mucosal immunity: lessons from the Holobiont Hydra. *MBio* 7:e01184-16. DOI: <https://doi.org/10.1128/mBio.01184-16>, PMID: 27803185
- Scott LD, Cahall DL. 1982. Influence of the Interdigestive Myoelectric complex on Enteric Flora in the rat. *Gastroenterology* 82:737–745. DOI: [https://doi.org/10.1016/0016-5085\(82\)90320-1](https://doi.org/10.1016/0016-5085(82)90320-1)
- Segata N, Izard J, Waldron L, Gevers D, Miropolsky L, Garrett WS, Huttenhower C. 2011. Metagenomic biomarker discovery and explanation. *Genome Biology* 12:R60. DOI: <https://doi.org/10.1186/gb-2011-12-6-r60>, PMID: 21702898
- Swaminathan M, Hill-Yardin E, Ellis M, Zygorodimos M, Johnston LA, Gwynne RM, Bornstein JC. 2016. Video imaging and Spatiotemporal maps to analyze gastrointestinal motility in mice. *Journal of Visualized Experiments* 1:53828. DOI: <https://doi.org/10.3791/53828>, PMID: 26862815
- Thielicke W, Stamhuis EJ. 2014. Pivlab—towards user-friendly, affordable and accurate Digital particle image Velocimetry in Matlab. *Journal of Open Research Software* 2:jors.bl. DOI: <https://doi.org/10.5334/jors.bl>
- Thorn RMS, Greenman J. 2012. Microbial volatile compounds in health and disease conditions. *Journal of Breath Research* 6:024001. DOI: <https://doi.org/10.1088/1752-7155/6/2/024001>, PMID: 22556190
- Thurber AR, Jones WJ, Schnabel K. 2011. Dancing for food in the deep sea: bacterial farming by a new species of Yeti crab. *PLOS ONE* 6:e26243. DOI: <https://doi.org/10.1371/journal.pone.0026243>, PMID: 22140426
- Tinevez J-Y, Perry N, Schindelin J, Hoopes GM, Reynolds GD, Laplantine E, Bednarek SY, Shorte SL, Eliceiri KW. 2017. Trackmate: an open and extensible platform for single-particle tracking. *Methods* 115:80–90. DOI: <https://doi.org/10.1016/j.ymeth.2016.09.016>, PMID: 27713081
- Toskes PP. 1993. Bacterial overgrowth of the gastrointestinal tract. *Advances in Internal Medicine* 38:387–407 PMID: 8438647.
- Trojanowski NF, Raizen DM, Fang-Yen C. 2016. Pharyngeal pumping in *Caenorhabditis elegans* depends on tonic and Phasic signaling from the nervous system. *Scientific Reports* 6:22940. DOI: <https://doi.org/10.1038/srep22940>, PMID: 26976078
- Vandeputte D, Falony G, Vieira-Silva S, Tito RY, Joossens M, Raes J. 2016. Stool consistency is strongly associated with gut Microbiota richness and composition, Enterotypes and bacterial growth rates. *Gut* 65:57–62. DOI: <https://doi.org/10.1136/gutjnl-2015-309618>, PMID: 26069274
- Vogel S. 2020. *Life in Moving Fluids: The Physical Biology of Flow-Revised And* Princeton University Press. DOI: <https://doi.org/10.2307/j.ctvzsmfc6>
- Wein T, Dagan T, Fraune S, Bosch TC, Reusch TB, Hülter NF. 2018. Carrying capacity and Colonization Dynamics of *Curvibacter* in the Hydra host habitat. *Frontiers in Microbiology* 9:443. DOI: <https://doi.org/10.3389/fmicb.2018.00443>
- Wheeler JD, Secchi E, Rusconi R, Stocker R. 2019. Not just going with the flow: the effects of fluid flow on bacteria and Plankton. *Annual Review of Cell and Developmental Biology* 35:213–237. DOI: <https://doi.org/10.1146/annurev-cellbio-100818-125119>, PMID: 31412210
- Wiles TJ, Wall ES, Schlomann BH, Hay EA, Parthasarathy R, Guillemin K. 2018. Modernized tools for streamlined genetic manipulation and comparative study of wild and diverse Proteobacterial lineages. *MBio* 9:e01877-18. DOI: <https://doi.org/10.1128/mBio.01877-18>, PMID: 30301859
- Wittlieb J, Khalturin K, Lohmann JU, Anton-Erxleben F, Bosch TC. 2006. Transgenic Hydra allow in vivo tracking of individual stem cells during Morphogenesis. *PNAS* 103:6208–6211. DOI: <https://doi.org/10.1073/pnas.0510163103>, PMID: 16556723

Yamamoto W, Yuste R. 2020. Whole-body imaging of neural and muscle activity during behavior in *Hydra Vulgaris*: effect of Osmolarity on contraction bursts. *ENeuro* 7:ENEURO.0539-19.2020. DOI: <https://doi.org/10.1523/ENEURO.0539-19.2020>, PMID: 32699071

Chapter III:

Multiple neuronal populations control the eating behavior in *Hydra* and are responsive to microbial signals

Accepted in *Current Biology* (2023)

Christoph Giez^{1*}, Denis Pinkle¹, Yan Giencke¹, Jörg Wittlieb¹, Eva Herbst¹, Tobias Spratte², Tim Lachnit¹, Alexander Klimovich¹, Christine Selhuber-Unkel², Thomas Bosch^{1*}

1. Zoological Institute, University of Kiel, Christian-Albrechts-Platz 4, 24118 Kiel, Germany
2. Institute For Molecular Systems Engineering and Advanced Materials (INSEAM), University Heidelberg, Im Neuenheimer Feld 225, 69120 Heidelberg, Germany

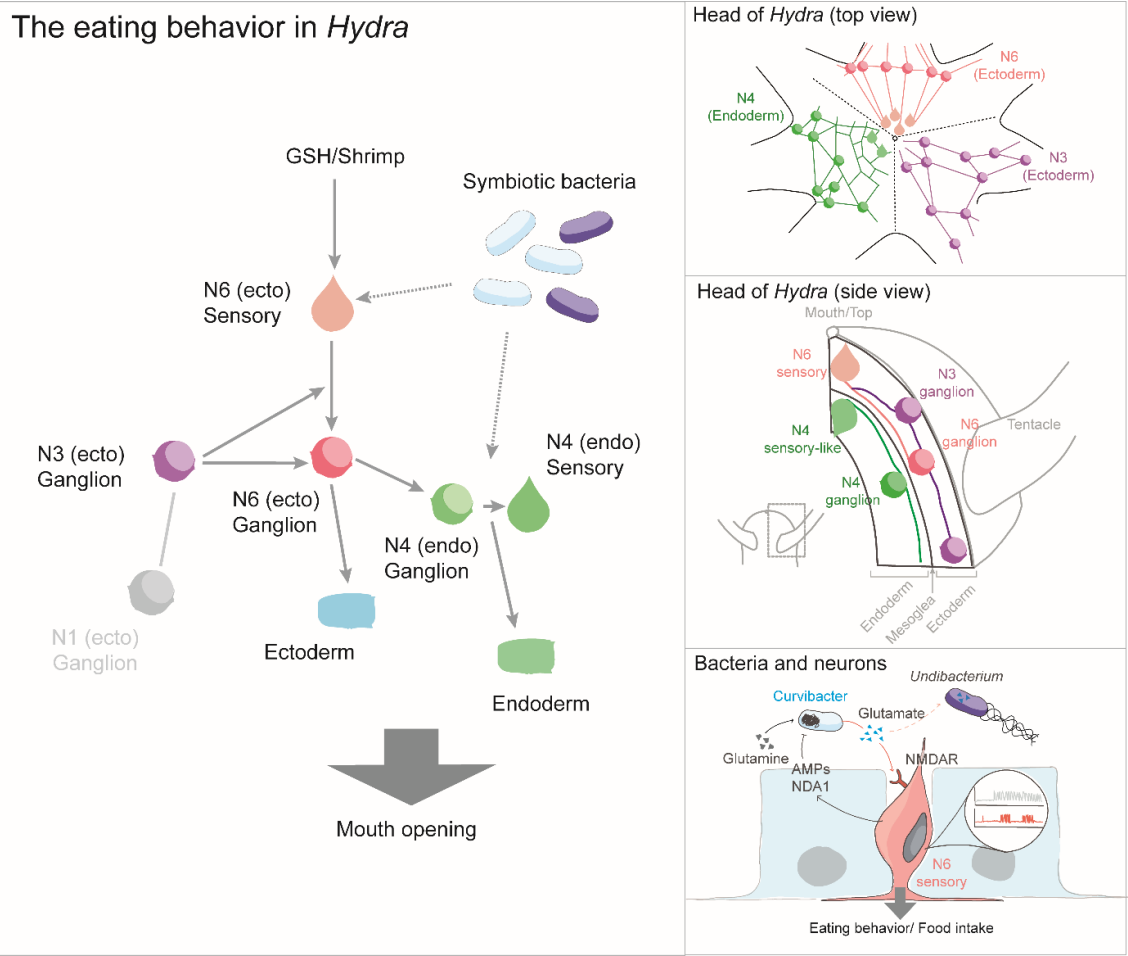
***Corresponding Authors:**

Christoph Giez, cgiez@zoologie.uni-kiel.de

Thomas C.G. Bosch, tbosch@zoologie.uni-kiel.de

DOI: doi.org/10.1101/2023.04.28.538719

Graphical abstract



Summary

Although recent studies indicate the impact of microbes on the central nervous systems and behavior, it remains unclear how the relationship between the functionality of the nervous system, behavior and the microbiota arise. We studied the eating behavior of *Hydra*, a host that has a simple nervous system and a low-complexity microbiota. To identify the neuronal subpopulations involved, we used a subpopulation specific cell ablation system and calcium imaging. The role of the microbiota was uncovered by reducing the diversity of the natural microbiota. Here, we demonstrate that different neuronal subpopulations are functioning together to control the eating behavior. The microbiota participates in control of the eating behavior since germ-free or mono-colonized animals have drastic difficulties in mouth opening. This was restored by adding a full complement of the microbiota. In summary, we provide a mechanistic explanation of how the eating behavior is controlled in *Hydra* and how microbes can affect the neuronal circuit.

Highlights

- Multiple neuronal modules and their networks control complex behavior in an animal lacking a central nervous system.
- Its associated microbes participate in these neuronal circuits and influence the eating behavior.
- Disorganization of the microbiota negatively impacts this eating behavior.
- Glutamate participates in an evolutionary ancient interkingdom language.

Keywords

Microbiota, eating, evolution, nervous system, Hydra, Cnidaria

Introduction

Understanding the neuronal basis of any behavior is a challenging task, given the complex interplay between neuronal circuits and the internal state of the organism such as hunger, fear or motivation^{1,2}. The neuronal basis for behavior has been studied in various animal hosts. In *Drosophila* larvae, food deprivation shapes the olfactory behavior, highlighting the role of state-dependent neuronal circuits in dynamic behaviors³. Another example is the mating and aggression behavior in mice and flies, where a small number of neurons appear to control both behaviors in a state-dependent manner⁴. To add another level of complexity, gut microbes can affect behavior as well as activity of the nervous system^{5–9}. For instance, the gut microbiota can affect aggression, fear, motivation, hunger, and emotional behaviors^{10–18}. However, how microbes actively regulate the nervous system and thereby affect internal states and behaviors remains mostly unknown. It can be expected that the myriad of neurochemicals produced by microbes that live in close association with their host can influence neuronal activity. For example, components of the bacterial cell wall such as muropeptides produced by the gut microbiota of mice are sensed by neurons expressing the Nod2 receptor in a specific region of the brain, which affects feeding behavior¹⁹.

Ideally, the complex interaction between behavior, internal state and microbes should be studied in a host that displays complex behavioral patterns, but also has a simple nervous system and a microbiota that is not too complex. Such a host is *Hydra* (Fig. 1A), a member of the phylum Cnidaria, which forms the sister group to the Bilateria in the Eumetazoa clade, which includes one of the earliest animals with a nervous system (Fig. 1B)²⁰. The nervous system of *Hydra* is composed of only two main neuronal cell types based on morphology, sensory and ganglion cells, that form a nerve net in the ectoderm and endoderm, respectively^{21–23}. The associated microbiota colonizes the glycocalyx a mucus-like structure that overlays the ectoderm and has direct contact to ectodermal sensory cells (Fig. 1C). There is no cephalization or ganglion formation, but regions along the body column have higher or lower densities of specific neuronal subpopulations (Fig. 1D)^{24,25}. These represent non-overlapping neuronal networks with differential activity²⁶. Already in 1744, Abraham Trembley recognized that *Hydra*'s behavior can be either spontaneous (such as contractions) or stimuli-evoked²⁷. An example of the latter is the eating behavior, schematically shown in Fig. 1E, that can be induced by food or food-associated

molecules such as reduced glutathione (GSH)^{28,29}. The pattern is stereotypical and consists of three different stages: tentacle writhing, tentacle ball formation, and mouth opening³⁰ (Fig. 1E, F, Suppl. Video 1). In animals without nerve cells this behavior is completely absent³¹. Previous work had indicated that neurons in the head region and not in the body column or tentacles were involved in the eating behavior^{32,33}. More recently, single cell RNA sequencing had identified different neuronal subpopulations including those in the head^{24,25,34}. This elaborate behavior also responds to an internal state, since a food stimulus given to well-fed animals does not result in a complete eating behavior response^{28,29,35}.

Interestingly, microbes present in the glycocalyx are in direct contact with the ectodermal sensory neurons (Fig. 1C)³⁶. Previous studies highlighted the capability of *Hydra*'s nervous system to sense and regulate this bacterial community^{25,36}. For instance, it was observed that by depriving *Hydra* of its microbial symbionts, spontaneous behaviors such as body contractions become less frequent³⁷.

Here, we studied the neuronal activity in freely moving *Hydra* during eating behavior, to uncover the neural circuitry involved. For this, we traced activity of individual neuronal populations using calcium imaging and interrogated their function using cell ablation approach. This revealed that *Hydra*'s eating behavior is controlled by multiple subpopulations of neurons that are activated in a temporally and spatially ordered manner, ultimately leading to mouth opening. In complete absence of microbes (germ-free animals) the mouth opening duration is significantly shortened. Adding the full complement of microbes back, restores this defect. Animals' mono-colonized with the major colonizer *Curvibacter* sp., also shows severe defect in mouth opening, possibly caused by the production of glutamate. The results demonstrate how, in an animal without a central nervous system, multiple networks of neuronal subpopulations form a neuronal circuit to control a complex behavior. Furthermore, the specific spatiotemporal pattern of neuron activity integrates specific microbial signals, demonstrating that eating behavior does not solely depend on the neuronal state of hunger or satiety: the bacterial community also modulates the neuronal circuits and their state. The evolutionary importance of these observations is discussed.

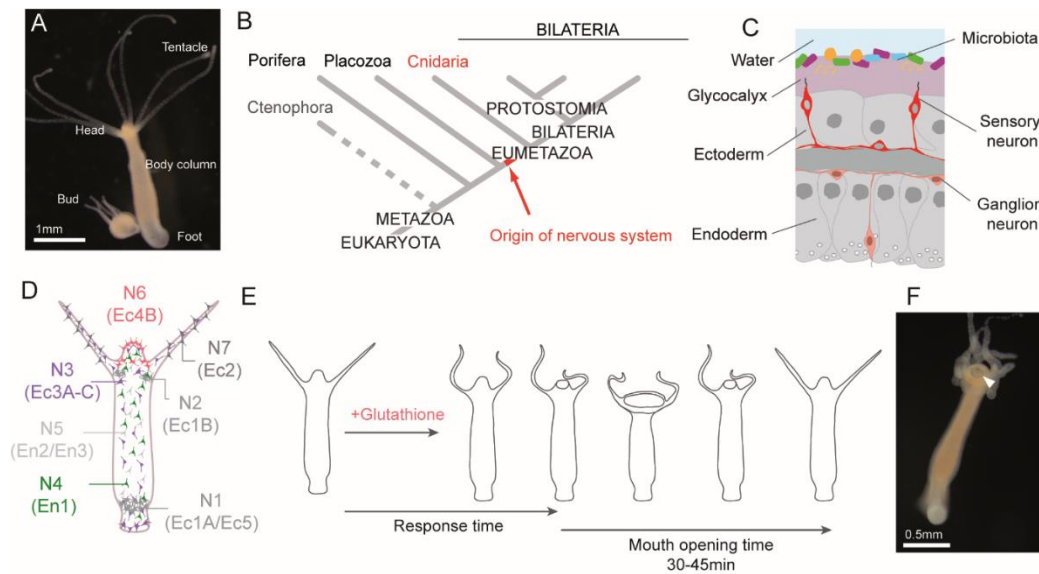


Figure 1. *Hydra vulgaris* AEP as a model system to study neuro-bacteria interactions.

A. *Hydra* polyp with a forming bud (asexual reproduction). Scale 1mm.

B. Phylogenetic position of *Hydra* in the phylum of Cnidaria which is the sister group of the Bilateria.

C. Tissue organization and localization of microbiota on the glycocalyx at the outside of the polyp.

D. Schematic presentation of the seven neuronal subpopulations and their distribution (after Siebert *et al.* 2019 and Klimovich *et al.* 2020)^{24,25}. The alternative nomenclature includes Ec for ectoderm and En for endoderm. The head region contains N6, N3 and N4 neurons.

E. The eating behavior of *Hydra* towards glutathione as defined by Loomis and Lenhoff^{28,29}. It can be quantified by the response time between stimulus and onset of mouth opening or tentacle movement, and by the duration of the mouth-opening time.

F. Picture of *Hydra* with an opened mouth (white arrow) and tentacles forming a ball shape that is typical of eating behavior. Scale 0.5mm.

Results:

Visualization of the neuronal subpopulations in the head of *Hydra*

First, we confirmed the old observation^{32,33} that *Hydra* polyps still open their mouths after the removal of both body column and tentacles (see suppl. Video V2), confirming that this property depended on head-specific neuronal regulation.

To visualize the various head specific neuronal subpopulations in *Hydra*, we produced multiple transgenic lines using subpopulation specific genes based on available single cell atlases. For this, we used the promoters of specifically

expressed genes, based on available single cell data sets of *Hydra*^{24,25} (See suppl. Fig. S1). The RFamide neuropeptide, (RFa, preprohormone-B, transcript ID²⁴: t2059aep) is exclusively expressed in the ectodermal subpopulation N6^{38–41}. The genetic target for the ectodermal subpopulation N3 is the neuropeptide Hym-355 (transcript ID: t12874aep)⁴². The marker for the endodermal neuronal subpopulation N4 is annotated as neurogenic differentiation factor 1-like (e-value: 3.03E-140, t14976aep). Their respective promoters were used in expression constructs to either drive the expression of a calcium indicator (GCaMP6s)^{26,43} or for the NTR-MTZ cell specific ablation approach (NTR-MTZ, explained below)^{44,45}.

Microscopic investigations of transgenic lines confirmed that the neuronal N6 subpopulation consists of two morphologically different cell types: sensory cells present in a dense cluster in the tip of the head where the mouth will form during feeding, and ganglion cells located in small packages at the basis of the head, close to where the tentacles originate (Fig. 2A-G). These two neuronal N6 types are interconnected by neurites that form radial functional connections (Fig. 2B, Suppl. Fig. 2). The ganglion cells are frequently circularly connected as well (Fig. 2B, F). A two-dimensional density plot confirmed the concentrated presence of N6 cells at the tip and the base of the head (Fig. 2G). In contrast, N3 neurons are found throughout the body (Fig. 2H). The spatial organization of N3 in the tip of the head is circular around the mouth region (Fig. 2I, K, L). Their density increases at the basis of the head (Fig. 2I-L). N4 neurons in the head reach the highest density at the base and between tentacles, while around the mouth their density is lower (Fig. 2M-S). The morphology of N4 neurons differs between body parts: around the mouth, the N4 neurites form a spider-web structure (Fig. 2R) with a morphology very similar to sensory cells (Fig. 2O, Suppl. Video 8). We call these N4 neurons sensory-like cells.

The density of N3 neurons was found the highest in the foot, followed by the head, whereas in the body column their density was lower (Fig. 2T). In contrast, most N4 neurons were present in the head with lower and similar numbers in body and foot (Fig. 2U). The distribution of the three neuron subpopulations (N6, N4 and N3) and their neurite networks in the head is summarized in Figure 2V. The individual subpopulations have a clear spatial distribution creating an ordered structure and resulting in a network of nerves with a relatively high complexity in the head region.

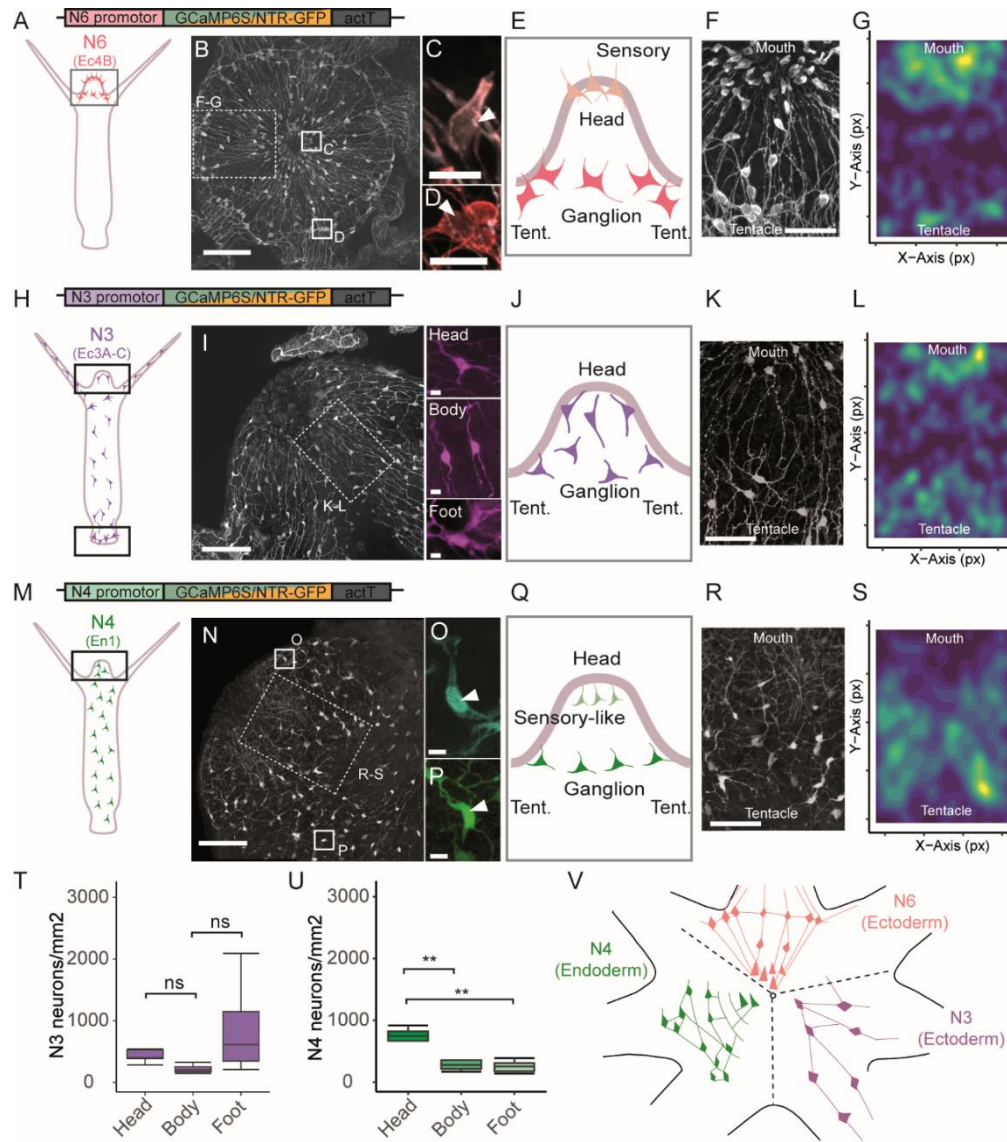


Figure 2. Visualization of the neuronal subpopulations in the head of *Hydra*.

A-G. Distribution, structure and morphology of ectodermal neuronal subpopulation N6. The constructs used for visualization and manipulation of N6 contains the promoter from an RFa neuropeptide (t2059aep, HVAEP9.T017227.1) regulating the expression of either GCaMP6S or NTR-GFP. **A:** Schematic of *Hydra* and the localization of N6 neurons. **B:** Immunohistochemistry of N6 neurons in the head (scale 100µm) stained with antibodies against GCaMP6S/GFP. **C-D:** Staining (artificial color added) of two representative enlargements showing the two different types of N6 neurons, with sensory neurons at the head tip (**C**) and ganglion neurons (**D**) found in groups around the head base (scale 10µm), as schematically presented in **E**. **F:** enlarged section of **A** with the neurites connecting the neurons (scale 50 µm). **G:** 2D-density plot of the distribution of neurons in a slice of the head (n=5). Higher densities of N6 neurons are present near the mouth and near the basis of the tentacles.

H-L. Ectodermal neuronal subpopulation N3, for which the construct included the promoter of the neuropeptide Hym-355 (t12874aep, HVAEP2.T004115.1). **H:** Schematic of the localization of N3 neurons in the head (**I**, scale 100µm) and in the body, tentacles and foot (scale 10µm). Their distribution in the head is summarized in **J**, with an enlarged section shown in **K** (scale 50µm). Higher densities are present in the tip and basis of the head (**L**, n=12).

M–S. Endodermal neuronal subpopulation N4 with the construct containing the promoter of a NEUROD1-like protein (t14976aep, HVAEP4.T008286.1). **M:** the localization of N4 neurons in the polyp. **N:** Overview of N4 neurons in the head (scale 100µm). **O–P:** Staining (artificial color added) of two representative enlargements showing the two different types of N4 neurons, with sensory-like neurons (**O**) and ganglion neurons (**P**, scale 10µm). In the head region, they are mostly present at the basis of the tentacles (**Q, R**, scale 50µm) with a lower density at the tip of the head (**S**, n=10).

T–U. Density of neurons/mm² in head, body and foot, for subpopulation N3 (**T**) and N4 (**U**). Highest densities of the latter are found in the head ($p < 0.01$, $n = 5-11$, ANOVA, Turkey post-hoc test).

V. Schematic representation of the distribution and organization of the different neuron subpopulations in the head, from tip (center) to tentacle base. The overlapping locations of the three subpopulations are separated here for clarity.

* $p \leq 0.05$; ** $p \leq 0.01$; *** $p \leq 0.001$

N6, N3 and N4 neurons are differentially active during the mouth opening

Animals were observed during mouth opening as part of their eating behavior and neuronal activity of head neurons was analyzed. The signals for the distinct sensory and ganglion cell types of N6 and N4 were recorded separately. Following the glutathione (GSH) stimulus, the mouth started to open by contraction of the epithelia³², which was recorded by plotting mouth width (Fig. 3A-C). After GSH stimulation, the first signal was recorded within 16.8 ± 26.5 s ($n = 6$) for N6 sensory cells, whereas the N6 ganglion cells responded 9.3 ± 5.3 s later (Fig. 3A, suppl. Video 3-4), at which time point the mouth started to open. As mouth opening continued, N6 cells activity slowly decreased (Fig. 3A). This was in contrast to the activity of N3 neurons, which at first sight seemed unresponsive to the GSH stimulus, both in the head and the foot region (Fig. 3B, suppl. Video 5-6). The N4 neurons responded strongly to the GSH stimulus. A faster response was observed for the N4 ganglion cells located at the base of the head, with a slightly slower response of the N4 sensory-like neurons (Fig. 3C, suppl. Video 7-8). After the delayed response of the N4 subpopulation, around 30s, the whole cell population started to spike in a synchronous manner (Fig. 3C, suppl. Fig. 4).

Interestingly, N3 neurons responded opposite to N4 to GSH stimulus, as their spiking frequency decreased significantly ($p < 0.001$, Fig. 3D-E). In individual polyps with a relatively frequent N3 spiking at the baseline (Fig. 3D), this became less frequent after glutathione administration. In individual polyps with a low baseline frequency, the firing of N3 neurons stopped completely (Fig. 3D). This was stepwise restored to higher frequencies in the late and end phase of feeding (330-420s post-stimulus and ~1800sec). In contrast to N3, the spiking frequency

of N4 neurons dramatically increased in response to GSH (Fig. 3F) and remained high during late phase of feeding (Fig. 3G). Since N6 cells did not produce pulses but showed continuous signal which increases or decreases (Fig3A), an analysis of the spiking frequency could not be performed.

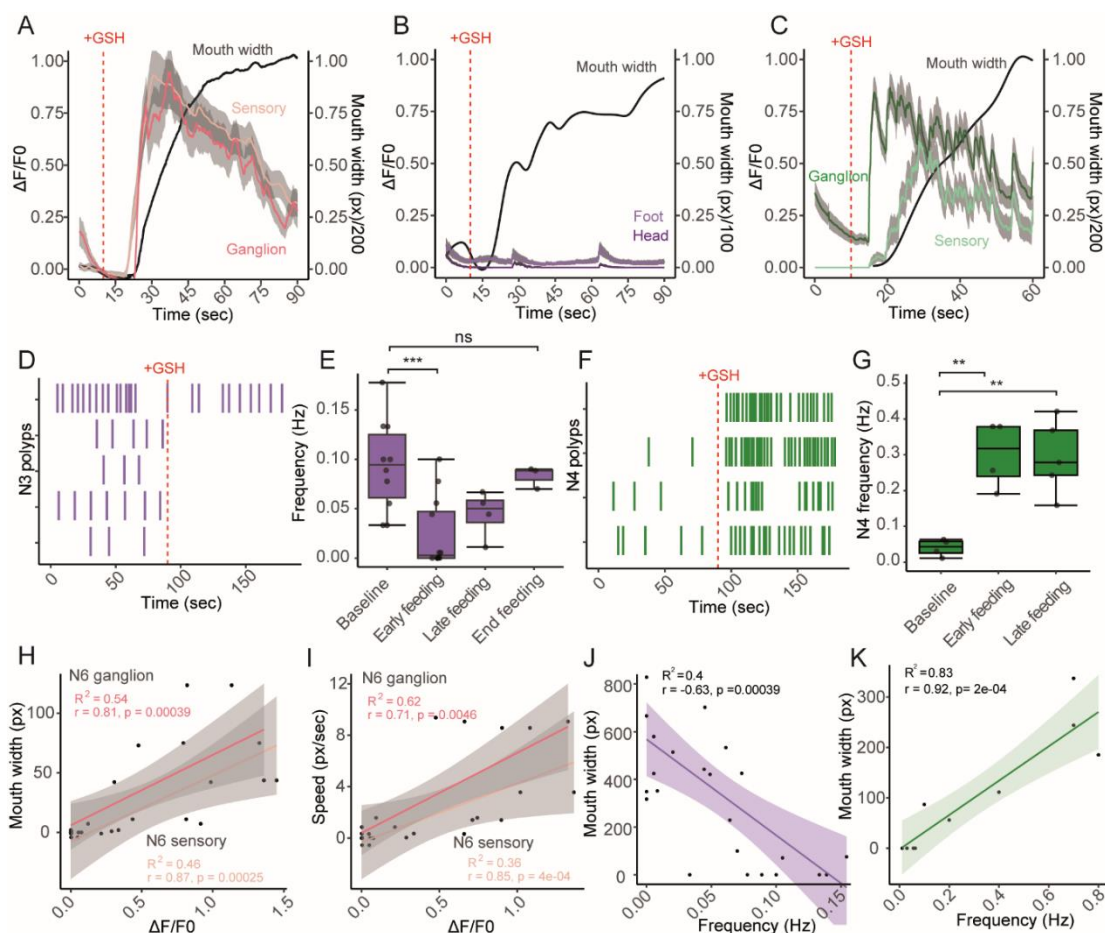


Figure 3. Neuronal response during the eating behavior.

A-C. Response of neuron subpopulations to a glutathione food stimulus. **A:** N6 neurons were differentiated into the sensory (red line) and ganglion cells (orange line). The sensory cells responded the ganglion neurons did. Lines represent the mean of either sensory or ganglion neuronal population from one representative animals with grey shading showing the standard deviation (see **suppl Fig. 3** for more animals). At the same time, mouth width was recorded (black line, in pixel). **B:** the spiking activity of N3 neurons in the head and foot was less obviously affected by glutathione administration. A slightly higher fluorescence change and baseline activity was recorded for neurons in the foot than in the head (one representative animal, see **suppl Fig. 4** for more animals). **C:** N4 neurons in the head responded strongly to glutathione administration, with a delay for the sensory cells (mean of population: light green line, light grey shading), whose reaction was also weaker than for the ganglion N4 neurons (dark green line, dark shading, one representative animal, see **suppl. Fig. 3** for more animals).

D-G. Spiking frequency of N3 and N4 neurons before and after glutathione administration. **D:** the spiking activity of N3 in 5 individual polyps decreased in frequency or stopped altogether after the GSH stimulus. **E:** the spiking frequency of N3 neurons at baseline (90s before glutathione, n=10) was significantly lowered during the early feeding response and mouth opening (0-90s post glutathione, n=10) and was restored during the later and end feeding response (late: 330-420s post

glutathione, n= 5; end: >1800sec, n=3). **F**: the spiking frequency of N4 neurons increased dramatically after glutathione administration (n= 4). **G**: This increase compared to baseline (n=4) was highly significant during early feeding (n=4, $p<0.01$, ANOVA, Turkey post-hoc test) and persisted during the late feeding response (n=4, $p<0.01$, ANOVA, Turkey post-hoc test).

H-K. Linear correlations of neuronal activity from before and after adding GSH with either mouth width or mouth opening speed. **H**. A positive correlation was found between N6 ganglion and sensory cells with mouth width (**H**, n=7) as well as with mouth opening speed (**I**). **J**. A negative linear correlation was observed between spiking frequency of N3 neurons with mouth width (**J**, n=15). **K**. A positive correlation existed between N4 neurons firing and mouth width (**K**, n=6). Correlation coefficients and p-value done via Spearman.

* $p\leq 0.05$; ** $p\leq 0.01$; *** $p\leq 0.001$

Next, we assessed whether there was a correlation between the mouth opening dynamics and neuronal activity. For this, a time window before and at the onset of neuronal activity was used and the determined change of fluorescence was correlated with either the mouth width (measured in pixel, px) or speed of mouth opening (px/sec, Fig. 3H-K). A linear positive correlation was observed for both effects, in sensory as well as ganglion N6 cells (Fig. 3H-I). Fitting the N6 data in a linear correlation for mouth width and speed, the correlation was slightly better for the ganglion cells than for the sensory cells (n = 7, Fig. 3H-I). This indicates that N6 ganglion cells were more likely involved in the mouth opening event and tissue movement, while the N6 sensory cells are receiving the sensory input. The negative correlation between N3 neuron firing and mouth width (Fig. 3J) suggested that a higher frequency of N3 neuron firing correlated with a smaller to no mouth opening ($R^2 = 0.4$, n= 18). The positive correlation between firing of the synchronous N4 neuron population and mouth width fitted with the highest correlation ($R^2=0.83$, n=4, Fig. 3K).

In combination, these data suggest that during eating behavior, N6 sensory neurons are active right before the mouth is opening. The activity of N6 ganglion cells correlates with the mouth opening and speed of tissue movement during mouth opening. The spiking of N3 decreases during eating while N4 cells fire more frequently, sending synchronized pulses through the complete polyp.

Multiple neuronal subpopulations are involved in eating behavior

To identify the contribution of individual neuronal subpopulation in the eating behavior we used the NTR-Mtz cell ablation system. Genetic constructs were used that contained nitroreductase (NTR) fused to GFP, to convert metronidazole

(Mtz) to a toxic product that induces apoptosis in the target cell population (suppl. Fig. 5A)⁴⁵. As a control, *H. magnipapillata* strain Sf1 polyps were included that lacks interstitial cells (neurons, nematocytes, gland cells and germline) after application of a heatshock⁴⁶.

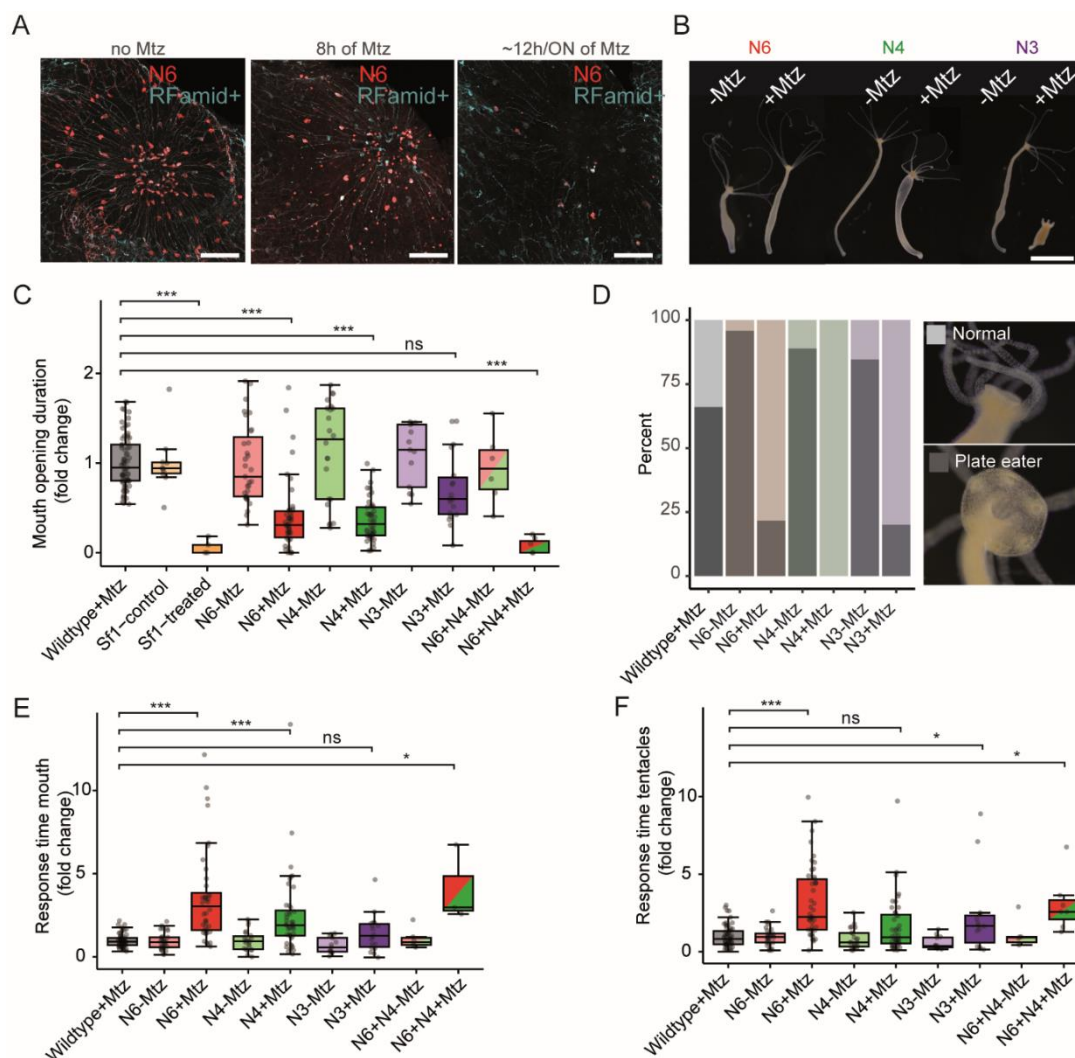


Figure 4. Ablation experiments highlight specific roles of the neuronal subpopulations.

A. Immunohistochemistry staining for GFP under the promoter for N6 (red) and RFamid (turquoise; expressed in N6 and other neurons) of polyp heads in absence and in presence of 10mM metronidazole (Mtz, 8h and 12h/overnight (ON)). Scale bar 50µm. Note the depletion of N6 neurons over time.

B. Different NTR transgenic lines of *Hydra* in absence and presence of 10mM Mtz for 12h. Note the inflated body shape following ablation of N4 and the fully contracted body in absence of N3.

C. The effect of ablating neuronal subpopulations on the mouth opening time. The measured mouth opening time was normalized to the mean response of the control within each experiment before pooling all data. The presence of i-cells is essential for mouth opening. Absence of N6 and N4 significantly ($p < 0.001$, N6: $n = 46$; N4: $n = 44$, N4+N6: $n = 7$) decreased mouth opening, and when lacking in combination it abolished the behavior. Ablation of N3 had no significant effect ($p > 0.05$). Treatments were compared to the "Wildtype+Mtz" group.

D. The percentage of animals displaying 'plate eating' behavior decreased when neuronal subpopulations were ablated (n=18-44). The ablation of N4 inhibited this behavior completely.

E. The mouth opening response time after administration of GSH was delayed following ablation of neuronal subpopulations. N6 and N4, alone or in combination, had a strong impact on the response time, but N3 did not. (N6: n=46; N4: n=44; N3: n =18; N4+N6: n = 3)

F. The tentacle movement response time was also affected by ablating the neuronal subpopulations, in particular by N6 (N6: n=46; N4: n=44; N3: n =18; N4+N6: n = 6).

All statistical analyses are based on Kruskal-Wallis's rank sum test and Dunn test as post-hoc with Bonferroni method.

* $p \leq 0.05$; ** $p \leq 0.01$; *** $p \leq 0.001$.

The N6 specific promoter caused a strong expression of the NTR-GFP fusion protein in Rfa-positive cells in the polyp's head (Fig. 4A). Indeed, 93% of Rfa+ cells were also GFP positive (GFP negative: 12 ± 5.57 cells, mean \pm sd), indicating that the N6 line was nearly fully transgenic. Incubation with 10mM Mtz eliminated the N6 neuronal subpopulation within 12h (Fig. 4A, suppl. Fig. 5B). Other neuronal populations remained intact, for instance Rfa+ cells in the tentacles remained detectable, demonstrating that the cell ablation was specific for the target N6 subpopulation. Mtz treatment of control animals containing the GCaMP6S construct had no effect (Suppl. Fig. 5D, G). Despite the ablation of N6 neurons, the transgenic animals had no changed phenotype (Fig. 4B, compare the polyp pair to the left, without and with Mtz treatment). Similar transgenic animals were produced for ablation of N4 and of N3 (Suppl. Fig. 5D-I). Polyps lacking N4 neurons that are normally present in head, body and foot, showed an inflated body shape (Fig. 4B, middle pair) and animals lacking N3 neurons (expressed in all body parts) were fully contracted (right-hand pair).

The effect of apoptotic removal of these different neuronal subpopulations on the eating behavior of the polyps was studied in freely moving *Hydra* individuals (Suppl. Fig. 6, Suppl. Video1, material and methods). Following GSH stimulation, the duration of the mouth opening period was recorded (how long the mouth stays open), as well as the response time required to initiate tentacle or mouth movement (how long till the first reaction). Results were reported as fold-change compared to control (Fig. 4C, E, F). Interestingly when using GSH as artificial food stimulus polyps attempted to ingest the chamber surface (Fig. 4D). This was

additionally scored as 'plate eating' and described as an extremely wide mouth opening.

As expected, presence of neurons is a pre-requisite for the eating behavior, as their absence in heat-treated Sf1 animals abolished mouth opening completely (Fig. 4C). Ablation of either N6 or N4 subpopulation resulted in a severe reduction in mouth opening time (fold-change compared to control: N4: 0.31 ± 0.398 , $n=44$, $p<0.0001$; N6: 0.32 ± 0.233 , $n=46$, $p<0.0001$; Fig. 4C). Removal of N3 caused a non-significant reduction of mouth opening time (0.599 ± 0.94 , $n=18$, $p>0.5$). When N4 and N6 neurons were removed in combination, the transgenic animals completely stopped opening their mouth (0 ± 0.09 , $n=7$; Fig. 4C). Plate eating was observed in 65% of control animals when the freely moving polyps spread their mouth wide over the surface of the chamber (Fig. 4D). Ablation of N4 neurons completely inhibited this extreme wide opening of the mouth (Fig. 4D). The response time to open the mouth after the GSH stimulus was affected by removal of N4 and N6 neurons but not by removal of N3 (Fig. 4E). Absence of the subpopulation N6 also strongly delayed tentacle movement ($p<0.001$, $n=46$, Fig. 4F).

Taken together, the data show that mouth opening duration, its response time and the response time for tentacle movement during eating behavior are all controlled by two distinct neuronal subpopulations endodermal N4 and ectodermal N6, with a degree of redundancy that adds some resilience to the functioning of this fitness-relevant and important behavior as single ablation could not completely inhibit mouth opening.

A global neuronal network of connected localized neuronal subpopulations regulates epithelial contraction

To investigate if neuronal subpopulations form synaptic-like connections, immunohistochemistry was performed with antibodies targeting the combined RFa⁺ neuronal subpopulations N1, N6 and N7, or the transgenic lines expressing GFP (Fig. 5, suppl. Fig. 7). This uncovered that N3 is connected to multiple other ectodermal neuronal subpopulations (Fig. 5F-H). Contacts suggestive of synaptic-like structures between N3 and N6^{RFa+} neurites were identified in the head (Fig. 5F), while in the foot N3 and N1^{RFa+} neurons were in close proximity (Fig. 5G). In the tentacles N3 was aligned in nerve bundles with neurites in contact with N7^{RFa+}

sensory neurons (Fig. 5H). Potential contacts between ectodermal and endodermal neuronal subpopulations (endodermal N4 with either N3 or N6) were not observed but regions of close proximity (Suppl. Fig. 7).

To investigate the sequential activity of the neurons in the neuronal circuit, we measured the time gap between the first neuronal activity (first activity in a single neuron, not whole neuronal population) and the onset of mouth opening (Time before mouth opening, Fig. 5A-B). A longer time-gap relates to an earlier response in the eating behavior. Figure 5A shows that the earliest responses were observed for sensory N6 cells, followed by N6 ganglion cells and then N4 ganglion/sensory cells (Fig. 5I, n=7-15). Since measuring the activity of neuronal populations in separate animals, high variability was observed (Fig. 5A). Measuring the population N4 and N6 in the same animal (double construct, see material and methods), a significant difference between the different populations was detected (Fig. 5B). Together, this suggests that sensory N6 cells detect the food stimulus first, to pass the signal on to ganglion N6 cells, before the N4 cells respond.

The number of primary neurites located in top part of the head and at its base was determined for N6 and N3 (Fig. 5C). The top of the head contained the fewest N6 neurites, and the base contained the most (Fig. 5C). This would enable a signal picked up by N6 sensory cells to be not only propagated but also enhanced via N6 neurites at the base, where a potential contact between N6 and N4 cells (cf. suppl. Fig. 7) ensures involvement of the latter. At the same time, contact between N6 and N3 would allow the inactivation of the N3 cells.

As mouth opening requires the contraction of epithelia, we also measured the time required to initiate contraction of both ectoderm and endoderm involved in mouth opening (see Methods for the application of calcium imaging constructs under control of an actin promoter for this)⁴⁷. First, we observed that the ectoderm of the head base contracted before the endoderm did (Fig. 5D, E). While the endoderm was activated in the whole head region at some point during the behavior, with a faster response at the top than at the base of the head (Fig. 5E), the ectoderm was only active at the base of the head, close to the tentacles (Fig. 5D). The time required for ectodermal contraction at the head base and for endodermal contraction till mouth opening differs.

All data taken together suggest that the reaction flow went from the N6 sensory cells to the ectodermal epithelium and to N6 ganglion cells, and from there to the N4 ganglion neurons and then to the endodermal epithelium. This is summarized in Figure 5I.

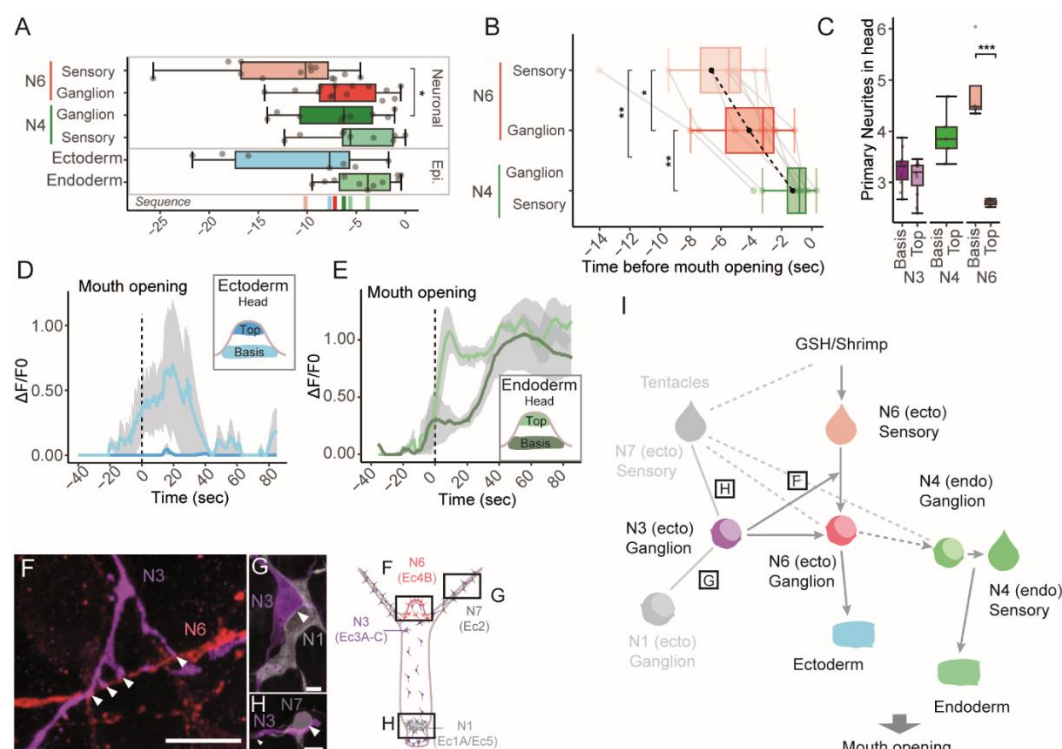


Figure 5. The model of the neuronal circuit controlling the eating behavior in *Hydra*.

A. Time gap between the first neuronal activity and the beginning of mouth opening (time point 0sec). The N6 subpopulation is split into sensory and ganglion cells. A lower value indicates a faster response to the food stimulus, as seen for N6 sensory cells (n=7-15, Kruskal-Wallis and Dunn post-hoc).

B. Analysis of the time sequence within the same animal (n = 8) highlighting the significant time difference between the different neuronal subpopulations (Repeated Measures ANOVA and pairwise t-test).

C. Number of primary neurons of the different neuronal populations in the head (n= 4-11). N6 ganglion cells have the most primary neurites.

D-E. Contraction response of the epithelia to the food stimulus, with ectoderm (**D**) and endoderm (**E**). The time point when the mouth opened is indicated by dashed line. No contraction of ectoderm in the head top was identified but a time relapse between contraction of endoderm at the head top and base is visible **C**. (n=4)

F-H. Identification of contact points between N3 and other ectodermal Rfa⁺ neurons by immunohistochemistry using antibodies targeting N1, N6, N7 in combination, and GFP for visualization of N3. Contact points (white arrows) are present between N3 and N6 in the head (**D**), where N1 and N7 are absent. In the foot (**E**) contact points are found between N3 and N1 and in the tentacles (**F**) they exist between N3 and N7.

I: The model of the neuronal circuit involved in the eating behavior. N6 sensory cells detect glutathione first and propagate the signal to N6 ganglion cells, where it spreads to the endodermal N4 ganglion cells. At the same time, the signal propagates to N3 cells which modulate the response and stops firing, leading to mouth opening. Contact between N3 ganglion cells and N1 and N7 neurons ensures further spread of the signal through the body of the polyp.

* $p \leq 0.05$; ** $p \leq 0.01$; *** $p \leq 0.001$

The role of bacteria: mono-association of *Curvibacter* sp. reduces mouth opening.

Since there are symbiotic bacteria in the immediate proximity of the head neurons³⁶, we next asked whether these bacteria might have an influence on the neuronal circuit identified here that control eating behavior. For this, germ-free (GF) animals were compared with wildtype (Wt) and recolonized with a number of pure cultures of native bacteria as described previously^{48,49}. Intriguingly, germ-free animals kept their mouths open much shorter than control animals did ($p < 0.01$, $n = 30$, Fig. 6A). Mono-association of polyps with single members of the core bacterial community, (including *Duganella*, *Pelomonas* or *Undibacterium* species, Fig. 6B) rescued this defect (Fig. 6A), although monoassociation with *Pseudomonas* or *Acidovorax* had no effect (Fig. 6A).

Completely unexpected results were obtained with animals that were mono-associated with *Curvibacter* sp., which is the most abundant representative in the wildtype *Hydra* AEP microbiota (Fig. 6B)^{48–50}. Exclusive presence of these bacteria reduced the mouth opening time to nearly zero ($n = 47$, Fig. 6A, C). The effect could be restored to some degree by co-addition of a second bacterial species, whereby all tested di-associations produced similar effects (Fig. 6C). The combination of *Curvibacter* with *Undibacterium* and *Duganella* restored the mouth opening time to normal (Fig. 6C).

The strong inhibitory effect on the mouth opening time by mono-association of *Curvibacter* led us to investigate the effect of these bacteria on the neuronal activity during eating behavior. For this, the neuronal activity of Wt, GF and polyps mono-associated with *Curvibacter* was compared by calcium imaging (Fig6 D-F). As shown in Figure 6D, the activity of N6 sensory neurons in germ-free animals was much lower compared to controls. Interestingly this could be restored by presence of the *Curvibacter* symbiont (Fig. 6D). The spiking frequency of N4 was

decreased in germ-free animals ($p < 0.01$) and in the presence of *Curvibacter* ($p < 0.05$, $n = 10-12$) (Fig. 6E). Activity of N3 neurons was not affected (Fig. 6F). Furthermore, no difference was observed in the number or morphology of neurons under the different treatments (Suppl. Fig. 9).

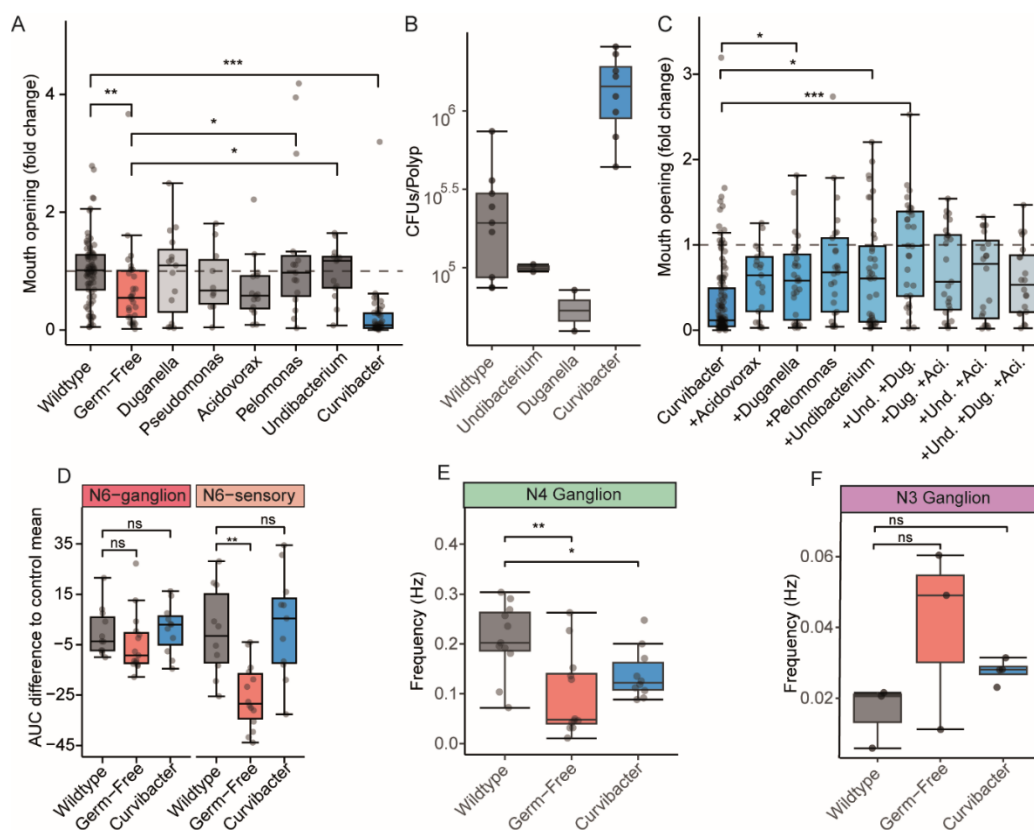


Figure 6. Mono-association of *Curvibacter* sp. inhibits mouth opening and changes neuronal activity in *Hydra*.

A.-C. Wildtype (Wt) *Hydra* was made germ-free (GF) with antibiotic (AB) treatment and then recolonized with single constituents of its native microbiota or combinations thereof.

A. Absence of bacteria decreased the mouth opening duration during feeding. This could be partially restored by recolonization with various bacterial species, but mono-association with *Curvibacter* sp. strongly inhibited mouth opening. Results of replicas ($5 > n < 105$) were normalized to the respective control (dotted line: mean of the control) before pooling experiments.

B. The inhibitory effect is not due to a lack of recolonization. Recolonization of the wildtype bacterial load, two bacteria which have a rescue effect (*Undibacterium*, *Duganella*) and *Curvibacter* who had a negative effect ($n = 3-9$).

C. The negative effect on the mouth opening time of mono-associated *Curvibacter* sp. was rescued by other bacterial species with increasing community complexity. Und: *Undibacterium* sp., Dug: *Dugonella* sp., Ac: *Acidovorax* sp. *Curvibacter* sp. was present in all.

D-F. Neuronal activity during eating behavior in transgenic animals with wildtype microbiota, germ-free animals or recolonization with *Curvibacter*.

D: the activity of N6 sensory cells was negatively affected by absence of bacteria, while recolonization of *Curvibacter* rescued this effect. N6 ganglion cells were not affected, Area under the curve (AUC) was calculated by taking the mean of respective controls and subtract this from treatment (n=8-10).

E: The spiking frequency is significantly reduced in animals mono-associated with *Curvibacter* within the first 400sec post GSH.(n=10-11).

F: Absence of bacteria or mono-association with *Curvibacter* did not affect N3 neural spiking frequency significantly during eating behavior (one experiment, n= 3-5).

***Curvibacter sp.* affects neuronal cells by means of glutamate**

To investigate the mechanism how *Curvibacter sp.* influences the eating behavior and neuron activity on a molecular level, gene expression pattern of *Curvibacter* in mono-association with *Hydra* was compared to the expression profile of the bacteria cultured in minimal growth medium R2A. Differentially expressed genes were identified and the metabolic pathways in which these genes were involved were examined. This approach identified pathways for alanine, aspartate and glutamate metabolism, among others (Fig. 7A). In particular, genes associated with glutamate metabolism were differentially expressed (Fig. 7A). While glutamine synthetase was downregulated in presence of the *Hydra* host, glutaminase, glutamate dehydrogenase (*gdhA*) and *glnM*, *glnP* and *glnQ* (glutamine transporters) were over-expressed (Fig. 7A). This points to a glutamate production during host-association. Since glutamine binding and uptake associated genes are also upregulated in host-association, we assume that host-associated *Curvibacter sp.* secretes glutamate while taking up glutamine.

Previous work had described a putative NMDA-like glutamate receptor in *Hydra* tissues to be involved in the eating behavior^{51–53}. Since N6 sensory cells express the NMDA receptor and glutamate receptors in general (Suppl. Fig. 8) we hypothesized that bacterial glutamate might bind to the glutamate receptors present on N6 sensory neurons. To test this, *Curvibacter sp.* was first cultivated *in vitro* in *Hydra* culture medium supplemented with 20mM glutamine. The glutamate concentration in this supernatant reached 332±34.9ng/μL. When *Curvibacter* was cultivated in *Hydra* culture medium with other amino acids, little

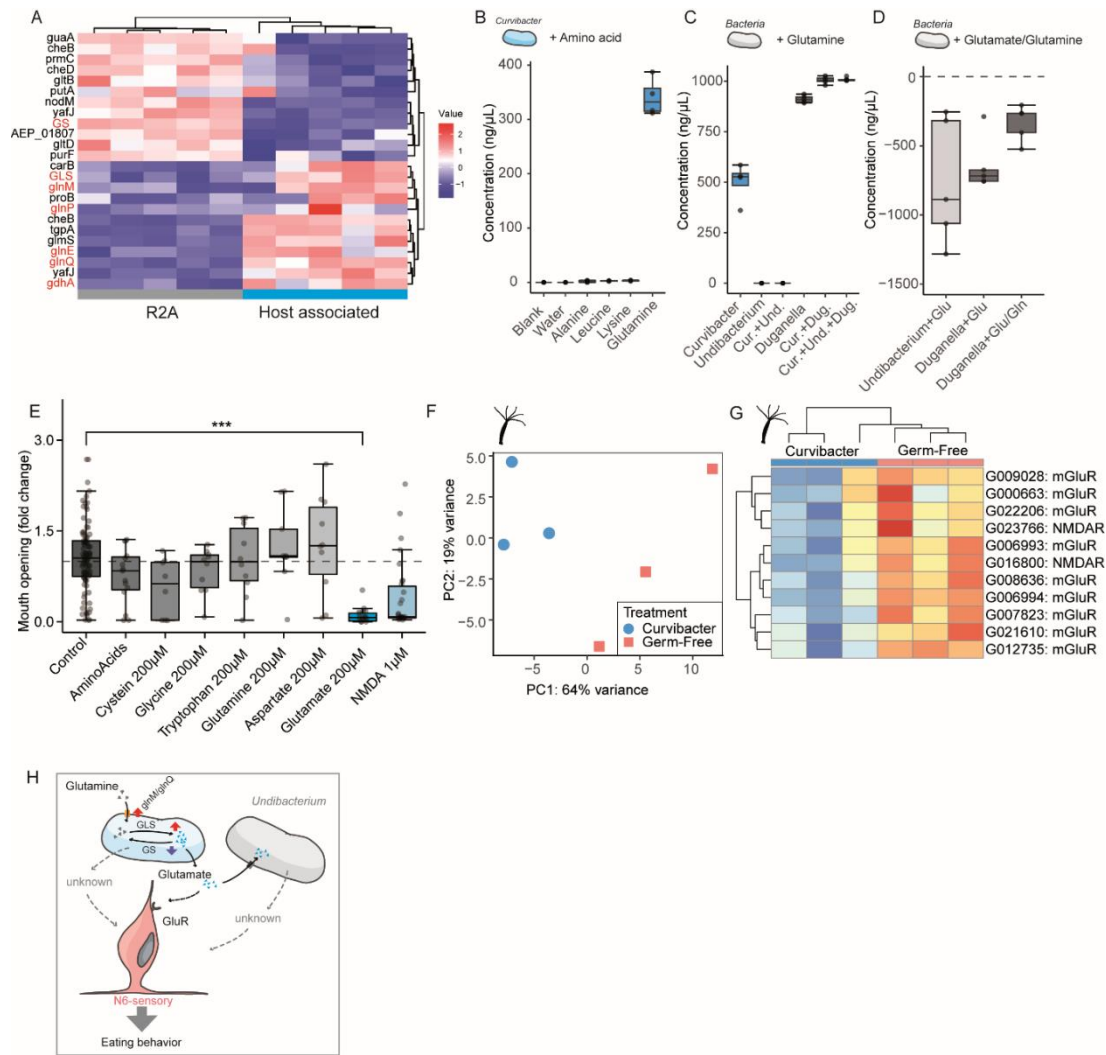


Figure 7. *Curvibacter* produces glutamate in host-association and thereby inhibits mouth opening duration.

A: Differentially expressed genes in *Curvibacter* sp. grown in minimal growth medium (R2A) and in mono-association with its host. Multiple genes are involved in glutamine/glutamate binding, transport and metabolism shown in red font.

B: *Curvibacter* sp. grown *in vitro* in *Hydra* culture medium supplemented with 20mM glutamine secreted glutamate into the medium (n = 5), whereas addition of other amino acids to the medium had no effect.

C: *Undibacterium* is cross-feeding on glutamate and cannot produce glutamate in the presence of glutamine. *Duganella*, can produce glutamate in the presence of glutamine and no cross-feeding observed in this setting (n = 5).

D: *Undibacterium* consumed 887±455 ng/μL and *Duganella* 717±198 ng/μL glutamate within 24h. *Duganella* consumed 265±130 ng/μL glutamate when both glutamate and glutamine were available in equal ratios. (Median, sd; n = 5)

E: Adding glutamate to the medium strongly inhibited mouth opening, but other amino acids had no effect. Addition of NMDA mimicked the glutamate inhibition (n=10).

F: *Hydra* showed a transcriptional response to mono-colonization with *Curvibacter* compared to germ-free PCA plot of (n= 3).

G: Down regulation of different glutamate receptor in the presence of *Curvibacter*.

H: Model of the rescue effect by co-culturing of *Curvibacter* and *Undibacterium* where glutamate is removed from the environment by *Undibacterium* (potential coress-feeding).

Kruskal-Wallis, Wilcoxon test, * $p \leq 0.05$; ** $p \leq 0.01$; *** $p \leq 0.001$

glutamate was secreted (Fig. 7B). Next, we tested if bacteria with a rescue effect on the eating behavior can also produce glutamate in the presence of 20mM glutamine and if co-culturing of those with *Curvibacter* decreases the concentration of glutamate in the supernatant. When *Undibacterium* was cultivated with either glutamine with and without *Curvibacter* or in 20 mM glutamate, no glutamate or glutamate concentration decrease was observed (Fig. 7C-D). In contrast, *Duganella* produced glutamate when cultured with or without *Curvibacter* in the presence of glutamine (Fig. 7C). In the presence of glutamate or a mixture of glutamate and glutamine (1:1 ratio, 10mM each), a decrease in glutamate was observed as well (Fig. 7D) suggesting both that *Duganella* rather prefers glutamate over glutamine and that it can use *Curvibacter*-produced glutamate. In a next step, we tested the effect of glutamate on the eating behavior. As shown in Figure 7E addition of glutamate inhibited mouth opening duration. Addition of NMDA had a similar inhibitory effect, corroborating the hypothesis of an NMDA-receptor being involved. Adding various other amino acids had little to none effect on mouth opening duration (Fig. 7E). Next, we tested if the host showed a potential response to the excessive glutamate by comparing the transcriptional profile of germ-free and *Curvibacter* mono-colonized animals (Fig. 7F-G). Indeed, various glutamate receptors are down regulated in the presence of *Curvibacter*. Taken together and in accordance with previous biochemical and functional evidence of the occurrence of putative NMDA-like glutamate receptors in *Hydra* tissues and with the fact that N6 sensory cells are equipped with this receptor and glutamate receptors are down regulated, we assume that *Curvibacter* produced glutamate can affect the N6 neurons via this receptor (Fig. 7H).

Discussion

Cnidarians emerge as informative models for neuroscience, as they have surprisingly complex neuronal circuits and enable the study of neuronal activity in complete organisms lacking a centralized nervous system^{20,26,54,55}. Neuronal control of behavior in cnidarians is dispersed and control takes place in neuronal subpopulations. Recent work in *Hydra* have highlighted that simple spontaneous behaviors are controlled by single neuronal subpopulations²⁶. *Hydra* has multiple non-overlapping neuronal networks, each of which can regulate a single behavior, but they are also collectively involved in mechanosensory processing⁵⁶. *Hydra* is also a well-described metaorganism which is colonized by a stable and functionally relevant microbiota^{37,48,50,57–59}. Here we studied the interplay and coordination between multiple neuronal subpopulations and epithelial cells that together with the microbial colonizers are involved in the eating behavior. Our work emphasizes the importance of the microbiota on neuronal circuits. The results offer an opportunity to unravel the evolution of the interplay between bacteria and the nervous system mechanistically.

The eating behavior requires coordination between multiple neuronal subpopulations

The eating behavior illustrates beautifully how, in the absence of any form of centralization, different neuronal subpopulations interact with each other to coordinate a complex behavior. In the presence of a chemical signal for food, for which we used reduced glutathione, different neuronal subpopulations were either activated or inactivated, to coordinate the epithelial movement leading to mouth opening (Fig. 3, Fig. 5I). First N6 sensory cells at the tip of the head are activated, followed by the N6 ganglion cells at the head base, while the local ectoderm contracts. When N6 ganglion cells are activated, the frequency of N4 spiking is increased and the signal spreads from the base back to the tip of the head, leading to contraction of the endoderm (Fig. 3, Fig. 5I). At the same time, N3 decreases in spiking frequency and the mouth is opening, suggesting these neurons have an inhibitory function on mouth opening (Fig. 3). Ablating N3 neurons did not inhibit the mouth opening, whereas ablating N4 and N6 did (Fig. 4C). Interestingly, these neuronal subpopulations control different aspects of the mouth opening and eating behavior: N4 regulates the mouth opening width (Fig. 4D), whereas N6 is involved in the recruitment of the tentacles and speed of

mouth opening (Fig. 3I and 4E-F). In combination, these three different neuronal subpopulations form the neuronal circuit controlling the epithelia involved in the eating behavior (Fig. 5I).

The fact that several non-overlapping neuronal subpopulations are involved to control different aspects of eating behavior suggests that they must be in contact with each other. One of the highest densities of neurons in *Hydra* is at the tentacle-head junctions at the base of the head^{60,61}. At this location, the densities of N3, N4 and N6 populations are particularly high, with increased numbers of primary neurites compared to the body column (Fig. 2G, L, S, Fig. 5C). In addition, in this region potential contact points between neurons of different neuronal subpopulations could be identified where neurites from different subpopulations came in close proximity (Fig. 5F-H, Suppl. Fig 7). In combination with the sequence of activity after glutathione stimulus (Fig. 3) this led us to the conclusion that the base of the head is the region where the different signals are being integrated and distributed to the endodermal and ectodermal networks. The complexity of neurites and synaptic structures in this region was already identified by electron microscopy^{60–65}. Our results highlight how a relatively simple neuronal network in *Hydra* can result in a stunning complexity in order to process sensory information into multiple responses to control the complex eating behavior. We note potential similarities to neuronal control mechanisms in the jellyfish *Clytia hemisphaerica*, where an apparently diffuse network of neurons is functionally subdivided into a series of spatially localized subassemblies whose synchronous activation controls food transfer from the tentacles to the mouth⁵⁴. However, that organism depends on functional modules, whereas in *Hydra* multiple subpopulations within a single circuit coordinate the behavior.

Eating behavior becomes severely impaired when the microbiota is disturbed.

Polyps mono-colonized with *Curvibacter sp.* had drastically reduced mouth opening time, suggesting a bacterial signal interfered with the neuronal circuit that controls this fitness relevant behavior. This striking inhibitory effect was all the more surprising, as *Curvibacter sp.* normally represents around 70% of the *Hydra* bacterial microbiota and has not been associated previously with any negative effect on the host⁵⁷. The inhibitory effect of *Curvibacter sp.* could be reversed by

increasing bacterial diversity while adding back specific members of the core microbial community (Fig. 6C).

The inhibitory effect of *Curvibacter sp.* on eating behavior was not accompanied by a detectable change in N6 and N3 neuronal activity compared with the control (Fig. 6D-F). Instead, mono-association of *Curvibacter sp.* reversed the effect of germ-freeness back to control conditions. This highlights that *Curvibacter sp.* affects neuronal activity and also that neurons are able to detect the presence of *Curvibacter sp.* Since the N6 sensory neurons are in close contact with the microbiota³⁶, their response was to be expected. Surprising was that *Curvibacter* reduced the spiking frequency of the endodermal subpopulation N4 (Fig. 6E) which was rather unexpected and suggests that *Curvibacter sp.* has a more global effect on the nervous system.

The transcriptional response of *Curvibacter sp.* to the host environment points to the secretion of glutamate in the presence of glutamine, which was supported by *in vitro* observations (Fig. 7B-D). The neuronal subpopulations N3, N4 and N6 express glutamate receptors and a NMDA receptor that could respond to bacterial glutamate and integrates this information into the neuronal circuit of the eating behavior (NMDAR and mGlu, see Suppl. Fig. 8). Interestingly, *Hydra* down regulates those glutamate receptors in the presence of *Curvibacter* (Fig. 7G) which also included the NMDA receptor. This additionally supports the role of glutamate. Since N4 and N6 but not N3 neurons showed a response to *Curvibacter sp.* (Fig. 6D-F), we assume that N4 and N6 receive and integrate the bacterial signal which may affect the downstream signaling instead of the neurons themselves. In the presence of other bacteria such as *Undibacterium*, glutamate gets scavenged, and the inhibitory effect abrogated (Fig. 6C and Fig. 7B-C, H). In case of *Duganella* it is more complex and other factors such as bacteria-bacteria interactions can come into play as described previously⁶⁶.

Our work shows that the old observation published by Lenhoff (1961)⁵² that glutamate has a negative effect on eating behavior in *Hydra* may find its explanation in the microbial colonization of *Hydra*.

Evolutionary perspective

Altogether, our findings confirm and expand on the idea that in animals without a central nervous system, a complex behavior is controlled by coordination of multiple subpopulations of neurons, forming circuits and modules⁵⁴. Our observations presented here show that this not only requires the coordination of multiple neuronal circuits, but also that signals from the microbial environment play an important role. We present data that support a model (Fig. 7H) in which in the critical phase of mouth opening, may be affected by microbially produced glutamate.

Already in 1963, the evolutionary biologist Tinbergen outlined an organizational framework that would control complex behavior^{67,68}. His research involved four levels of analysis: phylogenic, developmental, functional, and mechanistic investigations. Our findings of the influence of the microbiota on the neuronal control of *Hydra*'s eating behavior, which co-evolved with this host^{49,57}, adds this as an additional environmental perspective to be considered when studying complex behavior.

That bacteria are able to produce molecules that are active on neuronal cells has been known for quite some time^{69,70}, but most work has been carried out in mammals. Here we show that the integration of bacterial signals into neuronal circuits might be as evolutionary ancient as the first nervous system, as it already exists in cnidarians. Our observation that bacterial glutamate can play a crucial role in this interaction, together with the numerous findings on the influence of this molecule on mammalian intestinal physiology^{9,70}, support the idea that it is part of an ancestral interkingdom language.

Acknowledgements

This work was supported in part by grants from the Deutsche Forschungsgemeinschaft (DFG), the CRC 1182 "Origin and Function of Metaorganisms" (to TCGB.) and the CRC 1461 "Neurotronics: Bio-Inspired Information Pathways" (Project-ID 434434223 – SFB 1461) (to TCGB and AK). T.C.G.B. appreciates support from the Canadian Institute for Advanced Research. AK is supported by a DFG grant KL3475/2-1. C.S. and T.S. acknowledge funding by the DFG under Germany's Excellence Strategy 2082/1-390761711 (3D Matter

Made to Order). We thank Trudy Wassenaar for critical reading of the manuscript. We thank the members of the Bosch lab for support and discussion, and Andreas Tholey, Christoph Kaleta, Georgios Marinos and Karlis Moors for discussion. We also thank Urska Repnik and Marc Bramkamp from the Central Microscopy Facility at the Biology Department of the University of Kiel for excellent technical support. We highly appreciated the expertise provided by the sequencing facility at the Institute of Clinical Molecular Biology (IKMB) in Kiel, Germany.

Authors contribution

C.G. and T.C.G.B. conceptualized the project and wrote the manuscript. T.C.G.B., J.W., A.K., Y.G., D.P. and C.G. designed and performed experiments on transgenesis. T.C.G.B., D.P., C.S., T.S., E.H. and C.G. designed and performed histological, behavioral experiments. C.G., E.H., T.L. and T.C.G.B. designed and performed neuronal activity and microbiota experiments. T.L. and C.G. analyzed the data.

Declaration of interest

The authors declare no competing interests.

Data and code availability

- Source data reported in this paper will be shared by the lead contact upon request.
- Codes used for the analysis and statistical analysis will be shared by the lead contact upon request.
- Any additional information required to reanalyze the data in this paper will be shared by the lead contact upon request.

STAR Methods

Materials availability

The plasmids and transgenic *Hydra vulgaris* AEP generated in this study are available upon request.

Code availability

All codes used in this study are available upon request.

Data availability

All data presented in this study are available upon request.

Experimental Procedures

Hydra maintenance

In this study used *Hydra* polyps (*Hydra vulgaris* AEP, *Hydra magnipapillata sf1*) were cultured according to standard procedures in standard *Hydra* culture medium (CaCl₂ 0.042g/L; MgSO₄·7H₂O 0.081g/L; NaHCO₃ 0.042g/L, K₂CO₃ 0.011g/L in dH₂O)⁷¹. The animals were kept in 250mL glass beaker at 18°C with a 12/12h light cycle. The feeding regime was strictly three times per week with *Artemia* nauplii for at least two weeks before any experiment. Animals were starved for 1-3 days before either an ablation experiment or a calcium imaging analysis. There was no difference in the mouth opening duration between 1-3 days of starvation.

Generating germ-free animals and re-colonization

Germ-free animals were derived by treating animals for five days with an antibiotic cocktail containing rifampicin, ampicillin, streptomycin and neomycin in final concentrations of 50 µg/ml each and spectinomycin of 60 µg/ml, as previously described⁴⁹. Control polyps were incubated in 0.1% DMSO for the same time since rifampicin is dissolved in DMSO. The antibiotic cocktail was replaced after 72h of incubation. After 5 days in antibiotics, the animals were transferred to sterile *Hydra* culture medium and incubated for another 2 days. On the second day in sterile *Hydra* culture medium, animals were recolonized with defined bacteria or communities and medium was exchanged. After another 3 days of incubation with defined bacteria or communities, polyps were used for the behavioral assays or RNA sequencing. The germ-free status was checked twice

during the protocol, on the seventh day and the tenth day of the protocol via plating macerated polyps on R2A-agar plates. Random samples were also tested via PCR using universal rRNA primer Eub-27F and Eub1492R⁷². No colonies formed on the R2A agar plates after one week of incubation at room temperature and absence of amplification product confirmed the germ-free status.

Germ-free animals were monocolonized with pure bacteria cultures of the core members of *Hydras* microbiota: *Curvibacter* AEP 1.3 (NCBI:txid1844971), *Duganella* C 1.2 (NCBI:txid1531299), *Undibacterium* C 1.1 (NCBI:txid1531302), *Acidovorax* sp. AEP 1.4, *Pelomonas* AEP 2.2 (NCBI:txid1531300) and *Pseudomonas* sp.⁵⁰. Bacteria were cultured from existing isolate stocks in R2A medium at 18°C for three days and subcultured the day before recolonization (dilution depending on the bacterium). In all experiments we started from a fresh cryostock and identity of bacteria was regularly tested. From the overnight culture approximately 10⁵-10⁶ cells were added to the 50mL sterile *Hydra* culture medium containing 30-50 animals. For the different combinations of bacteria, each bacterium was added in at equal ratios. After three days the recolonization success was checked by plating three macerated polyps per treatment in a 1:1000 dilution on R2A agar plates and counting the CFUs after three to four days of incubation at 18°C. Recolonized animals were only used when recolonization was successful and in agreement with previous published values⁷³.

Promoter identification and extraction

Marker genes specifically expressed in the different neuronal subpopulations were identified using the single cell atlas previously published^{24,25} (suppl. Fig. 1). Genes were then mapped against the different available genomes of *Hydra* (nih.gov/HydraAEP) and their promotor were extracted as 1000-1500bp upstream of the gene, by including the first 30bp of the open reading frame. The sequence was then cloned into pGem-T Easy (Promega, cat# A1360) while restriction enzyme binding sites were inserted to further clone the construct into the LigAF vector (for sequences see suppl. Table 1).

Transgenesis and constructs

Transgenic *Hydra vulgaris* AEP were derived following the established protocol by Wittlieb *et al.*^{71,74} using a modified version of the LigAF vector. Different lines

were produced in which the specific promoters for desired expression in the neuronal subpopulation regulated either GCaMP6S (as in Dupre *et al.* ²⁶) with an actin terminator or the nitroreductase (NTR)⁴⁴ (*in silico* codon optimized) coupled to an eGFP at the C-terminus followed by an actin terminator sequence (see suppl. Table 1 for sequences). We generated single constructs for N3, N4 and N6 for NTR-GFP and GCaMP6S as well as a double construct with the promoter of N4 driving NTR-GFP and the promoter of N6 driving the expression NTR-GFP for ablating both population at once. The same construct was designed for GCaMP6S as well. As previously described, the construct was injected via microinjection in embryos resulting in mosaic animals. Animals were screened for transgenic neurons and selected to produce fully stable transgenic animals. We then induced embryogenesis in the transgenic lines and derived F1-generations which ensured that the construct was incorporated in all cells. This was successful for transgenic lines N4 and N6 while for N3 reached a non-mosaic stable population only (see suppl Table 1).

Histology

For antibody staining, *Hydra* polyps were relaxed with 2% urethan(Sigma-Aldrich, U2500) in *Hydra* culture medium for less than 2min and fixed for 2h (RT) or overnight (4°C) in Zamboni (Morphisto, cat#12773). Following 3 washes in PBS with 0.1% tween (PBST) followed by an incubation in PBS with 0.5% TritonX100 and an 1h of blocking in PBST with 1% bovine serum albumin (BSA, Roth, cat# 8076.1). Animals were then incubated overnight at 4°C with the primary antibody in PBST and 1% BSA. Primary antibodies used in this study were: anti-GFP (Biozol, cat# GFP-1010, 1:1000 dilution) and anti-FMRFamid (BMA Biomedicals, cat# T-4322, 1:1000 dilution). After the primary antibody incubation, four 15min washes in PBST with 1%BSA were performed before adding the secondary antibody. Secondary antibodies used in this study were: goat anti-chicken Alexa Fluor 488 (Invitrogen, cat# A11039, 1:1000 dilution) and donkey anti-rabbit Alexa Fluor 546 (Invitrogen, cat# A10040, dilution 1:1000). Animals were incubated for 2h at RT with the secondary antibody. After the secondary antibody another four 15min washes in PBST (here 0.5% tween) with 1% BSA were performed followed by a short 5min incubation in TO-PRO™-3 Iodide (642/661)(Invitrogen, cat# T3605, 1:1000 dilution). The animals were mounted in moviol with DAPCO on glass slides and stored at 4°C till imaging.

Imaging and analysis

Fixed and stained animals were imaged either with a LSM900 (Zeiss) or Axio Vert.A1 (Zeiss) using colibri 7 (Zeiss) as a light source. Further processing of the images was performed with Zen Blue 3.4 software (Zeiss) or Fiji⁷⁵. For the analysis of neuronal densities and distribution we used the Cell Counter plugin by Fiji. For counting, a rectangular area was subsampled from the images to count comparable areas (see Fig2B, I and N). For the densities, we calculated the density of neurons per mm². For the 2D density plots (Fig2G, L and S) we aligned the rectangle area using Fiji and extracted the x- and y-coordinates. Data were analyzed using R (v4.0.3)⁷⁶ over RStudio IDE⁷⁷ and for the visualization the plugin tidyverse (v1.3.1)⁷⁸ was used. For the characterization of the primary neurites, we counted all neurites originating from a neuron soma. In all cases at least five animals were analyzed. Multicolor images shown throughout are pseudo-colored composites (maximum projection), with brightness and contrast adjusted for clarity.

NTR and sf1 cell ablation experiments

Animals were incubated overnight in 10mM Metronidazole (Sigma, cat# M1547)^{44,45,54}. On the next morning animals were screened under a fluorescence microscope for absence of GFP⁺ cells. Once it was determined that the ablation had been successful, the animals were washed once in *Hydra* culture medium and used for behavioral assays or histology on the same day. Each experiment included a control of *Hydra vulgaris* wildtype and the corresponding GCaMP6S transgenic line with Metronidazole and the NTR-GFP transgenic line without Metronidazole. In all experiments at least 5 animals per treatment were used.

Hydra magnipapillata Sf1 were exposed to 28°C for 48h together with a control (*H. magnipapillata*) for the heat shock and afterwards kept for 19 days under standard culture conditions. Neurons were quantified on day 5, 8, 11, 14 and 19 using a cell maceration protocol²². Polyps were dissociated in maceration solution (1:1:13, Glycerol, Acidic acid, *Hydra* culture medium) at 32°C for 30 minutes. Afterwards cells were fixed in 8% PFA and spread out on gelatin-coated slides. Counting was done blinded.

Behavioral analysis

Acquisition

To analyze the effect of cell ablation and bacteria on the eating behavior, we developed a recording system where we can observe multiple animals at once and animals were minimally restrained. For this, a chamber was used where 5-6 animals could be observed under controlled fluid flow (Suppl. Fig. 6). The chamber consists of a two-piece aluminum case and two plexiglass pieces in which one cavity was milled and the other used as a lid (see suppl. Fig. 6). These were connected and liquid tight via braces. Animals could survive in the chamber for weeks as long as fresh *Hydra* medium was supplied. The chamber has a height of 0.4mm and two channels on both sides fitted with tubes through which medium can be manually supplied. The animals were recorded at 18°C in an insulated climate chamber to avoid external stimuli using M3C Wild Heerbrugg binocular microscopes and AxioCam 208 color (Zeiss), taking a picture every 2 seconds.

Mouth opening, tentacle response and analysis

The animals were given 10 min to adapt to the recording chamber before recording started and another 5-10 min before reduced glutathione (GSH, Roth, cat#6382.1) was supplied via the tube system. In all assays a final concentration of 10µM GSH was used, prepared in the same medium as the animals were kept in prior to the experiment using a 0.1M stock solution. Each animal was only recorded once. Acquired movies were blinded to their treatment and assigned with a random three-digit number before analysis. The behavior was manually annotated. The following different behaviors were scored: the mouth opening time, tentacle movement and the type of mouth opening (see suppl Video 1). As animals exhibited multiple mouth openings during the assay, for the mouth opening time only the first event was recorded. The raw data from the video analysis were further normalized by the mean of the respective controls within each experiment to obtain the fold-change information between treatments. The data were merged for analysis and plotting.

Mouth opening width

In order to correlate the mouth opening behavior and neuronal activity, we measured the width of the mouth opening during GCaMP6S recording via automated tracking of the opposite edges of the mouth. This tracking was done using icy⁷⁹ and the tracking plugin⁸⁰. Afterwards tracks were manually cleaned, and missing links were integrated. Using the track manager with the integrated function “Distance profiler” the distances between the two different tracks were calculated in pixel. The tracks were then smoothed using the integrated ksmooth function in R⁷⁶. As the mouth opening onset to analyze the time sequence of neuronal activation before mouth opening, the first increase in the slope was taken after the addition of GSH and where there is no decrease within a 20 sec window.

GCaMP6S imaging acquisition and calcium traces extraction

To analyze the neuronal activity during the eating behavior, we developed a system to record freely moving animals while adding GSH. The animals were placed in commercially available channel slides with a height of 0.2mm and a width of 5mm (Suppl. Fig. 6D.; Ibidi, cat# 80166). After an animal was placed in the channel sled, tubing was connected on both sides, and recording was started. GSH was added using a 1-ml syringe attached to one tube after 2-3min, depending on the behavior of the animal, and recording lasted for approximately 10min. GSH was only added when the animal stayed elongated and did not show contraction or somersaulting behavior. Imaging was performed using the Axio Vert. A1 (Zeiss) with the Colibri 7 as a light source (Zeiss) equipped with the fluorescence filter 38 HE (Zeiss), 5x and 10x Plan Apo objective, and the AxioCam 705 mono (Zeiss). Acquired videos were further processed with Zen Blue 3.4 (Zeiss) to 700x600px, 8-bit and aligned with the Fiji plugin Linear Stack Alignment with SIFT⁸¹. The aligned stacks were then used for tracing neurons as described by Lagach et al.⁸². Neurons were automatically traced in icy⁷⁹ using the protocol “Detection and Tracking of neurons with emc2”⁸² with individually adjusted parameters depending on the population, magnification, and animal size. Afterwards the quality of the tracks was manually controlled, and missing links were added, or false tracks were removed. For N6 and N4 neurons, tracks were manually separated for the different neuronal sensory (-like) and ganglion cell types.

GCaMP6S trace analysis

The raw traces were normalized to obtain the fluorescence change $\Delta F/F_0$ using the background fluorescence as F_0 . This background fluorescence was taken by selecting a frame without visible neuronal activity drawing the outline of the animal's body column and calculating the mean grey therein via Fiji. For further analysis the mean activity of each population or neuronal type was taken with the standard deviation to the mean since it summarized all major events (suppl. Fig. 6). All visualization and normalization were done using customized scripts in R⁷⁶. N3 and N4 spiking frequency was deconvoluted and analysed using either CASCADE⁸³ and/or MATLAB's (Mathworks) "findpeaks" function with manually adjusted parameters. In all experiments at least 4 animals were used. In Figure 3 A-C only, representative polyps were shown and the mean of the whole neuronal population with the standard deviation, for N4 and N6 divided into sensory and ganglion neurons. More replicates shown in the suppl. Fig. 3.

The time sequence of activation of the nerve subpopulation before an opening of the mouth was determined by the time difference between the first activation of the first cell and the opening of the mouth. As the timepoint of first neuronal response, the first activation of the first single cell was taken (shown in Fig. 5A-B). At least 7 animals pre transgenic line were taken.

To find a difference in N6 between germ-free and monocolonized with *Curvibacter* or wildtype microbiota, the area under the curve (AUC) was compared. For this purpose, the mean value of the wildtype microbiota AUC was taken and the difference to the other treatments was calculated. At least 8 animals per treatment were used.

GCaMP6S and mouth width analysis

For calculation of positive or negative correlations between the mouth opening and the mean activity of the different neuronal subpopulations, the smoothed mouth width data were used. The visualization was done using R and the tidyverse package (Fig. 2A-C)^{76,78}. The mouth opening width was adjusted to the scale of the fluorescence change as stated on the right y-axis title. To perform linear correlation analysis, for N6 we compared the fluorescence changes and in case of N3 and N4 the frequency to the mouth opening width at the given time

point. For N6, the GCaMP6S traces were divided into ganglion and sensory neurons. Since a continuous signal increase rather than a spiking pattern was observed in N6, we selected a time window of 10 sec before and 20 sec from the onset of neuronal activity compared this to the mouth width change in the same time window. For N4 and N3 we took the spiking frequency and the width of the mouth opening prior the GSH stimulus and post GSH stimulus (30sec windows). At least 6 animals per transgenic line were used.

RNA sequencing and analysis *Curvibacter*

Transcriptional analysis of *Curvibacter sp.* AEP1.3 was performed by RNA sequencing of bacteria in association with their host and when cultured in R2A without the host (Neogen, cat#NCM0188A). For the latter, 4mL of culture was collected before stationary phase was reached, at an OD₆₀₀ of 0.2-0.3, and centrifuged (4°C, 12000xg). For samples from host-associated *Curvibacter*, 5x500 mono-colonized polyps were prepared as described previously⁸⁴. *Curvibacter* was washed off these animals with PBS and the supernatant was collected and centrifuged (4°C, 12000xg). The bacterial pellet was dissolved in 750µL Trizol by vortexing and 250µL of chloroform was added and samples were centrifuged (12.000xg at 4°C). The aqueous phase was collected and 400µL of 99.9% ethanol was added. The solution was then transferred to silica columns of the ambion PureLink™ RNA Mini Kit (Thermo scientific). RNA was eluted with 35µL RNase free water and stored at -80°C until samples were submitted for sequencing.

Prior to sequencing isolated RNA was treated using the TruSeq stranded total RNA kit (Illumina) and Ribo-Zero Plus kit (Illumina). The remaining RNA was paired end sequenced using a NovaSeq 6000 (Illumina) with 2×150 bp. RNA sequences were analyzed using the platform Galaxy⁸⁵. The sequences were trimmed using CutAdapt⁸⁶ and Trimmomatic⁸⁷, and MultiQC for quality control⁸⁸. We aligned the reads against the public available *Curvibacter sp.* AEP1.3 genome (ASM216371v1)⁸⁴ using Bowtie2⁸⁹. Reads were counted with featureCounts⁹⁰. The normalization of reads and differential gene expression analysis was done using the DeSeq2 pipeline in R^{76,91} and data were visualized using tidyverse in R⁷⁸. All raw RNA-sequence read counts and analyzed data can be found in supplement table 2.

RNA sequencing and analysis *Hydra*

Transcriptional analysis of *Hydra vulgaris* AEP was performed by RNA sequencing of *Hydra* under germ-free conditions and in mono-association with *Curvibacter* sp. (the same experiment/animals as used for bacterial RNASeq). *Hydra* was dissolved in 750µL Trizol by vortexing and 250µL of chloroform was added and samples were centrifuged (12.000xg at 4°C). The aqueous phase was collected and 400µL of 99.9% ethanol was added. The solution was then transferred to silica columns of the ambion PureLink™ RNA Mini Kit (Thermo scientific). RNA was eluted with 35µL RNase free water and stored at –80°C until samples were submitted for sequencing.

Prior to sequencing isolated RNA was treated using the TruSeq stranded total RNA kit (Illumina) and polyA-enrichment (Illumina). The remaining RNA was paired end sequenced using a NovaSeq 6000 (Illumina) with 2×150 bp. RNA sequences were analyzed using the platform Galaxy⁸⁵. The sequences were trimmed using CutAdapt⁸⁶ and Trimmomatic⁸⁷, and MultiQC for quality control⁸⁸. We aligned the reads against the public available *Hydra vulgaris* AEP genome³⁴ using RNA Star⁸⁹. Reads were counted with featureCounts⁹⁰. The normalization of reads and differential gene expression analysis was done using the DeSeq2 pipeline in R^{76,91} and data were visualized using tidyverse in R⁷⁸. All raw RNA-sequence read counts and analyzed data can be found in supplement table 3.

Glutamate detection assay

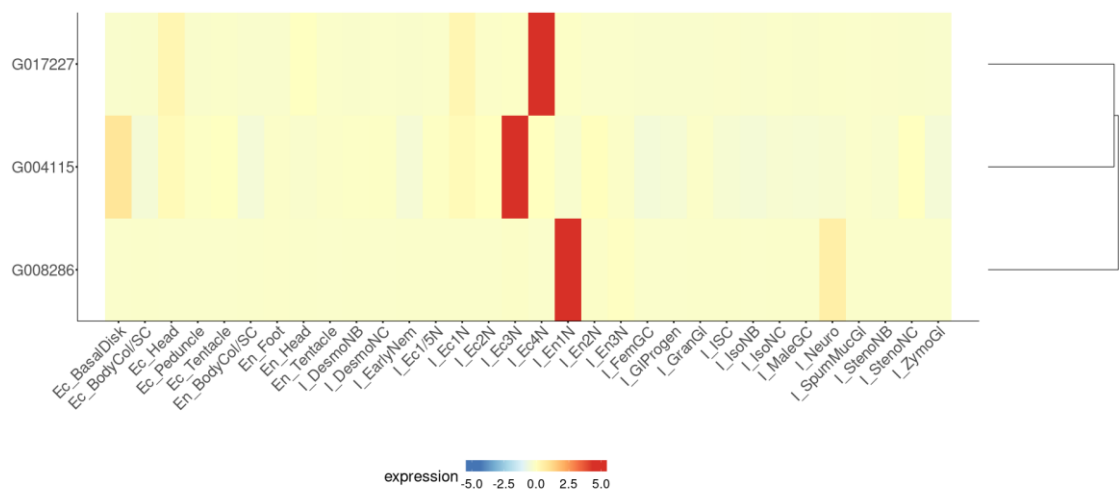
To test if *Curvibacter* and other bacteria can produce and export glutamate in the presence of glutamine we took the supernatant of *Curvibacter* in the presence of glutamine and determined the concentration of glutamate by using a glutamate detection kit (Sigma-Aldrich, cat#MAK004). The *Curvibacter* culture, in the exponential phase, was taken and washed twice with sterile *Hydra* culture medium via centrifugation and resuspension. Afterwards the bacterial pellet was dissolved in *Hydra* culture medium either supplemented with 20mM glutamine, 20mM respective other amino acids or nothing. The resuspended bacteria cultures were split into five times 2-5mL aliquots and incubated for 24h at 18°C. The bacteria were centrifuged down, and the supernatant was filtered with 0.2µm filters before freeze drying. Samples were dissolved in 1mL glutamate detection kit buffer before loading on a 96 well-plate in a randomized order. The instructions

given by the kit were followed for carrying out the measurement. The same procedure was done with *Undibacterium* and *Duganella*. For the co-culturing experiments, bacteria were mixed in a 1:1 or 1:1:1 ratio. In order to test the consumption of glutamate, 20mM glutamate solution in Hydra medium was taken instead of glutamine solution. After incubation the reduction in glutamate concentration was measured. For testing the preference of *Duganella* between glutamate or glutamine, glutamate and glutamine were mixed in a 1:1 ratio leading to a respective 10mM concentration.

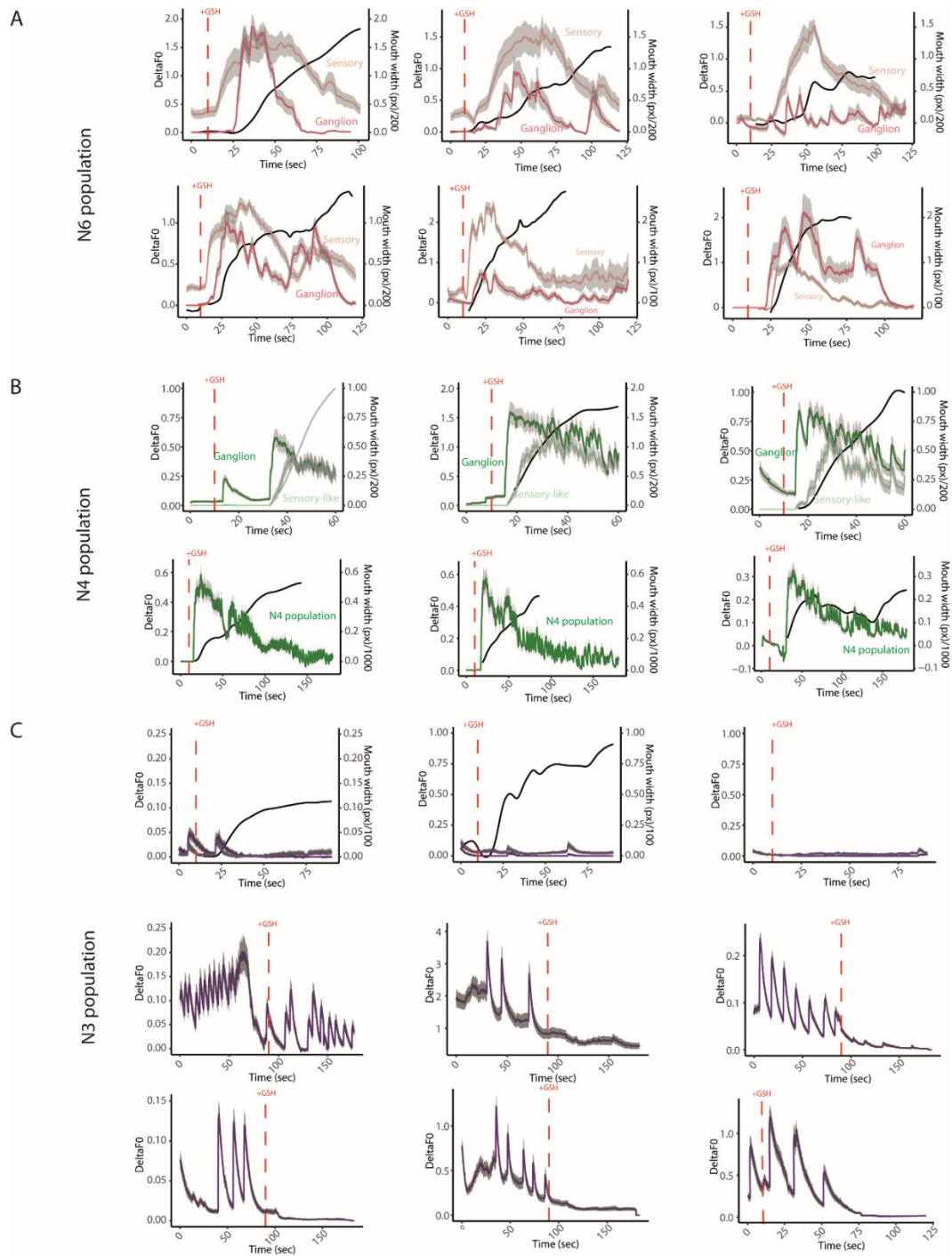
Statistics

All statistics were done using R and R-studio as IDE^{76,77}. In all cases data were tested for their equal variance using Levene's test and their normal distribution using Shapiro test. Depending on the outcome of those tests either a parametric (t-test, ANOVA, Turkey test) or non-parametric test (Kruskal-Wallis, (pairwise-) Wilcoxon test, Dunn test) were used. Correction for multiple testing was done using Bonferroni. The replicate number (n) for each dataset is indicated in the figure legends, along with the statistical method used for each comparison and the p value. For the linear correlation analysis, correlation coefficients and p-value was done via Spearman method using the R package "ggpubr". The cutoff for a significant difference was set as an $\alpha < 0.05$. Throughout the text, values are reported as median \pm standard deviation otherwise the difference is stated.

Supplemental Material



Supplement Figure 1. Expression of marker genes used for generating constructs shown in newest single cell atlas with their nomenclature¹. N6 (i_Ec4N) solely expresses G017227 (t2059aep). N3 (i_Ec3N) solely expresses G004115 (t12874aep). N4 (i_En1N) solely expresses G008286 (t14976aep).

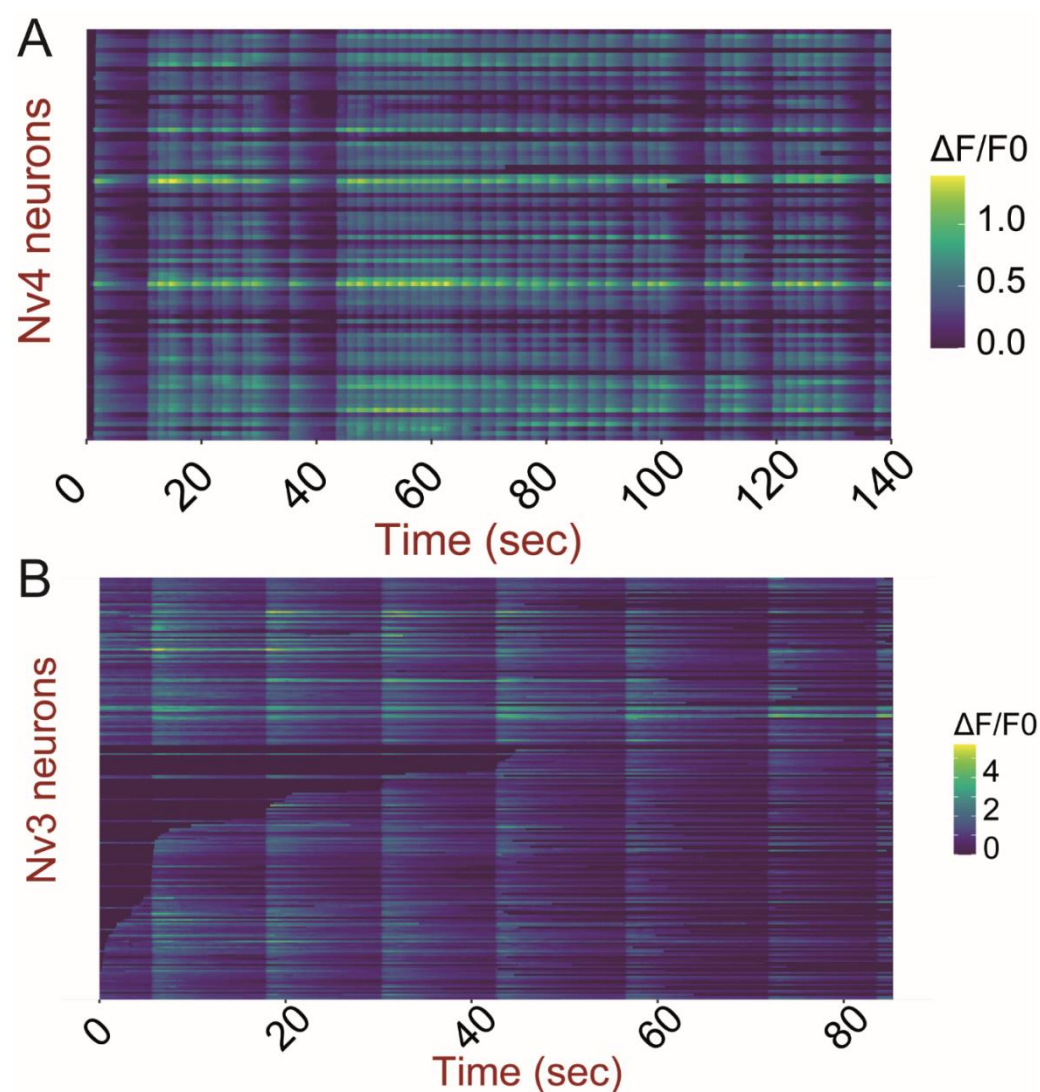


Supplement Figure 3.

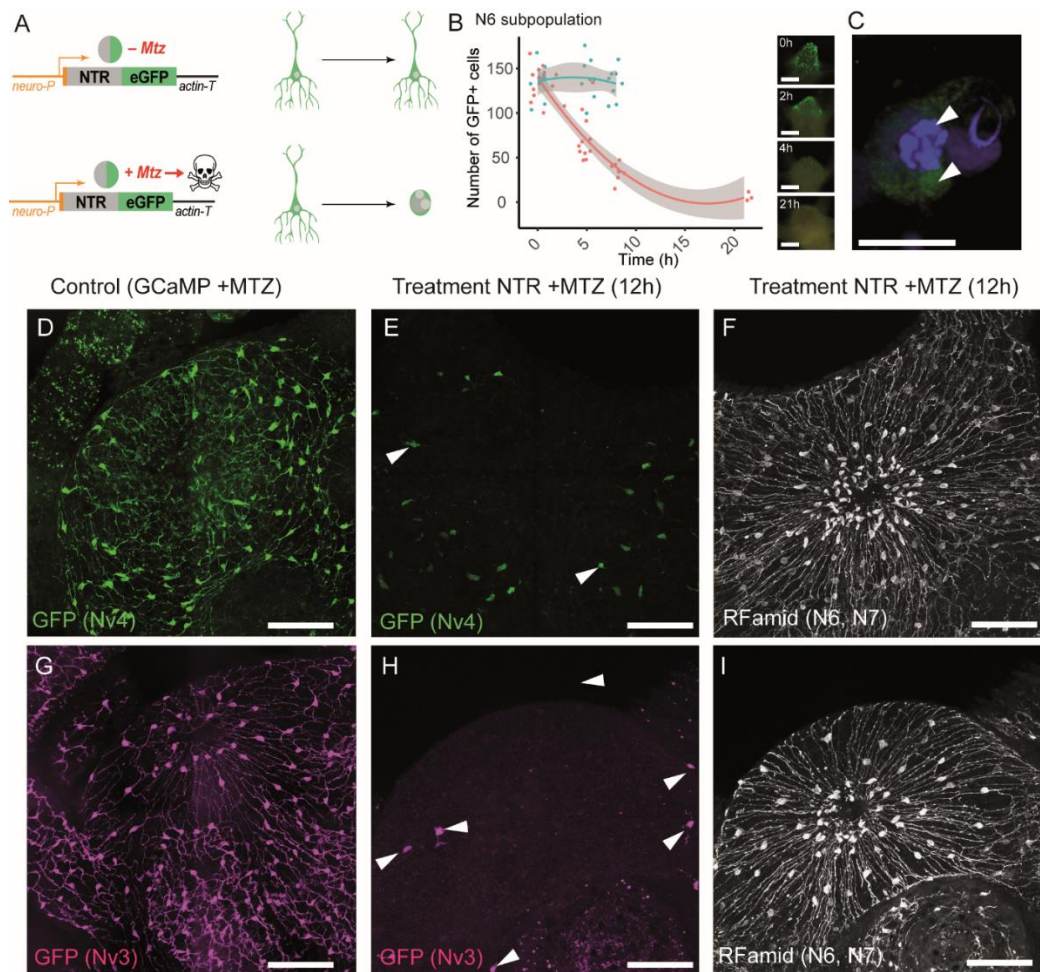
A. N6 subpopulation activated by GSH shown with GCaMP6S. Here shown multiple animals undergoing the eating behavior. Calcium traces were split into sensory and ganglion neurons. The mean of each cell type population is shown with the standard deviation. In addition, the mouth opening is shown as mouth width over time (measured in pixel) adjusted to the fluorescence change.

B. N4 subpopulation activated by GSH shown with GCaMP6S. Here shown multiple animals undergoing the eating behavior. Calcium traces were split into sensory-like and ganglion neurons in the first row otherwise the response of the whole population is shown (mainly ganglion). The mean of each cell type population is shown with the standard deviation. In addition, the mouth opening is shown as mouth width over time (measured in pixel) adjusted to the fluorescence change.

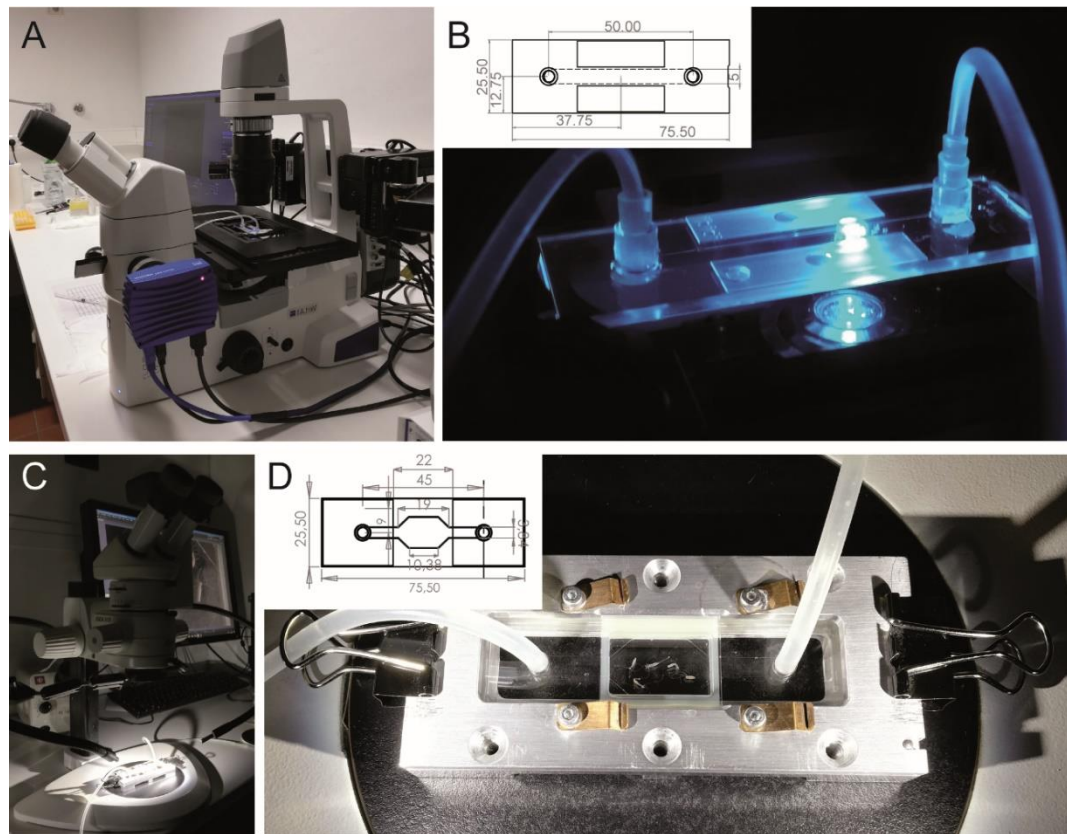
C. N3 subpopulation activated by GSH shown with GCaMP6S. Here shown multiple animals undergoing the eating behavior. Calcium traces were split into foot and head neurons in the first row otherwise the response of the whole population is shown. The mean of each cell type population is shown with the standard deviation. In addition, the mouth opening is included as mouth width over time (measured in pixel) adjusted to the fluorescence change in the first two plots.



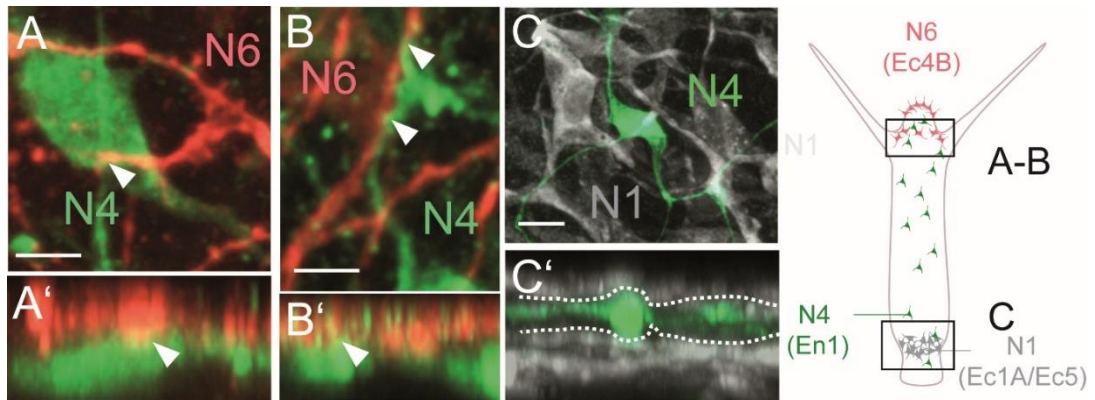
Supplement Figure 4. N3 and N4 synchronous firing. Neuronal populations N4 (**A**) and N3 (**B**) show synchronous firing activity in the whole population. **A.** Activity of N4 during the eating behavior. **B.** N3 during an activity episode before addition of GSH.



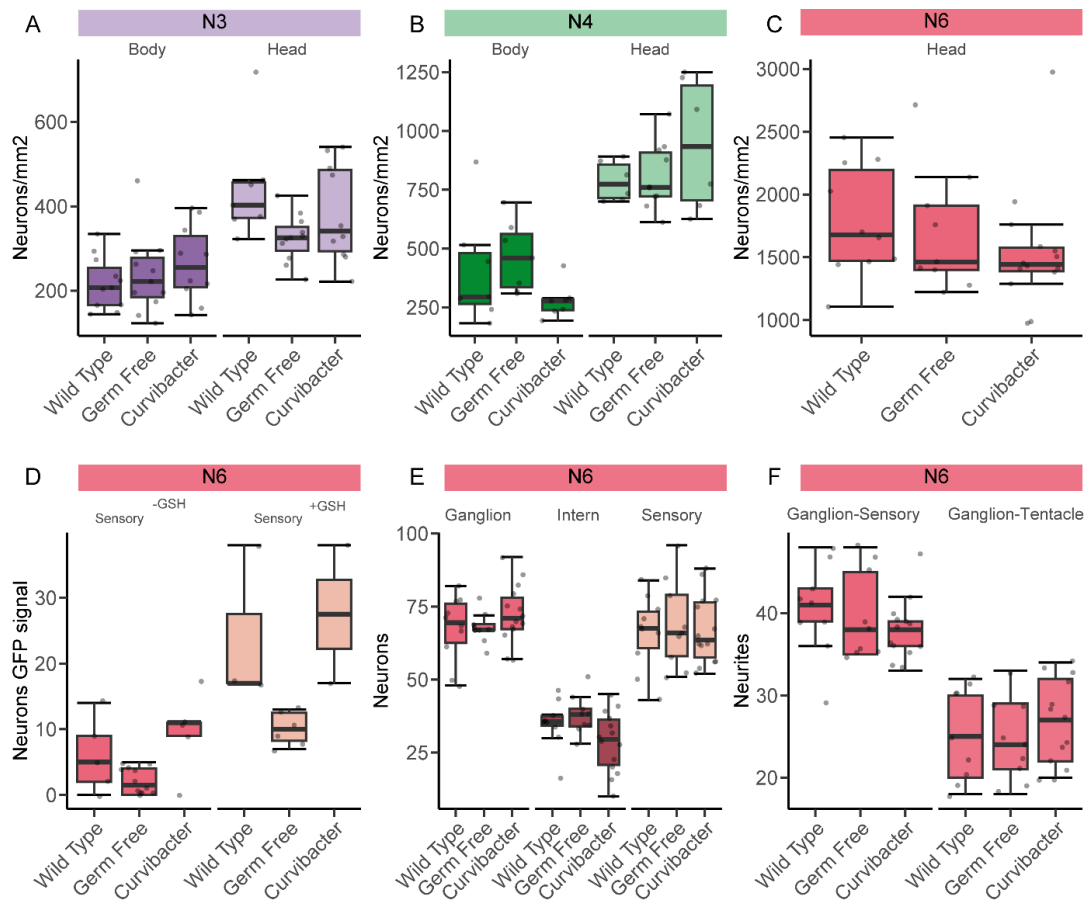
Supplement Figure 5. Cell ablation experiment. **A.** Schematic representation of the functioning of the NTR-MTZ system. **B.** Quantification of N6 GFP positive cells *in vivo* after 0h, 5h, 8h and 21h. After 8h till 21h almost all cells were lost. (Scale bar 200μm). **C.** Apoptotic GFP⁺ cell (Scale bar 10μm). **D-F.** Analysis of cell ablation of N4 neurons using antibody staining against GFP and RFamid. **D.** N4::GCaMP6S line with 10mM MTZ after >12h of incubation. **E-F.** N4::NTR-GFP with 10mM MTZ after >12h. **E.** Almost all GFP cells disappeared. **F.** Other neuronal populations are not affected. Here shown by RFamid positive cells (N6 and N7). **G-I.** Analysis of cell ablation of N3 neurons using antibody staining against GFP and RFamid. **D.** N3::GCaMP6S line with 10mM MTZ after >12h of incubation. **E-F.** N3::NTR-GFP with 10mM MTZ after >12h. **E.** Almost all GFP cells disappeared. **F.** Other populations are not affected. Here shown by RFamid positive cells (N6 and N7). Scale 100μm



Supplement Figure 6. Set up of recording animals for GCaMP6S and animal behavior. **A-B.** Experimental set up for GCaMP6S recordings. **A.** The inverse Zeiss microscope (Axio vert. A1, Zeiss). **B.** The chamber where animals were kept during recording with a technical drawing of the chamber (units in mm, Ibidi cat#80166). **C-D.** Experimental set-up for behavior analysis. **D.** The customized chamber for recording the behavior in the ablation and bacterial manipulation experiments. Technical drawing shown with units in mm.



Supplement Figure 7. Potential zones of contact between the ectodermal neuronal population N6 and the endodermal population N4. **A-B.** Regions of close contact in the head at the base of the hypostome, near the head-tentacle junctions. **C.** No similar structure or proximity observed between endodermal N4 and ectodermal N1.



Supplement Figure 9. Effect of bacteria and *Curvibacter* on neuronal subpopulations. **A.-C.** Densities of neuronal subpopulations (wildtype microbiota, germ-free and *Curvibacter*). No significant difference was observed in the change of neuronal densities compared to wildtype ($n = 10$). **D.** Count of sensory cells which showed a GCaMP6S signal either without glutathione (-GSH) or with glutathione (+GSH). In *Curvibacter*, the tendency shows that more sensory neurons are show a GCaMP6S signal without glutathione ($n = 4$). **E.** Quantification of N6 ganglion, N6 sensory and cells between locations of ganglion and sensory cells (Intern; $n = 8-13$). **F.** Quantification of neurites between ganglion and sensory cells (quantification of a half of a head, numbers are not per neuron, $n = 10$) and number of neurites reaching into tentacles (ganglion-tentacle, $n = 10$).

References:

1. Cazet, J.F., Siebert, S., Little, H.M., Bertemes, P., Primack, A.S., Ladurner, P., AchRAINER, M., Fredriksen, M.T., Moreland, R.T., Singh, S., et al. (2023). A chromosome-scale epigenetic map of the Hydra genome reveals conserved regulators of cell state. *Genome Res*, gr.277040.122. 10.1101/GR.277040.122.

Supplement Table 1. Construct sequences and lines.

Supplement Table 2. *Curvibacter* RNA Sequencing Raw reads, analyzed and annotated, related to Figure 7

Supplement Table 3 *Hydra* RNA Sequencing Raw reads, analyzed and annotated, related to Figure 6

Supplement Table 4 Statistical analysis of eating behavior and ablation of different neuronal subpopulations.

Supplement Video1: Behavior annotation, related to all behavioral analysis

Supplement Video2: Mouth opening without body and tentacles

Supplement Video3: N6 response to GSH 5xObjective, related to Figure 3

Supplement Video4: N6 response to GSH 10xObjective, related to Figure 3

Supplement Video5: N3 response to GSH 2xObjective, related to Figure 3

Supplement Video6: N3 response to GSH 10xObjective, related to Figure 3

Supplement Video7: N4 response to GSH 5xObjective, related to Figure 3

Supplement Video8: N4 response to GSH 10xObjective, related to Figure 3

References

1. Flavell, S.W., Gogolla, N., Lovett-Barron, M., and Zelikowsky, M. (2022). The emergence and influence of internal states. *Neuron* 110, 2545–2570. 10.1016/J.NEURON.2022.04.030.
2. Kennedy, A., Asahina, K., Hoopfer, E., Inagaki, H., Jung, Y., Lee, H., Remedios, R., and Anderson, D.J. (2014). Internal States and Behavioral Decision-Making: Toward an Integration of Emotion and Cognition. *Cold Spring Harb Symp Quant Biol* 79, 199–210. 10.1101/SQB.2014.79.024984.
3. Vogt, K., Zimmerman, D.M., Schlichting, M., Hernandez-Nunez, L., Qin, S., Malacon, K., Rosbash, M., Pehlevan, C., Cardona, A., and Samuel, A.D.T. (2021). Internal state configures olfactory behavior and early sensory processing in drosophila larvae. *Sci Adv* 7. 10.1126/sciadv.abd6900.
4. Anderson, D.J. (2016). Circuit modules linking internal states and social behaviour in flies and mice. *Nature Reviews Neuroscience* 2016 17:11 17, 692–704. 10.1038/nrn.2016.125.
5. Eisthen, H.L., and Theis, K.R. (2016). Animal–microbe interactions and the evolution of nervous systems. *Philosophical Transactions of the Royal Society B: Biological Sciences* 371. 10.1098/RSTB.2015.0052.
6. Carrier, T.J., and Bosch, T.C.G. (2022). Symbiosis: the other cells in development. *Development* 149. 10.1242/dev.200797.
7. Sharon, G., Sampson, T.R., Geschwind, D.H., and Mazmanian, S.K. (2016). The Central Nervous System and the Gut Microbiome. *Cell* 167, 915–932. 10.1016/J.CELL.2016.10.027.
8. Masuzzo, A., Montanari, M., Kurz, L., and Royet, J. (2020). How Bacteria Impact Host Nervous System and Behaviors: Lessons from Flies and Worms. *Trends Neurosci* 43, 998–1010. 10.1016/J.TINS.2020.09.007.
9. Nagpal, J., and Cryan, J.F. (2021). Microbiota-brain interactions: Moving toward mechanisms in model organisms. *Neuron* 109, 3930–3953. 10.1016/J.NEURON.2021.09.036.
10. Needham, B.D., Funabashi, M., Adame, M.D., Wang, Z., Boktor, J.C., Haney, J., Wu, W.L., Rabut, C., Ladinsky, M.S., Hwang, S.J., et al. (2022). A gut-derived metabolite alters brain activity and anxiety behaviour in mice. *Nature* 2022 602:7898 602, 647–653. 10.1038/s41586-022-04396-8.
11. Ogbonnaya, E.S., Clarke, G., Shanahan, F., Dinan, T.G., Cryan, J.F., and O’Leary, O.F. (2015). Adult hippocampal neurogenesis is regulated by the microbiome. *Biol Psychiatry* 78, e7–e9. 10.1016/j.biopsych.2014.12.023.
12. Valles-Colomer, M., Falony, G., Darzi, Y., Tigchelaar, E.F., Wang, J., Tito, R.Y., Schiweck, C., Kurilshikov, A., Joossens, M., Wijmenga, C., et al. (2019). The neuroactive potential of the human gut microbiota in quality of life and depression. *Nature Microbiology* 2019 4:4 4, 623–632. 10.1038/s41564-018-0337-x.
13. Zheng, P., Zeng, B., Zhou, C., Liu, M., Fang, Z., Xu, X., Zeng, L., Chen, J., Fan, S., Du, X., et al. (2016). Gut microbiome remodeling induces depressive-like behaviors through a pathway mediated by the host’s metabolism. *Molecular Psychiatry* 2016 21:6 21, 786–796. 10.1038/mp.2016.44.
14. Heijtz, R.D., Wang, S., Anuar, F., Qian, Y., Björkholm, B., Samuelsson, A., Hibberd, M.L., Forssberg, H., and Pettersson, S. (2011). Normal gut microbiota modulates brain development and behavior. *Proc Natl Acad Sci U S A* 108, 3047–3052. 10.1073/pnas.1010529108.
15. Mao, J.H., Kim, Y.M., Zhou, Y.X., Hu, D., Zhong, C., Chang, H., Brislawn, C., Langley, S., Wang, Y., Peisl, B.Y.L., et al. (2020). Genetic and metabolic links between the murine microbiome and memory. *Microbiome* 8, 1–14. 10.1186/s40168-020-00817-w.
16. Jia, Y., Jin, S., Hu, K., Geng, L., Han, C., Kang, R., Pang, Y., Ling, E., Tan, E.K., Pan, Y., et al. (2021). Gut microbiome modulates *Drosophila* aggression through octopamine signaling. *Nature Communications* 2021 12:1 12, 1–12. 10.1038/s41467-021-23041-y.

17. Dohnalová, L., Lundgren, P., Carty, J.R.E., Goldstein, N., Wenski, S.L., Nanudorn, P., Thiengmag, S., Huang, K.P., Litichevskiy, L., Descamps, H.C., et al. (2022). A microbiome-dependent gut–brain pathway regulates motivation for exercise. *Nature* 2022 612:7941–7947. 10.1038/s41586-022-05525-z.
18. Han, H., Yi, B., Zhong, R., Wang, M., Zhang, S., Ma, J., Yin, Y., Yin, J., Chen, L., and Zhang, H. (2021). From gut microbiota to host appetite: gut microbiota-derived metabolites as key regulators. *Microbiome* 2021 9:1–16. 10.1186/S40168-021-01093-Y.
19. Gabanyi, I., Lepousez, G., Wheeler, R., Vieites-Prado, A., Nissant, A., Wagner, S., Moigneu, C., Dulauroy, S., Hicham, S., Polomack, B., et al. (2022). Bacterial sensing via neuronal Nod2 regulates appetite and body temperature. *Science* (1979) 376. 10.1126/SCIENCE.ABJ3986.
20. Bosch, T.C.G., Klimovich, A., Domazet-Lošo, T., Gründer, S., Holstein, T.W., Jékely, G., Miller, D.J., Murillo-Rincon, A.P., Rentzsch, F., Richards, G.S., et al. (2017). Back to the Basics: Cnidarians Start to Fire. *Trends Neurosci* 40, 92–105. 10.1016/j.tins.2016.11.005.
21. Lentz, T.L., and Barnett, R.J. (1965). FINE STRUCTURE OF THE NERVOUS SYSTEM OF HYDRA. *Integr Comp Biol* 5, 341–356. 10.1093/ICB/5.3.341.
22. David, C.N. (1973). A Quantitative Method for Maceration of Hydra Tissue. *Wilhelm Roux' Archiv* 171, 259–268. 10.1007/BF00577724.
23. Epp, L., and Tardent, P. (1978). The Distribution of Nerve Cells in *Hydra attenuata* Pall. *Wilhelm Roux's Archives* 185, 185–193.
24. Siebert, S., Farrell, J.A., Cazet, J.F., Abeykoon, Y., Primack, A.S., Schnitzler, C.E., and Juliano, C.E. (2019). Stem cell differentiation trajectories in *Hydra* resolved at single-cell resolution. *Science* (1979) 365, eaav9314. 10.1126/science.aav9314.
25. Klimovich, A., Giacomello, S., Björklund, Å., Faure, L., Kaucka, M., Giez, C., Murillo-Rincon, A.P., Matt, A.-S., Willoweit-Ohl, D., and Crupi, G. (2020). Prototypical pacemaker neurons interact with the resident microbiota. *Proceedings of the National Academy of Sciences* 117, 17854–17863. 10.1073/pnas.1920469117.
26. Dupre, C., and Yuste, R. (2017). Non-overlapping neural networks in *Hydra vulgaris*. *Current Biology* 27, 1085–1097. 10.1016/j.cub.2017.02.049.
27. Trembley, A. (1744). Mémoires, pour servir à l'histoire d'un genre de polypes d'eau douce, à bras en forme de cornes (Chez Jean & Herman Verbeek).
28. Lenhoff, H.M. (1961). Activation of the feeding reflex in *Hydra littoralis*: I. Role played by reduced glutathione, and quantitative assay of the feeding reflex. *J Gen Physiol* 45, 331–344. 10.1085/jgp.45.2.331.
29. Loomis, W.F. (1955). Glutathione Control of the Specific Feeding Reactions of *Hydra*. *Ann N Y Acad Sci* 62, 211–227. 10.1111/j.1749-6632.1955.tb35372.x.
30. Koizumi, O., Haraguchi, Y., and Ohuchida, A. (1983). Reaction chain in feeding behavior of *Hydra*: Different specificities of three feeding responses. *Journal of Comparative Physiology A* 150, 99–105. 10.1007/BF00605293.
31. Campbell, R.D., Josephson, R.K., Schwab, W.E., Rushforth, N.B., and Campbell, R. D., et al. (1976). Excitability of nerve-free hydra. *Nature* 262, 388. 10.1038/262388a0.
32. Carter, J.A., Hyland, C., Steele, R.E., and Collins, E.M.S. (2016). Dynamics of Mouth Opening in *Hydra*. *Biophys J* 110, 1191–1201. 10.1016/j.bpj.2016.01.008.
33. Lauro, B.M., and Kass-Simon, G. (2018). *Hydra's* feeding response: Effect of GABAB ligands on GSH-induced electrical activity in the hypostome of *H. vulgaris*. *Comp Biochem Physiol A Mol Integr Physiol* 225, 83–93. 10.1016/j.cbpa.2018.07.005.
34. Cazet, J.F., Siebert, S., Little, H.M., Bertemes, P., Primack, A.S., Ladurner, P., Achraimer, M., Fredriksen, M.T., Moreland, R.T., Singh, S., et al. (2023). A chromosome-scale epigenetic map of the *Hydra* genome reveals conserved regulators of cell state. *Genome Res*, gr.277040.122. 10.1101/GR.277040.122.
35. Koizumi, O., and Maeda, N. (1981). Rise of feeding threshold in satiated *Hydra*. *J Comp Physiol* 142, 75–80. 10.1007/BF00605478.

36. Augustin, R., Schröder, K., Rincón, A.P.M., Fraune, S., Anton-Erxleben, F., Herbst, E.-M., Wittlieb, J., Schwentner, M., Grötzinger, J., and Wassenaar, T.M. (2017). A secreted antibacterial neuropeptide shapes the microbiome of *Hydra*. *Nat Commun* 8, 1–9. 10.1038/s41467-017-00625-1.
37. Murillo-Rincon, A.P., Klimovich, A., Pemöller, E., Taubenheim, J., Mortzfeld, B., Augustin, R., and Bosch, T.C.G. (2017). Spontaneous body contractions are modulated by the microbiome of *Hydra*. *Sci Rep* 7, 1–9. 10.1038/s41598-017-16191-x.
38. Darmer, D., Hauser, F., Nothacker, H.P., Bosch, T.C.G., Williamson, M., and Grimmelikhuijzen, C.J.P. (1998). Three different prohormones yield a variety of *Hydra*-RFamide (Arg-Phe-NH₂) neuropeptides in *Hydra magnipapillata*. *Biochemical Journal* 332, 403–412. 10.1042/BJ3320403.
39. Fujisawa, T. (2008). *Hydra* Peptide Project 1993–2007. *Dev Growth Differ* 50, S257–S268. 10.1111/J.1440-169X.2008.00997.X.
40. Moosler, A., Rinehart, K.L., and Grimmelikhuijzen, C.J.P. (1996). Isolation of Four Novel Neuropeptides, the *Hydra*-RFamides I–IV, from *Hydra magnipapillata*. *Biochem Biophys Res Commun* 229, 596–602. 10.1006/BBRC.1996.1849.
41. Norgaard Hansen, G., Williamson, M., and Grimmelikhuijzen, C.J.P. (2000). Two-color double-labeling in situ hybridization of whole-mount *Hydra* using RNA probes for five different *Hydra* neuropeptide preprohormones: Evidence for colocalization. *Cell Tissue Res* 301, 245–253. 10.1007/s004410000240.
42. Takahashi, T., Koizumi, O., Ariura, Y., Romanovitch, A., Bosch, T.C.G., Kobayakawa, Y., Mohri, S., Bode, H.R., Yum, S., Hatta, M., et al. (2000). A novel neuropeptide, Hym-355, positively regulates neuron differentiation in *Hydra*. *Development* 127, 997–1005. 10.1242/DEV.127.5.997.
43. Chen, T.W., Wardill, T.J., Sun, Y., Pulver, S.R., Renninger, S.L., Baohuan, A., Schreiter, E.R., Kerr, R.A., Orger, M.B., Jayaraman, V., et al. (2013). Ultrasensitive fluorescent proteins for imaging neuronal activity. *Nature* 499, 295–300. 10.1038/nature12354.
44. Guise, C.P., Grove, J.I., Hyde, E.I., and Searle, P.F. (2007). Direct positive selection for improved nitroreductase variants using SOS triggering of bacteriophage lambda lytic cycle. *Gene Therapy* 2007 14:8 14, 690–698. 10.1038/sj.gt.3302919.
45. Curado, S., Stainier, D.Y.R., and Anderson, R.M. (2008). Nitroreductase-mediated cell/tissue ablation in zebrafish: a spatially and temporally controlled ablation method with applications in developmental and regeneration studies. *Nature Protocols* 2008 3:6 3, 948–954. 10.1038/nprot.2008.58.
46. Sugiyama, T., and Fujisawa, T. (1978). Genetic analysis of developmental mechanisms in *Hydra*. II. Isolation and characterization of an interstitial cell-deficient strain. *J Cell Sci* 29, 35–52. 10.1242/JCS.29.1.35.
47. Yamamoto, W., and Yuste, R. (2020). Whole-Body Imaging of Neural and Muscle Activity during Behavior in *Hydra vulgaris*: Effect of Osmolarity on Contraction Bursts. *eNeuro* 7, 1–13. 10.1523/ENEURO.0539-19.2020.
48. Franzenburg, S., Fraune, S., Altmann, P.M., Künzel, S., Baines, J.F., Traulsen, A., and Bosch, T.C.G. (2013). Bacterial colonization of *Hydra* hatchlings follows a robust temporal pattern. *The ISME Journal* 2013 7:4 7, 781–790. 10.1038/ismej.2012.156.
49. Franzenburg, S., Walter, J., Künzel, S., Wang, J., Baines, J.F., Bosch, T.C.G., and Fraune, S. (2013). Distinct antimicrobial peptide expression determines host species-specific bacterial associations. *Proc Natl Acad Sci U S A* 110. 10.1073/pnas.1304960110.
50. Fraune, S., Anton-Erxleben, F., Augustin, R., Franzenburg, S., Knop, M., Schröder, K., Willoweit-Ohl, D., and Bosch, T.C.G. (2015). Bacteria-bacteria interactions within the microbiota of the ancestral metazoan *Hydra* contribute to fungal resistance. *ISME Journal* 9, 1543–1556. 10.1038/ismej.2014.239.
51. Pierobon, P., Sogliano, C., Minei, R., Tino, A., Porcu, P., Marino, G., Tortiglione, C., and Concias, A. (2004). Putative NMDA receptors in *Hydra*: A biochemical and functional study. *European Journal of Neuroscience* 20, 2598–2604. 10.1111/j.1460-9568.2004.03759.x.
52. Lenhoff, H.M., and Bovaird, J. (1961). Action of glutamic acid and glutathione analogues on the *Hydra* glutathione-receptor. *Nature* 189, 486–487. 10.1038/189486a0.

53. Pierobon, P. (2012). Coordinated modulation of cellular signaling through ligand-gated ion channels in *Hydra vulgaris* (Cnidaria, Hydrozoa). *International Journal of Developmental Biology* 56, 551–565. 10.1387/ijdb.113464pp.
54. Weissbourd, B., Momose, T., Nair, A., Kennedy, A., Hunt, B., and Anderson, D.J. (2021). A genetically tractable jellyfish model for systems and evolutionary neuroscience. *Cell* 184, 5854–5868.e20. 10.1016/j.cell.2021.10.021.
55. Wang, H., Swore, J., Sharma, S., Szymanski, J.R., Yuste, R., Daniel, T.L., Regnier, M., Bosma, M.M., and Fairhall, A.L. (2023). A complete biomechanical model of *Hydra* contractile behaviors, from neural drive to muscle to movement. *Proceedings of the National Academy of Sciences* 120, e2210439120. 10.1073/PNAS.2210439120.
56. Badhiwala, K.N., Primack, A.S., Juliano, C., and Robinson, J.T. (2021). Multiple neuronal networks coordinate *hydra* mechanosensory behavior. *Elife* 10. 10.7554/ELIFE.64108.
57. Fraune, S., and Bosch, T.C.G. (2007). Long-term maintenance of species-specific bacterial microbiota in the basal metazoan *Hydra*. *Proceedings of the National Academy of Sciences* 104, 13146–13151. 10.1073/pnas.0703375104.
58. Bosch, T.C.G. (2013). Cnidarian-microbe interactions and the origin of innate immunity in metazoans. *Annu Rev Microbiol* 67, 499–518. 10.1146/annurev-micro-092412-155626.
59. Bosch, T.C.G. (2014). Rethinking the role of immunity: lessons from *Hydra*. *Trends Immunol* 35, 495–502. 10.1016/j.it.2014.07.008.
60. Kinnamon, J.C., and Westfall, J.A. (1982). Types of neurons and synaptic connections at hypostome-tentacle junctions in *Hydra*. *J Morphol* 173, 119–128. 10.1002/jmor.1051730110.
61. Kinnamon, J.C., and Westfall, J.A. (1981). A three dimensional serial reconstruction of neuronal distributions in the hypostome of a *Hydra*. *J Morphol* 168, 321–329. 10.1002/jmor.1051680308.
62. Westfall, J.A. (1973). Ultrastructural evidence for a granule-containing sensory-motor-interneuron in *Hydra littoralis*. *J Ultrastruct Res* 42, 268–282. 10.1016/S0022-5320(73)90055-5.
63. Westfall, J.A., Yamataka, S., and Enos, P.D. (1971). ULTRASTRUCTURAL EVIDENCE OF POLARIZED SYNAPSES IN THE NERVE NET OF HYDRA. *Journal of Cell Biology* 51, 318–323. 10.1083/JCB.51.1.318.
64. Davis, L.E., Burnett, A.L., Haynes, J.F., Osborne, D.G., and Spear, M. Lou (1968). Histological and ultrastructural study of the muscular and nervous systems in *Hydra*. II. Nervous system. *Journal of Experimental Zoology* 167, 295–331. 10.1002/jez.1401670305.
65. Westfall, J.A., and Kinnamon, J.C. (1978). A second sensory-motor-interneuron with neurosecretory granules in *Hydra*. *J Neurocytol* 7, 365–379. 10.1007/BF01176999.
66. Deines, P., Hammerschmidt, K., and Bosch, T.C.G. (2020). Microbial species coexistence depends on the host environment. *mBio* 11, 1–13. 10.1128/mBio.00807-20.
67. Pfaff, D., Tabansky, I., and Haubensak, W. (2019). Tinbergen’s challenge for the neuroscience of behavior. *Proceedings of the National Academy of Sciences* 116, 9704–9710. 10.1073/PNAS.1903589116.
68. Tinbergen, N. (1963). On aims and methods of Ethology. *Z Tierpsychol* 20, 410–433. 10.1111/J.1439-0310.1963.TB01161.X.
69. Reigstad, C.S., Salmonson, C.E., Rainey, J.F., Szurszewski, J.H., Linden, D.R., Sonnenburg, J.L., Farrugia, G., and Kashyap, P.C. (2015). Gut microbes promote colonic serotonin production through an effect of short-chain fatty acids on enterochromaffin cells. *FASEB Journal* 29, 1395–1403. 10.1096/fj.14-259598.
70. Mazzoli, R., and Pessione, E. (2016). The neuro-endocrinological role of microbial glutamate and GABA signaling. *Front Microbiol* 7, 1–17. 10.3389/fmicb.2016.01934.
71. Klimovich, A., Wittlieb, J., and Bosch, T.C.G. (2019). Transgenesis in *Hydra* to characterize gene function and visualize cell behavior. *Nature Protocols* 2019 14:7 14, 2069–2090. 10.1038/s41596-019-0173-3.

72. Weisburg, W.G., Barns, S.M., Pelletier, D.A., and Lane, D.J. (1991). 16S ribosomal DNA amplification for phylogenetic study. *J Bacteriol* 173, 697–703. 10.1128/JB.173.2.697-703.1991.
73. Wein, T., Dagan, T., Fraune, S., Bosch, T.C.G., Reusch, T.B.H., and Hülter, N.F. (2018). Carrying capacity and colonization dynamics of *Curvibacter* in the hydra host habitat. *Front Microbiol* 9, 1–10. 10.3389/fmicb.2018.00443.
74. Wittlieb, J., Khalturin, K., Lohmann, J.U., Anton-Erxleben, F., and Bosch, T.C.G. (2006). Transgenic Hydra allow in vivo tracking of individual stem cells during morphogenesis. *Proc Natl Acad Sci U S A* 103, 6208–6211. 10.1073/pnas.0510163103.
75. Schindelin, J., Arganda-Carreras, I., Frise, E., Kaynig, V., Longair, M., Pietzsch, T., Preibisch, S., Rueden, C., Saalfeld, S., Schmid, B., et al. (2012). Fiji: an open-source platform for biological-image analysis. *Nature Methods* 2012 9:7 9, 676–682. 10.1038/nmeth.2019.
76. Team, R.C. (2020). R Core Team R: a language and environment for statistical computing. Foundation for Statistical Computing.
77. Team, R.S. (2022). RStudio: integrated development environment for R. R Studio, PBC, Boston, Massachusetts, United States of America.
78. Wickham, H., Averick, M., Bryan, J., Chang, W., D' L., McGowan, A., François, R., Grolemund, G., Hayes, A., Henry, L., et al. (2019). Welcome to the Tidyverse. *J Open Source Softw* 4, 1686. 10.21105/JOSS.01686.
79. De Chaumont, F., Dallongeville, S., Chenouard, N., Hervé, N., Pop, S., Provoost, T., Meas-Yedid, V., Pankajakshan, P., Lecomte, T., Le Montagner, Y., et al. (2012). Icy: an open bioimage informatics platform for extended reproducible research. *Nature Methods* 2012 9:7 9, 690–696. 10.1038/nmeth.2075.
80. Chenouard, N., Bloch, I., and Olivo-Marin, J.C. (2013). Multiple hypothesis tracking for cluttered biological image sequences. *IEEE Trans Pattern Anal Mach Intell* 35, 2736–2750. 10.1109/TPAMI.2013.97.
81. Lowe, D.G. (2004). Distinctive image features from scale-invariant keypoints. *Int J Comput Vis* 60, 91–110. 10.1023/B:VISI.0000029664.99615.94.
82. Lagache, T., Hanson, A., Pérez-Ortega, J.E., Fairhall, A., and Yuste, R. (2021). Tracking calcium dynamics from individual neurons in behaving animals. *PLoS Comput Biol* 17, e1009432. 10.1371/JOURNAL.PCBI.1009432.
83. Rupprecht, P., Carta, S., Hoffmann, A., Echizen, M., Blot, A., Kwan, A.C., Dan, Y., Hofer, S.B., Kitamura, K., Helmchen, F., et al. (2021). A database and deep learning toolbox for noise-optimized, generalized spike inference from calcium imaging. *Nature Neuroscience* 2021 24:9 24, 1324–1337. 10.1038/s41593-021-00895-5.
84. Pietschke, C., Treitz, C., Forêt, S., Schultze, A., Künzel, S., Tholey, A., Bosch, T.C.G., and Fraune, S. (2017). Host modification of a bacterial quorum-sensing signal induces a phenotypic switch in bacterial symbionts. *Proc Natl Acad Sci U S A* 114, E8488–E8497. 10.1073/pnas.1706879114.
85. Batut, B., van den Beek, M., Doyle, M.A., and Soranzo, N. (2021). RNA-Seq Data Analysis in Galaxy. *Methods in Molecular Biology* 2284, 367–392. 10.1007/978-1-0716-1307-8_20.
86. Martin, M. (2011). Cutadapt removes adapter sequences from high-throughput sequencing reads. *EMBnet J* 17, 10–12. 10.14806/EJ.17.1.200.
87. Bolger, A.M., Lohse, M., and Usadel, B. (2014). Trimmomatic: a flexible trimmer for Illumina sequence data. *Bioinformatics* 30, 2114–2120. 10.1093/BIOINFORMATICS/BTU170.
88. Ewels, P., Magnusson, M., Lundin, S., and Käller, M. (2016). MultiQC: summarize analysis results for multiple tools and samples in a single report. *Bioinformatics* 32, 3047–3048. 10.1093/BIOINFORMATICS/BTW354.
89. Langmead, B., Trapnell, C., Pop, M., and Salzberg, S.L. (2009). Ultrafast and memory-efficient alignment of short DNA sequences to the human genome. *Genome Biol* 10: R25. 10.1186/gb-2009-10-3-r25.
90. Liao, Y., Smyth, G.K., and Shi, W. (2014). featureCounts: an efficient general purpose program for assigning sequence reads to genomic features. *Bioinformatics* 30, 923–930. 10.1093/BIOINFORMATICS/BTT656.

91. Love, M.I., Huber, W., and Anders, S. (2014). Moderated estimation of fold change and dispersion for RNA-seq data with DESeq2. *Genome Biol* 15, 1–21. 10.1186/s13059-014-0550-8.

Chapter IV:

The internal metabolic state controls behavior in *Hydra* through an interplay of enteric and central nervous system-like neuron populations

Preprint on BioRxiv and submitted (2023)

Christoph Giez¹, Christopher Noack¹, Ehsan Sakib¹, Thomas Bosch¹

Zoological Institute, University of Kiel, Am Botanischen Garten 1-9, 24118 Kiel, Germany

Submitted manuscript (2023)

DOI: <https://doi.org/10.1101/2023.09.15.557876>

Abstract:

Hunger and satiety can have an influence on decision making, sensory processing, and motor behavior by altering the internal state of the brain. This process necessitates the integration of peripheral sensory stimuli into the central nervous system. Interestingly, even organisms without a brain, such as the Cnidaria, exhibit feeding dependent behavioral changes. The underlying mechanisms, however, remain unclear. In this study, we demonstrate that neuronal activity in two distinct neuronal populations, the ectodermal N3 neurons and the endodermal N4 neurons in *Hydra*, an ancestral metazoan animal with a diffuse nerve net spread throughout the body with no signs of centralization, are responsible for feeding dependent behavioral changes. Specifically, endodermal N4 neurons are essential for food intake and digestive functions, similar to the enteric nervous system, while the N3 population influences and inhibits other motor related behaviors, comparable to the central nervous system. This fascinating observation provides a new insight into the evolution and the complexity of a simple non-centralized nervous system.

Key words: Evolution, internal state, enteric nervous system, central nervous system, satiety, *Hydra*, Cnidaria

Introduction:

Most if not all animals exhibit behavioral responses in relation to food consumption or starvation. Satiety and hunger are two metabolic states which have a global effect and influence on decision making, sensory processing and motor behavior¹⁻³. In the majority of animals including human, the integration of such information occurs in the brain which then effects the outcome of behaviors. The signal of satiety emerges in the periphery, in the gastrointestinal tract and enteric nervous system⁴. Interestingly, internal states such as hunger or satiety can be already observed in organisms without a centralization of the nervous system and an enteric nervous system such as in the phylum Cnidaria⁵⁻⁸. Cnidaria (i.e., sea anemones, jellyfish, corals and *Hydra*) and Bilateria (i.e., vertebrates, sea stars, fruit flies), are sister groups that diverged around 600 million years ago (**Fig. 1A**)⁹. In the jellyfish *Clytia*, starvation had an influence on the food passing behavior⁵. In *Cassiopea* and *Hydra* a sleep-like state has been observed where they exhibit phases of quiescence^{6,7}. Further, *Hydra* seems to have a feeding state dependent phototaxis behavior where it is more attracted to light when starved⁸. However, the neuronal basis of those internal states has not been elucidated so far.

The tubular bodies of *Hydra* are radially symmetric and have only two layers, an ectodermal and an endodermal epithelium. A gastrovascular cavity has a single exterior opening that serves as both mouth and anus. Tentacles surround the mouth opening. Nerve cells are organized into two simple nerve nets, one ectodermal and the other endodermal, consisting of multiple neuronal populations that help coordinate muscular and sensory functions (**Fig. 1B - D**). Previous work has shown that the eating behavior of *Hydra* can be induced by reduced glutathione^{10,11}. Interestingly, after one GSH-induced full eating behavior a recovery period of over 24h has been described¹⁰. However, despite this, the polyps were still able to ingest living prey¹². The sensitivity to glutathione seems to depend on the feeding status since well-fed animals did not exhibit a feeding

response^{10,13}. Those papers already speculated about an internal state suggested to control the eating behavior¹⁴.

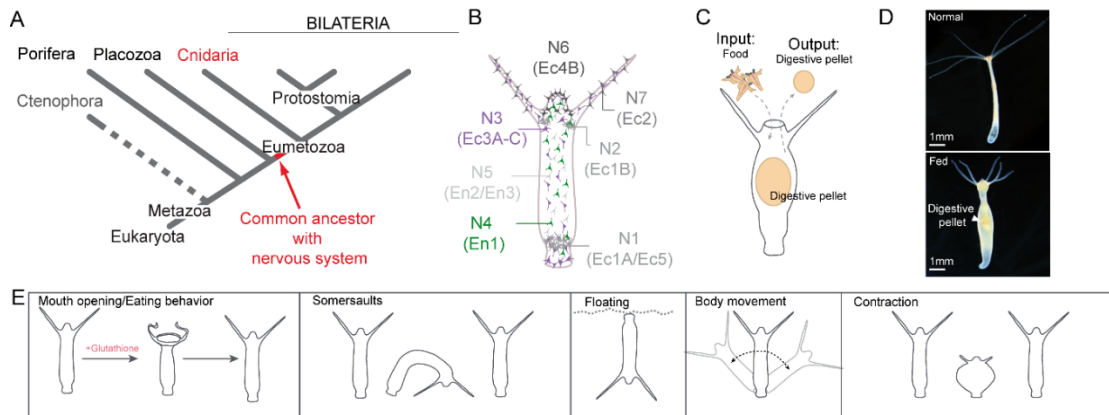


Figure 1. *Hydra* as a model system to study the evolution of the nervous system.

A. Phylogenetic positioning of *Hydra* at the origin of the nervous system with the same building tools than those of Bilaterian.

B. The different neuronal populations identified by single cell sequencing^{33–35}. The different nomenclature highlighted here.

C. Input of food and output of remaining digestive pellet is the same in *Hydra*.

D. *Hydra* not fed and *Hydra* 4 hours post feeding.

E. Different behavioral pattern in *Hydra*: Mouth opening due to glutathione, somersaults, floating at the surface, body movement or swaying and contractions.

Here we explored the possibility of satiety dependent behavioral changes in *Hydra* and the neuronal mechanism underlying the satiety-driven modifications that integrate information related to feeding status. Additionally, we examined whether there is a sub-functionalization of the nervous system regarding feeding-related behaviors and another for motor and information processing. Our study shows that *Hydra*'s behavior changes significantly depending on the degree of satiety. Immediately after the animal has taken food, *Hydra* stops contracting, somersaulting and shows no response to glutathione (food stimulus) but an increase in body movement (**Fig. 1E**). This drastic change in behavior arises from the ectodermal neuronal network N3 which shows a feeding dependent activity change. The genetic ablation of N3 neurons leads in well fed animals to a decrease in body movement, increased phototaxis and to a longer mouth opening

induced by glutathione. The endodermal neuronal network N4 responds differently depending on the presence and absence of a digestive pellet in the gastric cavity. Ablation of enteric-like N4 neurons leads to a bursting of the entire well-fed polyp beneath the hypostome since the animals lost the ability to spit out the digestive pellet. In summary, we identified the ectodermal neuronal network N3 as being responsible for encoding the metabolic internal state and an endodermal neuronal network N4 which is necessary for feeding and digestion associated behaviors. These findings may reflect an early separation of a diffuse neural network into a population of centralized and population-cooperating neurons and an enteric nervous system-like population.

Results

Ever since the eating behavior of the classical model organism *Hydra* has been described, multiple papers have reported that there is a refraction time or habituation to the stimulus of glutathione. Here, we did a first thorough investigation of this phenomenon and discovered that satiety of *Hydra* has a global effect on multiple behaviors but does not depend on glutathione exposure.

Satiety changes behavioral patterns in *Hydra*

To show that an exposure to glutathione or the extensive feeding of *Hydra* have an impact on the re-exposure to glutathione, we tested animals for their eating behavior which were either extensively fed with *Artemia* or exposed to glutathione (chemical food signal) for 2 hours. Animals which were extensively fed with *Artemia* showed only little response to glutathione until 10 hours post feeding while having normal behavior after 24 hours again (**Fig. 2A**). In a similar manner, their response time (the time until the mouth opens) was significantly slower within the first 8 hours post feeding while at 10 hours they responded normally fast again (**Fig. 2B**). In contrast, animals exposed to glutathione for 2 hours prior to the experiment showed a normal behavior after 4h post exposure (**Fig. 2A-B**). However, their response time was slightly slower over a longer period of time (**Fig. 2B**). In summary, only feeding *Artemia* resulted in a sensation of satiety with subsequent and long-lasting changes in mouth opening/eating behavior. Exposure to glutathione had only small effects.

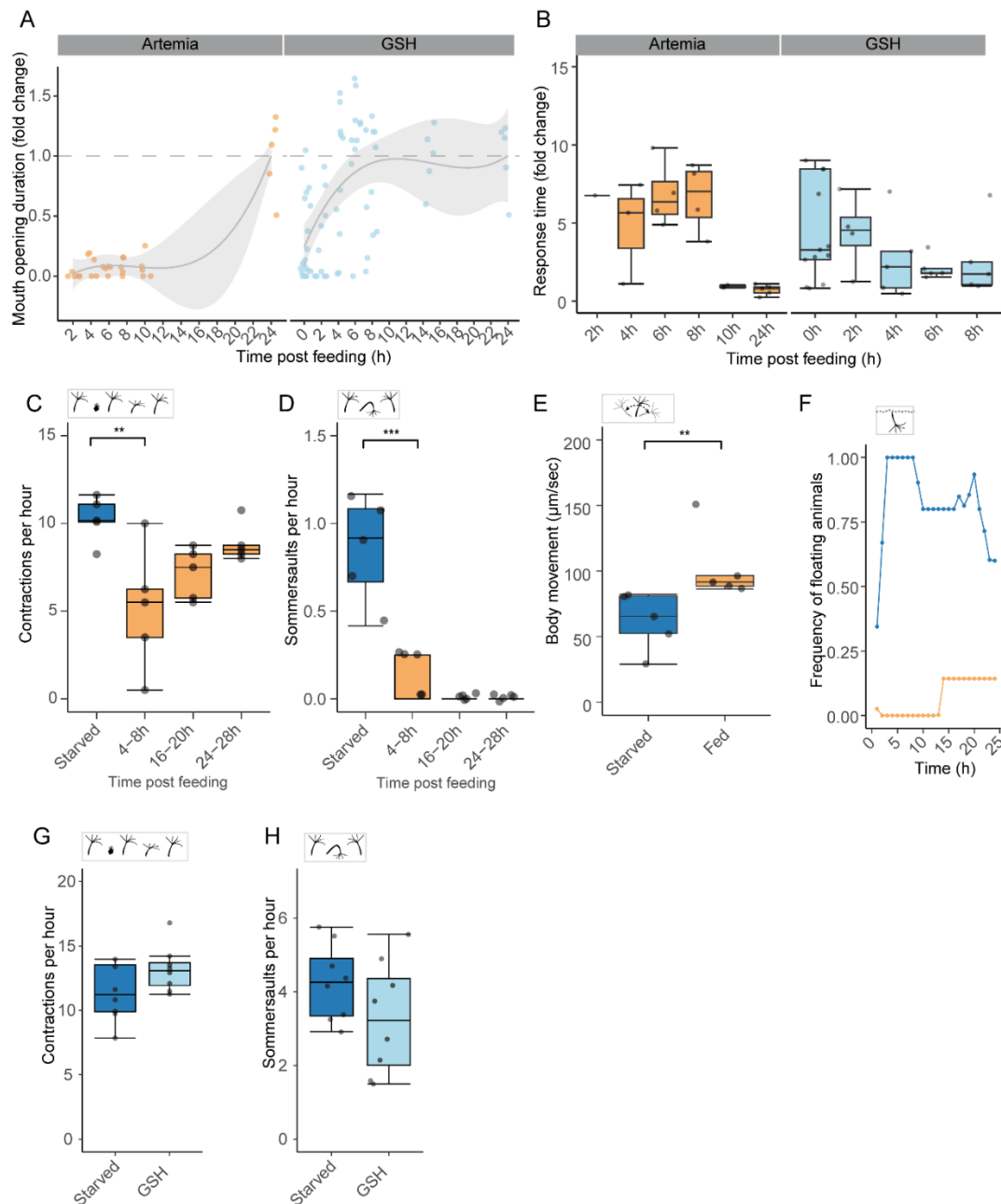


Figure 2. Satiety has a global impact on different behaviors and depends on the ingestion of digestible food.

A. After feeding animals extensively, the feeding response cannot be induced by reduced glutathione (GSH) till 10 hours post feeding (orange). The feeding cannot be mimicked by incubating animals for 2h in GSH prior experiment (light blue). $n = 5-10$

B. After feeding the response time to GSH is delayed for 8 hours post feeding whereas the effect of GSH exposure vanishes much faster ($n = 5-10$).

C. Comparing starved animals (10 days without feeding) to fed animals, a difference in contractions per hour was observed for 4-8 hours post feeding while afterwards the frequency returns to the starved conditions ($n = 5$, ANOVA, t-test, $p < 0.01$).

D. Somersaults were almost absent in fed animals whereas starved animals made 1 somersault per hour ($n = 5$, Kruskal-Wallis test, Dunn test, $p < 0.001$).

E. The movement of the body center by any kind of direction change was slightly increased in fed compared to starved animals ($n = 5$, Kruskal-Wallis test, Dunn test, $p < 0.01$).

F. Starved animals had a higher proportion of animals floating (detached and at the water surface) than fed animals ($n = 5$). The effect persisted over 24h.

G-H. The effect on contractions and somersaults could not be affected by pre-exposure to GSH (2h incubation). ($n = 5$)

Observing the effect of satiety on the eating behavior, we were curious if other movement patterns of *Hydra* such as spontaneous body contractions, somersaults, or movements in general were also affected. Therefore, we next explored a range of behaviors of animals after being fed and scored their behavioral patterns (**Fig. 1E**, **Fig. 2C-F**). We observed that contractions were significantly reduced ($p < 0.01$, $n = 5$) until 8 hours post feeding but increased thereafter and reached the contraction frequency of starved animals again around 24 hours post feeding (**Fig. 2C**). In case of somersaults, fed animals displayed a notable absence of somersaults which was significantly less than starved animals ($p < 0.001$, **Fig. 2D**). Interestingly, measurements of movement from the center of the body (see **Fig. 1E**) point to large overall movements of the polyps (**Fig. 2E**). Given the absence of observed somersault events, next we wanted to find out if starved animals are more frequently detached and float on the surface. By comparing the proportion of floating animals between starved and fed animals, we examined that starved animals were mainly floating whereas fed animals did not show any detachment until 13 hours post feeding (**Fig. 2F**). The behavioral changes were specific to animals which were fed with *Artemia* since the same behavioral changes could not be observed with glutathione exposure (**Fig. 2G-H**). In summary, satiety has a global and long-lasting effect on the behavior of the polyp *Hydra*. The stimulus responsible for this clearly comes from digestion and engulfment of real food and cannot be replaced by glutathione.

Neuronal populations 3 and 4 respond to satiety very differently

Intrigued by the behavioral changes, next we investigated if the effects are induced by changes in neuronal activity. To approach the nature of the neuronal control of satiety in *Hydra*, we conducted a systematic screening of different neuronal populations by using previously established calcium imaging lines. In a

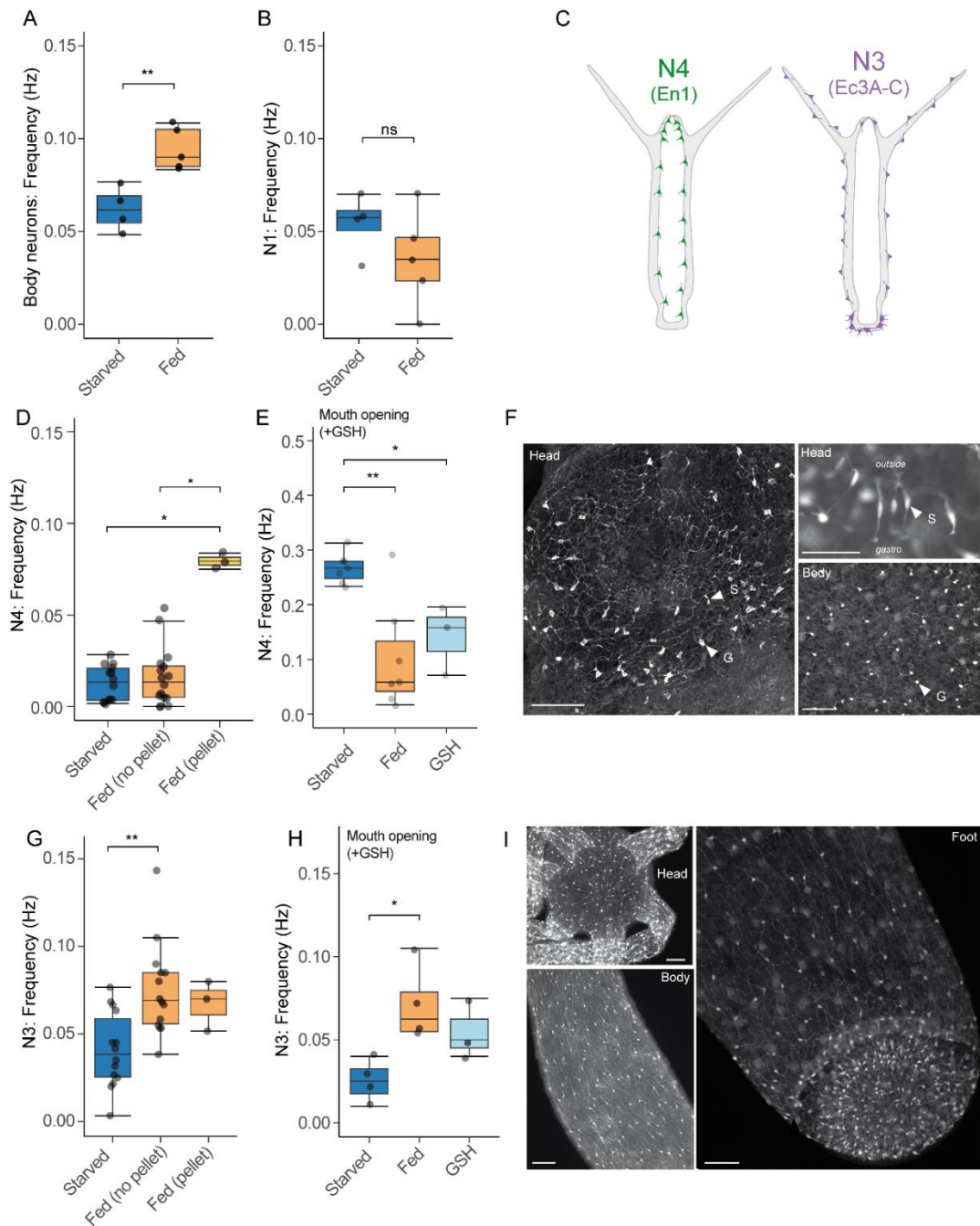


Figure 3. Two globally distributed neuronal networks respond differently 4 hours post feeding and do not respond normally to glutathione.

A. Neuronal activity increased in the body column of a pan-neuronal line after 4 hours post feeding compared to starved animals. All neuronal activity was analyzed, no differentiation between populations ($n = 5$, T-test).

B. Neuronal activity of the CB/N1 network in the foot of animals either starved or 4 hours post feeding showed no difference ($n = 4-5$, T-Test).

C. Schematic of the two different neuronal populations in *Hydra*. N3 in the ectoderm and distributed along the whole-body axis. N4 in the endoderm and only distributed in the body column and head.

D. Endodermal N4 neuronal population showed no difference 4 hours post feeding compared to starved animals when there is no pellet inside the animals. Animals with a digestion pellet showed a significant increase in spiking frequency. (n = 3- 16, ANOVA, Turkey)

E. Endodermal N4 population did not show an increase in spiking frequency as starved animals when exposed to reduced glutathione 4 hours post feeding or 1 hour post GSH exposure (n= 3-6, ANOVA, Turkey).

F. Immunohistochemistry of endodermal neuronal population N4 in different locations of *Hydra*. In the head N4 has a spiderweb similar arrangement with sensory cells (S) and ganglion cells. *Scale bar 100µm*

G. Ectodermal N3 population increased in spiking frequency 4 hours post feeding compared to starved animals. The presence or absence of a pellet did not affect the spiking frequency (n = 3-17, ANOVA, Turkey).

H. Ectodermal N3 population did not decrease in spiking frequency compared to starved animals when exposed to glutathione 4 hours post feeding or 1 hour post feeding. (n= 3-6, ANOVA, Turkey)

I. Immunohistochemistry of ectodermal population N3 at different locations in *Hydra*. Highest neuronal density is found in the foot. *Scale bar 100µm*

p-values: * p<0.05, ** p< 0.01, *** p< 0.001

first step, we took the advantage of a pan-neuronal *Hydra* line (alpha-tubulin promotor¹⁵) and investigated neuronal activity in the body column (**Fig. 3A**). We observed a significant increase in neuronal activity in the body column when comparing starved and 4 hours post feeding animals (p<0.01). However, it was not possible to distinguish between distinct neuronal subgroups and to identify the specific population accountable for the observed phenomenon. Therefore, we explored all different neuronal networks which were described so far (**Fig. 1 B, Fig. 3C**)^{16–18}. First, we examined the N1 neuronal network - previously named contraction burst (CB) - which was correlated with body contractions¹⁷. The N1 network showed a slight decrease in its frequency in fed animals (**Fig. 3B**). Second, we analyzed the spiking frequency of the endodermal neuronal population N4 (**Fig. 3C and F**). The N4 neuronal displayed no notable distinction between animals which were fed and had expelled their digestive pellet compared to starved animals (**Fig. 3D**). Most interestingly however, animals that had not expelled their pellet and still retained it in the gastric cavity behaved quite differently by showing a significant increase in their spiking frequency (p< 0.05, **Fig. 3D**). Finally, we analyzed the spiking frequency of the ectodermal neuronal population N3 (**Fig. 3C and I**). N3 neurons showed a significant increase in spiking, independent of the presence or absence of a digestive pellet in the gastric

cavity when compared to starved animals ($p < 0.01$, **Fig. 3G**). Since a change in the mouth opening duration has been observed in fed animals (**Fig. 2A-B**), we aimed to investigate whether there was a correlation between the significant

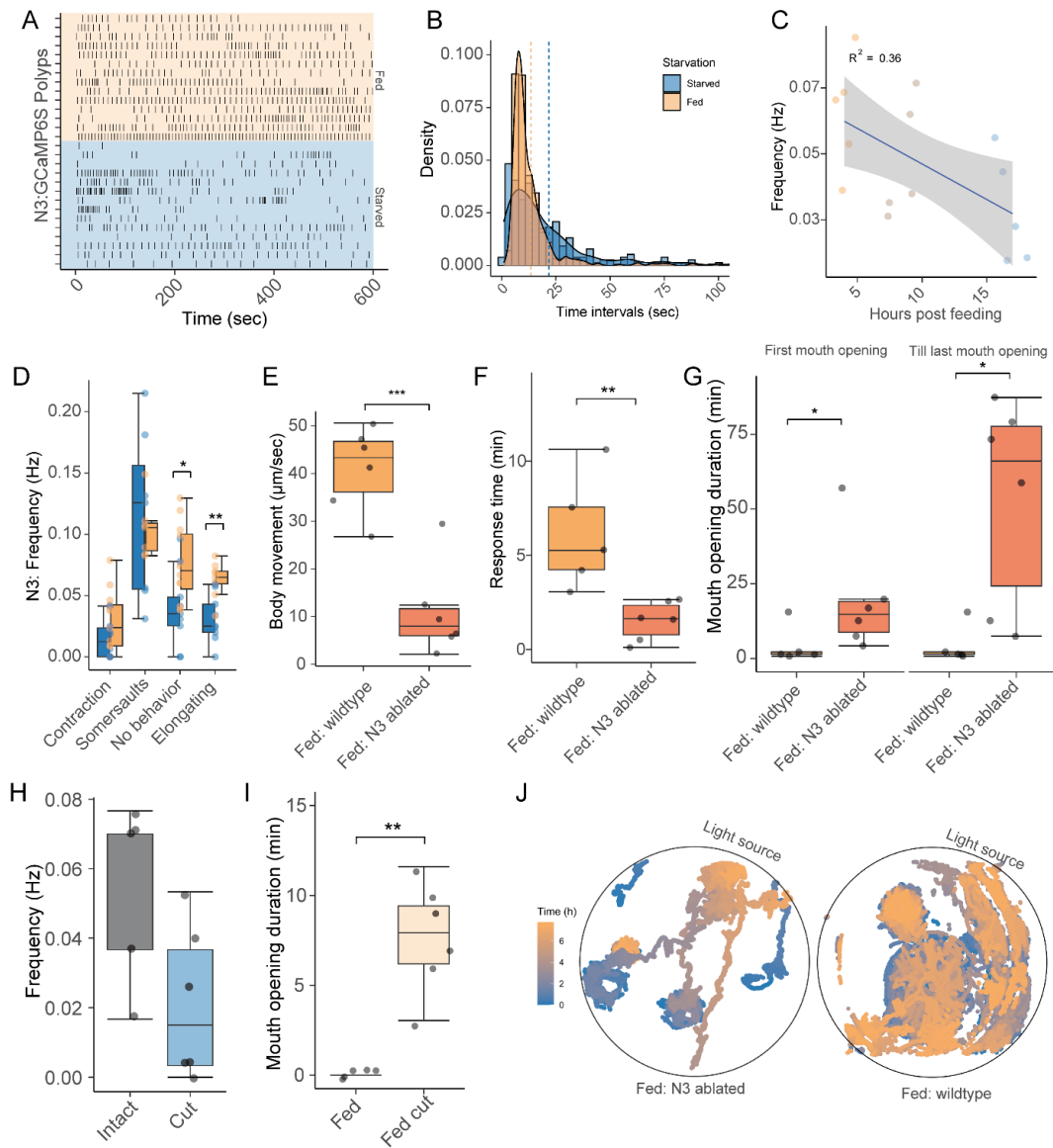


Figure 4. N3 neurons spikes regularly and prevents mouth opening as well as general body movement post feeding in a spiking frequency dependent manner.

A. Spiking trains of either fed (4 hours post feeding) and starved animals.

B. Inter spike intervals distribution across the two different treatments: starved and fed. More shorter and regular spikes observed in fed animals than starved.

C. Ectodermal N3 population decreased in spiking frequency post feeding and showed a negative correlation ($n = 5$). Each data point responds to an independent animal post the respective time of feeding.

D. N3 neurons exhibited different spiking frequency during different behaviors associated with N3. In fed animals (4h post feeding) the spiking frequency during elongation and non-behavior associated spiking is significantly increased. ($n = 5-10$, T-test)

E. In well fed animals where N3 neurons were ablated, almost no body movement was observed, whereas wildtype animals exhibited higher mobility. (n=6-7, T-test)

F. Ablation of N3 restored response time to glutathione of fed animals. Animals responded within 1.63 ± 1.04 min to GSH whereas fed animals responded 10 ± 35.8 min. (n = 5-6, Wilcox-Test)

G. Ablation of N3 led animals respond to GSH for a longer period than fed animals. N3 ablated animals showed multiple mouth openings (≥ 2). (n = 5-6, Wilcox-Test)

H. In animals without a foot the spiking frequency of N3 is decreased compared to intact polyps (n = 6).

I. When exposed to glutathione animals without a foot respond again with a mouth opening (n = 6).

J. Phototaxis behavior is elevated in N3 ablated animals, a behavior which is normally suppressed in fed animals. Tracks of six different is colored based on the time (blue: start, orange: end). (n = 6)

difference in activity observed in the two populations, N3 and N4 (**Fig. 3D and G**), and the altered mouth opening duration. To accomplish this, we investigated the neuronal activity during mouth opening with a previously established calcium imaging setup¹⁶. We observed that the endodermal N4 and the ectodermal N3 neuronal population responded significantly different compared to the starved control (**Fig. 3E and H**). The N4 population displayed a reduced frequency whereas N3 showed an increased frequency during the mouth opening induced by glutathione.

Ectodermal N3 neurons control motor behavior

With the ectodermal N3 neuronal population displaying an increase in activity after feeding, we next wanted to determine the implications of this altered activity pattern. The N3 neuronal network is distributed all over the polyp with a higher density in the foot region and displays synchronous firing (**Fig. 3C and I**). Fed animals had an increase in spiking which showed a striking regular spiking pattern after 4 hours post feeding compared to starved animals (**Fig. 4A-B**). The spiking frequency decreased over time post feeding until it reached a frequency similar to starved animals, approximately around 15 hours post feeding (**Fig. 4C**). The activity of N3 did change in a behavior specific manner. Elongation behavior had a significant increase in spikes compared to starved animals (**Fig. 4D**). Interestingly, non-visible behavior associated spikes also increased significantly (**Fig. 4D**). Since N3 previously has been associated with locomotion behavior in

*Hydra*¹⁷, we hypothesized that N3 plays a major role in motor behaviors and their regulation in fed animals. The causal role of N3 neurons became clear when we discovered in an ablation experiment a highly significant decrease in body movement in fed transgenic polyps compared to wildtype fed animals (**Fig. 4E**). N3 has also been proposed to have an inhibitory impact on the eating behavior and the mouth opening¹⁶. Therefore we next tested, if the absence of N3 neurons affects the response time or the mouth opening duration in animals 4 hours post feeding. Interestingly, N3 ablated animals responded significantly faster to glutathione than the fed control ($p < 0.01$, fed wildtype with MTZ) and showed a significant increase in mouth opening duration ($p < 0.05$, **Fig. 4F-G**). In addition, N3 ablated animals exhibited multiple mouth opening events which could not be observed in the control (**Fig. 4G**). To show that a change in frequency underlies the effect, we reduced the spiking frequency of N3 by cutting off the foot of animals and then tested their response to glutathione. As a result of the absence of artificial methods to decrease the spiking frequency, we observed that the excision of the animal's foot led to a reduction in the spiking frequency within the N3 population (**Fig. 4H**). In accordance with our predictions, cutting off the foot led to a significant increase of mouth opening duration in fed animals compared to starved ones ($p < 0.01$, **Fig. 4I**). In addition, we observed that the feeding dependent phototaxis behavior was changed in well fed N3 ablated animals. While normally an increased phototaxis behavior was observed in starved animals⁸, N3 ablated animals showed an increased movement behavior towards the light source (**Fig. 4J**).

Endodermal N4 neurons control food intake and the spitting out of the digestive pellet

Next, we studied the N4 neurons and noticed that the spiking frequency between starved and fed animals without a digestive pellet is rather similar. Animals that still had a digestive pellet in their gastric cavity, however, showed increased spikes and shorter inter spike intervals (**Fig. 5A-B**). The endodermal N4 population is distributed along the whole-body axis except for the tentacles with an increase in density in the hypostome area (**Fig 3 C**)¹⁶. Within the body, the population forms a network composed of ganglion neurons whereas in the head it forms a spiderweb-like structure with ganglion and sensory neurons which extend into the gastrovascular cavity (**Fig. 3F**). First, we have tested whether or not animals with an ablated N4 population could continue to ingest their prey. As

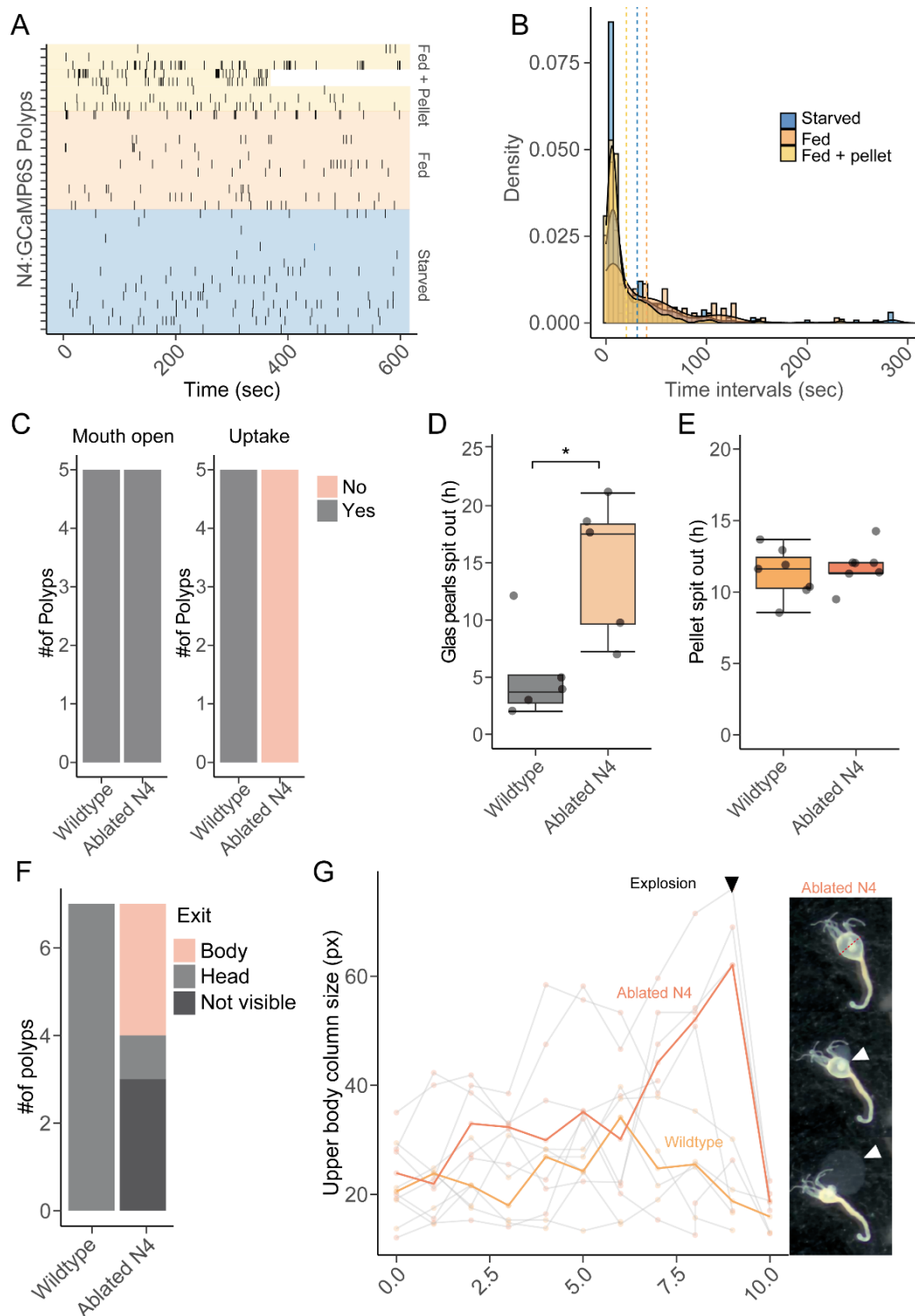


Figure 5. Endodermal N4 population regulates engulfment as well as spit out of digestive pellet.

A. Spike train of endodermal population N4 4 hours post feeding with (yellowish) and without pellet (orange) and starved (blue).

B. Inter spike interval distribution, fed with pellet has shorter intervals between consecutive spikes.

C. Animals with ablated N4 neurons can open their mouth but cannot engulf glass beads (n = 5).

D. Animals with ablated N4 neurons have difficulty to expel glass beads (n = 5, T-test).

E. Time till spit out of artemia did not differ in N4 ablated and wildtype animals (n =6)

F. The exit point of the digestive pellet varied between N4 ablated and wildtype. In N4 animals the pellet did not exclusively came out of the mouth (n = 6).

G. After 6h post feeding, animals with ablated N4 population have become inflated underneath the head till they exploded which led to pellet exit through the through the ruptured tissue (n = 6, picture series).

Hydra would not have been able to catch prey due to MTZ-treatment, we decided to use artificial food (here glass beads) for testing its ability to swallow the prey. Consistent with previously published data¹⁶, all N4 ablated animals could open their mouth. Surprisingly, however, they cannot swallow the glass beads and transport them into the gastric cavity (**Fig. 5C**). In contrast, the control group successfully engulfed all presented glass beads (**Fig. 5C**, control: wildtype + MTZ). N4 neurons also appear to be responsible for facilitating the digestive pellet to leave the gastric cavity. A significant time delay in spitting out glass beads was observed in N4 ablated animals, further supporting the role of N4 in the spit-out process ($p < 0.05$, **Fig. 5D**). We then investigated whether the expulsion time changes when using *Artemia* instead of glass beads. To our great surprise, although the expulsion time did not change (**Fig. 5E**), in N4 ablated polyps the pellet could not leave the gastric cavity via the normal exit, i.e., the mouth. Amazingly, fed animals without N4 neurons first became inflated like a balloon beneath the hypostome region, and then burst, releasing the digestive pellet through the ruptured tissue (**Fig. 5F und G**). N4 neurons, therefore, appear to be responsible for both controlling food intake and excreting the digestive pellet. To summarize our findings, we demonstrate here that *Hydra* has a long-lasting internal state which affects behavior and is controlled by two different neuronal networks. On one hand, the endodermal N4 network controls the response to the presence (or absence) of the digestive pellet and the ultimate spitting out of the pellet. On the other hand, the ectodermal N3 networks spiking frequency increases in a satiety dependent manner reducing the occurrence of other behaviors such as contractions and probably somersaults. Furthermore, N3 inhibits mouth opening when fed and ablation of N3 cancels the effect. These findings extend the recently described neuronal circuit of the eating behavior¹⁶

and show that in *Hydra* functions of the digestive system and the control of behavior are coordinated by two very distinct neuronal populations.

Discussion

Most animals adjust their behavior depending on whether they have ingested food or not. Often these behavioral changes are modulated by the brain which changes sensory processing based on the metabolic internal state and the enteric nervous system controlling food passage^{1,19}. Astonishingly, internal states can already be observed in animals that have no centralized nervous system. The underlying neuronal control is unknown⁵⁻⁸. Here we show in *Hydra* that neuronal population N3 with a polyp-wide spanning network has a metabolic state dependent change in its activity and controls behavior as well as repeated food intake. In addition, the endodermal neuronal population N4 controls behavior associated with the feeding and digestion process, including the expulsion of the digestive pellet. These findings highlight a sub-functionalization within *Hydras* nervous system into an ectodermal network controlling motor and physiological functions and an endodermal network controlling feeding associated behaviors.

Starved animals exhibit increased explorative behaviors

Behaviors associated with locomotion and mouth opening are reduced or even inhibited for more than 24 hours post feeding while contractions return much faster to a normal frequency (**Fig. 2A-F**). The exposure to glutathione in fed animals (food stimulus) did not result in a feeding response for more than 10 hours post feeding. Replacing the feeding with a pre-exposure to glutathione failed to reproduce the inhibiting effect for the same duration (**Fig. 2A**). This showed that the mere performance of the eating behavior could not prevent another feeding behavior 4h after the initial stimulus suggesting that the presence of real food is required to inhibit another response. A similar dependency was observed in locomotion associated behaviors. Somersaults were completely absent in fed animals for over 28h post feeding as well as fed animals did not detach from their substrate (**Fig. 2D, F**). Thoughts on the ecological relevance of the floating behavior of *Hydra* were already presented more than 60 years ago²⁰. It is to add, that fed animals were not motionless or devoid of activity, in fact they displayed higher levels of body movement compared to starved animals (**Fig. 2E**). However,

fed animals are rather stationary whereas starved animals seem to do more locomotion, contractions and floating behavior.

Neuronal control of digestion and internal state

The endodermal neuronal population N4 plays not only a crucial role in initiating the eating behavior of *Hydra* as previously shown¹⁶, but is also necessary for the downstream behavioral pattern. The N4 network displays an increased spiking frequency when a digestive pellet is present in the gastrovascular cavity, and this frequency is significantly reduced in the absence of the pellet (**Fig. 3D**). Further, cell ablation experiments demonstrate that N4 regulates the engulfment of the prey and the spit out of a digested pellet (**Fig. 5**). Both functions are supported by the presence of sensory cells in head of *Hydra*, extending into the gastrovascular cavity. These sensory cells are likely responsive to both chemical and mechanical stimuli (**Fig. 3F**). So far, N4 has not been associated with any other behavior and therefore we propose that N4 is mainly responsible for feeding-related behaviors and internal fluid transport.

The ectodermal neuronal population N3 is mainly involved in locomotion behavior and integrating physiological information such as the feeding state. The N3 network has previously been described to be involved in motor control of *Hydra* such as somersaulting and detachment¹⁸. Further, it counteracts the (contraction burst) N1 network^{14,17,18,21}, is associated with elongation behavior, responds to blue light, osmolarity, and has non-behavior associated activity^{18,21,22}. Here, we show that the activity of the N3 network increases and decreases in a feeding dependent manner and inhibits mouth opening while suppressing other behaviors such as body movement, phototaxis and somersaults (**Fig. 3G, Fig. 4**). The N3 neuronal network is unique due to its connectivity with the N1 network, as well as all other ectodermal neuronal populations and nematocytes, which allows for global modulation (**Fig. 3I**)^{16,18}. Intriguingly, N3 neurons appear to be multi-functional as they are involved in various behavioral patterns each characterized by a unique spiking frequency (**Fig. 4D**)^{17,18}. In the case of fed animals, the spiking pattern is strikingly regular and misses pattern such as bursts as seen in somersault behaviors¹⁸. This clearly shows that a single ectodermal neural population, population N3, possesses the ability to control numerous behaviors and to integrate comprehensive information about the organism's condition. Our findings suggest that the rise in activity triggered by feeding is the result of

modifications in the intrinsic neural activity, leading to substantial effects on adjacent circuits and the consequent regulation of behaviors. These observations indicate the existence of a hierarchical structure within the neuronal signaling system¹⁴.

Nevertheless, one question that has yet to be resolved is whether the alteration in activity of the N3 population can be attributed to endogenous regulation or exogenous influences. The activity of N3 has been associated to non-behavior associated activity (**Fig. 4D**)^{17,23,24}. Here, we observed a significant higher spiking frequency in non-behavior associated activity in fed animals suggesting an intrinsic activation. In addition, the activity of N3 mainly emerges from the foot region and the activity appears to counteract the activity of N1^{17,18}. Since there is no other ectodermal neuronal population that might trigger N3 and serve as the extrinsic driver, it is worth considering whether epithelial cells in the immediate proximity might not play an important role here. Perhaps subsequent work will provide clarity here.

In conclusion this work highlights the sub-functionalization of *Hydra*'s previously called "diffuse" nervous system into a subpopulation similar to the enteric nervous system (feeding associated behavior) and into a population that is performing central nervous system (physiology/motor) like functions. We further demonstrate that the ectodermal neuronal population changes its activity depending on the internal state and affects other behaviors. Taken together, *Hydra*'s nervous system serves as a remarkable illustration of how a simple nervous system can manifest intricate sub-functionalization; and perhaps for this reason it can be an important key to understanding the evolution of the Bilaterian nervous system.

Acknowledgements

This work was supported in part by grants from the Deutsche Forschungsgemeinschaft (DFG), the CRC 1182 "Origin and Function of Metaorganisms" (to TCGB.) and the CRC 1461 "Neurotronics: Bio-Inspired Information Pathways" (Project-ID 434434223 – SFB 1461) (to TCGB). T.C.G.B. appreciates support from the Canadian Institute for Advanced Research. We thank the whole Bosch Lab and in particular Lisa-Marie Hofacker for support during the preparation of the manuscript. We also thank Urska Repnik and Marc

Bramkamp from the Central Microscopy Facility at the Biology Department of the University of Kiel for excellent technical support.

Authors contribution

C.G. and C.N conceptualized the project and conducted the experiments. C.G. generated the transgenic constructs and designed experiments for behavioral analysis. C.G. and C.N. performed cell ablation experiments. C.G., C.N., and E.S. performed calcium imaging experiments. C.G. and C.N. did data analysis. C.G., C.N. and T.C.G.B wrote manuscript.

Declaration of interest

The authors declare no competing interests.

Data and code availability

- Source data reported in this paper will be shared by the lead contact upon request.
- Codes used for the analysis and statistical analysis will be shared by the lead contact upon request.
- Any additional information required to reanalyze the data in this paper will be shared by the lead contact upon request.

References

1. Flavell, S. W., Gogolla, N., Lovett-Barron, M. & Zelikowsky, M. The emergence and influence of internal states. *Neuron* **110**, 2545–2570 (2022).
2. Vogt, K. *et al.* Internal state configures olfactory behavior and early sensory processing in drosophila larvae. *Sci Adv* **7**, (2021).
3. Marques, J. C., Li, M., Schaak, D., Robson, D. N. & Li, J. M. Internal state dynamics shape brainwide activity and foraging behaviour. *Nature* **2019 577:7789** **577**, 239–243 (2019).
4. Chambers, A. P., Sandoval, D. A. & Seeley, R. J. Integration of Satiety Signals by the Central Nervous System. *Current Biology* **23**, R379–R388 (2013).
5. Weissbourd, B. *et al.* A genetically tractable jellyfish model for systems and evolutionary neuroscience. *Cell* **184**, 5854–5868.e20 (2021).
6. Kanaya, H. J. *et al.* A sleep-like state in Hydra unravels conserved sleep mechanisms during the evolutionary development of the central nervous system. *Sci Adv* **6**, eabb9415 (2020).
7. Nath, R. D. *et al.* The Jellyfish *Cassiopea* Exhibits a Sleep-like State. *Current Biology* **27**, 2984–2990.e3 (2017).
8. Kim, S. & Robinson, J. T. Phototaxis is a state-dependent behavioral sequence in *Hydra vulgaris*. *bioRxiv* 2023.05.12.540432 (2023) doi:10.1101/2023.05.12.540432.

9. Peterson, K. J. & Butterfield, N. J. Origin of the Eumetazoa: Testing ecological predictions of molecular clocks against the Proterozoic fossil record. *Proc Natl Acad Sci U S A* **102**, 9547–9552 (2005).
10. Lenhoff, H. M. Activation of the feeding reflex in *Hydra littoralis*: I. Role played by reduced glutathione, and quantitative assay of the feeding reflex. *J Gen Physiol* **45**, 331–344 (1961).
11. Loomis, W. F. Glutathione Control of the Specific Feeding Reactions of *Hydra*. *Ann N Y Acad Sci* **62**, 211–227 (1955).
12. Burnett, A. L., Davidson, R. & Wiernik, P. On the presence of a feeding hormone in the nematocyst of *Hydra pirardi*. doi.org/10.2307/1539399 **125**, 226–233 (1963).
13. Koizumi, O. & Maeda, N. Rise of feeding threshold in satiated *Hydra*. *J Comp Physiol* **142**, 75–80 (1981).
14. Passano, L. M. & McCullough, C. B. Pacemaker hierarchies controlling the behaviour of hydras. *Nature* **199**, 1174–1175 (1963).
15. Primack, A. S. *et al.* Differentiation trajectories of the *Hydra* nervous system reveal transcriptional regulators of neuronal fate. *bioRxiv* 2023.03.15.531610 (2023) [doi:10.1101/2023.03.15.531610](https://doi.org/10.1101/2023.03.15.531610).
16. Giez, C. *et al.* Microbes as part of ancestral neuronal circuits: Bacterial produced signals affect neurons controlling eating behavior in *Hydra*. *bioRxiv* 2023.04.28.538719 (2023) [doi:10.1101/2023.04.28.538719](https://doi.org/10.1101/2023.04.28.538719).
17. Dupre, C. & Yuste, R. Non-overlapping neural networks in *Hydra vulgaris*. *Current Biology* **27**, 1085–1097 (2017).
18. Yamamoto, W. & Yuste, R. Peptide-driven control of somersaulting in *Hydra vulgaris*. *Current Biology* **33**, (2023).
19. Wood, J. D. Enteric Nervous System. *Encyclopedia of Gastroenterology* 701–706 (2004) [doi:10.1016/B0-12-386860-2/00223-9](https://doi.org/10.1016/B0-12-386860-2/00223-9).
20. Lomnicki, A. & Slobodkin, L. B. Floating in *Hydra Littoralis*. *Ecology* **47**, 881–889 (1966).
21. Yamamoto, W. & Yuste, R. Whole-Body Imaging of Neural and Muscle Activity during Behavior in *Hydra vulgaris*: Effect of Osmolarity on Contraction Bursts. *eNeuro* **7**, 1–13 (2020).
22. Passano, L. M. & McCullough, C. B. the Light Response and the Rhythmic Potentials of *Hydra*. *Proceedings of the National Academy of Sciences* **48**, 1376–1382 (1962).
23. Passano, L. M. & McCullough, C. B. Co-Ordinating Systems and Behaviour in *Hydra*. II. the Rhythmic. *J Exp Biol* **42**, 205–231 (1965).
24. Hanson, A. Spontaneous electrical low-frequency oscillations: A possible role in *Hydra* and all living systems. *Philosophical Transactions of the Royal Society B: Biological Sciences* **376**, (2021).
25. Klimovich, A., Wittlieb, J. & Bosch, T. C. G. Transgenesis in *Hydra* to characterize gene function and visualize cell behavior. *Nature Protocols* 2019 14:7 **14**, 2069–2090 (2019).
26. Schneider, C. A., Rasband, W. S. & Eliceiri, K. W. NIH Image to ImageJ: 25 years of image analysis. *Nat Methods* **9**, 671–675 (2012).
27. Ershov, D. *et al.* TrackMate 7: integrating state-of-the-art segmentation algorithms into tracking pipelines. *Nature Methods* 2022 19:7 **19**, 829–832 (2022).
28. De Chaumont, F. *et al.* Icy: an open bioimage informatics platform for extended reproducible research. *Nature Methods* 2012 9:7 **9**, 690–696 (2012).
29. Lagache, T., Hanson, A., Pérez-Ortega, J. E., Fairhall, A. & Yuste, R. Tracking calcium dynamics from individual neurons in behaving animals. *PLoS Comput Biol* **17**, e1009432 (2021).
30. Team, R. C. R Core Team R: a language and environment for statistical computing. *Foundation for Statistical Computing* (2020).

31. Rupprecht, P. *et al.* A database and deep learning toolbox for noise-optimized, generalized spike inference from calcium imaging. *Nature Neuroscience* 2021 24:9 **24**, 1324–1337 (2021).
32. Team, R. S. RStudio: integrated development environment for R. R Studio, PBC, Boston, Massachusetts, United States of America. Preprint at (2022).
33. Siebert, S. *et al.* Stem cell differentiation trajectories in Hydra resolved at single-cell resolution. *Science* (1979) **365**, eaav9314 (2019).
34. Cazet, J. F. *et al.* A chromosome-scale epigenetic map of the Hydra genome reveals conserved regulators of cell state. *Genome Res* gr.277040.122 (2023) doi:10.1101/GR.277040.122.
35. Klimovich, A. *et al.* Prototypical pacemaker neurons interact with the resident microbiota. *Proceedings of the National Academy of Sciences* **117**, 17854–17863 (2020).

Material and Methods

The plasmids and transgenic *Hydra vulgaris* AEP generated in this study are available upon request.

Code availability

All codes used in this study are available upon request.

Data availability

All data presented in this study are available upon request.

Hydra maintenance

Hydra polyps (*Hydra vulgaris* AEP) were subjected to cultivation procedures in standard *Hydra* culture medium (i.e., CaCl₂ 0.042g/L; MgSO₄ x 7H₂O 0.081g/L; NaHCO₃ 0.042g/L; and K₂CO₃ 0.011g/L in dH₂O), in accordance with established protocols²⁵. The animals were cultured in 250mL glass beakers maintained at a temperature of 18°C, with a 12/12h light cycle. Feeding of the animals strictly occurred three times per week, utilizing *Artemia nauplii* for at least two weeks prior to any experimentation.

Behavioral analysis

Feeding behavior

To investigate the eating behavior and its dependency on the feeding state we followed a recently established protocol¹⁶. The animals were given a period of 10

minutes to adapt themselves to the recording chamber prior to the start of recording, followed by an additional interval of 5-10 minutes prior to the addition of reduced glutathione (Roth, cat#6382.1) through a tube system. A final concentration of 10 μ M glutathione was employed for all assays. The acquired recordings were blinded to their treatment and categorized with a random three-digit number before analysis. The conduct was manually annotated, with the following various behaviors being tallied (**Fig. 1E**): the duration of mouth opening and the response time. The duration of the mouth opening is the time the mouth stays open. The response time is the time an animal needs to show the first response to glutathione, here mouth opening.

Contractions, somersaults, body movement, and floating

Animals were placed into a custom-made chamber with a height of 5mm and a volume of 1.5-2mL which allowed the animals to move freely. Five animals were recorded at once with a frame rate of 0.5 frames per second. Further the recordings were blinded, and behaviors were manually annotated. For contraction behavior, all contractions were counted which reduced the animal length by a minimum of 33%. Somersaults were defined as the following sequence of behaviors: detachment of foot, attachment of head, contraction, bending and re-attachment of the foot in accordance with previously published work¹⁸. For the body movement, the body center of the animals was tracked by using Track Mate in ImageJ^{26,27} and the average speed (μ m/sec) was calculated. For the floating behavior the lid of the chamber was removed which then allowed animals to flow on the surface. Here, single animals were tracked, and behavior was annotated as attached or detached/floating (**Fig. 1E**).

GCaMP6S recording

In order to examine the neuronal activity in dependency of the feeding status, the animals were placed in commercially available channel slides that were 0.2 or 0.4mm in height and 5mm in width (Suppl. Fig. 6D.; Ibidi, cat#80166, cat#80176). Once an animal was placed in the channel slid, we led the animal adapt for 10 min to the new environment plus another 2min to the laser prior recording. Imaging was performed using the Axio Vert. A1 (Zeiss) with the Colibri 7 as a light source (Zeiss) equipped with the fluorescence filter 38 HE (Zeiss), 5x and 10x Plan Apo objective, and the AxioCam 705 mono (Zeiss). Acquired videos were

further processed with Zen Blue 3.4 (Zeiss) to 700x600px, 8-bit and analyzed via either ImageJ or ICY²⁸. The neurons were then tracked with a previously published pipeline²⁹. The acquired tracks were then merged to one by taking the mean fluorescence change to analyze the population activity pattern.

Neuronal activity analysis

The mean activity of each population or neuronal type was taken for further analysis with the standard deviation to the mean, as it summarized all major events. All visualization and normalization were performed using customized scripts in R³⁰. The spiking frequency of N3 and N4 was deconvoluted and analyzed using either CASCADE³¹ and/or MATLAB's (Mathworks) "findpeaks" function with manually adjusted parameters. At least 3 animals were used in all experiments.

Ablation experiments

To test the role of population N3 and N4 in modulating the behavior post feeding, we used animals carrying the NTR-MTZ system under the control of a N3- or N4-specific promoter¹⁶. We fed the animals extensively and transferred them into 10mM metronidazole (MTZ) after 30min post feeding. For analyzing the behavioral changes, animals were placed in the costume made chambers as described under behavioral analysis. For testing the ability to engulf glass beads, we incubated N4::NTR-GFP animals overnight in 10mM MTZ together with a control (without a construct) and performed the mock feeding assay.

Testing engulfment and spit-out (glass beads)

In order to test if animals lacking a certain neuronal population (N4) can still ingest prey and spit out the digestive pellet we force fed *Hydra* with glass beads with a diameter of 200-300µm (Sigma, #G9143). Animals were transferred into 10µM glutathione solution and then with a syringe or forceps stuffed with glass beads (>4<7 beads per animal). The ability to engulf a glass bead was scored. For testing the impact on the spit out time, animals were transferred into 10mM MTZ and recorded for 24h in the setup described under "Contraction, somersaults, body movement, and floating". The time point where all glass beads were spit out was noted.

Phototaxis assay

To investigate whether animals that have been adequately nourished (4-10 hours after feeding) exhibit alterations in their phototaxis behavior, and if these alterations are dependent on the N3 neuronal population, we conducted experiments using specially designed arenas. For this purpose, we utilized cell culture dishes with dimensions of 35x10mm (Eppendorf, cat#0030700112) and covered the walls with black tape, leaving a narrow opening measuring 0.5mm to allow light to enter the chamber. To provide the necessary light source, we employed a cold light source (Schott KL 1600 LED) with a high-power LED that emitted a maximum of 680 lumens and had a color temperature of approximately 5600 Kelvin. Prior to the commencement of the recordings, the animals were fed a substantial amount of *Artemia* until they were fully satiated and were then left at a temperature of 18°C for 30 minutes to initiate the digestion process. Following this 30-minute period, the animals were transferred into a solution of 10mM MTZ and were incubated for 4 hours in darkness at a temperature of 18°C. Subsequently, the animals were placed in the center of the arenas and were recorded for a duration of 24 hours at a temperature of 18°C. The recordings of the animals were captured at a frame rate of 0.5 frames per second, and the resulting movies were further processed using ImageJ²⁶. The tracking of the animals was performed using TrackMate, and the log-threshold approach was utilized for this purpose²⁷. The tracks obtained for each animal were subsequently subjected to additional processing and were visualized using R³⁰. For comparison, the control group in all experiments consisted of wildtype polyps (*Hydra vulgaris* AEP) subjected to the same experimental conditions as the transgenic animals.

Transgenic lines

The transgenic lines N4 (GCaMP6S and NTR-GFP) and N3 (GCaMP6S and NTR-GFP) have been generated in another study¹⁶. The pan-neuronal line was derived by isolating the promotor of a neuronal specific alpha tubulin (t14440aep/G019559, 1200bp) and this line has been already described¹⁵. Here, we derived this line to a F1 generation.

Histology

Immunohistochemical detection was performed on whole-mount *Hydra* preparations using as previously described¹⁶. The polyps were relaxed (Urethane), fixed (Zamboni), permeabilized (0.5% Triton X-100 in PBS), incubated with primary antibodies (1:1000) and secondary antibodies (1:1000). Confocal laser-scanning microscopy was then used for analysis (LSM900, Zeiss). As primary antibody was used: chicken-anti-GFP (Biozol, cat# GFP-1010) and as secondary antibody: goat anti-chicken Alexa Fluor 488 (Invitrogen, cat# A11039, 1:1000 dilution).

Data analysis

All statistical analyses were conducted using R and R-studio as the integrated development environment (IDE)^{30,32}. In all instances, data were evaluated for equal variance using Levene's test and normal distribution using the Shapiro test. Depending on the results of these tests, either a parametric (t-test, ANOVA, Turkey test) or non-parametric test (Kruskal-Wallis, pairwise or Wilcox test, Dunn test) was employed. Multiple testing correction was performed using Bonferroni. The number of replicates (n) for each dataset was indicated in the figure captions, along with the statistical method utilized for each comparison and the corresponding p-value. For linear correlation analysis, correlation coefficients and p-values were calculated using the Spearman method with the assistance of the R package "ggpubr". The cutoff for a significant difference was established as an $\alpha < 0.05$. Throughout the text, values are presented as median \pm standard deviation, unless otherwise specified.

Epilogue

Microbes and their metabolites have been consistently present throughout the evolution of metazoans, ultimately exerting a significant influence on their development (McFall-Ngai et al., 2013). Therefore, most eukaryotes are associated with a so-called microbiota which can range from a single bacterium to a highly complex community as well as from endo- to surface-associated symbionts (Alberdi et al., 2021). Over the past few decades, there has been an explosion of work exploring this fascinating partnership, which has resulted in a new perspective on organisms, as they are now regarded as metaorganisms (see Fig. 1 Introduction) (Bosch and McFall-Ngai, 2011). Furthermore, it led to paradigm shifts in diverse fields such as neuroscience since it has been shown that gut associated bacteria can influence neuronal physiology in the brain (see Fig. 2 Introduction) (Mayer et al., 2014). Yet, the mechanisms on how microbes can interact with neurons and influence complex behaviors has not been deciphered and often remains on a correlative level (Nagpal and Cryan, 2021). Major breakthroughs were often made in non-mammalian and non-vertebrate model systems (Douglas, 2019; Nagpal and Cryan, 2021). Therefore, work on *C. elegans*, *Drosophila melanogaster*, and zebrafish have majorly shaped our understanding of the interaction between host behavior and microbes. Nevertheless, there are much simpler organisms that have a nervous system but no brain such as Cnidarian which can help us to understand the fundamental functions of a nervous system and the interaction with symbiotic microbes (Bosch, 2014; Klimovich and Bosch, 2018; Schröder and Bosch, 2016b). In this thesis, I have studied the intriguing relationship between the nervous system of the Cnidarian *Hydra*, a simple freshwater polyp, and its microbial symbionts, approaching it from various angles, including fluid dynamics, behavioral analysis, neuronal circuits, microbial community analysis, and bacterial metabolism. This led us to come to the following major conclusions:

- 1.) Bacteria have been shown to modulate and reduce spontaneous contraction behavior in *Hydra* (Murillo-Rincon et al., 2017). However, the reason why microbes increase the frequency of contractions could not be explained. In **Chapter II**, we show that spontaneous contractions are a general principle of organisms to exchange their fluid boundary layer and thereby maintain a stable microbiota. While the host maintains control

over the microbial composition, the microbes derive significant advantages from the acquisition of fresh resources facilitated by the exchange of the fluid boundary layer.

2.) Eating behavior is a state-dependent behavior that is regulated by starvation and satiety. Most recently it has been shown that microbes can influence appetite as well (Han et al., 2021). However, how the bacterial signal gets integrated and influences the eating behavior remains underexplored. In **Chapter III**, we show that *Hydra* integrates bacterial signals into the control of eating behavior. Further, bacteria produce the excitatory neurotransmitter glutamate in a context-dependent manner and thereby block the eating behavior via sensory neurons. Therefore, bacteria have the potential to produce neuronal active components but if they do so is context dependent.

3.) Satiety and starvation can have an influence on multiple aspects of an animal's behavior ranging from decision making to motor control. The centralization of diverse peripheral information, particularly from the gastrointestinal tract, including the enteric nervous system and gut-associated microbiota, is essential. In **Chapter IV**, we observe that in *Hydra* two distinct neuronal populations take over the functions of the enteric and central nervous system. Highlighting the complexity of a simple nervous system and its fascinating sub-functionalization.

From these conclusions, I propose that bacterial influence on host behavior is context dependent. Furthermore, it is an environmental signal for the host. The host can use bacterial signals as an assessment of its surrounding environment thereby adapting to the specific situation. Therefore, the connection between associated microbes and host behavior can often rather be explained by a host-to-microbe or passive signaling by microbes than a bacteria-to-host active and directed mechanism. However, comprehending the “why” the host integrates microbial molecules into neuronal circuits or development is often a challenging task, demanding a multifaceted perspective and multidisciplinary approaches.

In the final section of my dissertation, I aim to discuss upon the subsequent overarching questions that have arisen from our investigation and consider the present state of the literature. I will first touch on the question of why animals have

evolved the integration of microbial signals and what the synthesis in the eating behavior and the microbiota across animals is. Finally, I will focus on the evolution of the nervous system, and if Cnidarians already have a brain while highlighting the contribution of this work in expanding our understanding of a primitive nervous system.

Connection between behavior, nervous system, and microbiota – can we understand the “why”?

Eating behavior is a behavior that is consistently modulated by microbes from early branching metazoan up to mammals. The nervous system monitors the gut microbiota and thereby regulates eating behavior such as appetite, food preference, and satiety. Besides the intake of new resources, spontaneous contractions, regulated by the enteric nervous system, help maintain our gut microbiota in a location where there is less competition for the same nutritional resources. This emphasizes that our eating habits are tightly interwoven with our microbes and an ancient role of the nervous system is to keep our symbionts on a leash.

Spontaneous contractions change the environment of symbionts.

The host controls its microbiota by sensing the composition and state of the microbial community and then changing the dynamics of the nested ecosystem accordingly. In **Chapter II**, we show that the microbial dependent spontaneous body contractions are a way for the host *Hydra* to control and maintain its symbionts (Murillo-Rincon et al., 2017; Nawroth et al., 2023). By contracting, the host facilitates the diffusion process and thereby exchanges the fluid environment. This can either remove waste or introduce new resources. In the end, a changed contraction frequency leads to a change in the microbial community composition. Furthermore, the modulation of contractions by the microbiota suggests a feedback loop in which the host detects the presence of bacteria that have yet to be identified in *Hydra* (Klimovich et al., 2020; Murillo-Rincon et al., 2017). Overall, those findings have a broader relevance since in the gastrointestinal tract of mammals, spontaneous contractions (also known as peristalsis) are also depending on the microbiota (Brophy et al., 2017; Obata et al., 2020). However, the reason for the dependency on microbial signals is still unclear as well. We propose that the host controls the microbiota by the

contractile behavior, creating a dynamic environment where resources are constantly newly introduced, or waste removed.

Spontaneous contractions to control the microbiota

Spontaneous rhythmic body wall contractions evolved to control and maintain a stable microbial community. The gastrointestinal tract forms a multitude of different environmental gradients (Donaldson et al., 2015). This ranges over pH, antimicrobials, oxygen, and gut motility. In the intestine, the pH and bacterial load are low whereas antimicrobials, oxygen, and spontaneous contractions are high (Donaldson et al., 2015). Disturbance of any of those factors leads to inflammation (Chikina & Matic Vignjevic, 2021). However, the most significant influence is the disruption of the contraction frequency as it can prompt alterations in all other factors that culminate in dysbiosis and the overgrowth of bacteria (Halfvarson et al., 2017; Sheehan et al., 2015; Toskes, 1993). The spontaneous contractions of the gut mix the lumen, ensuring an even distribution of host factors such as antimicrobials that would otherwise form diffusion-dependent gradients. The role of contractions, as supported by microfluidic models and simulations that mimic and replicate contraction and waterflow in the gastrointestinal tract, has led to the conclusion that these two factors alone are capable of explaining the microbial densities and composition within the gut. (Cremer et al., 2016, 2017; Ghosh & Good, 2022; Labavić et al., 2022). They further propose that fluid flow plays a key role in the ecological and evolutionary forces within the gut environment. This dynamic environment enhances neutral bacterial diversity and decreases large fluctuations of mutant frequencies (Ghosh & Good, 2022; Labavić et al., 2022). Yet, these predictions are interesting but require to be further validated in an animal model system. Nevertheless, in **Chapter II** we were able to confirm that contractions play a key role in maintaining a stable microbiota in *Hydra*. It also highlights that a specific behavior, which was initially considered inexplicable in terms of an animal's investment, serves a crucial function for the metaorganism. In conclusion, contractions of body walls such as the intestine or *Hydra* are crucial to maintain environmental gradients and thereby shape the biogeography as they link many factors together.

The enteric nervous system helps to keep the microbiota on a "leash"

The enteric nervous system senses and regulates the bacterial community and distribution to avoid competition for similar resources. When observing the biogeography of the gut, one can observe that the nutritional availability and the bacterial load are negatively correlated (McCallum and Tropini, 2023; Pereira and Berry, 2017). Phosphate and nitrogen are taken up to almost 90% in the intestine (Borgström et al., 1957; Sabbagh et al., 2011), making them a limited resource within the gut microbiota (Pereira and Berry, 2017; Reese et al., 2018). In contrast, gut motility and antimicrobials are positively correlated with nutrient availability (Donaldson et al., 2015; McCallum and Tropini, 2023). Furthermore, the mucus which forms the major habitat of the microbiota is much thicker in the distal regions than in the intestine (Chikina and Matic Vignjevic, 2021). The enteric nervous system has been shown to respond to the microbiota by changing the contraction frequencies of the gut (Obata et al., 2020). Additionally, there is a tight crosstalk between the enteric nervous- and the immune system regulating gut homeostasis (Schneider et al., 2022). Furthermore, the development and maturation of the enteric nervous system depend on microbial factors (Obata and Pachnis, 2016). In such a way that in germ-free mice the number of enteric neurons is reduced compared to animals with a microbiota (Anitha et al., 2012). The impact of the microbiota is continuously ongoing and already takes place in the womb (Collins et al., 2014). Based on these observations, one could speculate that the enteric nervous system is responsible for keeping symbiotic bacteria in the designated location and is responding and reacting as soon as this is breached. Interestingly, in the gastrovascular cavity of *Hydra*, no bacteria have been detected so far but the enteric nervous system like endodermal neurons (N4 population) respond to bacterial colonization (**Chapter III**). Additionally, antimicrobial peptides are mainly expressed in the endodermal epithelia (Cazet et al., 2023; Siebert et al., 2019). Similarly, to the enteric nervous system in vertebrates, the endodermal neuronal population controls radial contractions which could also increase the mixing of the antimicrobials in the gastric cavity making it hostile for microbes. It would be interesting to see if this can be connected which might highlight the ancient role of the enteric nervous system to keep the microbiota on a leash and in place where there is less competition for the same resources.

Impact of the microbiota on critical developmental windows

Microbiota-dependent changes in neuroanatomy and complex behaviors such as social behavior have a critical window during development where the input of microbial signals is required. This phenomenon has been mainly described for vertebrate model systems whereas in invertebrates there are only a few cases reported (John F. Cryan et al., 2019; Nagpal and Cryan, 2021). The effect of the microbiota on neurodevelopment in mammals starts as early as in the womb as has been shown in mice (Vuong et al., 2020). Microbial metabolites are transported to the fetus via serum and modulate axonogenesis. Colonization of autism spectrum disorder mice model offspring led to an altered defect in social behavior (Hsiao et al., 2013). In accordance, germ-free mice that show a socially impaired behavior are only partially rescuable when adult mice are recolonized (Desbonnet et al., 2013; Luczynski et al., 2016). Similar observations were also made in zebrafish where microglia and the remodeling of neuronal arbors are affected by microbes and lead to changes in social behavior (Bruckner et al., 2022). Here the effect is also only reversible when recolonizing zebrafish larvae in a specific developmental window. In invertebrates, the impact of bacteria on the aggression behavior in *Drosophila melanogaster* males is the only well-described behavior where a bacterial effect happens within a critical developmental window (Jia et al., 2021). The microbiome exhibit interactions with the diet during early development, which is critical for the appropriate expression of octopamine and the manifestation of aggression in adult fly males. It is fascinating that microbial signals are required in certain neurodevelopmental steps to ensure the proper development of the nervous system. This emphasizes the intimate relationship between microbes and the nervous system of multicellular hosts once again. However, why we have not more examples of such a relationship in invertebrates is interesting but might be because of a bias in the research focus towards vertebrate systems.

An invertebrate model that could be an insightful system to investigate the impact of microbes on neurogenesis in the future is *Hydra*. Yet, there have not been reports of any neuronal anatomy change under germ-free conditions. However, this might be because of wrong experimental designs or approaches. The fascinating thing about *Hydra* is that its stem cells are continuously proliferating and thereby also continuously doing neurogenesis (Bosch et al., 2010). However, the current experimental designs never took the time of

neurogenesis into account and lacked the appropriate tools to identify neuroanatomy changes. Most experiments worked in a 14- up to 21-day window but only up to 10 days post antibiotics in germ-free conditions (Harris, 2020; Murillo-Rincon et al., 2017), and recolonization even had a much smaller window of a maximum of five days. Further, the methods used for investigating the difference in the nervous system were determining the cell proliferation rate of the stem cells and the neuron-to-epithelia proportion so far. Both methods can only determine global changes and do not take spatial information into account. However, *Hydras* nervous system is not equally dense and consists of multiple distinct populations (Burnett and Diehl, 1964; Siebert et al., 2019). Also, major changes in other model organisms were rather concerning the morphology of the cells and not their number. Therefore, it would be interesting to investigate the neuronal anatomy and development while including spatial information as well. Ultimately, this could also be a possible explanation for why the spontaneous contraction phenotype could not be fully rescued. On the one hand, the recolonization lasted only 4 days and on the other hand, this could be too short a time window for changes to take place in the nervous system. (Murillo-Rincon et al., 2017). It may be interesting to systematically approach this and show that neurogenesis is also affected by microbes in an early branching metazoan, strengthening the evolutionary connection between microbes and neurons.

Eating behavior and microbes have a long consistent history

The eating behavior is one behavior that is consistently modulated by microbes from early branching metazoan up to mammals. Eating behavior can be roughly split into three major steps: (i) hunger and appetite; (ii) food preference and cravings; and (iii) eating, tasting and digestion. All three aspects can be affected by microbes. In mice, appetite can be regulated by a bacterial cell wall component (muropeptide), which can reach the brain and alters appetite and satiety via GABAergic neurons (Gabanyi et al., 2022). The work proposes that this forms a feedback loop for the host to monitor bacterial growth and regulate food intake respectively. This hypothesis can indeed be supported by other studies. It has been shown that there are multiple direct as well as indirect routes through which the gut microbiota can influence appetite (Han et al., 2021). Intriguingly, there is also evidence that bacterial growth triggers the release of satiety hormones, which suggests as well that satiety and bacterial growth are connected whereas systemic bacterial molecules directly activate appetite

pathways (Fetissov, 2016). In *Drosophila melanogaster* and *C. elegans*, the gut microbiota shapes food preferences as the host monitors the nutrient availability of the gut provided by the bacteria (Henriques et al., 2020; Kim et al., 2021; Rhoades et al., 2019). Finally, taste is most likely also affected by microbes in mammals even though mechanistic data are missing (Fetissov, 2016). However, there is mechanistic evidence that microbes modulate olfactory behavior and attract *Drosophila melanogaster* as well as *C. elegans* (Meisel et al., 2014; Wong et al., 2017). It cannot be denied that bacteria have an influence on eating behavior and the host ensures that there is a balance between food intake and bacterial growth. However, it is not clear if the modulation depends on single bacteria, on certain community composition, or just on bacterial growth. Therefore, our work in **Chapter III** provides valuable insights into the interplay between microbial composition and eating behavior.

Eating behavior depends on community composition

Eating behavior depends on the microbial community composition and bacteria-bacteria interactions. In *Hydra*, the eating behavior is modulated in a community-dependent manner (**Chapter III**) such as that a heavily disturbed community inhibits eating. This effect can be solely assigned to the main colonizer, *Curvibacter*, which exhibited an inhibitory effect on the mouth opening when mono-associated with the host. The underlying molecule is glutamate which seems to accumulate in the environment and interferes with the behavior. Interestingly, in a more complex community glutamate is taken up by other members and thereby the effect is abolished. Bacteria-bacteria interactions and cross-feeding have also been shown to be important in other systems (Henriques et al., 2020; Leitão-Gonçalves et al., 2017). Yet, whether glutamate is the only molecule in *Hydra* that affects the eating behavior remains an open question and further investigations are needed. However, the host downregulates glutamate receptors and upregulates excitatory amino acid transporter suggesting a specific response to an accumulation of glutamate (**Chapter III**). Another factor can be the bacterial load which is significantly higher in *Curvibacter* mono-association compared to any other bacteria. On one hand, this could potentially contribute to the accumulation of glutamate; however, on the other hand, it is possible for other factors to also accumulate. An increased bacterial load has been shown to trigger the release of satiety hormones in mammals (Fetissov, 2016). It is possible that in a similar way the eating behavior of *Hydra* is controlled by bacterial growth and

load as well. In summary, *Hydra* expands our understanding of the interaction between eating behavior and gut microbiota as it is a complex interplay between the host nervous system, and bacteria-bacteria interactions. A main colonizer has an inhibitory effect on the host in a context-dependent manner, highlighting the myriad of faces a bacterium can have in complex interaction.

Why does *Hydra* integrate bacterial signals into eating behavior?

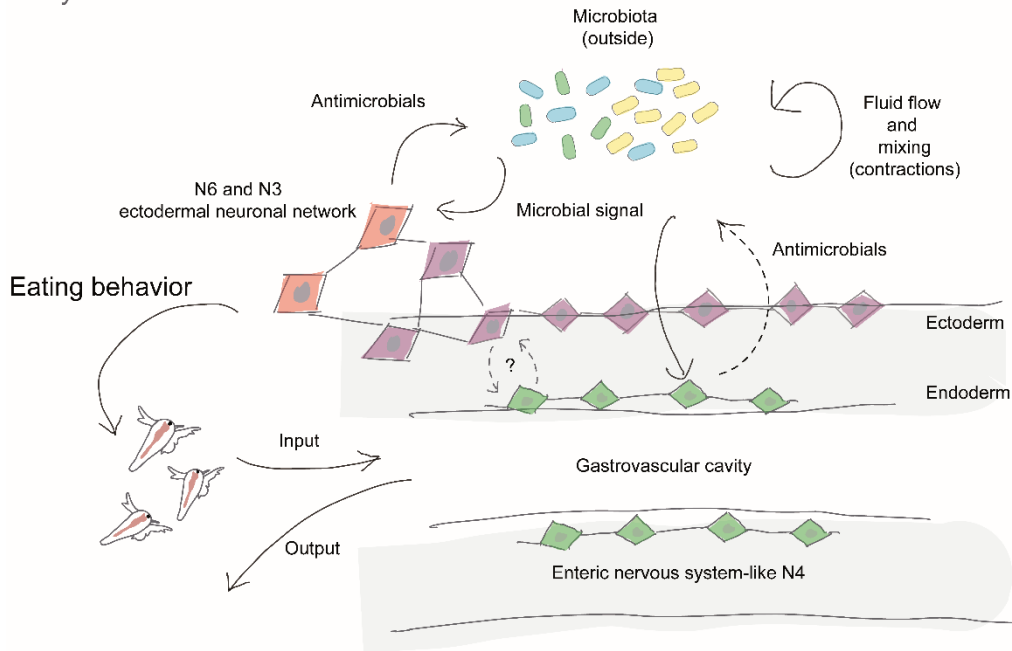
The reason why *Hydra* responds with a reduced eating behavior to *Curvibacter* or why such a feedback loop is integrated into the nervous system of *Hydra* is an interesting enigma. All examples show that bacteria can have a tremendous impact on eating behavior as different microbiota compositions have been associated with different eating disorders (de Wouters d'Oplinter et al., 2021). The absence of microbes leads to an overconsumption of palatable food in a reversible way, supporting the presence of a feedback loop to control satiety in animals (Ousey et al., 2023). In line with that thought, a disturbed microbiota completely changes the metabolic homeostasis in the colon (Zarrinpar et al., 2018). Furthermore, transplantation experiments highlight that different microbial communities have different impacts on the food choice of the host (Trevelline & Kohl, 2022). Nevertheless, all the aforementioned examples happen in a host who can choose their food and actively adapt their diet. However, given the limited ability of *Hydra* to actively select its prey to the extent of other systems, an interesting question arises as to why it integrates bacterial signals into its eating behavior. On one hand, a possible scenario is that the abundance of *Curvibacter* correlates with a well-fed *Hydra*, and this correlation is specific to *Curvibacter*, as demonstrated in **Chapter III**. On the other hand, alternatively, if the feedback loop rather solely depends on the bacterial load, it could serve as a mechanism for *Hydra* to prevent overgrowth by bacteria, similarly to other systems (Fetissov, 2016). It would be interesting to test this hypothesis further and manipulate the bacterial load. However, it is worth noting that under laboratory conditions, no other bacterium can attain a similar high bacterial load as *Curvibacter*. Identifying an equally good colonizer as *Curvibacter* might be highly informative and would help to understand the ecological relevance of the bacterial dependency of eating behavior. Nevertheless, the ecological relevance and the “why” of this interaction would be exciting future directions that would deepen the understanding of the connection between eating and bacteria.

Conserved functions of the nervous system from Cnidarian to mammals

Neurons have evolved to coordinate behavior, process, and integrate sensory stimuli from internal and external sources and to control the microbiota. Furthermore, neurons actively participate in keeping the “microbiota on a leash” (Foster et al., 2017). As discussed, the enteric nervous system monitors the gastrointestinal tract and responds appropriately by increasing the contraction frequency, modulating immune responses, and sending signals to the central nervous system which modulates eating behavior (Gabanyi et al., 2022; Han et al., 2021; Obata et al., 2020; Schneider et al., 2022). All of this involves neurons and is done to maintain a stable and beneficial microbiota which increases the accessibility to nutrients (Bäckhed et al., 2004; Krajmalnik-Brown et al., 2012; Rowland et al., 2017). The gut microbiota is kept in a place where almost 90% of the food-containing resources are already taken up by the host (Borgström et al., 1957). Thereby, the proliferation of the microbiota is limited by nitrogen and phosphate (Reese et al., 2018; Sabbagh et al., 2011). An increase in bacterial abundances together with food intake led to the release of satiety hormones preventing an overgrowth of bacteria and potential inflammation (Fetissov, 2016; Gabanyi et al., 2022; Han et al., 2021). With our work we can show that this feedback loop can be seen as a conserved function of the nervous system.

In *Hydra*, the nervous system is not yet as structured as in Bilaterian, but it contains all necessary components (**Chapters III and IV**). In *Hydra*, the microbiota is kept on the outside and is constrained from the gastrovascular cavity (Fraune et al., 2015). As in vertebrates, the nervous system of *Hydra* is involved in keeping the microbial community on a leash and stable (Fig. 4). Removing all neurons led to changes in the microbial composition (Fraune et al., 2009). This effect on the microbiota can have two underlying mechanisms that are not mutually exclusive but can go hand in hand. On one side, in the absence of neurons *Hydra* has no contraction behavior which is normally depending on bacteria and controls their composition (Murillo-Rincon et al., 2017; Nawroth et al., 2023). On the other hand, ectodermal neurons produce antimicrobial peptides that control the biogeography of the symbiotic bacteria (Augustin et al., 2017). Altogether, this shows high functional similarity with the gut of vertebrates where spontaneous contractions and antimicrobial compounds contribute to the biogeography of the microbiota as well (Fig. 4). However, in *Hydra*, most antimicrobial peptides are expressed in the endoderm where there are no bacteria

A. *Hydra*



B. Vertebrates

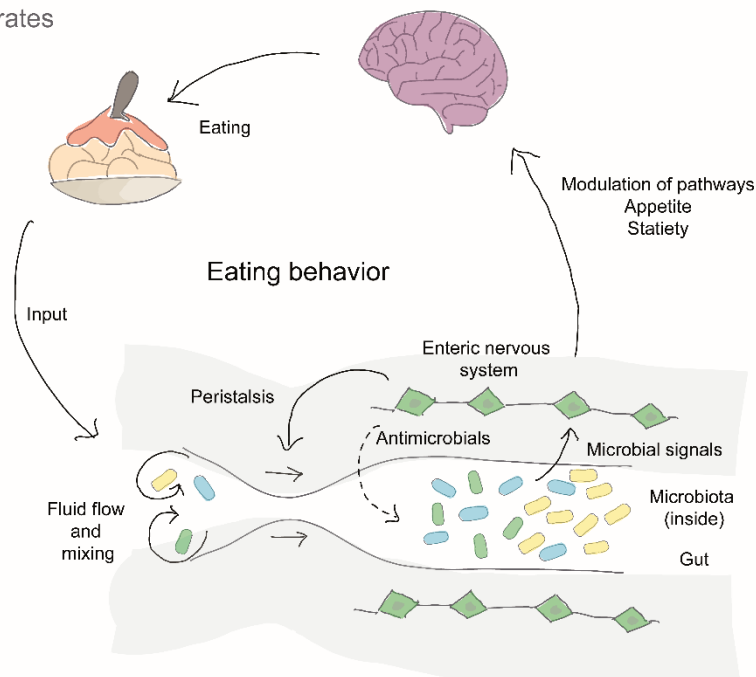


Figure 4. Similarities in eating behavior and microbiota between model systems. A. Schematic summary of the interaction between the microbiota, the nervous system, eating behavior and contractions in *Hydra*. **B.** Schematic simplification of the interaction between peristalsis, enteric nervous system, eating behavior and the microbiota in vertebrates. Functional similar structures are highlighted in similar colors.

found yet. Together with the fact that the endodermal neuronal population is responsive to microbial signals (direct or indirect needs to be resolved), suggests that here the situation is similar to the small intestine, where the number of bacteria is also drastically reduced (by 10^9 compared to the distal colon) and the number of antimicrobials is increased (Donaldson et al., 2015). One shared

reason can be – as was proposed – to avoid competition for the same nutritional resources. Overall, this may indicate that one of the ancient functions of the enteric nervous system is to control the microbiota. As the nutritional requirements get more complicated for the host and microbes are getting involved in providing resources and thereby need to be kept in the most convenient place. Moreover, symbiotic bacteria modulate food input and choice even though the reason is not always clear yet (Buchon et al., 2013; Kim et al., 2021). In summary, *Hydras* nervous system responds to microbial signals by secreting antimicrobial peptides, increasing contractions, and modulating the eating behavior, which suggests a similar relationship as in vertebrates (Fig. 4). Hereby, it may be inferred that a fundamental function of the nervous system is the regulation of its symbiotic bacteria, to keep them on a leash.

Does *Hydra* have a brain?

We move through our environment and always know where we are, what we smell, what we see, what we feel. The central nervous system processes and receives all those sensory information, which the brain integrates to adapt our behavior and determine our daily decisions (Chiel and Beer, 1997). Yet, the exact mechanism of how the brain does this remains an unresolved question even though we continuously decipher its mechanism (Pereira et al., 2020). Strikingly, certain animals, such as the Cnidarian, demonstrate already complex behaviors, yet they lack a central nervous system (Bosch et al., 2017). Cnidarians already exhibit associative memories (*Nematostella vectensis*, *Tripedalia cystophora*) (Bielecki et al., 2023; Botton-Amiot et al., 2023), sleeping behaviors as well as sleep deprivation (*Cassiopea xamachana*) (Abrams et al., 2023), visual processing with camera-type eyes (*Tripedalia sp.*) (Garm et al., 2007), aggression (Francis, 1973) and even courtship behavior (*Carybdea sivickisi*) (Werner, 1973). All those behaviors normally require a brain, yet they are possible without centralization. As a result, this phylum bears significant relevance in comprehending the fundamental principles governing nervous systems and the aforementioned behaviors.

We found that *Hydras'* complex behavior, the eating behavior, is controlled by a neuronal circuit that combines two non-overlapping global populations and one local neuronal population in the head. Furthermore, the two global networks can be divided into one central- and an enteric nervous system-like population (see **Chapters III** and **IV**). This highlights how sub-functionalized a decentralized nervous system already is and gives exciting insights into the evolution of the nervous system.

The enteric nervous system of *Hydra*

The central function of the enteric nervous system is the control of gastrointestinal motility and food transport (Constantinescu, 2016). Furthermore, it is quasi-autonomous and controls the tonus of the smooth muscle cells while also integrating bacterial signals (Brophy et al., 2017; Obata and Pachnis, 2016). Those features can be found from human to worm (Jiang et al., 2022; O'Donnell et al., 2020; Vidal et al., 2022). Here, we showed that it can even be found in one of the earliest nervous systems beyond Bilaterian. In *Hydra*, a freshwater Cnidarian, the endodermal neuronal network controls those exact tasks

(**Chapters III and IV**), which is in accordance with previous work (Shimizu et al., 2004). We were able to pin it down to one global spanning endodermal neuronal population, N4, which forms a homogenous network in the body column and has a higher density in the head (Giez et al., 2023b, 2023a). The endodermal population exhibits recurrent activity, with a slow periodicity of less than or equal to 0.01 Hz and increases during eating and digestion. So far, the slow recurring activity of the population seems to be quasi-autonomous as well. Furthermore, the spiking activity resembles striking similarity with the enteric nervous system of *C. elegans* where the DVB neurons exhibit a similar frequency and kinetics (Jiang et al., 2022). In addition, N4 has been associated with the contraction of the radial muscles which leads to peristaltic-like waves (Dupre and Yuste, 2017; Giez et al., 2023a). Additionally, it is essential for food intake and spitting out of digested remains as well as internal fluid control (Giez et al., 2023a). It seems to be mechanosensitive which is a property of the enteric nervous system as well (Mazzuoli-Weber and Schemann, 2015). Whether N4 senses the changes in the gastrovascular cavity solely by itself since it has sensory cells as well as the enteric nervous system (Furness and Stebbing, 2018), remains to be answered. A potential other route can be via the endodermal sensory population N5 since electron microscopic analysis has shown such connections (Fig. 5D-E) (Westfall et al., 1991). In conclusion, *Hydra* has an enteric nervous system-like nerve net in the endoderm based on high functional similarities.

The enteric nervous system is capable of perceiving environmental stimuli and regulating the gastrointestinal immune response, a function that is highly conserved across species. The endodermal neuronal population N4 responds to the microbiota. Nonetheless, the precise nature of this microbial impact needs to be eluded so far it is unclear if it is a direct or indirect effect. In contrast to most Bilaterian, *Hydras'* symbiotic microbial community sits on the outside and cannot be found in the gastrovascular cavity (Schröder and Bosch, 2016b). Interestingly, the enteric nervous system has been recently shown to control gastrointestinal immunity and environmental perception in mammals (Schneider et al., 2022). In *Hydra*, most antimicrobial peptides can be found in the endoderm as shown by the available single-cell data sets (Cazet et al., 2023; Franzenburg et al., 2013b; Siebert et al., 2019). Therefore, it might be possible that N4 regulates the concentration of antimicrobial peptides in the gastrovascular cavity of *Hydra*. Since N4 responds to the presence of bacteria, it could thereby ensure the absence of microbes as well. Assuming that the space in *Hydra* is truly germ-free,

one could speculate that the colonization of the gastrovascular or gastrointestinal tract is an invention of Bilaterian and the ancient "gut" was free of persisting symbiotic bacteria. For the increased nutritional requirements in Bilaterian, it might have been beneficial to evolve a "bioreactor" whereas *Hydra* does not depend on that. However, further investigations are required to substantiate these speculations. Nevertheless, with our discoveries, we may have established a framework for investigating and comprehending the evolutionary origin of the enteric nervous system and microbial regulation.

The central nervous system of *Hydra*

The evolutionary origin of the central nervous system might be traced back to a single neuronal network in one of the earliest nervous systems, the phylum Cnidarian. The key fundamental function of the central nervous system is the monitoring, sensing, and controlling of the entire body of an animal (Marcus and Jacobson, 2003; Pavelka and Roth, 2010). It is an invention of Bilaterian and the merging of two integrative centers, the apical nervous system and the blastoporal nervous system which are supposed to be present in earlier phyla (Arendt et al., 2015; Tosches and Arendt, 2013). Those two centers have been assigned two distinct functions: the apical nervous system is mainly responsible for sensing, locomotion, and neurosecretory functions whereas the blastoporal nervous system is responsible for feeding associated behaviors. However, these centers are mainly defined by morphology, location, and transcription factors and not by neuronal function. In **Chapter IV** we can provide functional and mechanistic evidence for the proposed trajectory of central nervous system evolution.

The ectodermal neuronal population N3 in *Hydra* has similar functions as the central nervous system in Bilaterian since it integrates physiological, internal states and environmental information, and modulates global behavioral patterns. The presence of an internal state or controlling instance in *Hydra* has been proposed for a long time (Koizumi and Maeda, 1981) but could not be shown. Here, we reported that the activity of N3 depends on the feeding state and thereby modulates almost all behaviors. In well-fed animals the spiking frequency of N3 is increased especially the activity which is associated with non-visible behavior. The increased spiking frequency suppresses and modulates other behaviors suggesting a hierarchical organization of activity which was proposed by electrophysiological measurements in 1963 (Passano and McCullough, 1963). In

the early work it has been already observed that rhythmic potentials are controlling and dominant over other activity systems. However, the electrical signal was not clearly associated with neurons yet and the proposed location was the endoderm while we identified it as an ectodermal network. Besides the feeding state, the ectodermal network N3 also integrates other environmental signals such as light, mechanical stimuli, and osmolarity and thereby changes behavioral patterns (Passano and McCullough, 1963; Yamamoto and Yuste, 2023, 2020b). Overall, N3 seems to be a higher order unit that integrates and modulates behavior similar to a central nervous system even though there is no centralization. This reveals a new mechanism of how animals with a rather diffuse nervous system can integrate information and coordinate their behavior in relation to their environment.

Now, with this new insight into a simple nervous system, it would be exciting to explore the concept of a single neuronal population that functions as an integration and processing unit which is globally distributed in other Cnidarians. Can one find a similar network in *Tripedalia* that integrates, processes visual information, and has associative learning? Or even more closely associated with our findings: does *Clythia* have a similar controlling system for preventing eating response post feeding and motor behaviors? In conclusion, we identified a neuronal network that integrates multiple information and thereby modulates behavioral patterns and acts as a central nervous system which will help us to understand the evolution and mechanism of our nervous system.

Low-frequency oscillations depend on internal states in *Hydra*

Low frequency spontaneous neuronal activity ($<0.1\text{Hz}$) is a phenomenon found in Cnidarians and the brain of vertebrates (Dupre and Yuste, 2017; Hanson, 2021; Hughes et al., 2011; Kropotov, 2022; Leung et al., 2019; Passano and McCullough, 1962). In human brains this spontaneous resting state network is called Default Mode Network (DMN) and is involved in processes such as episodic memory (Berger, 1929; Raichle, 2015). In *Hydra*, such low frequency activity is responsible for global behavioral modulation. Electrophysiological analysis in *Hydra* has already identified re-occurring rhythmic electrical activity, which was cryptic, as they were not associated with any behavior (Passano et al., 1965; Passano and McCullough, 1964, 1963). The underlying mechanism was proposed to be based on pacemaker cells which can intrinsically generate

rhythmic bursts. We and others have identified the responsible neuronal population for such low frequency re-occurring activity, the ectodermal N3 population (Dupre and Yuste, 2017). Investigating the different dynamics of N3, we identified different spiking frequencies associated with different behaviors (somersaults: $>0.1\text{Hz}$; contraction: < 0.02 ; elongating: > 0.025). However, the non-behavior associated activity was of particular interest since it depended on the feeding status as well, thus suggesting an integration of the metabolic state and downstream modulation of different behaviors. Removing N3 abolished its inhibitory effect on the mouth opening and response to food stimuli as well as on the phototaxis behavior. Further, it reduced the feeding state dependent increase in body movement. In conclusion, we could show that the neuronal network responsible for the low frequency rhythmic potentials serves as an organism-wide information integrator as proposed previously (Dupre and Yuste, 2017; Hanson, 2021). However, a question that remains unresolved pertains to whether the population denoted as N3 is strictly intrinsically activated or if it is rather extrinsically activated. Moreover, for this population to effectively integrate multiple sensory information, it is necessary that it has access to such information. How such access is achieved, however, remains to be resolved, notwithstanding the fact that we already have evidence for direct contact with other neuronal populations. Nevertheless, our observations have established a framework for investigating the integration of information in a simple nervous system and the modulation of different behavioral patterns. This will provide a stimulating insight into the evolution of the central nervous system.

How has our understanding of the nervous system of *Hydra* changed?

In this last part, I want to embed the identified mechanism of the nervous system of *Hydra* in the recent literature and draw a picture of how the nervous system of *Hydra* might work. In recent years, a new series of publications came out picking up on what electrophysiological analysis has identified decades before and stepwise completing the picture and understanding of *Hydras* nervous system.

The contraction and the elongation behavior are antagonistic and occur sequentially. The neuronal population N1 is associated with spontaneous body contraction and was previously identified as a contraction burst network (Dupre and Yuste, 2017; Passano and McCullough, 1963). In contrast the neuronal

population N3 (rhythmic potential 1) controls elongating behavior (Fig. 5A) (Passano and McCullough, 1963). Therefore, N1 and N3 are counteracting each other in a hierarchical way where N3 has a higher hierarchy than N1 as proposed (Passano and McCullough, 1963). Interestingly, they also interact similarly during other behaviors such as somersaulting which is mainly controlled by N3 (Fig. 5A, C) (Yamamoto and Yuste, 2023). Here, N3 increases in frequency and initiates the nematocytes and the detachment of the foot while inhibiting the activity of N1. As soon as the foot is loose, N1 is activated and leads to a body contraction that brings the body to the new location where the head has attached (Fig. 3J Introduction) (Yamamoto and Yuste, 2023). The interplay of these two populations in different behaviors nicely emphasizes the multifunctionality and required coordination between neuronal populations in this rather simple nervous system.

The coordination between neuronal populations in *Hydra* is required for different behaviors such as the eating behavior but the mechanism was unknown until our work (Fig. 5B). Similar to the agonistic coordination of N3 and N1 during contraction and elongation behavior, N3 modulates the eating behavior where an increased frequency prevents or reduces mouth opening. Additionally, during the eating behavior the ectodermal N6 transmits a signal to the endodermal N4 population which is required for the mouth opening. How the signal is spread and how both populations coordinate their activity is unknown. Recent work highlighted that there are no synaptic connections between ectodermal and endodermal neuronal networks (Athina et al., 2023). Nonetheless, this work has only investigated the body column and lacked a systematic investigation of other body parts such as the head. In contrast, early work on the ultrastructure of the nervous system of *Hydra* has found structures bridging the mesoglea and thereby connecting ecto- and endoderm (Kinnamon and Westfall, 1982, 1981). However, they could not determine if those were neuronal or epithelial structures and thereby did not further pursue it. Therefore, it is hard to say if there are synaptic contacts between ectodermal and endodermal neuronal networks and future work needs to elucidate the nature of neuronal connections in *Hydra*.

As proposed by Arendt *et al.* 2015, the nervous system of *Hydra* can be separated in an apical nervous system (ANS) responsible for the organism's overall physiology, settlement and locomotion, and a blastoporal nervous system (BNS) which coordinates eating behavior (Arendt et al., 2015). On one hand, the apical nervous system (ANS) is formed by the neuronal populations N3 (Ec3,

RP1), and N1 (Ec1/Ec5, CB; Fig. 5A). Both neuronal populations control overall physiology and locomotion behavior and have their highest densities in the foot of *Hydra*. The endodermal neuronal populations were not considered since their distribution is rather focused on the head and their function has not been associated with locomotion or settlement. On the other hand, the blastoporal nervous system is most likely formed by the neuronal populations N3 (Ec3, RP1), N4 (En1, RP2) and N6 (Ec4). All three neuronal populations control the eating behavior (Fig. 5B) (Giez et al., 2023b). Concluding that in *Hydra* the nervous

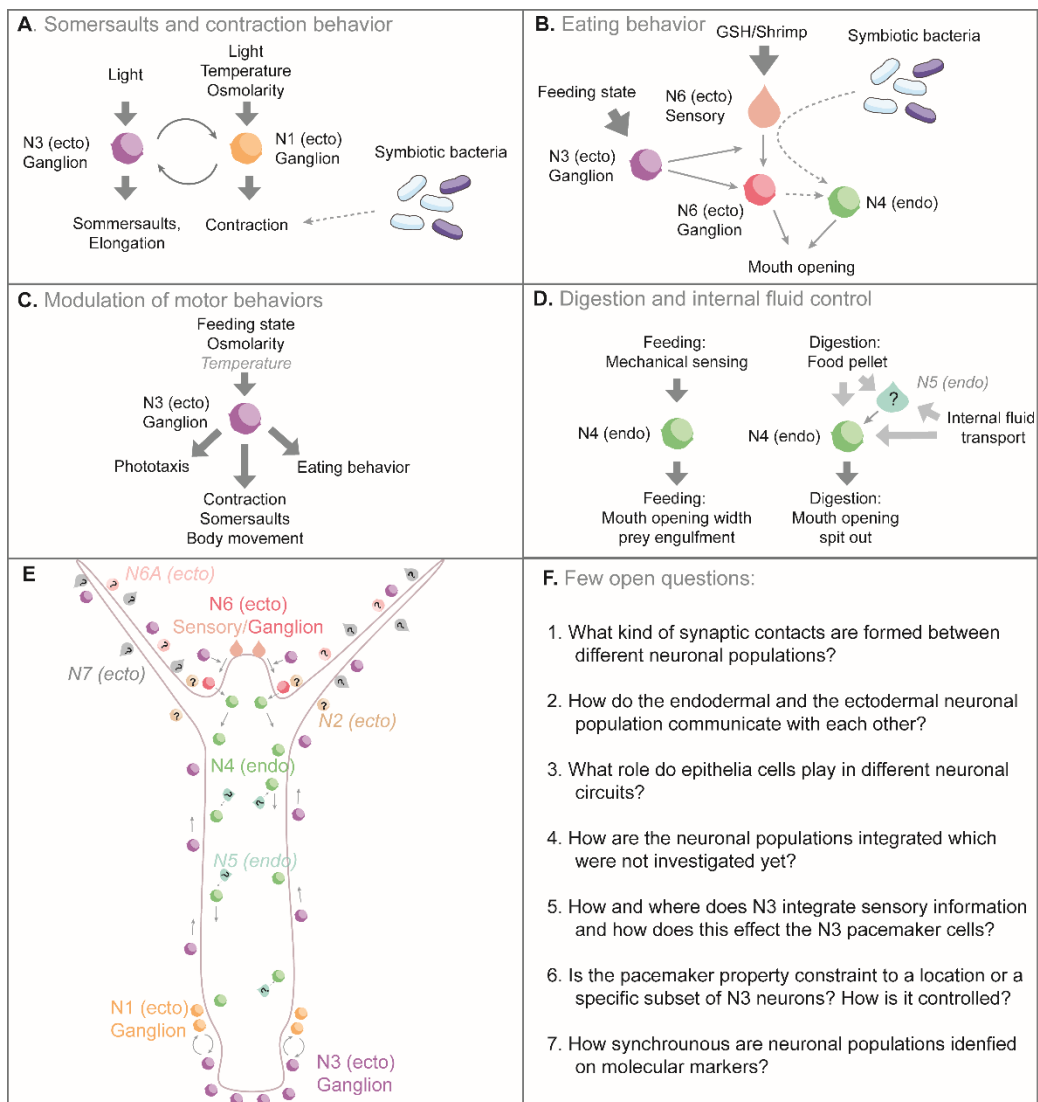


Figure 5. Identified neuronal circuits in *Hydra*. **A.** Somersaulting and contraction circuit. **B.** Eating behavior circuit. **C.** Integration of different sensory and internal information. **D.** Feeding and digestion related circuit. **E.** Schematic with all neuronal populations and known circuits unknown are highlighted with “?”. **F.** A few open questions about the nervous system of *Hydra*.

system can be roughly split into an apical- and blastoporal nervous system and confirms the proposed division into two centers.

However, the nervous system of *Hydra* is slightly more complicated than that and has a sub-functionalization into a more central and an enteric-like nervous system. The neuronal population N3 is involved in eating behavior as well as in locomotion behaviors and therefore connecting the apical- and blastoporal nervous systems. Besides connecting both systems, N3 also integrates external and internal stimuli and affects downstream behaviors (Fig. 5C). The ability to integrate and modulate behaviors makes N3 a central nervous system like population. On the other hand, the endodermal neuronal population N4 is mainly involved in eating associated behaviors which are characteristic of an enteric nervous system (Fig. 5D). Overall, this highlights that the rather simple nervous system of *Hydra* consists of multiple neuronal populations which are organized in a hierarchical manner where N3 has the highest order.

Since *Hydra* is colonized by microbes that affect different aspects of the host physiology, they also influence behavior and neuronal activity (Giez et al., 2023b). It has been shown that bacteria modulate the spontaneous contraction behavior, but the underlying mechanism could not be determined (Fig. 5A) (Murillo-Rincon et al., 2017). Since populations N3 and N1 are mainly associated with the contraction behavior so far, the question arises where the microbial signal can be integrated. One speculation is that N3 neurons could integrate bacterial signals and thereby affect behaviors such as spontaneous body contractions. However, further investigations are needed to elucidate the underlying mechanism of the interaction between bacteria and contractions in *Hydra*. Nevertheless, the eating behavior shows that the integration of bacterial signals into neuronal circuits is happening in *Hydra*. Here a disturbed community led to an accumulation of the bacterially produced neurotransmitter glutamate which affects N6 sensory neurons and thereby inhibits mouth opening (Fig. 5B). Overall, this work highlights that the integration of bacterial products is an ancient function of the nervous system and already evident in one of the earliest nervous systems.

Regardless of the described mechanism, there exist numerous unresolved questions concerning the way the nervous system interacts with the microbiota in *Hydra*. One such question pertains to whether microbial signals are also integrated into the N3 network or alternative neuronal networks, potentially

inducing alterations in contractions or other behaviors. In summary, while many functions of different neuronal populations in *Hydra* have been identified there are still many unanswered questions. Nonetheless, a framework has been created with our work to approach them now (Fig. 5E-F).

Taken together, the second part of my thesis has investigated the functional organization of the nervous system of *Hydra*. Advancing our understanding of the evolution of the nervous system, the systematical analysis of the neuronal populations in *Hydra* has provided new insight into the complex sub-functionalization and hierarchical organization of a rather simple nervous system. On one side the coordination of different neuronal populations to control a complex behavior such as the eating behavior. On the other side, the hierarchical organization is where one population is integrating multiple information and regulating other behaviors which is functionally like the central nervous system. Provocatively way one could say this neuronal population forms a pre-brain before the invention of centralization. Overall, this part of my work has shown that a rather simple nervous system has the potential to study conserved properties of nervous systems and to decipher the evolution of the nervous system.

References (Introduction and Epilogue)

- Abrams MJ, Zhang L, Emster K von, Lee BH, Zeigler H, Jain T, Jafri A, Chen Z, Harland RM. 2023. Sleep is required for neural network plasticity in the jellyfish *Cassiopea*. *bioRxiv* 2023.05.04.538973. doi:10.1101/2023.05.04.538973
- Akira S, Takeda K. 2004. Toll-like receptor signalling. *Nature Reviews Immunology* 2004 4:7 4:499–511. doi:10.1038/nri1391
- Akman Gündüz E, Douglas AE. 2008. Symbiotic bacteria enable insect to use a nutritionally inadequate diet. *Proceedings of the Royal Society B: Biological Sciences* 276:987–991. doi:10.1098/RSPB.2008.1476
- Alberdi A, Andersen SB, Limborg MT, Dunn RR, Gilbert MTP. 2021. Disentangling host–microbiota complexity through hologenomics. *Nature Reviews Genetics* 2021 23:5 23:281–297. doi:10.1038/s41576-021-00421-0
- Anitha M, Vijay-Kumar M, Sitaraman S V., Gewirtz AT, Srinivasan S. 2012. Gut Microbial Products Regulate Murine Gastrointestinal Motility via Toll-Like Receptor 4 Signaling. *Gastroenterology* 143:1006-1016.e4. doi:10.1053/J.GASTRO.2012.06.034
- Arendt D. 2020. The Evolutionary Assembly of Neuronal Machinery. *Current Biology* 30:R603–R616. doi:10.1016/J.CUB.2020.04.008
- Arendt D. 2018. Animal Evolution: Convergent Nerve Cords? *Current Biology* 28:R225–R227. doi:10.1016/J.CUB.2018.01.056
- Arendt D, Tosches MA, Marlow H. 2015. From nerve net to nerve ring, nerve cord and brain — evolution of the nervous system. *Nature Reviews Neuroscience* 2015 17:1 17:61–72. doi:10.1038/nrn.2015.15
- Athina K, Sandra S, Christina B, Cramer von LC, Bianca B, Willi S, Martin H, Olga A, M. GK, E. SR, Bert H, Thomas H, N. DC. 2023. A new look at the architecture and dynamics of the Hydra nerve net. *Elife* 12. doi:10.7554/ELIFE.87330
- Augustin R, Schröder K, Rincón APM, Fraune S, Anton-Erxleben F, Herbst E-M, Wittlieb J, Schwentner M, Grötzinger J, Wassenaar TM. 2017. A secreted antibacterial neuropeptide shapes the microbiome of Hydra. *Nat Commun* 8:1–9. doi:10.1038/s41467-017-00625-1
- Bäckhed F, Ding H, Wang T, Hooper L V., Gou YK, Nagy A, Semenkovich CF, Gordon JL. 2004. The gut microbiota as an environmental factor that regulates fat storage. *Proc Natl Acad Sci U S A* 101:15718–15723. doi:10.1073/pnas.0407076101
- Badhiwala KN, Primack AS, Juliano C, Robinson JT. 2021. Multiple neuronal networks coordinate hydra mechanosensory behavior. *Elife* 10. doi:10.7554/ELIFE.64108
- Bates JM, Mittge E, Kuhlman J, Baden KN, Cheesman SE, Guillemin K. 2006. Distinct signals from the microbiota promote different aspects of zebrafish gut differentiation. *Dev Biol* 297:374–386. doi:10.1016/j.ydbio.2006.05.006
- Bavaharan A, Skilbeck C. 2022. Electrical signalling in prokaryotes and its convergence with quorum sensing in *Bacillus*. *BioEssays* 44:2100193. doi:10.1002/BIES.202100193
- Benarroch JM, Asally M. 2020. The Microbiologist’s Guide to Membrane Potential Dynamics. *Trends Microbiol* 28:304–314. doi:10.1016/J.TIM.2019.12.008
- Berger H. 1929. Über das Elektrenkephalogramm des Menschen. *Arch Psychiatr Nervenkrankh* 87.
- Bielecki J, Nielsen SKD, Nachman G, Garm A. 2023. Associative learning in the box jellyfish *Tripedalia cystophora*. *Current Biology* 0. doi:10.1016/J.CUB.2023.08.056
- Bode H, Berking S, David CN, Gierer A, Schaller H, Trenkner E. 1973. Quantitative analysis of cell types during growth and morphogenesis in Hydra. *Wilhelm Roux Arch Entwickl Mech Org* 171:269–285. doi:10.1007/BF00577725/METRICS

- Boehme M, Guzzetta KE, Bastiaanssen TFS, van de Wouw M, Moloney GM, Gual-Grau A, Spichak S, Olavarria-Ramirez L, Fitzgerald P, Morillas E, Ritz NL, Jaggar M, Cowan CSM, Crispie F, Donoso F, Halitzki E, Neto MC, Sichiatti M, Golubeva A V., Fitzgerald RS, Claesson MJ, Cotter PD, O'Leary OF, Dinan TG, Cryan JF. 2021. Microbiota from young mice counteracts selective age-associated behavioral deficits. *Nature Aging* 2021 1:8 1:666–676. doi:10.1038/s43587-021-00093-9
- Borgström B, Dahlqvist A, Lundh G, Sjövall J. 1957. Studies of intestinal digestion and absorption in the human. *J Clin Invest* 36:1521–1536. doi:10.1172/JCI103549
- Bosch TCG. 2014. Rethinking the role of immunity: lessons from Hydra. *Trends Immunol* 35:495–502. doi:10.1016/j.it.2014.07.008
- Bosch TCG. 2013. Cnidarian-microbe interactions and the origin of innate immunity in metazoans. *Annu Rev Microbiol* 67:499–518. doi:10.1146/annurev-micro-092412-155626
- Bosch TCG, Anton-Erxleben F, Hemmrich G, Khalturin K. 2010. The hydra polyp: Nothing but an active stem cell community. *Dev Growth Differ* 52:15–25. doi:10.1111/j.1440-169X.2009.01143.x
- Bosch TCG, Klimovich A, Domazet-Lošo T, Gründer S, Holstein TW, Jékely G, Miller DJ, Murillo-Rincon AP, Rentzsch F, Richards GS, Schröder K, Technau U, Yuste R. 2017. Back to the Basics: Cnidarians Start to Fire. *Trends Neurosci* 40:92–105. doi:10.1016/j.tins.2016.11.005
- Bosch TCG, McFall-Ngai M. 2021. Animal development in the microbial world: Re-thinking the conceptual framework.
- Bosch TCG, McFall-Ngai MJ. 2011. Metaorganisms as the new frontier. *Zoology* 114:185–190. doi:10.1016/j.zool.2011.04.001
- Botton-Amiot G, Martinez P, Sprecher SG. 2023. Associative learning in the cnidarian *Nematostella vectensis*. *Proc Natl Acad Sci U S A* 120. doi:10.1073/pnas.2220685120
- Brophy JAN, Triassi AJ, Adams BL, Renberg RL, Stratis-Cullum DN, Grossman AD, Voigt CA, Bosch TCG, Klimovich A, Domazet-Lošo T, Gründer S, Holstein TW, Jékely G, Miller DJ, Murillo-Rincon AP, Rentzsch F, Richards GS, Schröder K, Technau U, Yuste R, Hadizadeh F, Walter S, Belheouane M, Bonfiglio F, Heinsen F-AA, Andreasson A, Agreus L, Engstrand L, Baines JF, Rafter J, Franke A, D'Amato M, Tropini C, Earle KA, Huang KC, Sonnenburg JL, Yang NJ, Chiu IM, Satterlie RA, Abrams MJ, Goentoro L, Hamner W, Jones M, Hamner P, Josephson RK, Macklin M, Sharon G, Sampson TR, Geschwind DH, Mazmanian SK, Takaku Y, Hwang JS, Wolf A, Böttger A, Shimizu H, David CN, Gojobori T, Jankipersadsing SA, Hadizadeh F, Bonder MJ, Tigchelaar EF, Deelen P, Fu J, Andreasson A, Agreus L, Walter S, Wijmenga C, Hysi P, D'Amato M, Zhernakova A, Trinh LA, McCutchen MD, Bonner-Fraser M, Fraser SE, Bumm LA, McCauley DW, Campbell, R. D. et al., Dobson AJ, Chaston JM, Newell PD, Donahue L, Hermann SL, Sannino DR, Westmiller S, Wong AC-N, Clark AG, Lazzaro BP, Douglas AE, Satterlie RA, Chaston JM, Dobson AJ, Newell PD, Douglas AE, Guder C, Pinho S, Nacak TG, Schmidt HA, Hobmayer B, Niehrs C, Holstein TW, Collins SM, Surette M, Bercik P, Franzénburg S, Walter J, Künzel S, Wang J, Baines JF, Bosch TCG, Fraune S, Hadizadeh F, Walter S, Belheouane M, Bonfiglio F, Heinsen F-AA, Andreasson A, Agreus L, Engstrand L, Baines JF, Rafter J, Franke A, D'Amato M, Kabouridis PS, Pachnis V, Cohen D, Melamed S, Millman A, Shulman G, Oppenheimer-Shaanan Y, Kacen A, Doron S, Amitai G, Sorek R, Abrams MJ, Basinger T, Yuan W, Guo C-L, Goentoro L, Beloussov L V. 2017. Stool frequency is associated with gut microbiota composition. *Gut* 66:559–560. doi:10.1136/gutjnl-2016-311935
- Bruckner JJ, Stednitz SJ, Grice MZ, Zaidan D, Massaquoi MS, Larsch J, Tallafuss A, Guillemin K, Washbourne P, Eisen JS. 2022. The microbiota promotes social behavior by modulating microglial remodeling of forebrain neurons. *PLoS Biol* 20:e3001838. doi:10.1371/JOURNAL.PBIO.3001838
- Bucher D, Anderson PAV. 2015. Evolution of the first nervous systems – what can we surmise? *Journal of Experimental Biology* 218:501–503. doi:10.1242/JEB.111799
- Buchon N, Broderick NA, Lemaitre B. 2013. Gut homeostasis in a microbial world: insights from *Drosophila melanogaster*. *Nature Reviews Microbiology* 2013 11:9 11:615–626. doi:10.1038/nrmicro3074

- Burkhardt P, Sprecher SG. 2017. Evolutionary origin of synapses and neurons – Bridging the gap. *BioEssays* **39**:1700024. doi:10.1002/BIES.201700024
- Burnett AL, Davidson R, Wiernik P. 1963. On the presence of a feeding hormone in the nematocyst of *Hydra pirardi*. doi.org/10.2307/1539399 **125**:226–233. doi:10.2307/1539399
- Burnett AL, Diehl NA. 1964. The nervous system of hydra. I. Types, distribution and origin of nerve elements. *Journal of Experimental Zoology* **157**:217–226. doi:10.1002/jez.1401570205
- Campbell RD, Josephson RK, Schwab WE, Rushforth NB, Campbell, R. D. et al. 1976. Excitability of nerve-free hydra. *Nature* **262**:388. doi:10.1038/262388a0
- Carrier TJ, Bosch TCG. 2022. Symbiosis: the other cells in development. *Development* **149**. doi:10.1242/dev.200797
- Cazet JF, Siebert S, Little HM, Bertemes P, Primack AS, Ladurner P, AchRAINER M, Fredriksen MT, Moreland RT, Singh S, Zhang S, Wolfsberg TG, Schnitzler CE, Baxevanis AD, Simakov O, Hobmayer B, Juliano CE. 2023. A chromosome-scale epigenetic map of the *Hydra* genome reveals conserved regulators of cell state. *Genome Res* gr.277040.122. doi:10.1101/GR.277040.122
- Chapman JA, Kirkness EF, Simakov O, Hampson SE, Mitros T, Weinmaier T, Rattei T, Balasubramanian PG, Borman J, Busam D, Disbennett K, Pfannkoch C, Sumin N, Sutton GG, Viswanathan LD, Walenz B, Goodstein DM, Hellsten U, Kawashima T, Prochnik SE, Putnam NH, Shu S, Blumberg B, Dana CE, Gee L, Kibler DF, Law L, Lindgens D, Martinez DE, Peng J, Wigge PA, Bertulat B, Guder C, Nakamura Y, Ozbek S, Watanabe H, Khalturin K, Hemmrich G, Franke A, Augustin R, Fraune S, Hayakawa E, Hayakawa S, Hirose M, Hwang JS, Ikeo K, Nishimiya-Fujisawa C, Ogura A, Takahashi T, Steinmetz PRH, Zhang X, Aufschneider R, Eder MK, Gorny AK, Salvenmoser W, Heimberg AM, Wheeler BM, Peterson KJ, Böttger A, Tischler P, Wolf A, Gojobori T, Remington KA, Strausberg RL, Venter JC, Technau U, Hobmayer B, Bosch TCG, Holstein TW, Fujisawa T, Bode HR, David CN, Rokhsar DS, Steele RE. 2010. The dynamic genome of *Hydra*. *Nature* **464**:592–596. doi:10.1038/nature08830
- Cheesman SE, Neal JT, Mittge E, Seredick BM, Guillemin K. 2011. Epithelial cell proliferation in the developing zebrafish intestine is regulated by the Wnt pathway and microbial signaling via Myd88. *Proceedings of the National Academy of Sciences* **108**:4570–4577. doi:10.1073/pnas.1000072107
- Chen H, Nwe PK, Yang Y, Rosen CE, Bielecka AA, Kuchroo M, Cline GW, Kruse AC, Ring AM, Crawford JM, Palm NW. 2019. A Forward Chemical Genetic Screen Reveals Gut Microbiota Metabolites That Modulate Host Physiology. *Cell* **177**:1217–1231.e18. doi:10.1016/J.CELL.2019.03.036
- Chevrot R, Rosen R, Haudecoeur E, Cirou A, Shelp BJ, Ron E, Faure D. 2006. GABA controls the level of quorum-sensing signal in *Agrobacterium tumefaciens*. *Proc Natl Acad Sci U S A* **103**:7460–7464. doi:doi.org/10.1073/pnas.06003131
- Chiel HJ, Beer RD. 1997. The brain has a body: adaptive behavior emerges from interactions of nervous system, body and environment. *Trends Neurosci* **20**:553–557. doi:10.1016/S0166-2236(97)01149-1
- Chikina A, Matic Vignjevic D. 2021. At the right time in the right place: How do luminal gradients position the microbiota along the gut? *Cells & Development* **168**:203712. doi:10.1016/J.CDEV.2021.203712
- Cohen LJ, Esterhazy D, Kim SH, Lemetre C, Aguilar RR, Gordon EA, Pickard AJ, Cross JR, Emiliano AB, Han SM, Chu J, Vila-Farres X, Kaplitt J, Rogoz A, Calle PY, Hunter C, Bitok JK, Brady SF. 2017. Commensal bacteria make GPCR ligands that mimic human signalling molecules. *Nature* **549**:48–53. doi:10.1038/nature23874
- Collins J, Borojevic R, Verdu EF, Huizinga JD, Ratcliffe EM. 2014. Intestinal microbiota influence the early postnatal development of the enteric nervous system. *Neurogastroenterology & Motility* **26**:98–107. doi:10.1111/NMO.12236
- Colosimo DA, Kohn JA, Luo PM, Piscotta FJ, Han SM, Pickard AJ, Rao A, Cross JR, Cohen LJ, Brady SF. 2019. Mapping Interactions of Microbial Metabolites with Human G-Protein-Coupled Receptors. *Cell Host Microbe* **26**:273–282.e7. doi:10.1016/J.CHOM.2019.07.002

- Concas A, Pierobon P, Mostallino MC, Porcu P, Marino G, Minei R, Biggio G. 1998. Modulation of γ -aminobutyric acid (GABA) receptors and the feeding response by neurosteroids in *Hydra vulgaris*. *Neuroscience* **85**:979–988. doi:10.1016/S0306-4522(97)00515-0
- Constantinescu M. 2016. The enteric nervous system. *Neuro-Immuno-Gastroenterology* **23**:38. doi:10.1007/978-3-319-28609-9_2/COVER
- Cooper GM. 2000. The Origin and Evolution of Cells.
- Costello EK, Stagaman K, Dethlefsen L, Bohannan BJM, Relman DA. 2012. The application of ecological theory toward an understanding of the human microbiome. *Science* (1979) **336**:1255–1262. doi:10.1126/science.1224203
- Cremer J, Arnoldini M, Hwa T. 2017. Effect of water flow and chemical environment on microbiota growth and composition in the human colon. *Proc Natl Acad Sci U S A* **114**:6438–6443. doi:10.1073/pnas.1619598114
- Cremer J, Segota I, Yang C, Arnoldini M, Sauls JT, Zhang Z, Gutierrez E, Groisman A, Hwa T. 2016. Effect of flow and peristaltic mixing on bacterial growth in a gut-like channel. *Proceedings of the National Academy of Sciences* **113**:11414–11419. doi:10.1073/pnas.1601306113
- Cryan John F, O’Riordan KJ, Cowan CSM, Sandhu K V, Bastiaanssen TFS, Boehme M, Codagnone MG, Cusotto S, Fulling C, Golubeva A V. 2019. The microbiota-gut-brain axis. *Physiol Rev*.
- Cryan John F., O’riordan KJ, Cowan CSM, Sandhu K V., Bastiaanssen TFS, Boehme M, Codagnone MG, Cusotto S, Fulling C, Golubeva A V., Guzzetta KE, Jaggar M, Long-Smith CM, Lyte JM, Martin JA, Molinero-Perez A, Moloney G, Morelli E, Morillas E, O’connor R, Cruz-Pereira JS, Peterson VL, Rea K, Ritz NL, Sherwin E, Spichak S, Teichman EM, van de Wouw M, Ventura-Silva AP, Wallace-Fitzsimons SE, Hyland N, Clarke G, Dinan TG. 2019. The microbiota-gut-brain axis. *Physiol Rev* **99**:1877–2013. doi:10.1152/physrev.00018.2018
- Currie CR. 2003. A Community of Ants, Fungi, and Bacteria: A Multilateral Approach to Studying Symbiosis. <https://doi.org/10.1146/annurev.micro551357> **55**:357–380. doi:10.1146/ANNUREV.MICRO.55.1.357
- Cusotto S, Sandhu K V., Dinan TG, Cryan JF. 2018. The Neuroendocrinology of the Microbiota-Gut-Brain Axis: A Behavioural Perspective. *Front Neuroendocrinol*. doi:10.1016/j.yfrne.2018.04.002
- Dagorn A, Chapalain A, Mijouin L, Hillion M, Duclairoir-Poc C, Chevalier S, Taupin L, Orange N, Feuilloley MGJ. 2013. Effect of GABA, a Bacterial Metabolite, on *Pseudomonas fluorescens* Surface Properties and Cytotoxicity. *International Journal of Molecular Sciences* **2013**, Vol **14**, Pages **12186–12204** **14**:12186–12204. doi:10.3390/IJMS140612186
- David CN. 1973. A Quantitative Method for Maceration of *Hydra* Tissue. *Wilhelm Roux’ Archiv* **171**:259–268. doi:10.1007/BF00577724
- De Petrocellis L, Melck D, Bisogno T, Milone A, Di Marzo V. 1999. Finding of the endocannabinoid signalling system in *Hydra*, a very primitive organism: Possible role in the feeding response. *Neuroscience* **92**:377–387. doi:10.1016/S0306-4522(98)00749-0
- de Wouters d’Oplinter A, Rastelli M, Van Hul M, Delzenne NM, Cani PD, Everard A. 2021. Gut microbes participate in food preference alterations during obesity. *Gut Microbes* **13**. doi:10.1080/19490976.2021.1959242
- Deines P, Hammerschmidt K, Bosch TCG. 2020. Microbial species coexistence depends on the host environment. *mBio* **11**:1–13. doi:10.1128/mBio.00807-20
- Depetris-Chauvin A, Galagovsky D, Chevalier C, Maniere G, Grosjean Y. 2017. Olfactory detection of a bacterial short-chain fatty acid acts as an orexigenic signal in *Drosophila melanogaster* larvae. *Scientific Reports* **2017** **7**:1 **7**:1–14. doi:10.1038/s41598-017-14589-1
- Desbonnet L, Clarke G, Shanahan F, Dinan TG, Cryan JF. 2013. Microbiota is essential for social development in the mouse. *Molecular Psychiatry* **2014** **19**:2 **19**:146–148. doi:10.1038/mp.2013.65

- Dohnalová L, Lundgren P, Carty JRE, Goldstein N, Wenski SL, Nanudorn P, Thiengmag S, Huang KP, Litichevskiy L, Descamps HC, Chellappa K, Glassman A, Kessler S, Kim J, Cox TO, Dmitrieva-Posocco O, Wong AC, Allman EL, Ghosh S, Sharma N, Sengupta K, Cornes B, Dean N, Churchill GA, Khurana TS, Sellmyer MA, FitzGerald GA, Patterson AD, Baur JA, Alhadeff AL, Helfrich EJN, Levy M, Betley JN, Thaïs CA. 2022. A microbiome-dependent gut–brain pathway regulates motivation for exercise. *Nature* 2022 612:7941 **612**:739–747. doi:10.1038/s41586-022-05525-z
- Donaldson GP, Lee SM, Mazmanian SK. 2015. Gut biogeography of the bacterial microbiota. *Nature Reviews Microbiology* 2015 14:1 **14**:20–32. doi:10.1038/nrmicro3552
- Douglas AE. 2019. Simple animal models for microbiome research. *Nature Reviews Microbiology* 2019 17:12 **17**:764–775. doi:10.1038/s41579-019-0242-1
- Dreosti E, Lopes G, Kampff AR, Wilson SW. 2015. Development of social behavior in young zebrafish. *Front Neural Circuits* **9**:155884. doi:10.3389/FNCIR.2015.00039/BIBTEX
- Dupre C, Yuste R. 2017. Non-overlapping neural networks in *Hydra vulgaris*. *Current Biology* **27**:1085–1097. doi:10.1016/j.cub.2017.02.049
- Dyall SD, Brown MT, Johnson PJ. 2004. Ancient Invasions: From Endosymbionts to Organelles. *Science (1979)* **304**:253–257. doi:10.1126/SCIENCE.1094884
- Epp L, Tardent P. 1978. The distribution of nerve cells in *Hydra attenuata* Pall. *Wilehm Roux Arch Dev Biol* **185**:185–193. doi:10.1007/BF00848677
- Erkosar B, Storelli G, Defaye A, Leulier F. 2013. Host-intestinal microbiota mutualism: “learning on the fly.” *Cell Host Microbe* **13**:8–14. doi:10.1016/j.chom.2012.12.004
- Erwin DH, Laflamme M, Tweedt SM, Sperling EA, Pisani D, Peterson KJ. 2011. The Cambrian conundrum: Early divergence and later ecological success in the early history of animals. *Science (1979)* **334**:1091–1097. doi:10.1126/science.1206375
- Fairclough SR, Chen Z, Kramer E, Zeng Q, Young S, Robertson HM, Begovic E, Richter DJ, Russ C, Westbrook MJ, Manning G, Lang BF, Haas B, Nusbaum C, King N. 2013. Premetazoan genome evolution and the regulation of cell differentiation in the choanoflagellate *Salpingoeca rosetta*. *Genome Biol* **14**:1–15. doi:10.1186/gb-2013-14-2-r15
- Fetissov SO. 2016. Role of the gut microbiota in host appetite control: bacterial growth to animal feeding behaviour. *Nature Reviews Endocrinology* 2016 13:1 **13**:11–25. doi:10.1038/nrendo.2016.150
- Foster KR, Schluter J, Coyte KZ, Rakoff-Nahoum S. 2017. The evolution of the host microbiome as an ecosystem on a leash. *Nature* 2017 548:7665 **548**:43–51. doi:10.1038/nature23292
- Francis L. 1973. Intraspecific aggression and its effect on distribution of *Anthopleura elegantissima* and some related sea anemones. *Biol Bull* **144**:73–92. doi:10.2307/1540148
- Franzenburg S, Fraune S, Altrock PM, Künzel S, Baines JF, Traulsen A, Bosch TCG. 2013a. Bacterial colonization of *Hydra* hatchlings follows a robust temporal pattern. *The ISME Journal* 2013 7:4 **7**:781–790. doi:10.1038/ismej.2012.156
- Franzenburg S, Fraune S, Kunzel S, Baines JF, Domazet-Lošo T, Bosch TCG. 2012. MyD88-deficient *Hydra* reveal an ancient function of TLR signaling in sensing bacterial colonizers. *Proceedings of the National Academy of Sciences* **109**:19374–19379. doi:10.1073/pnas.1213110109
- Franzenburg S, Walter J, Künzel S, Wang J, Baines JF, Bosch TCG, Fraune S. 2013b. Distinct antimicrobial peptide expression determines host species-specific bacterial associations. *Proc Natl Acad Sci U S A* **110**. doi:10.1073/pnas.1304960110
- Fraune S, Abe Y, Bosch TCG. 2009. Disturbing epithelial homeostasis in the metazoan *Hydra* leads to drastic changes in associated microbiota. *Environ Microbiol* **11**:2361–2369.
- Fraune S, Anton-Erxleben F, Augustin R, Franzenburg S, Knop M, Schröder K, Willoweit-Ohl D, Bosch TCG. 2015. Bacteria-bacteria interactions within the microbiota of the ancestral metazoan *Hydra* contribute to fungal resistance. *ISME Journal* **9**:1543–1556. doi:10.1038/ismej.2014.239

- Fraune S, Bosch TCG. 2010. Why bacteria matter in animal development and evolution. *BioEssays* **32**:571–580. doi:10.1002/bies.200900192
- Fraune S, Bosch TCG. 2007. Long-term maintenance of species-specific bacterial microbiota in the basal metazoan Hydra. *Proceedings of the National Academy of Sciences* **104**:13146–13151. doi:10.1073/pnas.0703375104
- Furness JB, Stebbing MJ. 2018. The first brain: Species comparisons and evolutionary implications for the enteric and central nervous systems. *Neurogastroenterology & Motility* **30**:e13234. doi:10.1111/NMO.13234
- Gabanyi I, Lepousez G, Wheeler R, Vieites-Prado A, Nissant A, Wagner S, Moigneu C, Dulauroy S, Hicham S, Polomack B, Verny F, Rosenstiel P, Renier N, Boneca IG, Eberl G, Lledo P-M. 2022. Bacterial sensing via neuronal Nod2 regulates appetite and body temperature. *Science* (1979) **376**. doi:10.1126/SCIENCE.ABJ3986
- Garm A, O'Connor M, Parkefeld L, Nilsson DE. 2007. Visually guided obstacle avoidance in the box jellyfish *Tripedalia cystophora* and *Chiropsella bronzie*. *Journal of Experimental Biology* **210**:3616–3623. doi:10.1242/JEB.004044
- Gensollen T, Iyer SS, Kasper DL, Blumberg RS. 2016. How colonization by microbiota in early life shapes the immune system. *Science* (1979) **352**:539–544. doi:10.1126/science.aad9378
- Ghosh OM, Good BH. 2022. Emergent evolutionary forces in spatial models of microbial growth in the human gut microbiota. *bioRxiv* 2021.07.15.452569. doi:10.1101/2021.07.15.452569
- Giez C, Noack C, Sakib E, Bosch T. 2023a. The internal metabolic state controls behavior in Hydra through an interplay of enteric and central nervous system-like neuron populations. *bioRxiv* 2023.09.15.557876. doi:10.1101/2023.09.15.557876
- Giez C, Pinkle D, Giencke Y, Wittlieb J, Herbst E, Spratte T, Lachnit T, Klimovich A, Selhuber-Unkel C, Bosch T. 2023b. Microbes as part of ancestral neuronal circuits: Bacterial produced signals affect neurons controlling eating behavior in Hydra. *bioRxiv* 2023.04.28.538719. doi:10.1101/2023.04.28.538719
- Grosberg RK, Strathmann RR. 2007. The Evolution of Multicellularity: A Minor Major Transition? <https://doi.org/10.1146/annurev.ecolsys.36.102403.114735> **38**:621–654. doi:10.1146/ANNUREV.ECOLSYS.36.102403.114735
- Grosvenor W, Bellis SL, Kass-Simon G, Rhoads DE. 1992. Chemoreception in hydra: specific binding of glutathione to a membrane fraction. *BBA - General Subjects* **1117**:120–125. doi:10.1016/0304-4165(92)90068-6
- Ha EM, Lee KA, Seo YY, Kim SH, Lim JH, Oh BH, Kim J, Lee WJ. 2009. Coordination of multiple dual oxidase–regulatory pathways in responses to commensal and infectious microbes in drosophila gut. *Nature Immunology* 2009 10:9 **10**:949–957. doi:10.1038/ni.1765
- Hadfield MG. 2010. Biofilms and Marine Invertebrate Larvae: What Bacteria Produce That Larvae Use to Choose Settlement Sites. <https://doi.org/10.1146/annurev-marine-120709-142753> **3**:453–470. doi:10.1146/ANNUREV-MARINE-120709-142753
- Halfvarson J, Brislawn CJ, Lamendella R, Walters WA, Bramer LM, Bonfiglio F, Gonzalez A, McClure EE, Dunklebarger MF, Knight R, Jansson JK, Directorate BS, Northwest P, Diego S, Directorate S, Northwest P, Unit E, Institutet K, Institutet K, Diego S, Diego S. 2017. Dynamics of the human gut microbiome in Inflammatory Bowel Disease. *Nat Microbiol* **2**. doi:10.1038/nmicrobiol.2017.4.Dynamics
- Han H, Yi B, Zhong R, Wang M, Zhang S, Ma J, Yin Y, Yin J, Chen L, Zhang H. 2021. From gut microbiota to host appetite: gut microbiota-derived metabolites as key regulators. *Microbiome* 2021 9:1 **9**:1–16. doi:10.1186/S40168-021-01093-Y
- Han S, Taralova E, Dupre C, Yuste R. 2018. Comprehensive machine learning analysis of Hydra behavior reveals a stable basal behavioral repertoire. *Elife* **7**:1–26. doi:10.7554/eLife.32605
- Hanson A. 2021. Spontaneous electrical low-frequency oscillations: A possible role in Hydra and all living systems. *Philosophical Transactions of the Royal Society B: Biological Sciences* **376**. doi:10.1098/RSTB.2019.0763

- Harold Urey BC. 1952. On the Early Chemical History of the Earth and the Origin of Life. *Proceedings of the National Academy of Sciences* **38**:351–363. doi:10.1073/PNAS.38.4.351
- Harris D. 2020. Metaorganism Metabolomics: Hydra as a tool for understanding the role of bacterial metabolites in shaping the metabolic landscape of the host. Kiel: Zoological Institute.
- Heijtz RD, Wang S, Anuar F, Qian Y, Björkholm B, Samuelsson A, Hibberd ML, Forssberg H, Pettersson S. 2011. Normal gut microbiota modulates brain development and behavior. *Proc Natl Acad Sci U S A* **108**:3047–3052. doi:10.1073/pnas.1010529108
- Henriques SF, Dhakan DB, Serra L, Francisco AP, Carvalho-Santos Z, Baltazar C, Elias AP, Anjos M, Zhang T, Maddocks ODK, Ribeiro C. 2020. Metabolic cross-feeding in imbalanced diets allows gut microbes to improve reproduction and alter host behaviour. *Nature Communications* 2020 **11**:1–15. doi:10.1038/s41467-020-18049-9
- Hinz RC, De Polavieja GG. 2017. Ontogeny of collective behavior reveals a simple attraction rule. *Proc Natl Acad Sci U S A* **114**:2295–2300. doi:10.1073/pnas.1616926114
- Hobert O, Carrera I, Stefanakis N. 2010. The molecular and gene regulatory signature of a neuron. *Trends Neurosci* **33**:435–445. doi:10.1016/j.tins.2010.05.006
- Hooper L V., Littman DR, Macpherson AJ. 2012. Interactions between the microbiota and the immune system. *Science (1979)* **336**:1268–1273. doi:10.1126/science.1223490
- Hooper L V., Wong MH, Thelin A, Hansson L, Falk PG, Gordon JI. 2001. Molecular analysis of commensal host-microbial relationships in the intestine. *Science (1979)* **291**:881–884. doi:10.1126/science.291.5505.88
- Hsiao EY, McBride SW, Hsien S, Sharon G, Hyde ER, McCue T, Codelli JA, Chow J, Reisman SE, Petrosino JF, Patterson PH, Mazmanian SK. 2013. Microbiota modulate behavioral and physiological abnormalities associated with neurodevelopmental disorders. *Cell* **155**:1451–1463. doi:10.1016/j.cell.2013.11.024
- Hufnagel LA, Kass-Simon G, Lyon MK. 1985. Functional organization of battery cell complexes in tentacles of *Hydra attenuata*. *J Morphol* **184**:323–341. doi:10.1002/jmor.1051840307
- Hughes SW, Lorincz ML, Parri HR, Crunelli V. 2011. Infra-slow (<0.1 Hz) oscillations in thalamic relay nuclei: basic mechanisms and significance to health and disease states. *Prog Brain Res* **193**:145. doi:10.1016/B978-0-444-53839-0.00010-7
- Jékely G, Paps J, Nielsen C. 2015. The phylogenetic position of ctenophores and the origin(s) of nervous systems. *Evodevo* **6**:1–9. doi:10.1186/2041-9139-6-1
- Jia Y, Jin S, Hu K, Geng L, Han C, Kang R, Pang Y, Ling E, Tan EK, Pan Y, Liu W. 2021. Gut microbiome modulates *Drosophila* aggression through octopamine signaling. *Nature Communications* 2021 **12**:1–12. doi:10.1038/s41467-021-23041-y
- Jiang J, Su Y, Zhang R, Li H, Tao L, Liu Q. 2022. *C. elegans* enteric motor neurons fire synchronized action potentials underlying the defecation motor program. *Nat Commun* **13**. doi:10.1038/S41467-022-30452-Y
- Kanaya HJ, Kobayakawa Y, Itoh TQ. 2019. *Hydra vulgaris* exhibits day-night variation in behavior and gene expression levels. *Zoological Lett* **5**:1–12. doi:10.1186/s40851-019-0127-1
- Kanaya HJ, Park S, Kim J, Kusumi J, Krenenou S, Sawatari E, Sato A, Lee J, Bang H, Kobayakawa Y. 2020. A sleep-like state in *Hydra* unravels conserved sleep mechanisms during the evolutionary development of the central nervous system. *Sci Adv* **6**:eabb9415. doi:10.1126/sciadv.abb9415
- Kass-Simon G, Pannaccione A, Pierobon P. 2003. GABA and glutamate receptors are involved in modulating pacemaker activity in hydra *Comparative Biochemistry and Physiology - A Molecular and Integrative Physiology*. Pergamon. pp. 329–342. doi:10.1016/S1095-6433(03)00168-5
- Kass-Simon G., Passano LM. 1978. A Neuropharmacological Analysis of the Pacemakers and Conducting Tissues of *Hydra attenuata*. *J Comp Physiol* **79**:71–79.

- Kass-Simon G, Passano LM. 1978. A neuropharmacological analysis of the pacemakers and conducting tissues of *Hydra attenuata*. *J Comp Physiol A Neuroethol Sens Neural Behav Physiol* **128**:71–79. doi:10.1007/BF00668375
- Kass-Simon G, Pierobon P. 2007. Cnidarian chemical neurotransmission, an updated overview. *Comparative Biochemistry and Physiology - A Molecular and Integrative Physiology* **146**:9–25. doi:10.1016/j.cbpa.2006.09.008
- Kass-Simon G, Scappaticci AA. 2004. Glutamatergic and GABAergic control in the tentacle effector systems of *Hydra vulgaris*. *Hydrobiologia* **530–531**:67–71. doi:10.1007/s10750-004-2647-7
- Kim B, Kanai MI, Oh Y, Kyung M, Kim EK, Jang IH, Lee JH, Kim SG, Suh GSB, Lee WJ. 2021. Response of the microbiome–gut–brain axis in *Drosophila* to amino acid deficit. *Nature* **2021 593:7860** **593**:570–574. doi:10.1038/s41586-021-03522-2
- Kim S, Robinson JT. 2023. Phototaxis is a state-dependent behavioral sequence in *Hydra vulgaris*. *bioRxiv* 2023.05.12.540432. doi:10.1101/2023.05.12.540432
- Kinnamon JC, Westfall JA. 1982. Types of neurons and synaptic connections at hypostome–tentacle junctions in *Hydra*. *J Morphol* **173**:119–128. doi:10.1002/JMOR.1051730110
- Kinnamon JC, Westfall JA. 1981. A three dimensional serial reconstruction of neuronal distributions in the hypostome of a *Hydra*. *J Morphol* **168**:321–329. doi:10.1002/jmor.1051680308
- Klimovich A, Giacomello S, Björklund Å, Faure L, Kaucka M, Giez C, Murillo-Rincon AP, Matt A-S, Willoweit-Ohl D, Crupi G. 2020. Prototypical pacemaker neurons interact with the resident microbiota. *Proceedings of the National Academy of Sciences* **117**:17854–17863. doi:10.1073/pnas.1920469117
- Klimovich A V, Bosch TCG. 2018. Rethinking the role of the nervous system: lessons from the *Hydra* holobiont. *BioEssays* **40**:1800060. doi:10.1002/bies.201800060
- Koizumi O, D-wilson J, Grimmelikhuijzen CJ, Westfall JA. 1989. Ultrastructural Localization of RFamide-Like Peptides in Neuronal Dense-Cored Vesicles in the Peduncle of *Hydra*. *J Exp Zool* **249–266**. doi:10.1002/jez.1402490105
- Koizumi O, Haraguchi Y, Ohuchida A. 1983. Reaction chain in feeding behavior of *Hydra*: Different specificities of three feeding responses. *Journal of Comparative Physiology A* **150**:99–105. doi:10.1007/BF00605293
- Koizumi O, Maeda N. 1981. Rise of feeding threshold in satiated *Hydra*. *J Comp Physiol* **142**:75–80. doi:10.1007/BF00605478
- Kommineni S, Bretl DJ, Lam V, Chakraborty R, Hayward M, Simpson P, Cao Y, Bousounis P, Kristich CJ, Salzman NH. 2015. Bacteriocin production augments niche competition by enterococci in the mammalian gastrointestinal tract. *Nature* **2015 526:7575** **526**:719–722. doi:10.1038/nature15524
- Krajmalnik-Brown R, Ilhan ZE, Kang DW, DiBaise JK. 2012. Effects of Gut Microbes on Nutrient Absorption and Energy Regulation. *Nutr Clin Pract* **27**:201. doi:10.1177/0884533611436116
- Kristan WB. 2016. Early evolution of neurons. *Current Biology* **26**:R949–R954. doi:10.1016/j.cub.2016.05.030
- Kropotov JD. 2022. The enigma of infra-slow fluctuations in the human EEG. *Front Hum Neurosci* **16**:928410. doi:10.3389/fnhum.2022.928410
- Kuner T, Seeburg PH, Guy HR. 2003. A common architecture for K⁺ channels and ionotropic glutamate receptors? *Trends Neurosci* **26**:27–32. doi:10.1016/S0166-2236(02)00010-3
- Labavić D, Loverdo C, Bitbol AF. 2022. Hydrodynamic flow and concentration gradients in the gut enhance neutral bacterial diversity. *Proc Natl Acad Sci U S A* **119**:e2108671119. doi:10.1073/pnas.2108671119
- Lagache T, Hanson A, Pérez-Ortega JE, Fairhall A, Yuste R. 2021. Tracking calcium dynamics from individual neurons in behaving animals. *PLoS Comput Biol* **17**:e1009432. doi:10.1371/JOURNAL.PCBI.1009432

- Lee KA, Kim SH, Kim EK, Ha EM, You H, Kim B, Kim MJ, Kwon Y, Ryu JH, Lee WJ. 2013. Bacterial-derived uracil as a modulator of mucosal immunity and gut-microbe homeostasis in drosophila. *Cell* **153**:797–811. doi:10.1016/j.cell.2013.04.009
- Lee YK, Mazmanian SK. 2010. Has the microbiota played a critical role in the evolution of the adaptive immune system? *Science* (1979) **330**:1768–1773. doi:10.1126/science.1195568
- Leitão-Gonçalves R, Carvalho-Santos Z, Francisco AP, Fioreze GT, Anjos M, Baltazar C, Elias AP, Itskov PM, Piper MDW, Ribeiro C. 2017. Commensal bacteria and essential amino acids control food choice behavior and reproduction. *PLoS Biol* **15**:e2000862. doi:10.1371/JOURNAL.PBIO.2000862
- Lenhoff HM. 1961. Activation of the feeding reflex in *Hydra littoralis*: I. Role played by reduced glutathione, and quantitative assay of the feeding reflex. *J Gen Physiol* **45**:331–344. doi:10.1085/jgp.45.2.331
- Lentz TL, Barnett RJ. 1965. FINE STRUCTURE OF THE NERVOUS SYSTEM OF HYDRA. *Integr Comp Biol* **5**:341–356. doi:10.1093/ICB/5.3.341
- Leung LC, Wang GX, Madelaine R, Skariah G, Kawakami K, Deisseroth K, Urban AE, Mourrain P. 2019. Neural signatures of sleep in zebrafish. *Nature* 2019 **571**:7764 **571**:198–204. doi:10.1038/s41586-019-1336-7
- Leys SP, Anderson PA V. 2015. Elements of a 'nervous system' in sponges. *Journal of Experimental Biology* **218**:581–591. doi:10.1242/JEB.110817
- Leys SP, Mackie GO. 1997. Electrical recording from a glass sponge. *Nature* 1997 **387**:6628 **387**:29–30. doi:10.1038/387029b0
- Li D, Wu M. 2021. Pattern recognition receptors in health and diseases. *Signal Transduction and Targeted Therapy* 2021 **6**:1 **6**:1–24. doi:10.1038/s41392-021-00687-0
- Logan SL, Thomas J, Yan J, Baker RP, Shields DS, Xavier JB, Hammer BK, Parthasarathy R. 2018. The *Vibrio cholerae* type VI secretion system can modulate host intestinal mechanics to displace gut bacterial symbionts. *Proc Natl Acad Sci U S A* **115**:E3779–E3787. doi:10.1073/pnas.1720133115
- Loomis WF. 1955. Glutathione Control of the Specific Feeding Reactions of *Hydra*. *Ann N Y Acad Sci* **62**:211–227. doi:10.1111/j.1749-6632.1955.tb35372.x
- Luczynski P, Neufeld KAMV, Oriach CS, Clarke G, Dinan TG, Cryan JF. 2016. Growing up in a Bubble: Using Germ-Free Animals to Assess the Influence of the Gut Microbiota on Brain and Behavior. *International Journal of Neuropsychopharmacology* **19**:1–17. doi:10.1093/IJNP/PYW020
- Mackie GO. 2013. Coelenterate ecology and behavior. Springer Science & Business Media.
- Madeira N, Oliveira RF. 2017. Long-Term Social Recognition Memory in Zebrafish. <https://home.liebertpub.com/zeb> **14**:305–310. doi:10.1089/ZEB.2017.1430
- Marcum BA, Campbell RD. 1978. Development of hydra lacking nerve and interstitial cells. *J Cell Sci* **Vol. 29**:17–33. doi:10.1242/jcs.29.1.17
- Marcus EM, Jacobson S. 2003. An Overview of the Central Nervous System. *Integrated Neuroscience* 1–21. doi:10.1007/978-1-4615-1077-2_1
- Martín-Durán JM, Hejnal A. 2021. A developmental perspective on the evolution of the nervous system. *Dev Biol* **475**:181–192. doi:10.1016/J.YDBIO.2019.10.003
- Massaquoi MS, Kong GL, Chilin-Fuentes D, Ngo JS, Horve PF, Melancon E, Kristina Hamilton M, Eisen JS, Guillemin K. 2023. Cell-type-specific responses to the microbiota across all tissues of the larval zebrafish. doi:10.1016/j.celrep.2023.112095
- Masuzzo A, Manière G, Viallat-Lieutaud A, Avazeri É, Zugasti O, Grosjean Y, Kurz CL, Royet J. 2019. Peptidoglycan-dependent NF-κB activation in a small subset of brain octopaminergic neurons controls female oviposition. *Elife* **8**. doi:10.7554/ELIFE.50559
- Masuzzo A, Montanari M, Kurz L, Royet J. 2020. How Bacteria Impact Host Nervous System and Behaviors: Lessons from Flies and Worms. *Trends Neurosci* **43**:998–1010. doi:10.1016/J.TINS.2020.09.007

- Mayer EA, Knight R, Mazmanian SK, Cryan JF, Tillisch K. 2014. Gut Microbes and the Brain: Paradigm Shift in Neuroscience. *Journal of Neuroscience* **34**:15490–15496. doi:10.1523/JNEUROSCI.3299-14.2014
- Mazzuoli-Weber G, Schemann M. 2015. Mechanosensitivity in the enteric nervous system. *Front Cell Neurosci* **9**:408. doi:10.3389/FNCEL.2015.00408
- McCallum G, Tropini C. 2023. The gut microbiota and its biogeography. *Nature Reviews Microbiology* 2023 1–14. doi:10.1038/s41579-023-00969-0
- Mccullough CB. 1965. Pacemaker interaction in Hydra. *American Zoologist* **5**:499–504. doi:10.1093/icb/5.3.499
- McFadden GI, Van Dooren GG. 2004. Evolution: Red Algal Genome Affirms a Common Origin of All Plastids. *Current Biology* **14**:R514–R516. doi:10.1016/J.CUB.2004.06.041
- McFall-Ngai M, Hadfield MG, Bosch TCG, Carey H V., Domazet-Lošo T, Douglas AE, Dubilier N, Eberl G, Fukami T, Gilbert SF, Hentschel U, King N, Kjelleberg S, Knoll AH, Kremer N, Mazmanian SK, Metcalf JL, Nealson K, Pierce NE, Rawls JF, Reid A, Ruby EG, Rumpho M, Sanders JG, Tautz D, Wernegreen JJ. 2013. Animals in a bacterial world, a new imperative for the life sciences. *Proc Natl Acad Sci U S A* **110**:3229–3236. doi:10.1073/pnas.1218525110
- Mcvey Neufeld KA, Mao YK, Bienenstock J, Foster JA, Kunze WA. 2013. The microbiome is essential for normal gut intrinsic primary afferent neuron excitability in the mouse. *Neurogastroenterology & Motility* **25**:183-e88. doi:10.1111/NMO.12049
- Meisel JD, Panda O, Mahanti P, Schroeder FC, Kim DH. 2014. Chemosensation of bacterial secondary metabolites modulates neuroendocrine signaling and behavior of *C. elegans*. *Cell* **159**:267–280. doi:10.1016/j.cell.2014.09.011
- Michellod D, Bien T, Birgel D, Violette M, Kleiner M, Fearn S, Zeidler C, Gruber-Vodicka HR, Dubilier N, Liebeke M. 2023. De novo phytosterol synthesis in animals. *Science* **380**:520–526. doi:10.1126/science.add7830
- Miri S, Yeo JD, Abubaker S, Hammami R. 2023. Neuromicrobiology, an emerging neurometabolic facet of the gut microbiome? *Front Microbiol* **14**:1098412. doi:10.3389/fmicb.2023.1098412
- Moroz LL, Kocot KM, Citarella MR, Dosung S, Norekian TP, Povolotskaya IS, Grigorenko AP, Dailey C, Berezikov E, Buckley KM, Ptitsyn A, Reshetov D, Mukherjee K, Moroz TP, Bobkova Y, Yu F, Kapitonov V V., Jurka J, Bobkov Y V., Swore JJ, Girardo DO, Fodor A, Gusev F, Sanford R, Bruders R, Kittler E, Mills CE, Rast JP, Derelle R, Solovyev V V., Kondrashov FA, Swalla BJ, Sweedler J V., Rogaev EI, Halanych KM, Kohn AB. 2014. The ctenophore genome and the evolutionary origins of neural systems. *Nature* 2014 510:7503 **510**:109–114. doi:10.1038/nature13400
- Moroz LL, Kohn AB. 2016. Independent origins of neurons and synapses: insights from ctenophores. *Philosophical Transactions of the Royal Society B: Biological Sciences* **371**. doi:10.1098/RSTB.2015.0041
- Mortzfeld BM, Taubenheim J, Fraune S, Klimovich A V., Bosch TCG. 2018. Stem cell transcription factor FoxO controls microbiome resilience in hydra. *Front Microbiol* **9**:1–10. doi:10.3389/fmicb.2018.00629
- Murillo-Rincon AP, Klimovich A, Pemöller E, Taubenheim J, Mortzfeld B, Augustin R, Bosch TCG. 2017. Spontaneous body contractions are modulated by the microbiome of Hydra. *Sci Rep* **7**:1–9. doi:10.1038/s41598-017-16191-x
- Nagpal J, Cryan JF. 2021. Microbiota-brain interactions: Moving toward mechanisms in model organisms. *Neuron* **109**:3930–3953. doi:10.1016/J.NEURON.2021.09.036
- Nawroth JC, Giez C, Klimovich A, Kanso E, Bosch TC. 2023. Spontaneous body wall contractions stabilize the fluid microenvironment that shapes host–microbe associations. *Elife* **12**. doi:10.7554/ELIFE.83637
- Nyholm S V., McFall-Ngai MJ. 2021. A lasting symbiosis: how the Hawaiian bobtail squid finds and keeps its bioluminescent bacterial partner. *Nature Reviews Microbiology* 2021 19:10 **19**:666–679. doi:10.1038/s41579-021-00567-y

- Obata Y, Castaño Á, Boeing S, Bon-Frauches AC, Fung C, Fallesen T, de Agüero MG, Yilmaz B, Lopes R, Huseynova A. 2020. Neuronal programming by microbiota regulates intestinal physiology. *Nature* **578**:284–289. doi:10.1038/s41586-020-1975-8
- Obata Y, Pachnis V. 2016. The Effect of Microbiota and the Immune System on the Development and Organization of the Enteric Nervous System. *Gastroenterology* **151**:836–844. doi:10.1053/J.GASTRO.2016.07.044
- Obeng N, Bansept F, Sieber M, Traulsen A, Schulenburg H. 2021. Evolution of Microbiota–Host Associations: The Microbe’s Perspective. *Trends Microbiol* **29**:779–787. doi:10.1016/j.tim.2021.02.005
- O’Donnell MP, Fox BW, Chao PH, Schroeder FC, Sengupta P. 2020. A neurotransmitter produced by gut bacteria modulates host sensory behaviour. *Nature* **583**:415–420. doi:10.1038/s41586-020-2395-5
- Ousey J, Boktor JC, Mazmanian SK. 2023. Gut microbiota suppress feeding induced by palatable foods. *Current Biology* **33**:147–157.e7. doi:10.1016/J.CUB.2022.10.066
- Parker A, Romano S, Ansorge R, Aboelnour A, Le Gall G, Savva GM, Pontifex MG, Telatin A, Baker D, Jones E, Vauzour D, Rudder S, Blackshaw LA, Jeffery G, Carding SR. 2022. Fecal microbiota transfer between young and aged mice reverses hallmarks of the aging gut, eye, and brain. *Microbiome* **2022 10:1** 10:1–25. doi:10.1186/S40168-022-01243-W
- Passano LM, McCullough CB. 1965. Co-Ordinating Systems and Behaviour in Hydra. II. The Rhythmic Potential System. *J Exp Biol* **42**:205–231. doi:10.1242/jeb.42.2.205
- Passano L. M., McCullough CB. 1964. Co-Ordinating Systems and Behaviour in Hydra: I. Pacemaker System of the Periodic Contractions. *Journal of Experimental Biology* **41**:643–664. doi:10.1242/JEB.41.3.643
- Passano LM, McCullough CB. 1963. Pacemaker hierarchies controlling the behaviour of hydras. *Nature* **199**:1174–1175. doi:10.1038/1991174a0
- Passano LM, McCullough CB. 1962. The Light Response and the Rhythmic Potentials of Hydra. *Proceedings of the National Academy of Sciences* **48**:1376–1382. doi:10.1073/pnas.48.8.1376
- Pavelka M, Roth J. 2010. Central Nervous System: Neuron, Glial Cells. *Functional Ultrastructure* 316–317. doi:10.1007/978-3-211-99390-3_162
- Pereira FC, Berry D. 2017. Microbial nutrient niches in the gut. *Environ Microbiol* **19**:1366. doi:10.1111/1462-2920.13659
- Pereira TD, Shaevitz JW, Murthy M. 2020. Quantifying behavior to understand the brain. *Nature Neuroscience* **23**:1537–1549. doi:10.1038/s41593-020-00734-z
- Phelps D, Brinkman NE, Keely SP, Anneken EM, Catron TR, Betancourt D, Wood CE, Espenschied ST, Rawls JF, Tal T. 2017. Microbial colonization is required for normal neurobehavioral development in zebrafish. *Scientific Reports* **2017 7:1** 7:1–13. doi:10.1038/s41598-017-10517-5
- Pierobon P. 2015. Regional modulation of the response to glutathione in Hydra vulgaris. *Journal of Experimental Biology* **218**:2226–2232. doi:10.1242/jeb.120311
- Pierobon P. 2012. Coordinated modulation of cellular signaling through ligand-gated ion channels in Hydra vulgaris (Cnidaria, Hydrozoa). *International Journal of Developmental Biology* **56**:551–565. doi:10.1387/ijdb.113464pp
- Pierobon P, Concas A, Santoro G, Marino G, Minei R, Pannaccione A, Mostallino MC, Biggio G. 1995. Biochemical and functional identification of GABA receptors in Hydra vulgaris. *Life Sci* **56**:1485–1497. doi:10.1016/0024-3205(95)00111-I
- Pierobon P, Minei R, Porcu P, Sogliano C, Tino A, Marino G, Biggio G, Concas A. 2001. Putative glycine receptors in Hydra: A biochemical and behavioural study. *European Journal of Neuroscience* **14**:1659–1666. doi:10.1046/j.0953-816X.2001.01792.x
- Pierobon P, Sogliano C, Minei R, Tino A, Porcu P, Marino G, Tortiglione C, Concas A. 2004a. Putative NMDA receptors in Hydra: A biochemical and functional study. *European Journal of Neuroscience* **20**:2598–2604. doi:10.1111/j.1460-9568.2004.03759.x

- Pierobon P, Tino A, Minei R, Marino G. 2004b. Different roles of GABA and glycine in the modulation of chemosensory responses in *Hydra vulgaris* (Cnidaria, Hydrozoa). *Hydrobiologia* **530–531**:59–66. doi:10.1007/s10750-004-2690-4
- Pietschke C, Treitz C, Forêt S, Schultze A, Künzel S, Tholey A, Bosch TCG, Fraune S. 2017. Host modification of a bacterial quorum-sensing signal induces a phenotypic switch in bacterial symbionts. *Proc Natl Acad Sci U S A* **114**:E8488–E8497. doi:10.1073/pnas.1706879114
- Pisani D, Pett W, Dohrmann M, Feuda R, Rota-Stabelli O, Philippe H, Lartillot N, Wörheide G. 2015. Genomic data do not support comb jellies as the sister group to all other animals. *Proc Natl Acad Sci U S A* **112**:15402–15407. doi:10.1073/pnas.1518127112
- Raichle ME. 2015. The Brain's Default Mode Network. <https://doi.org/10.1146/annurev-neuro-071013-014030> **38**:433–447. doi:10.1146/ANNUREV-NEURO-071013-014030
- Rakoff-Nahoum S, Foster KR, Comstock LE. 2016. The evolution of cooperation within the gut microbiota. *Nature* **2015 533:7602** **533**:255–259. doi:10.1038/nature17626
- Rathje K, Mortzfeld B, Hoepfner MP, Taubenheim J, Bosch TCG, Klimovich A. 2020. Dynamic interactions within the host-associated microbiota cause tumor formation in the basal metazoan *Hydra*. *PLoS Pathogens*. doi:10.1371/journal.ppat.1008375
- Rawls JF, Samuel BS, Gordon JI. 2004. Gnotobiotic zebrafish reveal evolutionarily conserved responses to the gut microbiota. *Proc Natl Acad Sci U S A* **101**:4596–4601. doi:10.1073/pnas.0400706101
- Reese AT, Pereira FC, Schintlmeister A, Berry D, Wagner M, Hale LP, Wu A, Jiang S, Durand HK, Zhou X, Premont RT, Diehl AM, O'Connell TM, Alberts SC, Kartzinel TR, Pringle RM, Dunn RR, Wright JP, David LA. 2018. Microbial nitrogen limitation in the mammalian large intestine. *Nature Microbiology* **2018 3:12** **3**:1441–1450. doi:10.1038/s41564-018-0267-7
- Rhoades JL, Nelson JC, Nwabudike I, Yu SK, McLachlan IG, Madan GK, Abebe E, Powers JR, Colón-Ramos DA, Flavell SW. 2019. ASICs Mediate Food Responses in an Enteric Serotonergic Neuron that Controls Foraging Behaviors. *Cell* **176**:85-97.e14. doi:10.1016/J.CELL.2018.11.023
- Richter SH, Garner JP, Würbel H. 2009. Environmental standardization: cure or cause of poor reproducibility in animal experiments? *Nature Methods* **2009 6:4** **6**:257–261. doi:10.1038/nmeth.1312
- Robertson MP, Joyce GF. 2012. The origins of the RNA world. *Cold Spring Harb Perspect Biol* **4**:a003608. doi:10.1101/cshperspect.a003608
- Roshchina V V. 2016. New trends and perspectives in the evolution of neurotransmitters in microbial, plant, and animal cells. *Adv Exp Med Biol* **874**:25–77. doi:10.1007/978-3-319-20215-0_2/COVER
- Rowland I, Gibson G, Heinken A, Scott K, Swann J, Thiele I, Tuohy K. 2017. Gut microbiota functions: metabolism of nutrients and other food components. *European Journal of Nutrition* **2017 57:1** **57**:1–24. doi:10.1007/S00394-017-1445-8
- Ruggieri RD, Pierobon P, Kass-Simon G. 2004. Pacemaker activity in hydra is modulated by glycine receptor ligands. *Comparative Biochemistry and Physiology - A Molecular and Integrative Physiology* **138**:193–202. doi:10.1016/j.cbpb.2004.03.015
- Rushforth NB. 1971. Behavioral and Electrophysiological Studies of *Hydra*. I. Analysis of Contraction Pulse Patterns. *Biol Bull* **140**:255–273. doi:10.2307/1540073
- Rushforth NB. 1965. Inhibition of contraction responses of hydra. *Integr Comp Biol* **5**:505–513. doi:10.1093/icb/5.3.505
- Rushforth Norman B, Hofman F. 1972. Behavioral and Electrophysiological Studies of *Hydra*. III. Components of Feeding Behavior. *Bulletin* **142**:110–131.
- Rushforth Norman B., Hofman F. 1972. Behavioral and Electrophysiological Studies of *Hydra*. III. Components of Feeding Behavior. *Biol Bull* **142**:110–131. doi:10.2307/1540250
- Ryan JF, Pang K, Schnitzler CE, Nguyen AD, Moreland RT, Simmons DK, Koch BJ, Francis WR, Havlak P, Smith SA, Putnam NH, Haddock SHD, Dunn CW, Wolfsberg TG, C.Mullikin J, Martindale MQ, Baxevanis AD. 2013. The genome of the ctenophore

- Mnemiopsis leidyi and its implications for cell type evolution. *Science* (1979) **342**. doi:10.1126/science.1242592
- Sabbagh Y, Giral H, Caldas Y, Levi M, Schiavi SC. 2011. Intestinal Phosphate Transport. *Adv Chronic Kidney Dis* **18**:85. doi:10.1053/J.ACKD.2010.11.004
- Sagan L. 1967. On the origin of mitosing cells. *J Theor Biol* **14**:225-IN6. doi:10.1016/0022-5193(67)90079-3
- Scappaticci AA, Kass-Simon G. 2008. NMDA and GABAB receptors are involved in controlling nematocyst discharge in hydra. *Comparative Biochemistry and Physiology - A Molecular and Integrative Physiology* **150**:415–422. doi:10.1016/j.cbpa.2008.04.606
- Schluter J, Foster KR. 2012. The Evolution of Mutualism in Gut Microbiota Via Host Epithelial Selection. *PLoS Biol* **10**:e1001424. doi:10.1371/JOURNAL.PBIO.1001424
- Schneider KM, Kim J, Bahnsen K, Heuckeroth RO, Thaiss CA. 2022. Environmental perception and control of gastrointestinal immunity by the enteric nervous system. *Trends Mol Med* **28**:989–1005. doi:10.1016/J.MOLMED.2022.09.005
- Schretter CE, Vielmetter J, Bartos I, Marka Z, Marka S, Argade S, Mazmanian SK. 2018. A gut microbial factor modulates locomotor behaviour in Drosophila. *Nature* **563**:7731 **563**:402–406. doi:10.1038/s41586-018-0634-9
- Schröder K, Bosch TCG. 2016a. The origin of mucosal immunity: Lessons from the holobiont Hydra. *mBio*. doi:10.1128/mBio.01184-16
- Sharma R, Schumacher U. 1995. Morphometric analysis of intestinal mucins under different dietary conditions and gut flora in rats. *Digestive Diseases and Sciences* **1995** **40**:12 **40**:2532–2539. doi:10.1007/BF02220438
- Sheehan D, Moran C, Shanahan F. 2015. The microbiota in inflammatory bowel disease. *J Gastroenterol* **50**:495–507. doi:10.1007/s00535-015-1064-1
- Shigenobu S, Watanabe H, Hattori M, Sakaki Y, Ishikawa H. 2000. Genome sequence of the endocellular bacterial symbiont of aphids Buchnera sp. APS. *Nature* **2000** **407**:6800 **407**:81–86. doi:10.1038/35024074
- Shikuma NJ, Antoshechkin I, Medeiros JM, Pilhofer M, Newman DK. 2016. Stepwise metamorphosis of the tubeworm Hydroides elegans is mediated by a bacterial inducer and MAPK signaling. *Proc Natl Acad Sci U S A* **113**:10097–10102. doi:10.1016/j.molmed.2022.09.005
- Shimizu H, Koizumi O, Fujisawa T. 2004. Three digestive movements in Hydra regulated by the diffuse nerve net in the body column. *J Comp Physiol A Neuroethol Sens Neural Behav Physiol* **190**:623–630. doi:10.1007/s00359-004-0518-3
- Shimomura T, Yonekawa Y, Nagura H, Tateyama M, Fujiyoshi Y, Irie K. 2020. A native prokaryotic voltage-dependent calcium channel with a novel selectivity filter sequence. *Elife* **9**. doi:10.7554/ELIFE.52828
- Sieber M, Pita L, Weiland-Bräuer N, Dirksen P, Wang J, Mortzfeld B, Franzenburg S, Schmitz RA, Baines JF, Fraune S, Hentschel U, Schulenburg H, Bosch TCG, Traulsen A. 2019. Neutrality in the Metaorganism. *PLoS Biol* **17**:e3000298. doi:10.1371/JOURNAL.PBIO.3000298
- Sieber M, Traulsen A, Schulenburg H, Douglas AE. 2021. On the evolutionary origins of host-microbe associations. *Proc Natl Acad Sci U S A* **118**:e2016487118. doi:10.1073/pnas.2016487118
- Siebert S, Farrell JA, Cazet JF, Abeykoon Y, Primack AS, Schnitzler CE, Juliano CE. 2019. Stem cell differentiation trajectories in Hydra resolved at single-cell resolution. *Science* (1979) **365**:eaav9314. doi:10.1126/science.aav9314
- Smith P, Willemsen D, Popkes M, Metge F, Gandiwa E, Reichard M, Valenzano DR. 2017. Regulation of life span by the gut microbiota in the short-lived african turquoise killifish. *Elife* **6**:1–26. doi:10.7554/eLife.27014
- Sommer F, Bäckhed F. 2013. The gut microbiota — masters of host development and physiology. *Nature Reviews Microbiology* **2013** **11**:4 **11**:227–238. doi:10.1038/nrmicro2974

- Squire L, Berg D, Bloom FE, Du Lac S, Ghosh A, Spitzer NC. 2012. Fundamental neuroscience. Academic press.
- Stednitz SJ, McDermott EM, Ncube D, Tallafuss A, Eisen JS, Washbourne P. 2018. Forebrain Control of Behaviorally Driven Social Orienting in Zebrafish. *Current Biology* **28**:2445-2451.e3. doi:10.1016/j.cub.2018.06.016
- Stednitz SJ, Washbourne P. 2020. Rapid Progressive Social Development of Zebrafish. <https://home.liebertpub.com/zeb> **17**:11–17. doi:10.1089/ZEB.2019.1815
- Strandwitz P. 2018. Neurotransmitter modulation by the gut microbiota. *Brain Res* **1693**:128–133. doi:10.1016/J.BRAINRES.2018.03.015
- Tardent P, Frei E, Borner M. 1976. The Reactions of Hydra Attenuata Pall. to Various Photoc Stimuli. *Coelenterate Ecology and Behavior* 671–683. doi:10.1007/978-1-4757-9724-4_69
- Tardent P, Weber C. 1976. A Qualitative and Quantitative Inventory of Nervous Cells in Hydra Attenuata Pall. *Coelenterate Ecology and Behavior* 501–512. doi:10.1007/978-1-4757-9724-4_52
- Taubenheim J, Miklós M, Tökölyi J, Fraune S. 2022. Population Differences and Host Species Predict Variation in the Diversity of Host-Associated Microbes in Hydra. *Front Microbiol* **13**:799333. doi:10.3389/FMICB.2022.799333/BIBTEX
- Taubenheim J, Willoweit-Ohl D, Knop M, Franzenburg S, He J, Bosch TCG, Fraune S. 2020. Bacteria- And temperature-regulated peptides modulate β -catenin signaling in hydra. *Proc Natl Acad Sci U S A* **117**:21459–21468. doi:10.1073/pnas.2010945117
- Tosches MA, Arendt D. 2013. The bilaterian forebrain: an evolutionary chimaera. *Curr Opin Neurobiol* **23**:1080–1089. doi:10.1016/J.CONB.2013.09.005
- Toskes PP. 1993. Bacterial overgrowth of the gastrointestinal tract. *Adv Intern Med* **38**:387–407.
- Tran CM, Fu S, Rowe T, Collins EMS. 2017. Generation and Long-term Maintenance of Nerve-free Hydra. *JoVE (Journal of Visualized Experiments)* **2017**:e56115. doi:10.3791/56115
- Trembley A. 1744. Mémoires, pour servir à l'histoire d'un genre de polypes d'eau douce, à bras en forme de cornes. Chez Jean & Herman Verbeek.
- Trevelline BK, Kohl KD. 2022. The gut microbiome influences host diet selection behavior. *Proc Natl Acad Sci U S A* **119**:e2117537119. doi:10.1073/pnas.2117537119
- Tzouanas CN, Kim S, Badhiwala KN, Avants BW, Robinson JT. 2021. Hydra vulgaris shows stable responses to thermal stimulation despite large changes in the number of neurons. *iScience* **24**. doi:10.1016/j.isci.2021.102490
- Uribe A, Alam M, Midtvedt T, Smedfors B, Theodorsson E. 2009. Endogenous Prostaglandins and Microflora Modulate DNA Synthesis and Neuroendocrine Peptides in the Rat Gastrointestinal Tract. <http://dx.doi.org/10.3109/00365529708996520> **32**:691–699. doi:10.3109/00365529708996520
- Vallet-Gely I, Lemaitre B, Boccard F. 2008. Bacterial strategies to overcome insect defences. *Nature Reviews Microbiology* 2008 **6**:4 **6**:302–313. doi:10.1038/nrmicro1870
- van der Vaart M, van Soest JJ, Spaink HP, Meijer AH. 2013. Functional analysis of a zebrafish myd88 mutant identifies key transcriptional components of the innate immune system. *Dis Model Mech* **6**:841–854. doi:10.1242/dmm.010843
- Venturini G. 1987. The hydra GSH receptor. Pharmacological and radioligand binding studies. *Comparative Biochemistry and Physiology Part C, Comparative* **87**:321–324. doi:10.1016/0742-8413(87)90015-6
- Venturini G, Carolei A. 1992. Dopaminergic receptors in Hydra. Pharmacological and biochemical observations. *Comparative Biochemistry and Physiology Part C: Comparative Pharmacology* **102**:39–43. doi:10.1016/0742-8413(92)90040-E
- Vidal B, Gulez B, Cao WX, Leyva-Diaz E, Reilly MB, Tekieli T, Hobert O. 2022. The enteric nervous system of the C. elegans pharynx is specified by the Sine oculis-like homeobox gene ceh-34. *Elife* **11**. doi:10.7554/ELIFE.76003

- Vien TN, DeCaen PG. 2016. Biophysical Adaptations of Prokaryotic Voltage-Gated Sodium Channels. *Curr Top Membr* **78**:39–64. doi:10.1016/BS.CTM.2015.12.003
- Vuong HE, Pronovost GN, Williams DW, Coley EJJ, Siegler EL, Qiu A, Kazantsev M, Wilson CJ, Rendon T, Hsiao EY. 2020. The maternal microbiome modulates fetal neurodevelopment in mice. *Nature* **586**:281–286. doi:10.1038/s41586-020-2745-3
- Weissbourd B, Momose T, Nair A, Kennedy A, Hunt B, Anderson DJ. 2021. A genetically tractable jellyfish model for systems and evolutionary neuroscience. *Cell* **184**:5854–5868.e20. doi:10.1016/j.cell.2021.10.021
- Werner B. 1973. Spermatzeugmen und Paarungsverhalten bei *Tripedalia cystophora* (Cubomedusae). *Mar Biol* **18**:212–217. doi:10.1007/BF00367987
- Westfall JA. 1973. Ultrastructural evidence for a granule-containing sensory-motor-interneuron in *Hydra littoralis*. *J Ultrastruct Res* **42**:268–282. doi:10.1016/S0022-5320(73)90055-5
- Westfall JA, Epp LG. 1985. Scanning electron microscopy of neurons isolated from the pedal disk and body column of *Hydra*. *Tissue Cell* **17**:161–170. doi:10.1016/0040-8166(85)90085-0
- Westfall JA, Kinnamon JC. 1984. Perioral synaptic connections and their possible role in the feeding behavior of *Hydra*. *Tissue Cell* **16**:355–365. doi:10.1016/0040-8166(84)90055-7
- Westfall JA, Kinnamon JC. 1978a. A second sensory-motor-interneuron with neurosecretory granules in *Hydra*. *J Neurocytol* **7**:365–379. doi:10.1007/BF01176999/METRICS
- Westfall JA, Kinnamon JC. 1978b. A second sensory-motor-interneuron with neurosecretory granules in *Hydra*. *J Neurocytol* **7**:365–379. doi:10.1007/BF01176999
- Westfall JA, Kinnamon JC, Sims DE. 1980. Neuro-epitheliomuscular cell and neuro-neuronal gap junctions in *Hydra*. *J Neurocytol* **9**:725–732. doi:10.1007/BF01205015
- Westfall JA, Wilson JD, Rogers RA, Kinnamon JC. 1991. Multifunctional features of a gastrodermal sensory cell in *Hydra*: three-dimensional study. *J Neurocytol* **20**:251–261. doi:10.1007/BF01235543
- Westfall JA, Yamataka S, Enos PD. 1971. ULTRASTRUCTURAL EVIDENCE OF POLARIZED SYNAPSES IN THE NERVE NET OF HYDRA. *Journal of Cell Biology* **51**:318–323. doi:10.1083/JCB.51.1.318
- Wiles TJ, Jemielita M, Baker RP, Schlomann BH, Logan SL, Ganz J, Melancon E, Eisen JS, Guillemin K, Parthasarathy R. 2016. Host Gut Motility Promotes Competitive Exclusion within a Model Intestinal Microbiota. *PLoS Biol* **14**:1–24. doi:10.1371/journal.pbio.1002517
- Wiles TJ, Schlomann BH, Wall ES, Betancourt R, Parthasarathy R, Guillemin K. 2020. Swimming motility of a gut bacterial symbiont promotes resistance to intestinal expulsion and enhances inflammation, *PLoS Biology*. doi:10.1371/journal.pbio.3000661
- Williams CG, Lee HJ, Asatsuma T, Vento-Tormo R, Haque A. 2022. An introduction to spatial transcriptomics for biomedical research. *Genome Med* **14**:1–18. doi:10.1186/s13073-022-01075-1
- Wong ACN, Wang QP, Morimoto J, Senior AM, Lihoreau M, Neely GG, Simpson SJ, Ponton F. 2017. Gut Microbiota Modifies Olfactory-Guided Microbial Preferences and Foraging Decisions in *Drosophila*. *Current Biology* **27**:2397–2404.e4. doi:10.1016/J.CUB.2017.07.022
- Woznica A, Cantley AM, Beemelmanns C, Freinkman E, Clardy J, King N. 2016. Bacterial lipids activate, synergize, and inhibit a developmental switch in choanoflagellates. *Proc Natl Acad Sci U S A* **113**:7894–7899. doi:10.1073/pnas.1605015113
- Yamamoto W, Yuste R. 2023. Peptide-driven control of somersaulting in *Hydra vulgaris*. *Current Biology* **33**. doi:10.1016/J.CUB.2023.03.047

- Yamamoto W, Yuste R. 2020b. Whole-Body Imaging of Neural and Muscle Activity during Behavior in *Hydra vulgaris*: Effect of Osmolarity on Contraction Bursts. *eNeuro* **7**:1–13. doi:10.1523/ENEURO.0539-19.2020
- Ye L, Bae M, Cassilly CD, Jabba S V., Thorpe DW, Martin AM, Lu HY, Wang J, Thompson JD, Lickwar CR, Poss KD, Keating DJ, Jordt SE, Clardy J, Liddle RA, Rawls JF. 2021. Enteroendocrine cells sense bacterial tryptophan catabolites to activate enteric and vagal neuronal pathways. *Cell Host Microbe* **29**:179-196.e9. doi:10.1016/J.CHOM.2020.11.011
- Zarrinpar A, Chaix A, Xu ZZ, Chang MW, Marotz CA, Saghatelian A, Knight R, Panda S. 2018. Antibiotic-induced microbiome depletion alters metabolic homeostasis by affecting gut signaling and colonic metabolism. *Nature Communications* **2018** *9*:1 **9**:1–13. doi:10.1038/s41467-018-05336-9
- Zhou C, Rao Yong, Rao Yi. 2008. A subset of octopaminergic neurons are important for *Drosophila* aggression. *Nat Neurosci* **11**:1059–1067. doi:10.1038/nn.2164
- Zhu S, Zhu M, Knoll AH, Yin Z, Zhao F, Sun S, Qu Y, Shi M, Liu H. 2016. Decimetre-scale multicellular eukaryotes from the 1.56-billion-year-old Gaoyuzhuang Formation in North China. *Nature Communications* **2016** *7*:1 **7**:1–8. doi:10.1038/ncomms11500
- Zwarts L, Versteven M, Callaerts P. 2012. Genetics and neurobiology of aggression in *Drosophila*. *Fly (Austin)* **6**:35–48. doi:10.4161/fly.19249